

# Historic amphibian settlements in the northwestern Nile delta - a geoarchaeological perspective

## Dissertation

zur Erlangung des Doktorgrades der Naturwissenschaften

*(Dr. rer. nat.)*

vorgelegt beim Fachbereich Geowissenschaften/Geographie (FB11)

der Johann Wolfgang Goethe-Universität

in Frankfurt am Main



von

M. Eng., Dipl. Geogr. Andreas Ginau  
aus Niddatal

July 28, 2020

---

vom Fachbereich Geowissenschaften/Geographie (FB11) der  
Johann Wolfgang Goethe-Universität als Dissertation angenommen

Dekan:

**Prof. Dr. Georg Rumpker**  
Institut für Geowissenschaften  
Johann Wolfgang Goethe-Universität

Gutachter:

**Prof. Dr. Jürgen Wunderlich**  
Institut für Physische Geographie  
Johann Wolfgang Goethe-Universität

**Prof. Dr. Christian Opp**  
Fachbereich Geographie  
Philipps-Universität, Marburg

## Abstract

No concise picture of the archaeological and palaeoecological evolution can be drawn for the northwestern Nile delta, and archaeological records show significant population dynamics that still need explanation and spur the need for further palaeoenvironmental research. This study delivers a set of new methods especially in the fields of remote sensing and data analytics that can be regarded as important milestones and foundations for further palaeoenvironmental research in the area. Additionally, it shows new insights for individual time slices.

This geoarchaeological project is a cooperation with the archaeological excavations of the German Archaeological Institute (DAI) in Buto and Kom el'Gir. It expands the work of Wunderlich (1989) which laid important foundations in understanding the origin of the initial landscape that was later colonized in different cultural stages showing different dynamics, settlement intensities and even long phases of abandonment or breaks in between. This forms the starting point for relating the population dynamics of the different cultural phases reaching from Predynastic (prior to 3150 before Christ) up to the Greco-Roman era (~anno Domini 650) to the environmental history and events that occurred in the area. It is very likely that environmental changes such as the shifting of major water routes, inundation or paludification of larger areas or other environmental events affected settlements and human life in the area.

In the fields of remote sensing new methods are presented to complete information on the location of ancient settlements, and complex workflows are developed that allow the tracing of subsurface structures via indirect analysis of vegetation growth in larger time series data. It was verified that a relationship exists between vegetation performance, the appearance of archaeological material in the topsoil, and the location of former Nile river branches. Together with a new high resolution digital elevation model (DEM) based on TanDEM-X data, new interpretations with a high spatial significance are possible. For individual time slices, namely the Late Dynastic and Greco-Roman era, this work delivers a detailed landscape description suggesting a finely ramified subdelta, with all settlements placed on alluvial levees. This explains the massive increase in settlements in the Ptolemaic, Roman and in particular late Roman periods (4<sup>th</sup> century before Christ – anno Domini 7<sup>th</sup> century).

We sampled the Nile delta clays together with the channels and the material of the archaeological excavations in vibracores and profile walls. This geologic inspection of the subsurface together with geochemical results from a handheld portable X-ray fluorescence device (pXRF) allowed new interpretations of the landscape and environmental history. For example, we used geochemical data to distinguish between artificial and natural channels as a measure for the anthropogenic influence, a proxy for past environmental characteristics and lastly as a basis for a new dating method. Many of the channels, for instance, were dated by our own  $^{14}\text{C}$  datings, comparisons with the previous work of Wunderlich (1989) and application of new dating approach based on machine learning with artificial neural networks. Additionally, we run a full methodological approach, and examine the applicability of pXRF methods in general, and test the quality of the data to detect distinct geochemical differences between the main settlement phases with advanced methods in data analytics. The dating is based, for example, on the training of artificial neural networks with pXRF data from archaeological material of well-dated context to date test data of cultural layers within the vibracores. With this method the homogeneous Nile alluvium, cultural layers and channels can be dated roughly and, as a result, fundamental changes in the landscape can be linked with the settlement history of Buto and neighboring tells.

## Kurzzusammenfassung

Trotz einer Jahrzehnte umfassenden Forschungsgeschichte, die das nordwestliche Nildelta erfahren hat, kann noch immer kein zusammenhängendes Bild der archäologischen und paläoökologischen Umweltgeschichte gezeichnet werden. Gerade die im archäologischen Kontext aufgedeckten Populationsschwankungen mit einhergehender Verlagerung bzw. Aufgabe von Siedlungen bedarf der Erforschung der vergangenen Umweltbedingungen, um Ursachen und Zusammenhänge für ebensolche bedeutenden Entwicklungen zu finden.

Um diese Wissenslücken zu schließen, wurden seit 2012 in Kooperation mit dem Deutschen Archäologischen Institut (DAI) geoarchäologische Forschungen durchgeführt mit dem Ziel, die Arbeiten von Wunderlich (1989), welche Grundlagen im Verständnis des spätpleistozänen bis frühholozänen Entstehungsprozesses dieses Siedlungsraumes geschaffen haben, fortzuführen. Ziel dieser Dissertation ist die Erforschung von Umweltdynamiken während der verschiedenen Besiedlungsphasen in Buto und Umgebung, die durch Populationsschwankungen und langen Phasen der Siedlungsaufgabe gekennzeichnet sind und zeitlich gesehen von der Vorgeschichte (vor 3150 vor Christus) bis hin zur Griechisch-Römischen Zeit (~anno Domini 650) reichen. Es ist sehr wahrscheinlich, dass die Verlagerung von Flussarmen, Vernässung und Versumpfung von Gebieten oder andere Naturereignisse das Schicksal der Menschen in den verschiedenen Kulturphasen bestimmt haben.

Diese Studie liefert eine Fülle an neuen Methoden insbesondere im Bereich der Fernerkundung und Datenanalyse, um genau solche Entwicklungen besser erklären und erforschen zu können. Dabei werden für einzelne Zeitabschnitte neue Erkenntnisse und Grundlagen über den vorgestellten Raum zu Tage gebracht.

Die fernerkundlichen Methoden dieser Arbeit zielen darauf ab, das Netzwerk bekannter historischer Siedlungsstätten zu vervollständigen und komplexere fernerkundliche Routinen für Satellitenbildzeitreihen zu entwickeln, die Strukturen im Untergrund dank ihres indirekten Einflusses auf das Pflanzenwachstum sichtbar machen. So konnte ein Zusammenhang zwischen einer hohen Vegetationsleistung der Pflanzen und dem Vorhandensein von archäologischem Material im Oberboden nachgewiesen werden, der auch mit der Nähe zu den früheren Flussarmen korreliert. Vervollständigt werden die fernerkundlichen Methoden durch die Verarbeitung und Analyse von hochauflösenden global verfügbaren Geländemodellen aus TanDEM-X Daten. Diese

eröffnen völlig neue Perspektiven auf das Nildelta und ermöglichen neue Interpretation für diesen Raum in einer für paläoökologische Verhältnisse sehr hohen räumlichen Auflösung. Gerade für den griechische-römischen Zeitabschnitt (viertes Jahrhundert vor Christus – siebtes Jahrhundert nach Christus) konnte ein detailliertes Landschaftsbild mit einem fein aufgegliederten Flussnetz geschaffen werden, an dessen Ufern fast ausschließlich alle historischen Siedlungen liegen, die mit fernerkundlich oder archäologischen Methoden prospektiert wurden.

Während verschiedener Geländekampagnen wurden das Delta, die Umgebung der Siedlungen und das Siedlungsmaterial selbst mit Hilfe von Bohrungen und durch Probennahme in anstehenden Profilwänden beprobt. Diese geologische Prospektion, ergänzt um chemische Analysen mit einem handgehaltenen Röntgenfluoreszenzmessgerät (pXRF) sind Kernstück des methodischen Inventars für die angestrebte diachrone Landschafts- und Umweltanalyse. So können auf Basis von geochemischen Daten künstliche und natürliche Rinnen unterschieden, der anthropogene Einfluss detektiert, vergangene Umweltbedingungen mit Elementproxies erhoben und die Sedimente datiert werden. Letzteres ist ein Kernstück dieser Arbeit und stellt eine Möglichkeit dar, die Datierungsmethoden zu erweitern, welche derzeit in Ägypten aufgrund des Ausfuhrverbots limitiert sind. Der gewählte Ansatz basiert auf der Anwendung von Maschinenlernen mit künstlichen neuronalen Netzwerken. Dabei wurde ein ganzheitlicher Untersuchungsansatz gewählt, der die Anwendbarkeit und Qualität von pXRF-Messungen an dem Probenmaterial bewerten soll. In der Datenanalyse wurde mittels multivariater und anderer statistischer Verfahren überprüft, ob es Unterschiede zwischen Siedlungsmaterial und den alluvialen Deltasedimenten gibt und ob sich diese Unterschiede bis hin zu Material aus verschiedenen Kulturphasen verfolgen lassen. Die Datierung basiert auf dem Training des neuronalen Netzwerkes mit Probenmaterial der verschiedenen archäologischen Schichten bekannten Kontextes und der Anwendung auf Material der umgebenden Bohrungen, welche Kulturschichten, Flussrinnen oder anderes beinhalten. Auf diese Weise können die in den Bohrungen zu Tage gebrachten Zeugen der früheren Landschaftsgeschichte mit der Siedlungs- und Kulturgeschichte der archäologischen Grabung zusammengebracht werden.

## Zusammenfassung

Trotz einer Jahrzehnte umfassenden Forschungsgeschichte, die das nordwestliche Nildelta erfahren hat, kann noch immer kein zusammenhängendes Bild der archäologischen und paläoökologischen Umweltgeschichte gezeichnet werden. Die in der Vergangenheit durchgeführten archäologischen Arbeiten konnten das Bild einer schwer zugänglichen und als Siedlungsstandort ungeeigneten Sumpflandschaft revidieren und zeigen, dass sich spätestens seit dem vierten Jahrtausend vor Christus Siedlungsspuren in der Region finden lassen. Weiterhin konnte ein detaillierteres Bild der Siedlungsaktivität entworfen werden, welches von mehreren Besiedlungsphasen unterschiedlicher Intensität ausgeht, zwischen denen zum Teil längere Siedlungslücken existierten. Gerade die im archäologischen Kontext aufgedeckten Populationsschwankungen mit einhergehender Verlagerung bzw. Aufgabe von Siedlungen bedarf der Erforschung der vergangenen Umweltbedingungen, um Ursachen und Zusammenhänge für ebensolche bedeutenden Entwicklungen zu finden.

Um diese Wissenslücken zu schließen, wurden seit 2012, in Kooperation mit dem Deutschen Archäologischen Institut (DAI), geoarchäologische Forschungen durchgeführt, die an die Arbeiten von Wunderlich (1989), welche Grundlagen im Verständnis des spätpleistozänen bis frühholozänen Entstehungsprozesses dieses Siedlungsraumes geschaffen haben, anknüpfen. Ziel dieser Arbeit ist es die kulturgeschichtliche und paläoökologische Entwicklung im nordwestlichen Nildelta diachron von der Spätvorgeschichte bis in die frühislamische Zeit zu entschlüsseln und miteinander zu verknüpfen. Die Dissertation liefert Grundlagen für die Erforschung von Umweltdynamiken während der verschiedenen Besiedlungsphasen in Buto und Umgebung, die durch Populationsschwankungen und langen Phasen der Siedlungsaufgabe gekennzeichnet sind und zeitlich gesehen von der Vorgeschichte (vor 3150 vor Christus) bis hin zur Griechisch-Römischen Zeit (~anno Domini 650) reichen. Es ist sehr wahrscheinlich, dass die Verlagerung von Flussarmen, Vernässung und Versumpfung von Gebieten oder andere Naturereignisse das Schicksal der Menschen in den verschiedenen Kulturphasen bestimmt haben.

Diese Studie liefert eine Fülle an neuen Methoden insbesondere im Bereich der Fernerkundung und Datenanalyse, um genau solche Entwicklungen besser erklären und erforschen zu können. Dabei werden für einzelne Zeitab-

schnitte neue Erkenntnisse und Grundlagen über den vorgestellten Raum zu Tage gebracht.

Gerade fernerkundliche Methoden erfahren einen immensen Bedeutungszuwachs in den Geowissenschaften. Gründe hierfür sind die hohe räumliche Verfügbarkeit von Daten, neue technische Entwicklungen und die unentgeltliche Bereitstellung von Fernerkundungsmaterial. Letzteres gilt insbesondere für den wissenschaftlichen Bereich.

Auch in dieser Arbeit wird auf das große Potential fernerkundlicher Methoden zurückgegriffen und es werden diese weiterentwickelt. Es werden neue überwachte Klassifizierungstechniken vorgestellt, um antike Siedlungshügel auf Basis von mehreren Landsat 8 Satellitenbildern zu klassifizieren. Antike Siedlungshügel sind ein wichtiger Indikator für den Verlauf früherer Nilarme und sie sind als wichtiges Kulturgut gefährdet, da sie zunehmend in landwirtschaftliche Flächen umgewandelt werden, der Urbanisierung zum Opfer fallen oder als Dünger für die Felder abgebaut werden. Dass Ihre Lage mit den Nilverläufen zusammenhängt und fast alle Siedlungshügel im nordwestlichen Nildelta an ehemaligen Wasserläufen liegen, konnte in dieser Arbeit erstmals nachgewiesen werden. Dabei zielen die fernerkundlichen Methoden dieser Arbeit nicht nur darauf ab, das Netzwerk oberflächlich sichtbarer historischer Siedlungsstätten zu vervollständigen. Es werden zudem komplexe fernerkundliche Routinen für Satellitenbildzeitreihen entwickelt, die Strukturen im Untergrund dank ihres indirekten Einflusses auf das Pflanzenwachstum sichtbar machen. So konnte ein Zusammenhang zwischen einer hohen Vegetationsleistung der Pflanzen und dem Vorhandensein von archäologischem Material im Oberboden nachgewiesen werden, der auch mit der Nähe zu den früheren Flussarmen korreliert. Es zeigt sich aber auch, dass die Vegetationsleistung mit anderen Faktoren, wie der Verfügbarkeit von Bewässerungswasser und der Salinität zusammenhängt. Bei der hier berechneten Vegetationsleistung handelt es sich um ein eigenes Indiz, das sich aus verschiedenen Parametern, die das Pflanzenwachstum beschreiben, zusammensetzt. Diese wären der mittlere NDVI und die Anzahl der Feldrotationen in der betrachteten Satellitenbildzeitreihe, sowie Wachstumsstatistiken, die für eine Fruchtfolge im Sommer 2014 berechnet wurden.

Vervollständigt werden die fernerkundlichen Methoden durch die Verarbeitung und Analyse von hochaufgelösten global verfügbaren Geländemodellen aus TanDEM-X Daten, die im Rahmen eines wissenschaftlichen Forschungsantrags seitens des Deutschen Zentrums für Luft- und Raumfahrt (DLR) bewilligt wurden. Diese eröffnen völlig neue Perspektiven auf das Nildelta und ermöglichen neue Interpretationen für diesen Raum in einer für paläoökologische Verhältnisse sehr hohen räumlichen Auflösung. Um bessere Genauigkeitsangaben für den Untersuchungsraum treffen zu können, wurde die vertikale Auflösung durch Vergleich mit ICESAT Daten näher bestimmt. Die Ergebnisse zeigen, dass die Residuen zwischen ICEAT and TanDEM-X



Daten bei 0.7 m ( $1\sigma$ ) liegen, was einer für Radardaten sehr hohen relativen vertikalen Auflösung entspricht und in der geringen Reliefierung des Nildeltas begründet ist. Diese Auflösung ist ausreichend um gerade für den griechisch-römischen Zeitabschnitt ein detailliertes Landschaftsbild mit einem fein aufgegliederten Flussnetz zu rekonstruieren. An den Flussläufen liegen fast ausschließlich die historischen Siedlungen, die mit den zuvor genannten fernerkundlichen oder archäologischen Methoden prospektiert wurden.

Während verschiedener Geländekampagnen wurden Deltasedimente, die Umgebung der Siedlungen und das Siedlungsmaterial selbst mit Hilfe von Bohrungen und durch Probennahme in anstehenden Profilwänden beprobt. Die Bohrungen konzentrieren sich zum einen auf die beiden antiken Siedlungen Buto und Kom el'Gir und deren Umgebung, als auch auf einzelne Transekte, die ausgehend von den Siedlungen in die entfernteren Deltabereiche verlaufen. Diese geologische Prospektion, ergänzt um chemische Analysen mit einem handgehaltenen Röntgenfluoreszenzmessgerät (pXRF), sind Kernstück des methodischen Inventars für die angestrebte diachrone Landschafts- und Umweltanalyse und erlauben eine detaillierte Untersuchung der in den Fernerkundungsdaten aufgedeckten Strukturen. Gerade den geochemischen Analysen kommt in dieser Arbeit eine hohe Bedeutung zu. Dies lässt sich generell in den angewandten Naturwissenschaften, insbesondere Geologie, Geomorphologie und Bodenkunde bestätigen, in denen pXRF Analysen zunehmend für Umweltanalysen und Landschaftsrekonstruktionen eingesetzt werden. Die recht einfache Anwendbarkeit der pXRF, die daraus resultierende hohe Anzahl an Messungen sowie die erwähnte Vielfalt der erfassten chemischen Parameter führen zu immer größeren Datenmengen, die auch schon in kleineren Projekten die Handhabung der Daten in Datenbanken (DB) mittels Datenbankmanagementsystemen (DBMS) erforderlich machen. In dieser Arbeit kommt dabei insbesondere PostgreSQL mit der Erweiterung POSTGIS zu Anwendung, welche die Speicherung von Geometrien erlaubt und GIS Analysen auf Datenbankebene ermöglicht. In der Datenanalyse kommt die statistische Programmiersprache R zum Einsatz und es konnten räumliche Analysen und multivariate oder andere statistische Verfahren miteinander kombiniert werden. Zudem erfordert die Analyse der Elementkompositionen speziell darauf ausgerichtete statistische Methoden und Verfahren, auf die in der Programmiersprache R mit den Programmbibliotheken „Compositions“ und „robCompositions“ zurückgegriffen wurde.

In der Anwendung zeigt sich, dass auf Basis von geochemischen Daten und der erhobenen Felddaten künstliche und natürliche Wasserrinnen in den Sedimenten unterschieden werden können. Beispielsweise zeigen künstliche und natürliche Wasserläufe erhebliche Unterschiede in den Al/Ti und Cu/Zn Ratios. Im Vergleich zu regulierten künstlichen Kanälen zeigen Se-

dimente natürlicher Wasserläufe stark variierende Ti/Al Ratios. An unterschiedlichen Stellen im Untersuchungsgebiet wurden mehrere Meter tief eingeschnittene Rinnen identifiziert, bei denen es sich teils um natürliche Flussbetten oder auch künstliche Kanäle handelt, die vermutlich verbunden waren und einen Versuch der damaligen Menschen darstellen, die Siedlungen mit den benachbarten Flussläufen zu verbinden. Im Detail konnte für die als künstliche Kanäle identifizierten Rinnen gezeigt werden, dass zahlreiche Eigenschaften in den Sedimenten und geochemischen Parametern auf das Vorherrschen von Stillwasserbedingungen hinweisen.

Weitergehend wurden Methoden geschaffen, den anthropogenen Einfluss an Hand der geochemischen Daten zu detektieren und zu datieren. Dies ist ein Kernstück dieser Arbeit und stellt eine Möglichkeit dar, die Datierungsmethoden zu erweitern, welche derzeit in Ägypten aufgrund des Ausfuhrverbots von Sedimentproben limitiert sind. Dabei wurde auf neue Techniken der Datenspeicherung, -analyse, -selektion zurückgegriffen und ein ganzheitlicher Untersuchungsansatz gewählt, der die Anwendbarkeit und Qualität von pXRF-Messungen an dem Probenmaterial bewerten soll. Die Qualität der Messungen konnte insbesondere auf Basis von wiederholten Standard-Messungen und der Berechnung des Variationskoeffizienten für die einzelnen Elemente nachvollzogen werden. Zusätzlich wurden einzelne Befunde mehrfach beprobt, um die Streuung der geochemischen Werte innerhalb eines Befundes zu bewerten. Dies erlaubte eine Beurteilung postsedimentärer Effekte auf die geochemische Zusammensetzung des Probenmaterials und es konnte gezeigt werden, dass die Elemente Ca, Cl, Fe, Mn, P, S und Sr hohe Fluktuationen innerhalb desselben Befundes aufweisen. Dies ist insbesondere auf lokale Lösungs- und Kristallisationseffekte zurückzuführen, welche die Elementzusammensetzung der Befunde nachträglich verändern. Auf Basis dieser und anderer Untersuchungen konnte eine Auswahl von Elementen getroffen werden, die Eingang in die weiterführende Datenanalyse und Datierung mit neuronalen Netzen finden. Zuvor wurden die Daten jedoch weiter aufbereitet und bereinigt. Fehlende Werte oder Nullen in den Datensätzen wirken sich fatal für die Datenvisualisierung und die statistische Datenanalyse auf, da sie eine Anwendung vieler statistischer Verfahren verhindern. Entsprechend präsentiert diese Arbeit einen Arbeitsablauf, der Nullen oder fehlende Werte als Werte unterhalb des Detektionslimits behandelt und mittels spezieller Verfahren, die für die Anwendung auf Kompositionsdaten wie XRF Daten entwickelt wurden, durch künstlich simulierte Daten ersetzt und somit entfernt. Die Analysen zielen insbesondere darauf ab, die Unterschiede in den geochemischen Signalen zwischen Siedlungsmaterial und den alluvialen Deltasedimenten aufzudecken. Weiterhin ist zu klären, ob sich diese Unterschiede bis hin zu Material aus verschiedenen Kulturphasen verfolgen lassen und sich somit für die angestrebte Entwicklung einer Datierungsmethode eignen. Um dies genauer beurteilen zu können wurden die

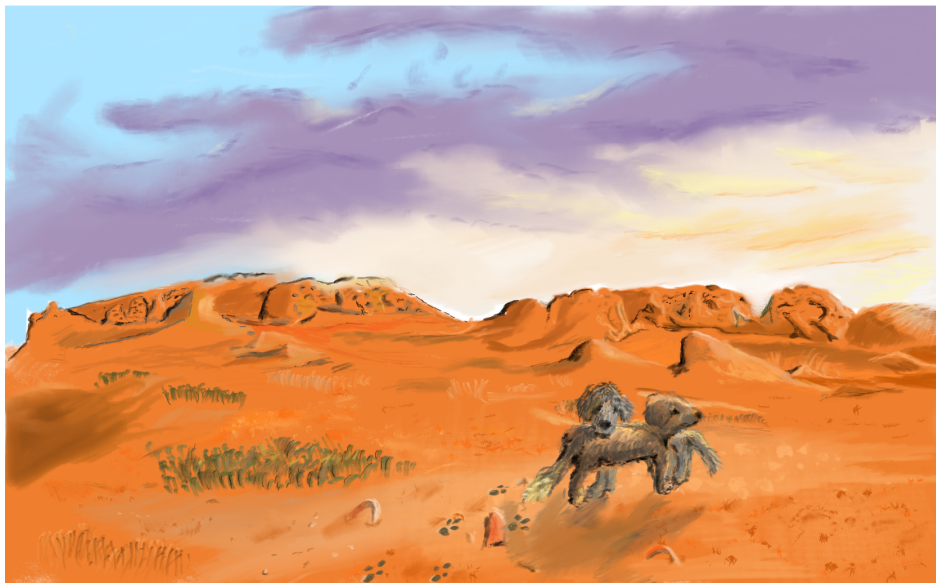
statistischen Verfahren mit räumlichen Analysen kombiniert.

Der gewählte Datierungsansatz basiert auf der Anwendung von Maschinenlernen mit künstlichen neuronalen Netzwerken. Hierbei wurde auf das Paket `neuralnet` in R zurückgegriffen und ein Netzwerk mit „resilient backpropagation“ und „weight backtracking“ gewählt. Das Training des neuronalen Netzwerkes erfolgte mit Probenmaterial der verschiedenen archäologischen Schichten bekannten Kontextes. Hierfür wurden archäologische Profilwände und Flächen aus den archäologischen Grabungen von Ulrich Hartung und Pascale Ballet beprobt.

Die Beprobung der archäologischen Profilwände erfolgte gezielt für verschiedene archäologische Befunde der in Buto erschlossenen Kulturphasen. Die Profile selbst liegen über verschiedene Niveaus verteilt und beinhalten Schichten aus verschiedenen Kulturphasen, die im Rahmen dieser Arbeit auf drei wesentliche Phasen reduziert wurden. Hierbei handelt es sich um Material aus Prädynastischer Zeit (>3150 vor Christus, BC), Frühdynastisch bis Altes Reich (3150 - 2181 BC) und Material aus der Spätzeit bis Griechisch-Römischen Zeit (332BCE - 641 CE). Dabei wurden Ziegel von Mauern, Laufhorizonte, Öfen, Gruben und Ascheschichten einzeln beprobt. Somit konnte überprüft werden, welche geochemischen Signale eine bestimmte Kulturphase kennzeichnen und in welchen Befunden sich dies am besten widerspiegelt. Gerade diese Analysen ermöglichen die Auswahl der Daten, die sich bestens für das Training der neuronalen Netze eignen. An dieser Stelle konnte gezeigt werden, dass Laufhorizonte und Mauern deutliche Unterschiede in den geochemischen Signalen der verschiedenen Kulturphasen aufweisen und nur Daten dieser Befunde fanden daher Eingang in das Training des neuronalen Netzwerkes. In der Trainingsphase lernt das Netz von den ausgewählten Trainingsdaten. Lernen meint hier die Änderung der Gewichtung bei der Weitergabe eines Signals innerhalb des neuronalen Netzes. Deswegen kommen der Qualität und Auswahl der Trainingsdaten besondere Bedeutung zu. Zusätzlich wurde ein weiteres neuronales Netz entwickelt, für welches das Training verbessert wurde. Für das Training des zweiten Netzes wurden für die einzelnen Proben neue Werte simuliert. Somit konnte nachweislich die Robustheit des neuronalen Netzes durch künstliche Simulation von Trainingsdaten verbessert werden. In der Simulation wurden die berechneten Variationskoeffizienten der einzelnen Elemente genutzt und es konnten die elementspezifischen Fehlerwerte innerhalb des neuronalen Netzes berücksichtigt werden. Die Ergebnisse beider neuronalen Netze, mit und ohne Simulation von Trainingsdaten, weichen dabei voneinander ab, und es zeigt sich, dass gerade die Simulation und Vervielfältigung der Trainingsdaten die Präzision der Ergebnisse wesentlich erhöht hat und das Netz generell eine geringere Fehlerquote aufweist. Dies konnte durch den Vergleich mit  $^{14}\text{C}$  und Keramikdatierungen eingeschätzt werden. Die Anwendung der trainierten neuronalen Netze erfolgte dann auf Material der

umgebenden Bohrungen, welche zum Beispiel Kulturschichten, Flussrinnen oder Hochflutsedimente beinhalten. Dabei ließen sich die drei betrachteten Kulturphasen gut identifizieren. Trotzdem zeigt sich der Einfluss postsedimentärer Prozesse. In der Regel ist besonders die Oberfläche von Salzausblühungen gekennzeichnet und verwendete Trainingsdaten für die römische Kulturphase lagen ausschließlich oberflächennah, was entsprechend Einfluss auf die Ergebnisse zeigt. Trotzdem konnten innerhalb der verschiedenen Bohrtransekte tiefliegende Kulturschichten identifiziert werden, die Rinnen zuzuordnen sind. Westlich von Buto konnten römische Sedimente und Sedimente, die in dem Zeitabschnitt Frühdynastisch bis Altes Reich fallen, mit 4 m unterhalb des Meeresspiegels nachgewiesen werden. Östlich des Kom el’Gir lässt sich ebenfalls eine auf 9 m unterhalb des Meeresspiegels liegende Rinne identifizieren, die mit ausschließlich römischen Material verfüllt ist und gut mit aktuellen geophysikalischen Messungen zusammenpasst. Generell identifiziert das neuronale Netz für den Kom el’Gir nur römische Proben, was ebenfalls gut mit den Grabungsergebnissen übereinstimmt, da der Kom el’Gir erst in der römischen Zeit besiedelt wurde. Für die Datierung mit neuronalen Netzen konnten in dieser Arbeit erste Ansätze geschaffen werden, die innovative Techniken der Datenaufbereitung und -verbesserung einschließen. Diese Ansätze gilt es weiterzuentwickeln, denn auf diese Weise können die in den Bohrungen zu Tage gebrachten Zeugen der früheren Landschaftsgeschichte mit der Siedlungs- und Kulturgeschichte der archäologischen Grabung zusammengebracht werden.

For my father, family and Marlen, Janne and Matti



**What was once a city of clay, are now the ruins of Tell el-Fara'in.**

## Acknowledgements

This dissertation was integrated in the work of the German Archaeological Institute (DAI) on the former city of Buto in the north western Nile delta. It was the predecessor of an ongoing research project funded by the Deutsche Forschungsgemeinschaft.

My working life outside the university has already started and parts of this thesis were completed part-time while employed. Looking back on my research years, I loved being a researcher. I enjoyed being responsible for my own project, solving difficulties and new problems and designing new creative methods to get more out of my data. But I must also admit that many times I strut and fret long hours upon the researcher's desk and felt the importance of endurance and then - for the benefit of all geographers doing field work - I was ever motivated by the countless hours of fieldwork in the beautiful biblical landscape of the north western Nile delta with the contrasting influence of modern society. I will always keep this time of solitary working, wonderful and exhausting field work, presentation at international science meetings and scientific writing in memory as a positive and fruitful experience, and I feel proud to say that I was an active researcher once, and I will keep on solving problems in a scientific manner.

To complete such a work, help from other people is needed, and I thank everyone who participated in this work and who helped me reaching this goal. First of all I thank my supervisor Prof. Dr. Jürgen Wunderlich, who initiated the project in Egypt and motivated me to continue when even at times the odds to progress with the project were at stake during the Yasmine revolution and the continuing problems with the Egyptian authorities. He supported the free space that was necessary to find a balance between my thesis, family and part-time study and allowed a friendship to grow that let me encounter science in a friendly, appreciative and open-minded atmosphere.

Another friend I met on this long voyage is my archaeological colleague Robert Schiestl, whom I accompanied starting with the first missions in Buto and who participated in most of my field campaigns while he conducted a survey of the surroundings and the neighboring tell Kom el'Gir. He had a major part in the success of this project as he constantly addressed scientific questions that let us advance. He took a great part in organization and administration of the campaigns, and besides the motivating time we

always shared in Egypt, showed a contagious fascination for the science we were carrying out there.

I also thank Marina Altmeyer as my number one student assistant and contributor. She joined me in several missions, mirrored fascination for the topic and contributed with her Bachelor thesis to the work in Egypt.

Special thanks are also dedicated to Dr. Daniel Steiniger, who took part in several campaigns and with endurance and resistance made the pXRF measurements possible. Many have tried to import such a device to Egypt and, to my knowledge, he is the only one who not only once but several times in a row succeeded, thanks to his iron serenity, expertise and motivation that very much aided the success of our work.

Furthermore I thank the excavation team in Buto with Dr. Ulrich Hartung, Rita Hartmann, Wiebke Kreibig for all the assistance they gave in the administration of our missions, logistic organization and sampling the archaeological excavation walls. And I want to express my gratefulness for the dating of archaeological artifacts to Peter French who together with Rita Hartmann was able to date the tiny fragments found in our corings. My dearest thanks are dedicated to Prof. Dr. Stephan Seidlmayer, head of the DAI Cairo, who from the beginning was convinced of the importance of the project and supported the supply of necessary equipment as well as resources and personal efforts to make it a story of success.

I am very grateful for the support in publication and scientific organisation from Martin Seeliger, who is a very team-oriented cooperative character and I am thankful that he stepped into the project. Thanks are also addressed to Prof. Dr. Pascale Ballet for providing us with documentation data and the opportunity to sample her Roman excavation layers.

With pleasure, I look back on all the members of the working group of Prof. Dr. Wunderlich and the friendly, collaborative atmosphere we shared in addressing scientific questions in a sometimes heated but positive manner. Thanks to Dirk Nowacki, Carolin Langan and Nabila Ibrahim. To Doris Bergmann-Doerr and Dagmar Schneider, I direct my dearest thanks for the continuous and patient support of laboratory analyses in Frankfurt. Additionally, I am thankful for the assistance of Dr. Markus Helfert in providing means for the application of pXRF measurements in Frankfurt. And I thank the Egyptian workers for sharing their strong efforts in the fields to recover the precious clay material. Out of these, special thanks are directed to Mohammed and Mounir, who took part in most of the coring work. Lastly, I thank Janice M. Schiestl for proofreading of the articles and the thesis.

My warmest thanks go to my parents Monika and Theodor Ginau, who shaped the most important points in my life that enable such achievements; I believe they are very proud of me now. Lastly I thank my own family,

especially Marlen Ginau, for their unconditional support and confidence, and the time they invested in me. Much of the time I invested here, I should have spent raising my two sons Janne and Matti together with my wife. I think they will never read my research, but I thoroughly believe that when looking back in the future, they will be glad that I brought this research to an end and that I progressed in my life.



# Contents

<b>List of Figures</b>	<b>xxi</b>
<b>List of Tables</b>	<b>xxiii</b>
<b>1 Introduction</b>	<b>1</b>
1.1 Geoarchaeological research in Buto . . . . .	2
1.2 Aims, research design and outline of the study . . . . .	3
1.2.1 Aim 1: Identification of the large-scale water net and localization of settlement sites . . . . .	5
1.2.2 Aim 2: Inspection of the fine-scaled sedimentological subsurface .	6
1.2.3 Aim 3: Characterization and dating of settlement layers within coring transects . . . . .	7
<b>2 Methodology</b>	<b>9</b>
2.1 Fieldwork . . . . .	9
2.2 Remote Sensing . . . . .	10
2.3 Geochemical analysis . . . . .	10
2.4 Data analytics . . . . .	11
<b>3 Identification of historic landscape features and settlement mounds in the Western Nile delta by means of remote sensing time series analysis and the evaluation of vegetation characteristics</b>	<b>13</b>
3.1 Abstract . . . . .	14
3.2 Introduction . . . . .	14
3.3 Study area . . . . .	18
3.4 Material and methods . . . . .	18
3.4.1 Identification of high tells . . . . .	20
3.4.2 Identification of lost tells . . . . .	22
3.5 Results . . . . .	29
3.5.1 Classification of high tells . . . . .	29
3.5.2 Classification of lost tells . . . . .	29
3.6 Discussion . . . . .	34

## CONTENTS

---

3.6.1	Classification of high tells . . . . .	34
3.6.2	Classification of lost tells . . . . .	34
3.6.3	Geometric difficulties in the analyzes . . . . .	35
3.6.4	NDVI patterns in the Nile delta . . . . .	36
3.6.5	Influence of palaeorivers on the vegetation performance . . . . .	36
3.6.6	Soil salinization and other applications . . . . .	38
3.7	Conclusion . . . . .	40
3.8	Acknowledgments . . . . .	42
<b>4</b>	<b>Integrative geoarchaeological research on settlement patterns in the dynamic landscape of the northwestern Nile delta</b>	<b>43</b>
4.1	Abstract . . . . .	44
4.2	Introduction . . . . .	44
4.3	Historical and Geological setting of the Nile delta . . . . .	45
4.3.1	Research history on the fluvial landscape of the Nile delta . . . . .	45
4.3.2	Research history of ancient settlements in the study region . . . . .	49
4.3.3	Physical setting and environmental history . . . . .	49
4.4	Methods . . . . .	52
4.4.1	Archaeological methods . . . . .	52
4.4.2	TanDEM-X digital elevation model . . . . .	53
4.4.3	Corings and geochemical analyzes . . . . .	54
4.5	Results and Discussion . . . . .	55
4.5.1	Archaeological results . . . . .	56
4.5.2	Larger channels in the area under study, a large scale perspective . . . . .	57
4.5.3	Fine scaled sedimentological inspection of the connection between settlements and their surrounding . . . . .	62
4.6	Conclusion . . . . .	71
4.7	Acknowledgments . . . . .	72
<b>5</b>	<b>What settlements leave behind - pXRF compositional data analysis of archaeological layers from Tell el-Fara'in (Buto, Egypt) using machine learning</b>	<b>75</b>
5.1	Abstract . . . . .	76
5.2	Introduction . . . . .	76
5.3	An overview of pXRF analyzes in geoarchaeological contexts . . . . .	79
5.4	Methods . . . . .	80
5.4.1	Sampling of archaeological layers on-site . . . . .	80
5.4.2	Sampling of sediment corings . . . . .	80
5.4.3	Sample preparation . . . . .	82
5.4.4	pXRF measurements . . . . .	82
5.4.5	Data management and analysis . . . . .	84
5.5	Results and discussion . . . . .	86
5.5.1	XRF methodology . . . . .	88

5.5.2 Geostatistical analysis . . . . .	90
5.6 Conclusions . . . . .	100
5.7 Acknowledgments . . . . .	104
<b>6 Synthesis and conclusions</b>	<b>105</b>
6.0.1 Ad aim 1: Reconstruction of the large scale water net with location of settlement sites . . . . .	105
6.0.2 Ad aim 2: Inspection of the fine-scaled sedimentological underground . . . . .	107
6.0.3 Ad aim 3: Characterization and dating of settlement layers within coring transects . . . . .	108
6.0.4 Summary and outlook . . . . .	109
<b>References</b>	<b>111</b>
<b>Appendices</b>	<b>121</b>
<b>A additional figures</b>	<b>123</b>
<b>B corings</b>	<b>131</b>

## CONTENTS

---

# List of Figures

1.1	Research design . . . . .	4
3.1	Location of the study area . . . . .	15
3.2	Classification of different tell types in the Nile delta . . . . .	16
3.3	Distance mapping of plant nutritious elements . . . . .	17
3.4	Presumed relation of tell material and vegetation performance . . . . .	19
3.5	Flowchart with applied analyzes . . . . .	20
3.6	Feature space of NIR (x) and STDEV(NIR) . . . . .	22
3.7	Acquisition dates of satellite scenes used for the identification of lost tells . . . . .	23
3.8	Workflow of the crop rotation analysis . . . . .	26
3.9	Workflow of the field growth analysis . . . . .	28
3.10	Classification of high tells . . . . .	30
3.11	Spatial distribution of the overall performance of the vegetation . . . . .	31
3.12	Spatial distribution of vegetation describing parameters . . . . .	33
3.13	Estimation of the number of harvests . . . . .	37
3.14	Vegetation performance in contrast to former palaeorivers . . . . .	39
4.1	Research design . . . . .	46
4.2	Location of the study area . . . . .	51
4.3	Quality of TanDEM-X . . . . .	54
4.4	TanDEM-X DEM . . . . .	58
4.5	Thresholded TanDEM-X DEM . . . . .	59
4.6	Transformation of levees . . . . .	61
4.7	Location of sedimentological transects . . . . .	63
4.8	Cross sections of sedimentological transects . . . . .	65
4.9	Categorization of channels . . . . .	67
4.10	Data distribution between channels with different energy domains . . . . .	69
4.11	Spiderplot showing pXRF profiles . . . . .	70
5.1	Location of archaeological profiles . . . . .	78
5.2	Archaeological records targeted by pXRF measurements . . . . .	81
5.3	Sampling of the southwestern wall in profile section E18 . . . . .	81
5.4	Normalization factor in relation to the different grain-size classes . . . . .	84

## LIST OF FIGURES

---

5.5	Location of sedimentological corings analyzed with pXRF . . . . .	87
5.6	Selection of elements . . . . .	90
5.7	Post-sedimentary affected elements . . . . .	91
5.8	Chemical differences along large-scale transects . . . . .	93
5.9	Spiderplot showing pXRF profiles . . . . .	94
5.10	Chemical differentiation between archaeologic records and main epochs for selected elements . . . . .	96
5.11	Neural network results . . . . .	98
5.12	Neural network results . . . . .	99
5.13	Neural network results . . . . .	101
5.14	Neural network results . . . . .	102
6.1	Research papers . . . . .	106
A.1	Profile walls PB15 and PB19 . . . . .	124
A.2	Profile walls E9, E14 and E18 . . . . .	125
A.3	On site sample preparation . . . . .	126
A.6	Structural design of the neural network . . . . .	127
A.7	Post-sedimentary affected elements . . . . .	128
A.8	Chemical differentiation between archaeologic records and main epochs for selected elements. . . . .	129
A.9	Chemical differentiation between archaeologic records and main epochs for selected elements . . . . .	130
B.1	Location of sediment corings . . . . .	132
B.2	Coring descriptions G1-G5 . . . . .	133
B.3	Coring descriptions G6-G10 . . . . .	134
B.4	Coring descriptions G11-G15 . . . . .	135
B.5	Coring descriptions G16-G20 . . . . .	136
B.6	Coring descriptions G21-G25 . . . . .	137
B.7	Coring descriptions G26-G30 . . . . .	138
B.8	Coring descriptions G31-G35 . . . . .	139
B.9	Coring descriptions G36-G40 . . . . .	140
B.10	Coring descriptions G41 . . . . .	141

# List of Tables

3.1	Landsat 8 scenes used for classification of high tells . . . . .	21
3.2	Training sites used for the supervised classification of high tells . . . . .	22
3.3	List of land cover classes together with the area in pixels and the number of fields or sites that were sampled. . . . .	25
3.4	Quality assessment for the classification of high tells . . . . .	32
4.1	Coefficients of variation for elements used within this study. . . . .	56
5.1	Linear regression parameters for the relationship between x:mean and y:standard deviation . . . . .	83
5.2	Limits of detection (LOD) for selected elements . . . . .	88
5.3	Coefficient of variation (CV) for selected elements . . . . .	89

## LIST OF TABLES

---



# 1

## Introduction

For decades, the Nile delta and specifically the area around Buto (Tell el-Fara'in) in the northwestern Nile delta has been subject to archaeological excavations and prospections. The research history of geoarchaeological work in the delta is best described in Wunderlich (1989, 1993); Wunderlich & Ginau (2016) and shows that there exist many studies with a focus on the relation between landscape and human life in the delta. Such approaches reach back to the pioneering work of Butzer (1975), who shed light on the relation between landscape and the former settlements in the Nile delta. He presented a concise picture of the geologic design of the delta and described its Holocene development with special emphasis on the palaeoecologic and -hydrologic characteristics. He related these physical developments to cultural findings from archaeological excavations and written sources and presented new explanations for colonization and land use history of the delta. In the context of archaeological excavation in Tell el-Dab'a/Auaris Bietak (1975) reconstructed changes of the former water net on the basis of elevation contour lines, corings and literary sources and related his findings to changes in settlement patterns such as the abandonment of the city of Pi-Ramesse and its shift to Tanis. These studies exemplify the need of geoarchaeological research as it allows integration of geoscientific methods and concepts in archaeology and relates landscape changes to findings of archaeological excavations, literary or other sources. Since then, more and more studies mushroomed with the aim of unraveling this interrelation between landscape and archaeology. Key questions of geoarchaeological work in the delta are the reconstruction of the former water net (see 4.3.1) and the reconstruction of the coastline (Arbouille & Stanley, 1991; Flaux *et al.*, 2012, 2013; Hamroush, 1987; Marriner *et al.*, 2012a; Stanley *et al.*, 1992; Trampier *et al.*, 2013; Wunderlich, 1989). Often the outcome of such studies bears a scientific significance for recent environmental studies. Anthony *et al.* (2014) - for example - gathered archaeological records and  $^{14}\text{C}$  datings from geoarchaeological and archaeological projects in the Nile delta to develop a chronostratigraphy on the spatial and temporal changes of isostatic movements in the delta and shed more light on the subsidence the delta experiences nowadays together with a rising sea level. This shows how interdisciplinary geoarchaeological work con-

## 1. INTRODUCTION

---

tribute to knowledge of actual problems of climate change, natural hazards and sea level rise.

### 1.1 Geoarchaeological research in Buto

Especially for the northwestern Nile delta, no concise picture of the archaeological and palaeoecological evolution can be drawn, and archaeological records show significant population dynamics and long lasting abandonment of sites that still need explanation. It is still unknown if ecological reasons were responsible for the variable occupation of the northwestern delta and consequently there is still need for further palaeoenvironmental research. First studies and excavations reach far back in the past, and for more than three decades the ancient settlement site Tell el-Fara'in (Buto) and its surroundings have been the target of archaeological excavations and prospections conducted under the umbrella of the German Archaeological Institute (DAI) (Faltings *et al.*, 2000; Hartung, 2014; Hartung *et al.*, 2009; von der Way, 1997) and the Paris Nanterre University (Ballet & Marouard, 2015; Ballet *et al.*, 2011).

From the beginning, these excavation works in Buto were accompanied by geoarchaeological research. This allowed a first inspection of the connections between the landscape changes and the archaeological records (Wunderlich, 1988, 1989, 1993). Large-scale placement of sediment cores as a typical geoscientific method allowed the study of the occurrence and distribution of cultural debris and settlement layers of the relevant time periods dating back from Predynastic to Early Dynastic times hidden below several meters thick alluvial Nile deposits or layers with younger cultural material. Other research goals were the reconstruction of the former palaeorelief in the vicinity of Buto, the reconstruction of the former water network, and the analysis of the development of the coastline in the context of sea level changes, subsidence and sediment supply.

In the northwestern delta, Wunderlich (1988, 1989, 1993) related landscape changes to the archaeological findings, and developed a concise picture that describes landscape and cultural changes in the late Pleistocene and early to middle Holocene. He showed the change from brackish-lagoonal conditions with deposition of peat layers on top of the former Pleistocene surface with a maximum southern extent of the shoreline at about 5000 cal before Christ (BC) to the development of the modern Nile floodplain with constantly aggrading clastic sediments reaching a thickness of about 7 to 10 m (see Fig. 3.4) today.

In recent decades, field surveys focused on the history of ancient settlements in the area (see 4.3.2) (Ballet & von der Way, 1993; Schiestl, 2012a,b, 2015; Schiestl & Rosenow, 2016; Spencer, 1992; Wilson, 2012a,b, 2015; Wilson & Grigoropoulos, 2009). These investigations showed that most of the settlement sites were founded in the Ptolemaic, Roman and, in particular, late Roman periods (332 BC - anno Domini (AD) 641). Buto, on the other hand, shows a remarkable settlement continuity in the region. It was founded in the 4<sup>th</sup> millennium BC with the latest traces of occupation from the Early Islamic period. Nevertheless, this continuity shows a major gap between the late Old Kingdom (late 3<sup>rd</sup> millennium BC) and the Third Intermediate Period (early 1<sup>st</sup>

## 1.2 Aims, research design and outline of the study

---

millennium BC) of almost 1500 years. The reasons for the abandonment of Buto and other sites from the Middle Kingdom till the New Kingdom are unknown, and possibly reflect a significant decline due to environmental changes in the area. Butzer (1998, 2002) describes that Nile floods reached a famous climax between 2000 and 1500 BC. As a consequence, high floods may have reached the settlements or the shape of the water network may have changed drastically as branches may have shifted their courses to distant depth lines after significant floodings, which is typical for levee-river systems (Aslan & Autin, 1999). Such changes could have easily decided the fate of societies at that time as people depended on the river system.

The continuation of settlement activity in the Late Period and the recolonization of the northwestern delta with the rise of new settlements in Ptolemaic and Roman times prove the existence of favorable conditions for colonization after the Late Period. Yet the reasons for these significant cultural changes with a registered total decline of settlement activity in the Middle till the New kingdom and the rise of settlements starting in the Late Period are unknown and were the starting point for interdisciplinary geoarchaeological work that was initiated in 2012. The work since 2012 focused on the area around Buto and the neighboring smaller settlement mound Kom el'Gir on which the work of Schiestl (2015); Schiestl & Rosenow (2016) concentrates (see Fig. 4.2).

## 1.2 Aims, research design and outline of the study

This study supports the archaeological excavations and survey activities of the German Archaeological Institute (DAI) in Buto and Kom el'Gir and seeks to relate changes in settlement activities of certain periods to environmental changes that occurred in the research area. Results and methods of this study are the precursor of a larger ongoing DFG research project (WU 206/1 0-1, Jürgen Wunderlich) and set its scientific starting point. The primary aim of the DFG project is to develop an integrative, diachronical, geoarchaeological reconstruction of the settlement and landscape history in the northwestern Nile delta reaching back from Predynastic to Roman times that can explain the major push backs or growth phases in the settlement history mentioned previously.

This study focuses on individual time slices, specifically the end of the Late Period and the Greco-Roman era, and reveals that a massive increase of settlements over the northwestern delta in Classical Antiquity was spurred by multiple river branches that served important human needs in transportation, food and water supply, irrigation and agriculture. Highlight and one major aim of this work is the development of a toolbox of new methods comprising

- i time series analysis on remote sensing data to identify ancient settlements and detect former river branches,
- ii analysis and accuracy estimation of TanDEM-X elevation models to reconstruct former river patterns and

# 1. INTRODUCTION

iii multivariate statistics on geochemical data in combination with a new machine learning approach to date sediments.

Applying these new and highly sophisticated methods should allow for reaching the overall aims of the integrated geoarchaeological research which are summarized in Fig. 1.1 and will be described in detail within the following sections.

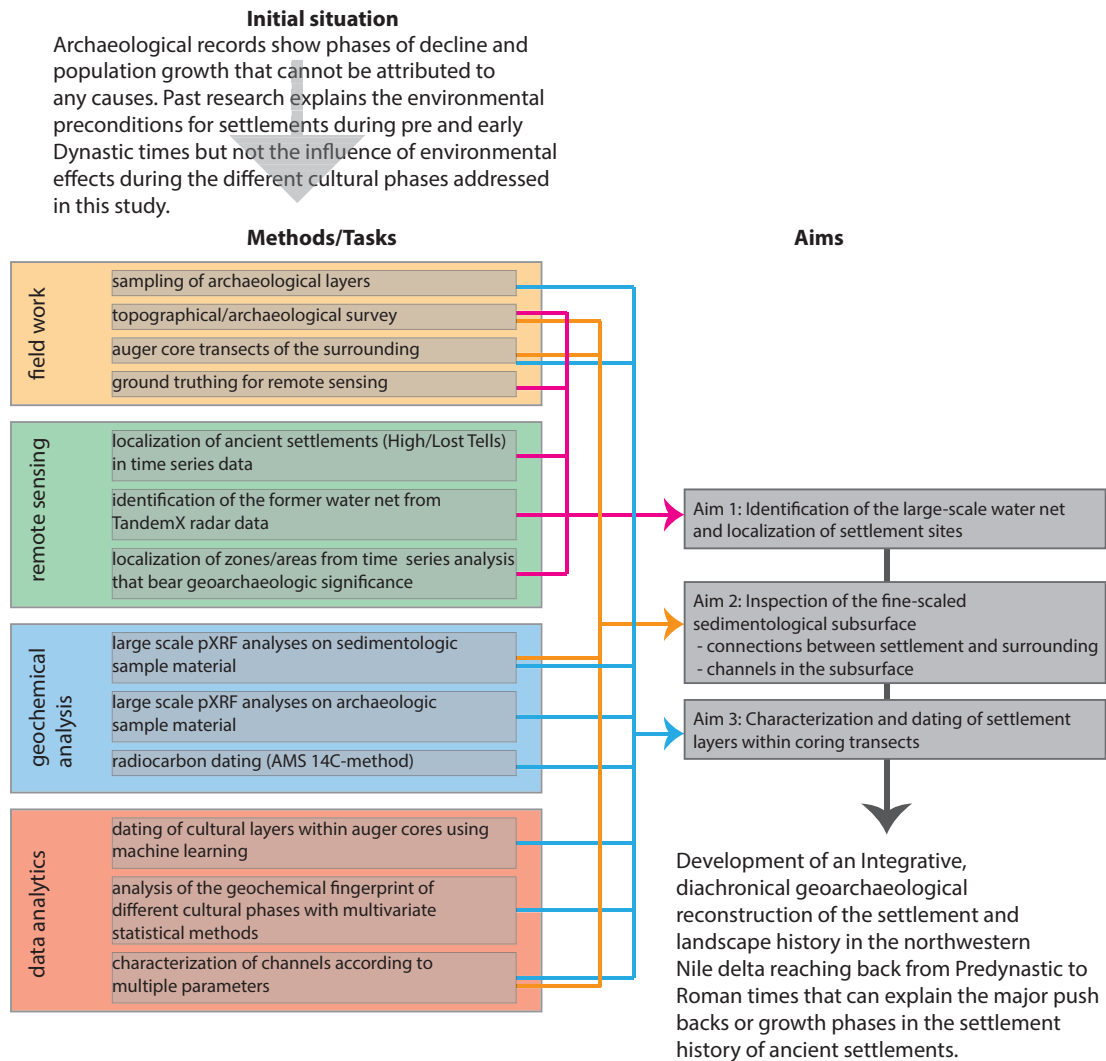


**Fig. 1.1: Research design** - Overall research design including the central question, methods and aims of this study.

### 1.2.1 Aim 1: Identification of the large-scale water net and localization of settlement sites

Human life in the delta centered on its waterscape, a system of connected rivers or canals that, like today, satisfies essential needs for transport, irrigation and food supply. For this reason, colonization of the area probably happened along the former water courses, and settlements lie along major river branches, or were artificially connected with neighboring branches.

Consequently, the first essential aim is the localization of former settlements and the identification of river levees in topographical data as both the rivers and location of settlements should fall together. To detect the network of settlements an archaeological survey was initiated (Schiestl, 2012a,b, 2015) and is described in detail in chapter 4.4.1. It is set in the region bordered approximately by Kom Sidi Salem in the north, the modern towns of Qellin in the South, Kafr esh-Sheikh in the East and by Buto (Tell el-Fara'in) in the West (Schiestl, 2012b, Fig. 1). No prior systematic survey of the region exists and the archaeological investigation had three aims: Firstly, location and identification of ancient sites, secondly, documentation and prospection of these sites, and thirdly, dating of archaeological material. Major method of this archaeological subproject is the localization of ancient sites by the manual analysis of remote sensing material, see chapter 3. Besides mapping existing high tells that are not completely occupied and still show tell material on the surface, Schiestl (2012b) focused on a group of sites which is generally classified as lost tells. These are small leveled tells in cultivated land that were harvested for additional space or as fertilizer and completely removed from the delta surface and can only be localized via distinctive shapes of field boundaries that are associated with them in topographic maps.

The manual detection of tells in topographic data or other sources such as Google Earth is time consuming and ambiguous. This study seeks a new remote sensing approach to automatically detect the different categories of tells in multitemporal satellite images and a large set of time series data. The network of existing high tells is completed with supervised classification techniques on the basis of multitemporal Landsat 8 images that involves synthetic image layers. To register lost tells, the overall vegetation performance is analyzed in a large stack of time series image data. Here a completely new approach is presented to automate the identification of lost tells and indirectly identify them as hot spots in images describing the vegetation growth. This relies on the fact that tell material is enriched in plant nutritious elements as was verified by own pXRF geochemical measurements. Vegetation growth itself is described as a new measure invented within this study that represents the product of different measures describing the plant growth, namely the mean Normalized Difference Vegetation Index *NDVI*, growth statistics and crop rotations derived from a large set of multitemporal *NDVI* images. A more detailed description of the different tell classes is given in Fig. 3.2.

The second main aim is the reconstruction of the ancient waterscape of the larger area to allow the juxtaposition with the localized settlements. This juxtaposition is one of the key questions ascertained in chapter 4 and will be addressed in this study based

## 1. INTRODUCTION

---

on the analysis of a new high resolution DEM based on TanDEM-X radar data (see chapter 4). Application of TanDEM-X radar data is a central approach in this study that also involves a precision estimation based on the comparison with ICESAT laser data. Compared to prior approaches based on contour lines derived from topographic maps or analysis of SRTM data, this new high resolution global elevation model allows a completely new perspective on the deltas topography.

### 1.2.2 Aim 2: Inspection of the fine-scaled sedimentological subsurface

Central aspect of the fieldwork is the verification of the results of the remote sensing analysis via corings and application of geochemical measurements on sample material retrieved from the corings. This combination of remote sensing, fieldwork and geochemistry allows to investigate landscape conditions at the end of the Late Period and the Greco-Roman era in high detail and reveals new astonishing results for the northwestern Nile delta in this time period. Especially the results of the large scale reconstruction of the ancient waterscape can be verified and further analyzed.

With the application of sediment corings the subsurface conditions were inspected at various locations and depths. Especially the extraction of sediments via corings keeps sedimentary structures and boundaries between different layers intact and allows identification of different stratigraphic units such as channels or levee deposits. This way it could be verified if channels present in the TanDEM-X data can be identified as such within the sediments. The area around the settlements is often very disturbed and channels are hard to recognize in the TanDEM-X data and only corings allow identification of channels in this area. Additionally, more information on these channels such as depth, shape or age via the collection of datable material, carbon or ceramic sherds, was gathered. Besides channel deposits, elevated levees visible in the DEM were sampled. The geochemical work concentrated on finding new measures to differentiate between different categories of channels within the transects. Specifically, field results and measures based on geochemical pXRF data of sample material of these channels allow a discrimination between high and low energy watercourses, representing natural rivers and artificial canals respectively. This is very important to answer the question as to how Buto and Kom el'Gir were connected with the supra-regional water network and how their connection was held intact when rivers changed their courses in this dynamic landscape. Moreover, the sedimentological transects in the study area help to understand the complex fluvial processes and the changing nature of the Holocene delta landscape and waterscape.

The general stratigraphy of the in the study region was developed earlier by Wunderlich (1989). Another major aim of the field work was to target these different stratigraphic units and analyze them with new geochemical methods. The upper clayey alluvial Nile deposits that especially occur in greater distance to settlements or waterways lack any visible structures or significant color changes. On the other hand, they have the potential to store information on past landscape changes in form of geochemical signatures. Clay has a very low porosity resulting in slow drainage and strong

cohesion forces attract and store elements. This leaves behind a geochemical archive and allows to explore and find new geochemical ratios or parameters that give more information on past landscape changes. That is why a central task of this working branch is to determine the geochemical composition of the different stratigraphic units and to collect the results in a data-store for further analysis and comparison. A special focus was laid on the transition zones near the settlements. Here these homogeneous clay deposits are interrupted or enriched with cultural material from the settlements that intermixed with alluvial Nile material. This embedded cultural material can be an important source for dating (see 1.2.3) to chronify the geochemical information. Another primary target in the transition zones are the canals that were filled with cultural material and it is possible to date the fillings with the new method based on pXRF data. This way a terminus postquem can be established that dates when the different channels ceased to exist. Nevertheless, it must be admitted that modern dating techniques which are indispensable in geoarchaeology are not available in Egypt. Another aspect is that sample transport is totally restricted in Egypt except during the 2012 campaign. That led to the exploration of new dating techniques based on the inventory of geochemical signatures collected in this working branch (see 1.2.3).

### 1.2.3 Aim 3: Characterization and dating of settlement layers within coring transects

The temporal relations between the results of the fine-scaled sedimentologic inspection and the archaeological excavations in the settlements are poorly understood. Only a small fraction of the ceramic material found within the corings is datable and - as it has been prior stated - other dating techniques are not available in Egypt.

A key question is whether it is possible to establish a chronostratigraphy based on geochemical fingerprints from different cultural deposits found within the coring transects. This new method is based on a machine learning approach that allows to draw temporal relationships between the well documented and dated settlement layers of the archaeological excavations and the undated cultural debris found in the corings of the transition zones. The question is, if archaeological remains which have been exposed during the excavations at Buto can be used for our new machine learning approach. Physically, these are profile walls or archaeological planes that cut deep into the settlement mound and were left behind by the ongoing excavations. The settlement mound itself is a unique archive comprising layers of all cultural phases which were documented and dated and now qualify as perfect training material to date cultural layers or material in the corings of the transition zones.

This is a completely new approach that is used on pXRF data of sediment samples and requires to examine methodological prerequisites in detail. In a first step, the distinct geochemical properties of the transition zones need to be described and it is necessary to show whether the sediments located in the transition zone nearby are influenced by material from the settlements. This flux of elements from the settlements into the surrounding is necessary for the approach and tested with the help of multivari-

## 1. INTRODUCTION

---

ate statistics in combination with spatial analyses. With this proven, artificial neural networks can be used to reference the geochemistry of a certain layer to a specific cultural phase. Often machine learning approaches are described as “black boxes”. That is why the usability of pXRF data for machine learning techniques is tested in terms of accuracy and applicability in a larger geostatistical approach (see chapter 5). Prior to the dating with artificial neural networks, geochemical differences of material of the different cultural phases were analyzed, and material taken from different archaeological records was measured. In the course of this methodological approach many questions had to be solved: Which elements are usable? Does there really exist a geochemical difference between archaeological and alluvial Nile material? Do there exist differences in the geochemical signature between cultural stages and how does this vary over different archaeological records? How did erosion, leaching and so on postsedimentarily affect the sediments and their geochemistry? Which records resemble differences in the geochemical properties best?

A subset of the training data is chosen to ensure that the artificial network is trained with valid data. For example, a detailed description of erroneous elements is needed as these are better dropped from the training set. On the other hand, archaeological records that show the highest chemical differences between the cultural stages need to be identified and used for training. Lastly, the results of the neural network and its accuracy were improved by changing its design, taking into account results on the usability of elements and dropping out data of the neural network analysis or by artificially enlarging the dataset and emulating data within the error ranges of the pXRF device for the different elements. Especially, the latter might allow the artificial neural network to compensate for lower measurement quality of certain elements.

In closure, this is an entirely new innovative approach and there are still many uncertainties and challenges that are tackled within this work. The results are preliminary and touch on just a small fraction of what is possible with the application of machine learning techniques.



## 2

# Methodology

As has been mentioned in the previous chapter, this study focuses on the development of new methods for geoarchaeological research in the northwestern Nile delta and it is primarily individual time slices that are analyzed. In the following a brief description and synthesis of the methods used in the different research papers is given.

## 2.1 Fieldwork

Overall nine field campaigns between autumn 2012 and autumn 2018 were carried out. During the Egyptian protests in 2012 and 2013, scientific campaigns were restricted due to security issues in Egypt. The field campaigns focused on the sampling of the lithology of the subsurface with a vibracoring device (Wacker BH65) and open steel auger heads with varying diameters (6.0, 5.0 and 4.0 cm) and 1 m length. The retrieved sediments were described in detail in the field according to Eckelmann *et al.* (2006) and organic material as well as indicative chert or faunal or floral remains were sampled additionally to the normal sediment samples and stored. Dateable ceramic fragments were analyzed by Peter French and Rita Hartmann. For individual samples  $^{14}\text{C}$  age estimation was carried out (Beta Analytics, Florida, USA). The dates taken from the samples and from other sources such as the work of Wunderlich (1989) were calibrated with Calib Rev 7.1 using IntCal13 and stated using the 2 sigma error range.

The cores were placed either along different transects leading away from the settlement sites of Buto and Kom el’Gir, crossing important levees in the north or in the Bahr Nashart depression lying east of Kom el’Gir or in close vicinity of the two previous named settlement sites. Over the course of the nine field campaigns 52 open steel augerhead cores and five closed corings were placed in the study region, and 2365 samples were collected. Out of these, 1790 samples were measured with the pXRF device.

On-site sampling focused on archaeological material from the archaeological excavations of Ulrich Hartung and Pascale Ballet (see Fig. 5.1). Material targeted in the archaeological profiles belonged to records such as bricks, floors, ovens, pits and ash

## 2. METHODOLOGY

---

layers, or other forms of burned residues. Additionally, soil samples from squares taken during excavation works were added to the inventory. In total for 688 samples out of 708 archaeological samples, pXRF data was generated.

Position measurements for core positions, tracks for the generation of elevation models, height profiles crossing individual levees were measured with a Topcon DGPS (Gr50) with  $\pm 2$  cm vertical and horizontal accuracy. Lastly, for a land cover classification (see chapter 3) land use classes were marked in the field with a handheld GPS during three days, day before, at and after sensing time of a RapidEye that was tasked on 23<sup>rd</sup> of October 2014.

### 2.2 Remote Sensing

In chapter 3 a processing chain for the identification of High and Lost tells is developed that incorporates multispectral classification techniques and development of our own scripting routines for the analysis of NDVI time series. High tells were classified using four Landsat 8 scenes acquired in the year 2013 that were atmospherically corrected with GrassGIS using dark object subtraction. For better classification results synthetic statistical layers were added to the image stack. For the classification of Lost tells 69 satellite scenes covering a period of six years were used in the study. Scripts and routines were developed to quantify the vegetation performance in the area under study either via statistics or temporal dynamics derived from a time series of *Normalized Difference Vegetation Index* (NDVI) images (see section 3.4.2.1). To calibrate the results of the vegetation performance for different crop types a supervised classification of a tasked RapidEye scene was performed that had been ordered over the BlackBridge science application platform <https://resa.blackbridge.com>.

Elevation data from the TanDEM-X satellite formation was analyzed and used in this study. The TanDEM-X digital elevation model (DEM) is available globally and shows a pixel spacing of up to 12 m and with less than 10 m absolute vertical accuracy and around 2 m relative vertical accuracy in flat terrains (DLR Product Specification). This data was made available for the project via the DLR science application platform. To give better quality information, the relative vertical accuracy was estimated via comparison with ICESAT elevation data and our DGPS core measurements. In a first approach, elevation models were generated from TanDEM-X CoSSC data with SARscape (<https://www.harrisgeospatial.com/Software-Technology/ENVI-SARscape>) but later additional ready generated DEM tiles from the DLR science application platform were used.

### 2.3 Geochemical analysis

Samples from corings and archaeological profiles were prepared in special XRF cylinders and analyzed with a Niton XL3t 980He portable XRF (pXRF) analyser equipped with a Ag-Anode. Preparation steps include drying, pestling and pressing in the cylin-

ders equipped with a thin xrf foil. A helium purge was used to enhance quantitative measurements of light elements, of which phosphorus is most important. With the help of certified reference materials (SiO<sub>2</sub>, NIST2780, Till4) and our own local standards that were measured during each measurement series, results could be optimized and validated. This was the essential step for the collection of geochemical element spectra and fingerprints from the different archives and cultural layers. Overall 3062 pXRF measurements were carried out for 2514 different samples that were measured with the device during six campaigns.

## 2.4 Data analytics

Especially chapter 5 deals with application of data analytics on the pXRF data. Generally, large amounts of pXRF data, field data and GPS data were collected in the project and require new methods of data storage, selection and analysis. In consequence, our data is stored in a “relational database management system”(RDBMS, PostGIS) that allows querying and selection of data based on attribute values and spatial relations. Data is inserted in the warehouse via automatic processing chains realized with Pentaho Geokettle. Analyzes such as robust factor analysis (PFA), clusterization, or machine learning techniques are performed using the statistical scripting language R (<https://www.r-project.org/>) together with the spatial functions offered by PostGIS (<https://postgis.net/>).

Main tasks in data analytics are calculation of precision values and statistics to gather information on the accuracy of the pXRF device. This is realized via repeated measurement of pXRF standards and our own reference material. For example, precision of measurement is expressed with the coefficient of variation also known as relative standard deviation (RSD).

Furthermore, the data needs to be prepared in order to remove missing values or exclude elements that lie below the detection limit. The presence of zeros has consequences for plotting, descriptive statistics, estimation of parameters or statistical tests (van den Boogaart & Tolosana-Delgado, 2013). Zero values are considered as trace zeros, meaning that values are below the detection limit (BDL) and the measurement method is not precise enough to actually distinguish the true value from zero. They are replaced with EM-based algorithm (Palarea-Albaladejo *et al.* (2007), function `impRZilr` from `robCompositions`). In the exclusion preparation, only elements are chosen that were measured in more than 50 % of the sediment or archaeological sample material.

The third main task of data analytics is the application of multivariate statistics and clusterization combined with spatial information. For example, chemical differences along the large-scale sedimentological transects are analyzed with a robust factor analysis (see 5.5.2.1) or the contents of plant nutritious elements are related to the distance to the next neighboring tell (see 3.3).

Lastly, the described steps are preparation steps for the application of neural networks that are used to register patterns within the data that allow “indirect” dating of the sediments (see 5.4.5). In order to perform the neural network analysis with the

## 2. METHODOLOGY

---

R-package neuralnet (Guenther & Fritsch, 2010). The training set comprises in total 539 samples, 95 dated sediment samples from the corings, 141 dated archaeological samples taken from walls and floors of the archaeological profiles, and 303 samples from alluvial Nile material. The latter are the sediment samples surrounding dated pottery in the corings. To ensure that cultural sediments are not included, training data for the alluvial Nile material is selected as samples lying outside a 600 m radius of settlements and in depths below 6 m. Considering the quantities for the different cultural phases, the training data consist of 74 Roman, 109 Dynastic, 47 Predynastic, and 303 alluvial Nile samples.

### **3**

# **Identification of historic landscape features and settlement mounds in the Western Nile delta by means of remote sensing time series analysis and the evaluation of vegetation characteristics**

The identical content of this chapter was published in different formatting in:

Ginau, A., Schiestl, R., Kern, F., Wunderlich, J., 2017. Identification of historic landscape features and settlement mounds in the Western Nile delta by means of remote sensing time series analysis and the evaluation of vegetation characteristics. *Journal of Archaeological Science: Reports* 16, 170-184.

#### 3.1 Abstract

Remote sensing techniques gain increasing importance in landscape archaeological research. Traditional archaeological excavation techniques are slow and time in the Nile delta is running out. The Nile delta has been settled and used for agricultural cultivation since the Neolithic period and is shaped by the interplay of urbanization and agriculture. In particular, the study of ancient settlement mounds (tells) and landscape archaeological features such as former river channels requires urgent action. This study seeks to develop supervised classification techniques on the basis of multitemporal Landsat 8 images to easily monitor existing high tells in the delta that have not been destroyed yet. In the 19<sup>th</sup> and early 20<sup>th</sup> centuries many tells were destroyed, because tell sediments (sebakh) were harvested on an industrial scale in order to be used as fertilizer. These activities continued on a smaller scale into the mid to later 20<sup>th</sup> century. Geochemical analysis of ancient settlement material (sebakh) has confirmed the high content of nutrients. In a second step which is based on these geochemical findings, we seek to identify the category of lost tells which had been transformed into agricultural areas. We suggest that the presence of ancient settlement material enhances the overall vegetation performance and indirectly allows identification of lost tells via describing the vegetation performance. In general, the vegetation performance is a new measure and invented within this study. It is calculated as the product of different measures describing the plant growth, namely the mean *NDVI* (Normalized Difference Vegetation Index), growth statistics and crop rotations derived from a large set of multitemporal *NDVI* images. Our results show that there exists a relationship between vegetation performance and the appearance of archaeological material in the topsoil and such information can be useful for planning of non-invasive archaeological surveys. Remarkably the vegetation performance corresponds with the location of former Nile branches that are currently investigated by the authors on the basis of TanDEM-X elevation data and sedimentological investigations of the area. Several factors such as water availability and salinity also affect plant growth and mask this relationship. Additionally, our methods to describe the number of crop rotations or growth statistics from *NDVI* time series help to analyze the agricultural areas in the Nile delta. Therefore, the methods used in this study may offer important insights on aspects of urban sprawl and agricultural areas in the Nile delta and beyond.

#### 3.2 Introduction

The Nile delta has been settled and used for agricultural cultivation since the Neolithic period and is shaped by the interplay of urbanization and intensive agriculture. It makes up 2.8 % of Egypt's territory and is home to 63 % of Egypt's population, namely 50 million people (Hamza, 2010). Awareness is increasing that the intensification of land use by the rising population and urbanization leads to transformation of fertile agricultural land into urban areas. But Egypt's agricultural land does not only suffer transformation but also severe degradation of the soil, meaning that the

potential capability of the soil to produce agricultural goods is lowered. Both processes drastically increase the pressure on the use of land and, therefore, increase the rate of land degradation (Abdel Kawy & Ali, 2012).

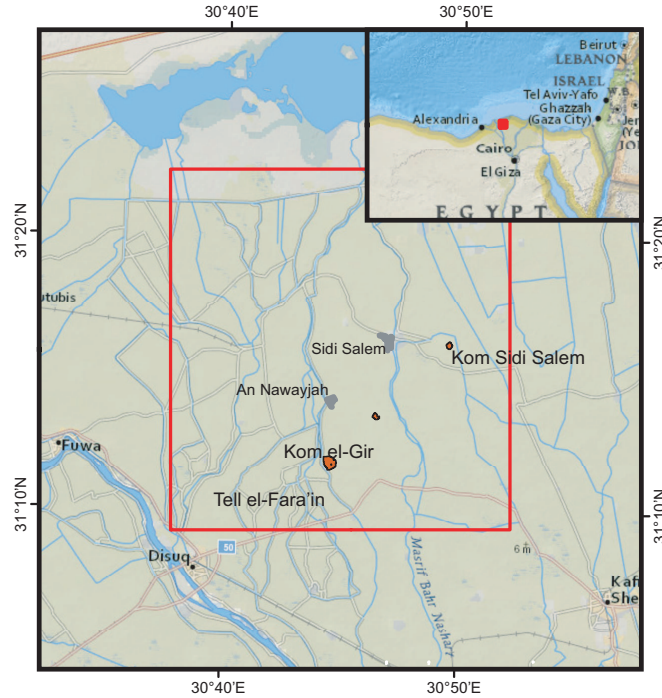


**Fig. 3.1: Location of the study area** - The study area (red rectangle) is located in the northwestern Nile delta. Important tells (ancient settlements) are shown in red as well as the location of the most important modern settlements.

In this context, Schiestl (2012a) focused on the fate of archaeological sites which disappear due to the rising demand for new agricultural land or settlements and were harvested at industrial scale as 'sebakh' (ancient settlement debris) and spread as an important fertilizer. Awareness is increasing that the intensification of land use by the rising population and urbanization leads to the destruction of archaeological and landscape features. Remote sensing data are often the only available source of data for some sites and are gaining increasing importance. Their application allows archaeologists and ge archaeologists to uncover unique data on a high spatial level compared to the punctual and site based design of archaeological excavations. With remote sensing techniques, archaeological or landscape features and sites can either be identified, characterized or analyzed directly or indirectly. Directly via their specific shape, spectral signature and other remotely measurable characteristics or indirectly via their influence on entities such as vegetation or surface characteristics. Lastly, traditional archaeological excavation techniques require a long time.

This study focuses on an area that covers approximately 560 km<sup>2</sup>. It stretches from Lake Burullus in the north, the city of Desouk in the southwest and the city of

### 3. ARTICLE 1, REMOTE SENSING ANALYSIS

---

Kafr el-Sheikh in the southeast (Fig. 3.1). In roughly the southern half of this area the German Archaeological Institute (DAI) is conducting the archaeological excavation on Tell el-Fara'in, the former city of Buto, as well as the above mentioned survey conducted by Robert Schiestl to get a better understanding of the former landscape and the network of settlements that were connected with Buto.

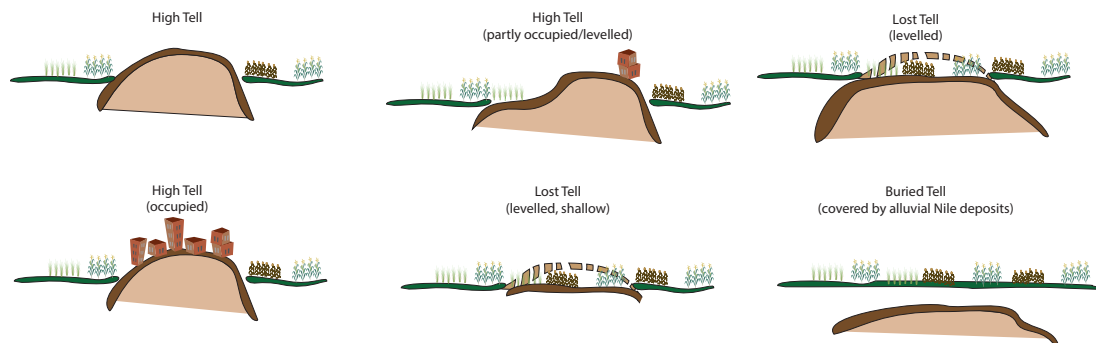


**Fig. 3.2: Classification of different tell types in the Nile delta** - Different tell types that occur within the delta plain. Primary classes are the prominent high tells and lost tells that are consumed by agricultural colonization or buried by Nile mud. Based on a classification by Schiestl (2012a).

The majority of archaeological sites in the Western Nile delta are tells, a man-made mound, “[...] whose sediment matrices are for the most part culturally derived, the sediment itself may be treated as an artifact” (Rosen, 1986). Numerous studies have been undertaken to identify former settlements from space in order to get a better understanding of former settlement patterns. A study dealing with this topic and going beyond previous qualitative approaches (Schiestl, 2012a; Sherratt, 2004; Trampier, 2009) is the work of Menze & Ur (2012). Menze & Ur (2012) name three distinctive characteristics of tells, dense surface artefacts, moundedness and anthropogenic sediments “anthrosols” for Near Eastern sites that might be remotely traceable. It is here argued these characteristics also hold true for sites in the Nile delta. Additionally, Menze & Ur (2012) state that texture, hydrological and reflective properties of these anthrosols often differ significantly from the surrounding land in the region under study, the Upper Khabur Basin in northeastern Syria. To assess these differences, they proposed a multitemporal classification strategy on the basis of multiple multispectral Aster scenes. This multitemporal approach is adopted for our study area in the Western Nile delta, but conditions in the Nile delta are quite different. Here we are dealing with an intensively used agricultural area that allows different characteristics of the surface to be classified, such as the surface variability or temporal vegetation patterns. Specifically, for this study area, we use remote sensing workflows and processing techniques to allow monitoring of existing high tells that are not completely occupied, that show tell material on the surface (see Fig. 3.2) and lack agricultural or other usage due to protection and conservation by the Egyptian ministry for Antiquities. This tell material on the surface is the target of the classification via the direct analysis of surface



characteristics and their robust unchanging behavior over time. In general, the fate of high tells is shaped by the interplay of archaeological protection and conservation, population pressure and the need for new agricultural and industrial areas. Even though sites are protected, the latter processes can consume these areas, which emphasizes the need for robust monitoring techniques that allow estimations of the deterioration of these sites.

On the other hand, this study searches for means to locate lost tells. This proves to be a much more complicated task as the methods can only trace the indirect influence that lost tells exert on the vegetation growing and feeding from tell material underneath. In some cases the tell material may be covered with shallow deposits of alluvial Nile material. In the latter case, the accumulation of Nile mud surpassed accumulation rates of the tell material leading to the burying of the tell (see Schiestl, 2012a). The classification tries to identify lost tells or buried tells (Fig. 3.2), but the deeper the buried tells are covered with Nile mud, the more does the influence of anthrosols on the vegetation performance diminish.

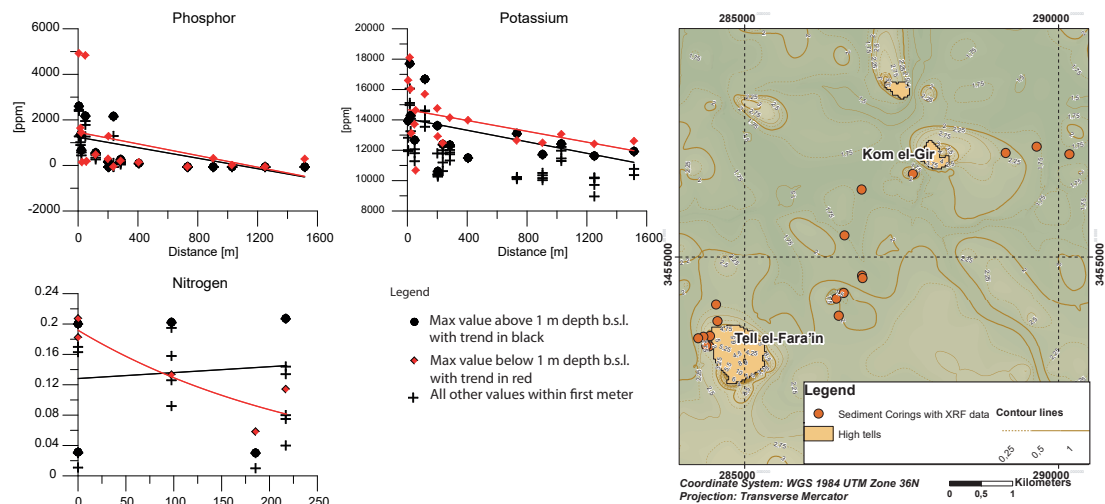


**Fig. 3.3: Distance mapping of plant nutritious elements** - Relation between the distance to the next neighboring tell and the amount of plant nutritious elements (Phosphor, Potassium and Nitrogen) within core profiles that were analyzed with a pXRF device. This relation is shown for the upper first meter b.s.l. and samples of the whole coring. Solid lines show the linear regression for the different categories of points

Menze & Ur (2012) already referred to visible differences in anthrosols. We found additional differences in anthrosols on the basis of geochemical findings. In particular, enhanced performance of the vegetation might be related to distinct soil properties of archaeological sites which have especially raised values of plant nutritious elements. This study is embedded in a larger project dedicated to deciphering Holocene landscape change in the area around Buto in which we retrieved data from corings and sedimentological analyzes. The geochemical results were obtained using a handheld

### 3. ARTICLE 1, REMOTE SENSING ANALYSIS

---

portable X-ray fluorescence spectrometer (pXRF) from Analyticon Instruments (Niton xl3t) on sample material retrieved during geoarchaeologic field work in 2014. The analysis shows elevated content of nutritious elements in these culturally derived sediments on the tell itself and in sediments of the surrounding area of these archaeological sites. The sediments surrounding these sites are affected by the influx of chemical elements. Fig. 3.3 illustrates that especially phosphate, nitrogen and potassium show a negative correlation with the distance to the next tell, meaning that their values decrease with increasing distance from a tell. Additionally, these three elements belong to the most important chemical fertilizers used in Egyptian agriculture (Zeydan, 2005) and largely affect plant growth and the overall performance of the vegetation. In this study, the performance of the vegetation is quantified via statistics or temporal dynamics derived from Normalized Difference Vegetation Index (*NDVI*) images and time series (see section 3.4.2.1) calculated from Landsat 8 and RapidEye images. It needs to be emphasized, however, that numerous variables affect plant growth and, therefore, affect the *NDVI* value (Ma *et al.*, 2001) as well as the vegetation performance. Fig. 3.4 outlines the preconceived relation between tell material and vegetation performance and gives a general overview of the typical stratigraphic situation in the area of Buto stretching out north to lake Burullus.

### 3.3 Study area

According to Wunderlich & Andres (1991) the present morphology of the Nile delta is defined by the smoothly arched coastline, the promontories of the Damietta and Rosetta branches, the marsh and lagoon belt close to the coast and the flat now nearly entirely cultivated delta plain further south. The delta plain successively developed during Holocene times. This study focuses on the flat cultivated delta plain whose genesis is best described in the works of (Butzer, 1975; Said, 1981; Stanley & Warne, 1993).

Today the Nile delta can be described as a patchwork of different and constantly changing agricultural cultivation stages. This patchwork is densely dissected by canals, roads and cities. In the north of the study area fish farms are situated along the southern margin of lake Burullus. Important channels and means for water supply are the canals Bahr Nashart, leading from east of Tell el-Fara'in to the north through the city of Sidi Salem, and Bahr es-Saidi, which leads from the southwest of the study area along el-Mandura to the north. Here the Bahr es-Saidi forms a lobe-shaped agricultural area within the area of fish farms in the north.

### 3.4 Material and methods

As it was outlined in the introduction and the preceding chapter, this work aims to develop remote sensing workflows and processing techniques that allow monitoring of existing high tells and identification of the category of lost tells and buried tells.

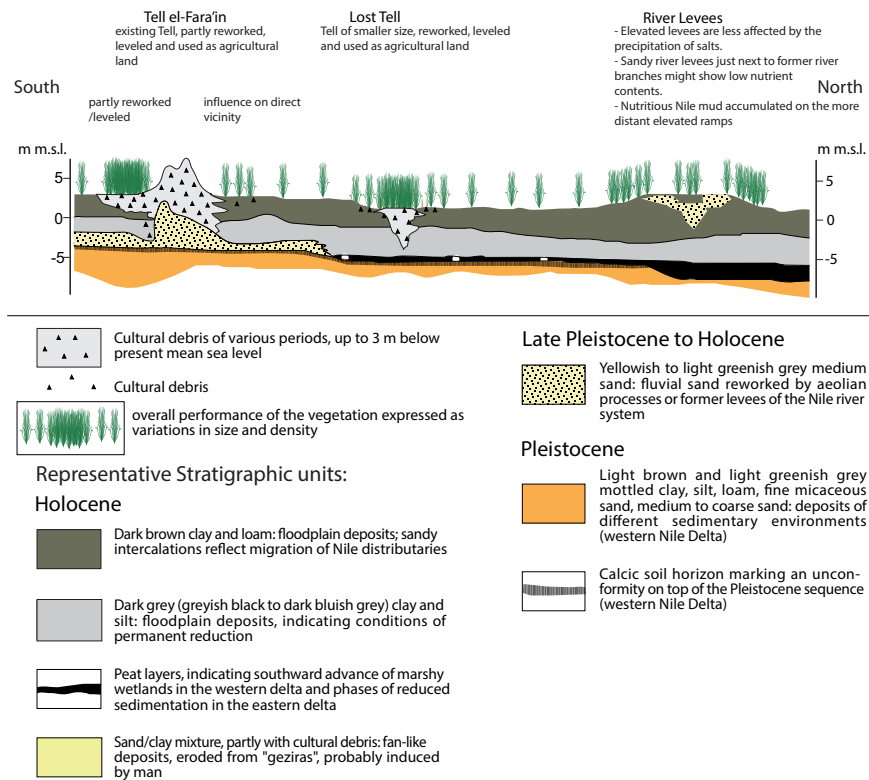


**Fig. 3.4: Presumed relation of tell material and vegetation performance - Main stratigraphic units and tells embedded within. The density of plant symbols refers to the supposed vegetation performance.**

### 3. ARTICLE 1, REMOTE SENSING ANALYSIS

Fig. 3.5 shows a flowchart that helps to understand the steps of the analyzes. The different elements of this flowchart refer to the sections of this chapter. High tells are identified using supervised classification techniques (chapter 3.4.1), whereas lost tells only manifest themselves within the delta via their indirect influence on the vegetation (chapter 3.4.2). The performance of the vegetation is described by the amount of crop rotations, the overall mean *NDVI* of all multispectral satellite products taken into consideration and by the properties of the growth curves different field uses showed during spring to autumn 2014. The relevant preprocessing steps and the methods for retrieving these parameters is described in section 3.4.2.

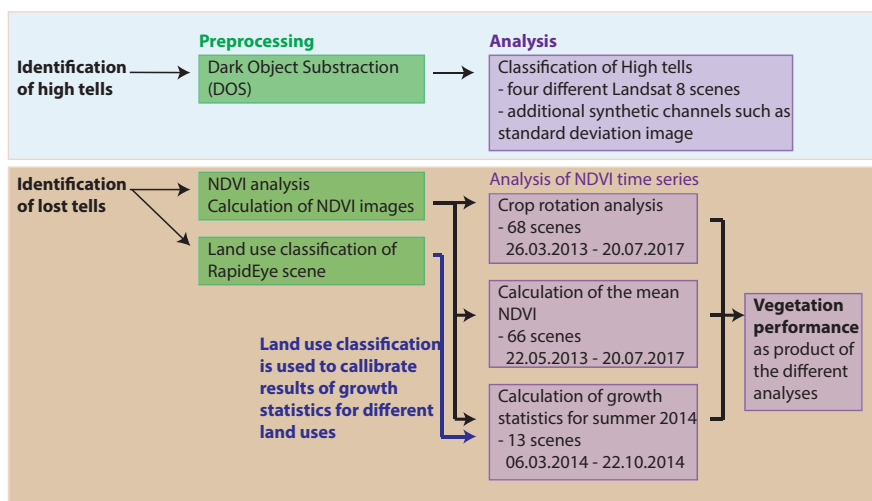


**Fig. 3.5: Flowchart with applied analyzes** - Relevant preprocessing steps and analyzes for the identification of high tells and lost tells

#### 3.4.1 Identification of high tells

This section deals with identifying high tells in the area under study. High tells are classified using four Landsat 8 scenes acquired in the year 2013. Generally the classification should be easily applicable requiring only a minimal set of scenes with no clouds. On the other hand, it should allow a yearly monitoring and, therefore, only scenes from one year are used in the classification. The acquisition dates lie within the dry period of 2013 and show no clouds over the land area.

##### 3.4.1.1 Preprocessing of Landsat 8 images

As multiple scenes are used to classify high tells, it should be ensured that they are not differentially altered by different atmospheres. Before classification, images are corrected to surface radiance and surface reflectance values. Corrections are applied using *i.landsat.toar* module in *Grass 6.4.4* applying the *Dark Object Subtraction (DOS)* model.

As stated in Moran *et al.* (1992) the *DOS* model’s main advantages are that it is strictly an image-based procedure and does not require in-situ field measurements. Its application is simple and straightforward. Chavez (1996) concludes that the basic idea of this model lies in the fact that some image pixels are in complete shade and their radiances received at the satellite are due to atmospheric scattering induced by Rayleigh and Mie scattering effects (path radiance). For example, reflectance with a substantial component of atmospheric scattering can often be retrieved from lakes and oceans, as they show low reflectance in the short wavelengths and, therefore, act as dark objects.

Equations used for application of the *DOS4* atmospheric correction model are stated in the `i.landsat.toar` documentation. Resulting float values of atmospheric correction are min-max stretched and reduced to 8-bit quantization.

#### 3.4.1.2 Classification of high tells

Classification of ancient settlement mounds and the retrieval of their modern outlines is achieved via the analysis of a multitemporal set of Landsat 8 scenes. Images are differentiated into a limited number of main classes including agricultural fields, settlement mounds, modern settlements and cities, river channels, sandy areas and ocean water, see table 3.2. A supervised Nearest Neighbor Classification is carried out with *ERDAS IMAGINE* on a single layer stack containing four Landsat 8 scenes with different acquisition dates (see table 3.1).

**Table 3.1:** Landsat 8 scenes used for classification of high tells

ID	DATE ACQUIRED
LC81770382013142LGN01	22.05.2013
LC81770382013158LGN00	07.06.2013
LC81770382013206LGN00	25.07.2013
LC81770382013254LGN00	11.09.2013

Synthetic layers are added to the image stack, namely *NDVI* images of the four scenes as well as the mean *NDVI* and the calculation of the standard deviation between the different color bands of the individual scenes. Especially the calculation of the standard deviation triggers the discrimination between tells and agricultural fields, Fig. 3.6. Training regions are marked according to topographic maps, *Google Earth* images and the results of former field campaigns. The clustering of the different land uses in the feature space of a near infrared channel with the standard deviation of the near infrared shows that fields as well as tells show similar overlaying grey values in the infrared but different standard deviations. This can be explained by the fact that land uses of the fields are continually changing, whereas tells more or less show the same land cover (open flat silty soil) throughout the year. Without taking the standard deviation

### 3. ARTICLE 1, REMOTE SENSING ANALYSIS

into consideration, this surface is easily confused with barren fields in the classification.

**Table 3.2:** Training sites used for the supervised classification of high tells

no.	fieldtype	amount of pixels (training sites)
1	riverine vegetation	12,234
2	cities	11,120
3	coast	8,761
4	fields, type 1	21,518
5	fields, type 2	7,575
6	fields, type 3	24,605
7	fields, type 4	4,534
8	water	1,025,110
9	clouds	46,749
10	high tells	1,424

Results are recoded masking the high tells to 1 and everything else to 0. Finally, focal median filtering is performed in order to eliminate single false pixels.

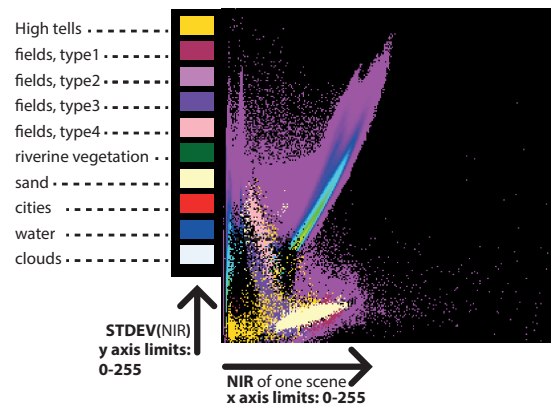


**Fig. 3.6:** Feature space of NIR (x) and STDEV(NIR) - Correlation of one NIR image with the standard deviation of all four images. Fields and tells cluster in the same area on the x axis as they show similar NIR values, whereas they become separated by their y values that tend to describe their changing states.

#### 3.4.2 Identification of lost tells

In general the identification of lost tells is retrieved from a high number of satellite scenes. This performance does not manifest itself in an individual scene as the Nile delta reflects a patchwork of different land uses that are constantly changing. It is rather

derived from *NDVI* growth curves or statistic measures such as the arithmetic mean of this number of scenes (see Fig. 3.7). Such measures allow comparison of different areas/pixels and they tend to describe the vegetation performance of the region under observation.

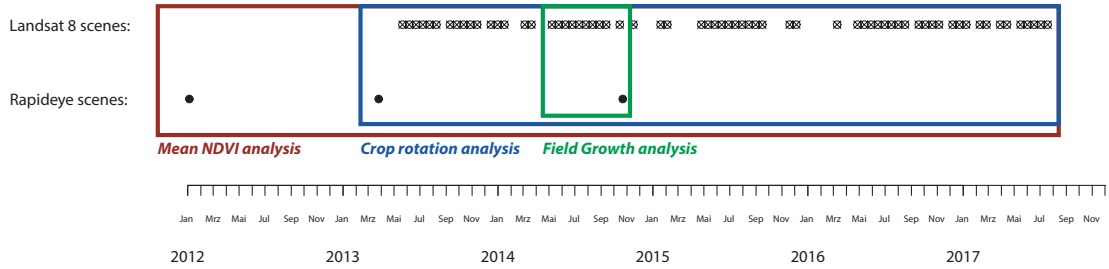


**Fig. 3.7: Acquisition dates of satellite scenes used for the identification of lost tells** - Overview of the acquisition dates of Landsat 8 surface reflectance data products and RapidEye Level 3A scenes that were used in this study. The colored rectangles indicate which scenes are used for the different steps of analysis. One RapidEye scene from spring 2011 is omitted in this Fig. but used in the context of the Mean *NDVI* analysis.

### 3.4.2.1 Preprocessing

Overall 69 satellite scenes covering a period of six years are used in this study. Fig. 3.7 gives an overview of the temporal allocation of the different scenes. Prior to the calculation of *NDVI* images and the calculation of the number of crop rotations or analyzing the vegetation growth statistics, images are resampled to fit the same pixel geometry as in the Landsat images (reduction of ground resolution from 5 m to 30 m) and cropped to the dimensions of the region under study.

#### NDVI Analysis

The performance of the vegetation is quantified either via statistics or temporal dynamics derived from *Normalized Difference Vegetation Index (NDVI)* images and time series. Generally the ratio of energy reflected from an object to the object's energy incident is called reflectance. Spectral reflectance of plants or crops differ in the *near Infrared (NIR)* and *Visible Red (VIS)* region of the electromagnetic spectrum (Kumar & Silva, 1973). Due to chlorophyll absorption, they generally show low reflectance in the blue and red portion of the electromagnetic spectrum. On the other hand *NIR* radiation is strongly reflected. This strong contrast between the red and *NIR* reflectance is known as “red edge”. The amount of reflected *NIR* depends especially on the leaf tissues of the plants. Ma *et al.* (2001) hint at the interaction of these plant specific characteristics and environmental factors such as soil moisture, nutrient status, salinity or leaf development stage. Govaerts & Verhulst (2010) name the *NDVI* an important indice that has been correlated with many variables such as crop nutrient deficiency, final yield or long-term water stress. The *NDVI* should be considered as an amalgamated measure

### 3. ARTICLE 1, REMOTE SENSING ANALYSIS

---

of plant growth that reflects various plant growth factors. The physical characteristics detected by the index might be related to canopy density or total biomass.

Considering the effective and intact irrigation system established in the Nile delta, water or soil moisture can be excluded as limiting factors for plant growth. The *NDVI* within the region under study is related to nutrient contents, development stage and possibly soil salinity. *NDVI* values are calculated with *ERDAS* using equation 3.1. In the case of the Landsat datasets, the *NDVI* images are calculated from atmospherically corrected surface reflectance data products to allow better comparison of the data within this long time-spanning series covering different seasons and atmospheric conditions. Only three RapidEye *NDVI* images are used in the analysis. They are produced from original Level 3A scenes, but as image bands are related in a quotient, atmospheric effects are reduced.

$$NDVI = \frac{NIR - VIS}{NIR + VIS} \quad (3.1)$$

where:

- NDVI* = Normalized Differenced Vegetation Index
- NIR* = Near Infrared
- VIS* = Visible Red
- Landsat8* = Band combinations: 5(*NIR*), 4(*VIS*)
- RapidEye* = Band combinations: 5(*NIR*), 3(*VIS*)

#### Land cover classification of RapidEye scene

Land cover classification of a RapidEye scene taken on the 23rd of October 2014 is performed with *ERDAS* Imagine via supervised Nearest Neighbor classification of a single scene. The scene was shot one day after field work in which we retrieved positions of training areas for classification. The ground truth focused on the retrieval of the crop type growing on different test regions.

Therefore, only land uses were marked in the field and later the polygon of the complete field was digitized on the basis of high-resolution Google Earth satellite images as the borders of the fields and their size remain stable over years or decades. This allowed the fast retrieval of training areas in the field. These digitized fields were used as test-regions for classification and for the quality assessment. Quality assessment is carried out on the basis of an error confusion matrix. It has to be admitted that sites used in the quality assessment had to be used in the classification due to the small area of the individual fields. This leads to an overestimation of the kappa coefficient 0.912 (91.2 %) and can be regarded as a rough estimate on whether certain land uses are differentiated well enough or confused with each other. They show that user accuracies concerning the field uses greenhouse (0.01), reed (0.2), rice (0.2), sugarcane (0.45) and tomato (0.2) are very low. The main reason for the low accuracy in differentiating these land covers lies in the fact that only few or individual fields were marked for these land covers as they only appear in very low numbers and can be ignored for the area under



**Table 3.3:** List of land cover classes together with the area in pixels and the number of fields or sites that were sampled.

no.	fieldtype	amount of pixels (training sites)	number of training sites
1	barren field	3,439	39
2	beet	1,321	13
3	clover	1,111	16
4	cotton	1,489	12
5	fish farm	13,901	30
6	greenhouse	56	1
7	maize	222	6
8	reed	39	2
9	rice	37	1
10	sugarcane	37	1
11	tomato	24	1
12	village	64,792	3
13	water	50,404	8

study. On the other hand, greenhouses show the same surface material as appears in villages, and they are easily confused. User accuracy values for the other land covers are above 0.7 and differentiation of clover and beet as well as villages and barren fields show the highest error values among these. The results of the land cover classification enable the comparison of the growth curves of different crop types.

#### 3.4.2.2 Analyzing NDVI time series

Analyzes describing the vegetation growth all deal with the analysis of a set of *NDVI* images acquired at different times. Crop rotation analysis and field growth analysis deal with patterns and changes in *NDVI* curves. All analytical steps take advantage of Landsat 8 Surface Reflectance quality assessment band (<https://www.usgs.gov/land-resources/nli/landsat>) and its new sensor configuration including Landsat 8 Cirrus band (Band 9). In detail, clouds and cirrus clouds can be easily isolated on the basis of the Pixel QA band, which includes information for different atmospheric or surface conditions encoded in the binary representation of the band's values. Clouds, Cloud confidence levels high and medium, Cirrus confidence level high and cloud shadows defined by the Pixel QA band are masked from the *NDVI* images. In conclusion, *NDVI* curves of different pixel locations in both steps of analysis are cleaned for cloud values. The removal of cloud pixels is also applied for calculating the mean *NDVI* value of all scenes as part of the field growth analysis.

### 3. ARTICLE 1, REMOTE SENSING ANALYSIS

#### Crop rotation analysis

The crop rotation analysis is performed with R (<https://www.r-project.org/>) and based on 66 Landsat 8 scenes and two RapidEye scenes. The scenes cover a time period of five years from 26.03.2013 to 20.07.2017. Fig. 3.8 gives an overview of the different analytical steps and shows functions and definitions used for calculating the number of crop rotations. The first steps of analysis comprise cropping to the extent of the study region, calculation of *NDVI* images and resampling of RapidEye scenes to fit the 30 m pixel resolution of Landsat 8 image products. In a next step, the scenes are stacked and scaled to *NDVI* values ranging between -100 and 100 %. Vegetation canopy tends to show positive values (say 30 to 80) percent while water or clouds show negative values. Then image data are transferred into a data list that is analyzed for significant drops and rises related to changes in the field use. The way the algorithm calculates the number of crop rotations is also described in Fig. 3.8. For each individual pixel the algorithm identifies the highest and lowest values around the mean and creates a simplified *NDVI* curve. Then each *NDVI* value of the simplified curve is compared to the mean and if the absolute value of a vector between the mean and the *NDVI* value exceeds a certain threshold it is counted as a field change.

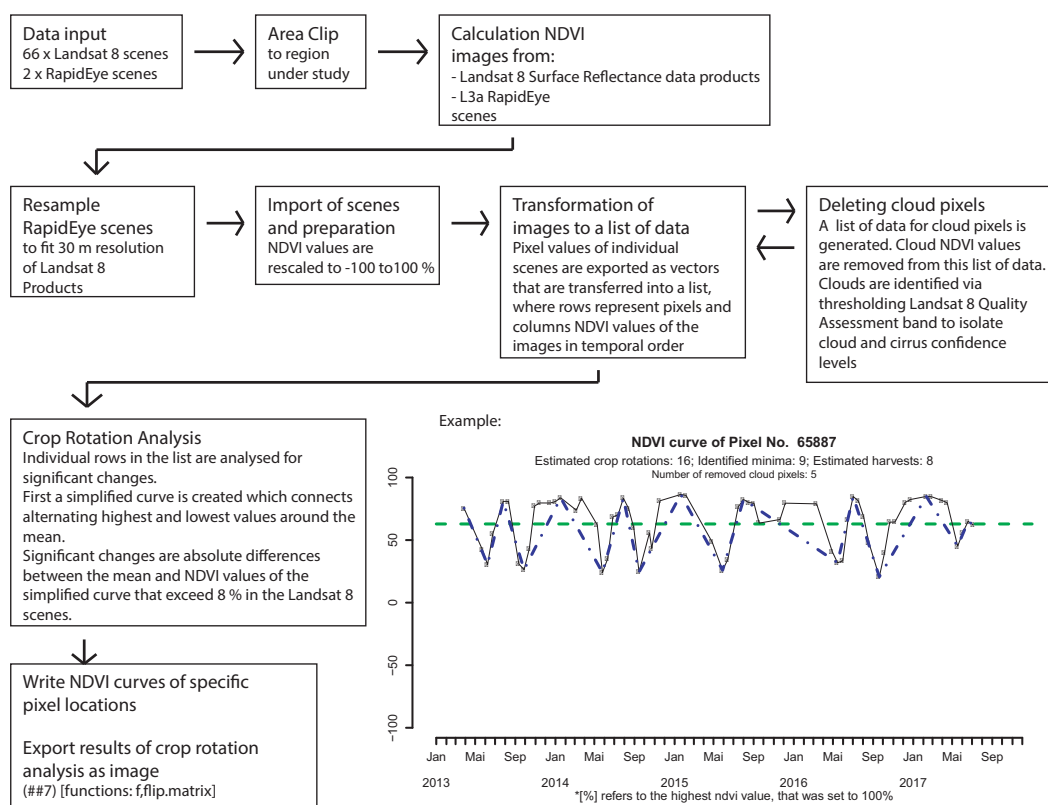


**Fig. 3.8: Workflow of the crop rotation analysis** - Overview of the main processing steps to estimate the number of crop rotations between 26.03.2013 and 22.10.2014.

#### Calculation of the mean *NDVI* and growth statistics for summer 2014

In a first attempt to measure the vegetation performance, named mean *NDVI* analysis, the overall performance of the vegetation is described in R using the mean *NDVI* of all 66 Landsat 8 surface reflectance scenes. This can be compared with the calculation of the seasonally integrated *NDVI* (*SINDVI*) (Hope *et al.*, 2003; Stow *et al.*, 2003). It represents the sum of all *NDVI* values for each pixel during the growing season. The *SINDVI* can reflect inter-annual variability compared to the *NDVI*. Egypt's agriculture does not have fixed growing seasons and this study does not seek to compare growing seasons of certain years. By taking the mean of *NDVI* values, this study aims to find areas where site characteristics such as nutrients, soil or water delivery are best and contribute to elevated *NDVI* values. These might not be visible within an individual scene as the *NDVI* depends on the development stages of the plant or crop type but they might appear in the mean *NDVI* value. Generally, results should be better with an increasing number of scenes.

In a second attempt to measure the vegetation performance, growth statistics of the growing season in summer 2014 are calculated with R and plotted as raster images. In the course of this study this step is referred to as field growth analysis. It takes 13 scenes that were acquired during 2014 into consideration. These are 12 Landsat 8 scenes and one RapidEye scene. They cover a time period ranging from 06.03.2014 to 23.10.2014. The different steps of analysis are presented in Fig. 3.9. First steps of the analysis comprise cropping of the image data to the study region, calculation of *NDVI* images (see 3.4.2.1), resampling of RapidEye image products to fit the resolution of Landsat 8 data, importing into R and transformation into a list of data. The different pixels are analyzed for the shape of the growth curve and its statistics (mean growth rate, maximal growth rate and total growth). Overall the algorithm identifies the growth curve as lying within the lowest and highest *NDVI* value of scenes covering the time interval presented. Statistics are exported as images and adjusted according to their field use. This adjustment respects the fact that different crop types show different growth curves, soil coverages and so on. As a consequence, the results of the field growth analysis are made comparable via min-max stretch for the individual field uses identified in the field use classification (see results of RapidEye classification).

Land covers such as rice and tomato fields are not adjusted as they occur only in very low number. Field uses adjusted are beet, clover, cotton, maize and rice. Barren fields are interpreted as harvested rice fields, their *NDVI* curves show a peak in the period before harvest and the drop of the *NDVI*. During the survey nearly all of the investigated barren fields showed remains of dry rice plants. Results individually adjusted for different crop types are combined to single images showing growth rate, maximal growth rate and total growth for the region under study. The last step deals with the calculation of the vegetation performance (Fig. 3.11) within the area under study. It is calculated as the product of the number of crop rotations, the total growth that occurred during the summer period in 2014 and the mean *NDVI* of all Landsat and RapidEye scenes. Therefore, this calculation represents a rough estimate of the vegetation performance and should be handled as such.

### 3. ARTICLE 1, REMOTE SENSING ANALYSIS

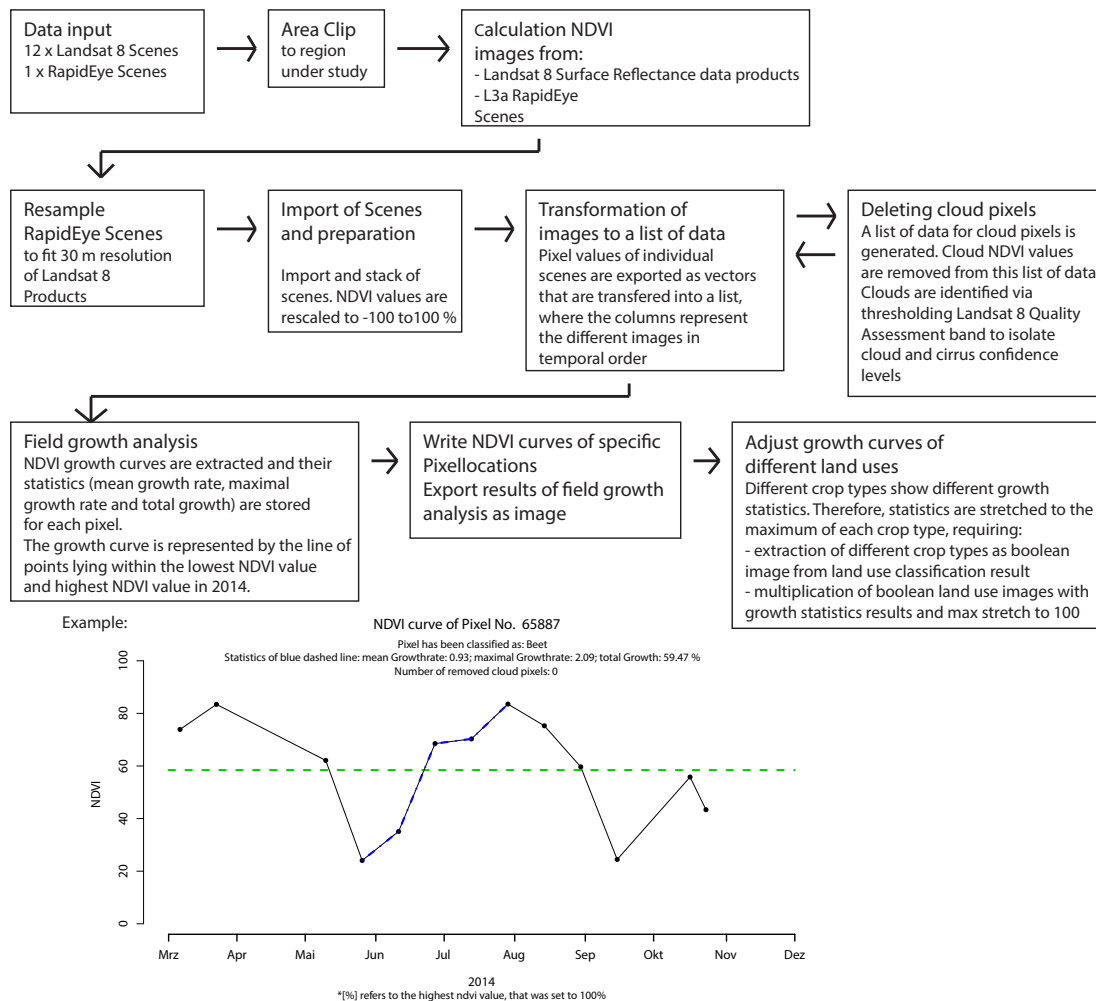


**Fig. 3.9: Workflow of the field growth analysis** - Overview of the main processing steps to estimate the mean growth rate, maximal growth rate and total growth in *NDVI* curves covering satellite scenes lying between 06.03.2014 and 22.10.2014.

## 3.5 Results

The Classification results of high tells and lost tells are presented in the following. As expected, the differentiation of high tells worked out very well, as these are differentiated directly by their surface characteristics. In contrast, the differentiation of lost tells is based indirectly on the performance of the vegetation which shows connections to and dependencies on other influences beside the presence of nutritious archaeological sediment material.

### 3.5.1 Classification of high tells

Classification results of the high tells are very good and the contour of the tells is matched precisely (see Fig. 3.10). The results are cleaned by morphological closing and singular and separate pixels are excluded from the results. Additionally, the area of the tells is enlarged by one pixel; this includes surrounding mixed pixels. In summary, most high tells in the area under study have been identified plus a number of barren areas. Quality assessment is achieved via comparison of the digitized high tells in the area with the classification results. Precisely, 30 of the 34 high tells are correctly identified. Five tells are confused with barren areas at the edges of modern settlements (Fig. 3.10 and table 3.4). These show similar surface characteristics and are, therefore, classified as tells. Overall four tells were not found. Three of these were covered with cemeteries and thick bush canopies. Table 3.4 gives a complete overview on the quality of the classification for the identification of tells and also shows the percentages for the correctly classified areas. The overlapping area of 21 % compared to the area of the high tells within the study area results especially from the overlapping Landsat pixels and the contribution of the mixed pixels as described earlier.

### 3.5.2 Classification of lost tells

As the fields tend to be very small and show a lot of variation it is better to view the results on larger scales. Therefore, the performance is illustrated on a 300 m pixel grid in the overview map and 150 m resolution for the magnified tells. It is important to clarify that these pixels represent the zonal mean of the results of the vegetation performance with a spatial resolution of 30 m, whereas non-vegetated areas have been excluded from the calculation.

Results uncover a general difference between the north and the south with higher vegetation performances occurring in the south. Additionally, large areas of higher performances coincide with the presence of dense canals or river arms. Especially, vegetation performances are high in the central part of the southern half between the Bahr Nashart (east of Tell el-Fara'in along Kom el'Gir and Sidi Salem) and the canal running west of Tell el-Fara'in, where a dense canal and river network is present. This area encompasses the large settlement site Tell el-Fara'in and remnants of a former settlement network including Kom el'Gir and Kom el-Dab'a. Enhanced performances are also observable in the north of Kom esh-Sheikh Ismail where the Bahr es-Saidi

### 3. ARTICLE 1, REMOTE SENSING ANALYSIS

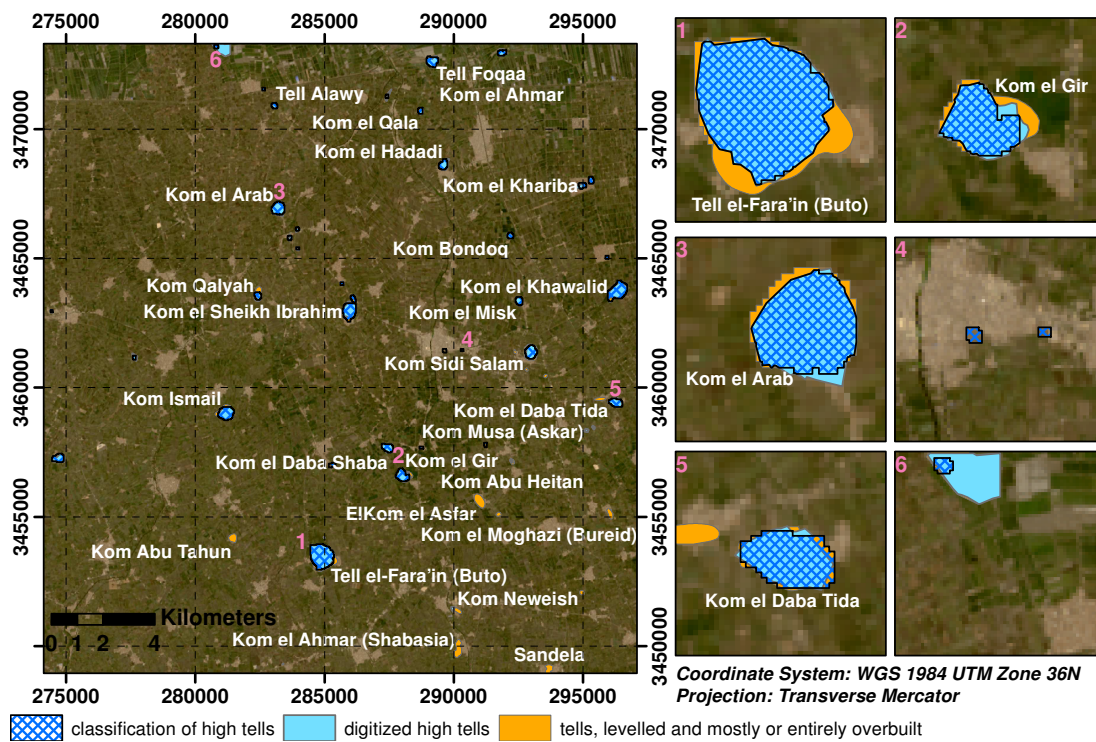


**Fig. 3.10: Classification of high tells** - Results of the Landsat 8 classification for identifying high tells. Illustrated are the outlines of the classified high tells, digitized high tells derived from recent Google imagery and tells investigated in the course of the survey of Buto combining various sources such as historic maps, classification results and survey results. The latter should comprise all known tells of the area.

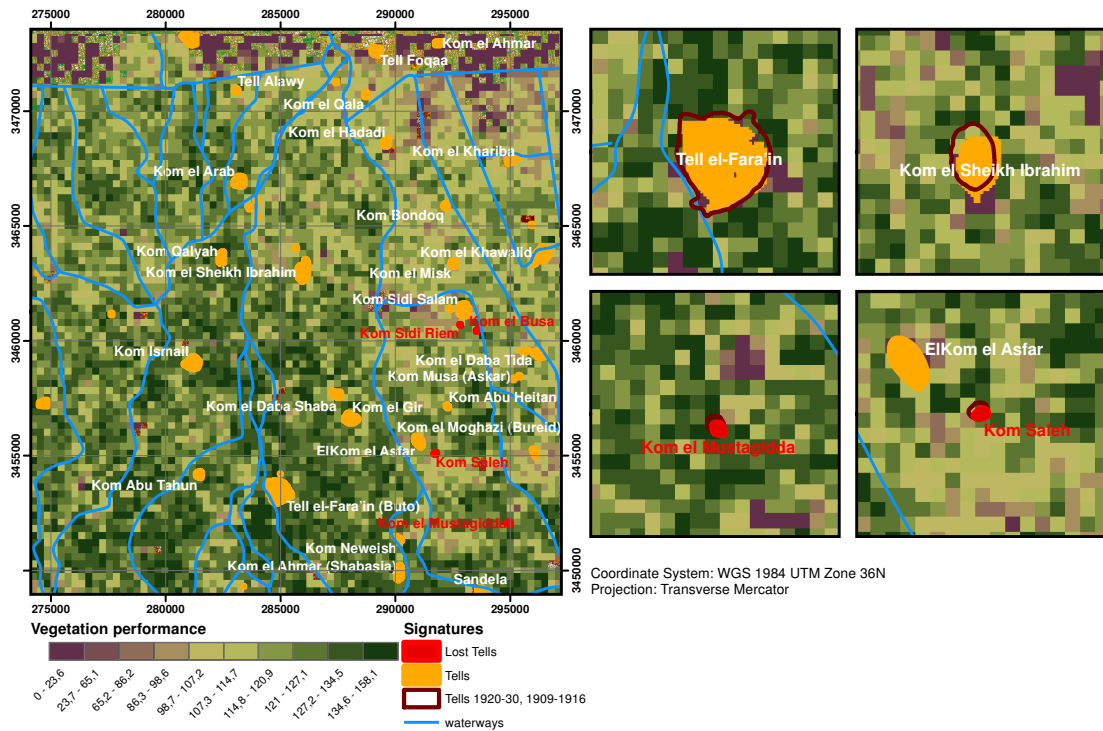


**Fig. 3.11: Spatial distribution of the overall performance of the vegetation -** The vegetation performance is calculated as the product of the number of crop rotations, the total growth that occurred during the summer period in 2014 and the mean *NDVI* of all Landsat and RapidEye scenes. On the left of the Fig. the vegetation performance is shown for the whole region under study on the basis of a 300 m grid. The small Figs illustrate this parameter with 150 m pixels for four important settlement mounds.

### 3. ARTICLE 1, REMOTE SENSING ANALYSIS

---

**Table 3.4:** Quality assessment for the classification of high tells

Category	Remark	
Number of high tells in the study area		<b>34</b>
Identified as tells		<b>35</b>
<b>Of the Identified tells:</b>		
correctly classified		30
falsely classified	mostly barren areas in cities	5
not found	3 of these are covered with cemeteries and thick bush canopy	4
<b>Classified area as percentage of the total area of high tells:</b>		
correctly classified		86%
overlapping area	due to overlapping Landsat pixels	21%
not classified area	in most cases tells were partly covered with cemeteries or thick bushes	14%

splits into several arms. The northern half shows a very diverse pattern, lacking the presence of larger areas with higher performances. Superimposed are the influences of the tells on the vegetation performance. Compared to their larger surrounding, the close vicinities of high tells often show higher performances. Fig. 3.11 exemplifies this for 4 different sites that show vegetation performances for a 150 m pixel grid. Results are also compared to former tell outlines in the very detailed series of the Survey of Egypt maps, 1:25000, from the 1920s and 30s. In the case of Kom esh-Sheikh Ibrahim it is observable that vegetation performances are higher in the northwest of the tell, especially within the red contour representing the tell area as it existed before 1930. Also the surrounding of Tell el-Fara'in and the areas that once constituted Kom el-Mustagidda show higher values.

The spatial patterns of the individual parameters contributing to the vegetation performance and additionally the maximal growth rate in summer 2014 (Fig. 3.12) also hint at different influences on the soils or the availability of water. The number of crop rotations is higher in regions with a dense network of canals. This is especially true for areas where the larger canals such as the Bahr es-Saidi, which leads from the southwestern corner of the map past el-Mandura to the north, and the Bahr Nashart, leading from east of Tell el-Fara'in to the north along the city of Sidi Salem, divert. The maximum growth rate determined for the summer period of 2014 also shows enhanced values in these areas, but these appear to be more restricted to the area between Tell el-Fara'in and Kom el'Gir or where the Bahr es-Saidi diverges. The total growth, meaning the total change of the *NDVI* value between the start and the end of the growing period in 2014, displays a clear north-south contrast with higher values in the south and in the area around and between the two larger canals Bahr es-Saidi and



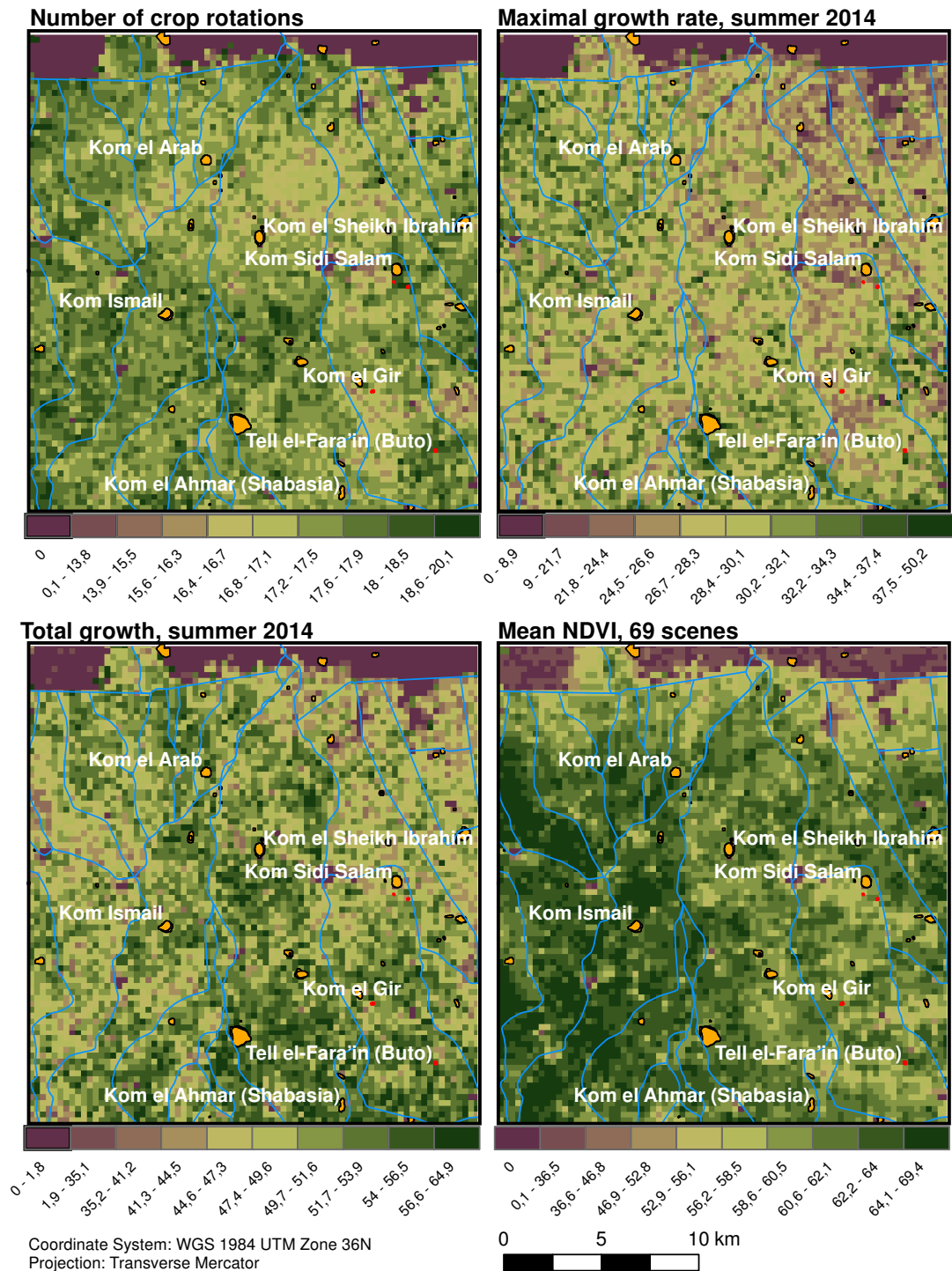


**Fig. 3.12: Spatial distribution of vegetation describing parameters** - Juxtaposition of different parameters that tend to describe the vegetation performance for the study area. These parameters are the number of crop rotation, the maximum growth rate meaning the highest increase in the NDVI curve in summer 2014, the total growth (difference between the lowest and highest NDVI value) that occurred in summer 2014 and the mean NDVI value. The maximal growth rate and the total growth are adjusted to the different crop types to allow comparison between them, see chapter 3.4.

### 3. ARTICLE 1, REMOTE SENSING ANALYSIS

---

Bahr Nashart. Enhanced values that are related to the presence of ancient settlement material especially occur in parameters describing the growth statistics of the vegetation period in summer 2014. Both parameters, the maximal growth rate and total growth, show increased values in the vicinity of tells. Lastly, the mean *NDVI* of all scenes that were analyzed reveal a contrast between the agricultural area supplied by the Bahr es-Saidi and the area supplied by the Bahr Nashart. Here, the areas fed by the Bahr es-Saidy show higher values. Additionally, mean *NDVI* values in the north, just south of the area with fish farms, are very low.

## 3.6 Discussion

### 3.6.1 Classification of high tells

The position of modern high tells is known and they are recognizable in high-resolution Google Earth images. Nevertheless, this study tried to develop methods for an automatic classification of modern tell outlines. The study used four L8 satellite scenes for classification and made use of the calculation of the standard deviation between them. This allows a fast classification. In essence, the method is an ideal tool for automated monitoring of existing tells, which could be easily adopted for the complete Nile delta area. As mentioned in the results, problems arose in differentiating tells from barren areas which show similar spectral characteristics and lack a seasonal change of their land use. Nevertheless the adopted methods allow a robust differentiation between tells and ploughed fields, which was responsible for the magnitude of the false classified pixels. The applied classification routine worked out very well with the coarse spatial resolution of the Landsat 8 image products. Even smaller high tells encompassing monadic pixel numbers are clearly identifiable with the presented method.

Far less accurate is the classification of lost tells due to the fact that various parameters such as the availability of water, nutrients, manuring and so on exert influence on the strength and growth characteristics of the vegetation. Possible sources of error affecting all steps of the analysis are discussed. Both results of the field change analysis and field growth analysis were calculated for individual pixels, namely the  $30 \times 30 \text{ m}^2$  pixels of the Landsat 8 scenes.

### 3.6.2 Classification of lost tells

Knowledge of the category of lost tells is scarce and overall four lost tells are located in the area under study that have been verified and studied. These are only of a very small size. Elevated vegetation performances appear in the area surrounding Kom Saleh and Kom el Mustagidda, whereas at the site Kom Sidi Riem this relation is not traceable. Additionally, the surrounding area of the existing high tells within the area under study often shows elevated values. This is due to the fact that the surroundings are possibly a leveled part of the tell or they might be enriched with tell material. Erosion of tell material is often intensified by the cutting off of tell material as a means to enlarge

agricultural fields. Results on Kom esh-Sheikh Ibrahim reveal that the tell previously had extended further to the north and northwest (see Fig. 3.12) as higher performances occur in these areas. This is corroborated by the former outlines shown on maps from the 1920-30. Clearly the harvesting and spreading of 'sebakh' (Schiestl, 2012a) resulted in additional noise and randomness of the data, but still geochemical results in Fig. 3.3 illustrate the negative relationship between distance to a tell and amount of nutritious elements very well. This relationship has been elaborated based on several corings and settlement sites which corroborate a higher positive influence of in-situ settlement material compared to remote areas very likely affected by the spreading of 'sebakh'. In our view only thin layers were added to these remote areas that do not show a long lasting benefit or comparable benefits as thick in-situ and site adjacent layers of settlement material. The areas next to tells were affected throughout the time the tell existed by erosion of tell material and show comparably higher amounts of nutritious elements.

In summary, results of the vegetation performance can offer valuable information for archaeological surveying and should be considered along with other non-invasive methods. Looking at the results at a larger scale, it becomes also evident that larger tells in the area (e.g. Tell el-Fara'in, Kom el'Gir, Kom el-Dab'a, Kom esh-Sheikh Ismail) are situated in areas that in general show higher vegetation performances. Buto (Tell el-Fara'in) itself sits on top of an elevated lobe that runs out to the north. The higher elevation might reduce salinization effects as the groundwater table sits deeper below the surface and therefore ascension of groundwater and precipitation of salts is alleviated. This was also a benefit in the past and might explain why agriculturally used areas do not occur north of Tell el-Fara'in in the atlas of the Description de l'Égypte (1798–1801) as these areas are significantly lower. These environmental aspects are discussed separately in the following.

### 3.6.3 Geometric difficulties in the analyzes

Both analyzes face the problem that the geometry of the pixel is not aligned with the geometry of the fields. Mostly fields tend to describe narrow, long rectangles with varying orientation. As the pixel area covers 30 x 30 m<sup>2</sup> several fields may be contained in one pixel. This can be roughly verified using the polygonized and 'cleaned' results of the extracted field borders from high-resolution RapidEye scenes. The segmentation is based on finding stable features via application of canny edge detector, bilateral filtering and Standard Deviation analysis (similar to the approach by Perko *et al.* (2010)) of the different RapidEye scenes. 'Cleaned' means that polygons of very small size or very large size are erased from the field polygons as well as polygons covering the non-agricultural areas.

The average field size within the area under study measures 2600 m<sup>2</sup>. Results show that nearly half of all the pixels cover only one field and one quarter cover two fields. Pixels covering more than two fields are rare and make up only 5 %. A remaining quarter corresponds to fields that lie within non-agricultural areas or excluded areas.

### 3. ARTICLE 1, REMOTE SENSING ANALYSIS

---

Additionally, it has to be considered that water canals, small irrigation lines between fields, roads and non-agricultural areas also belong to the set of different land uses and features of the pixels area and affect the *NDVI* value. If land uses and features occurring within a particular pixel show completely contrasting land uses such as barren fields and fields or non-agricultural areas and fields, *NDVI* values might either be enhanced or detracted. Detraction of the values is suggested to occur quite often on the border between agricultural areas and non-agricultural areas. As mostly only one field allocates a significant share of a pixel area, only slight *NDVI* variations due to mixed pixel effects are suggested to occur. The analysis of the number of crop rotations counterbalances this with a threshold counting only *NDVI* changes greater than 10 % as a field change, so that slight drops are excluded.

#### 3.6.4 *NDVI* patterns in the Nile delta

Another parameter influencing the quality of the results is the temporal resolution of the resulting *NDVI* curve. Egyptian winter from October to March is characterized by a drop of average temperatures from 26° C (July/August) to 13° C (January). The low temperatures are accompanied by rainfalls reaching 50 mm in December to January and ~30 mm in November to February. Therefore, cloudless satellite images are less available in the winter, resulting in a seasonal fluctuating temporal resolution of the *NDVI* curve. A major problem is that this period with low temporal resolution coincides with Egypt's important growing season in winter. This has been compensated by a pixel based exclusion of cloud pixels in the calculation of growth statistics, crop rotations and the mean *NDVI*.

On the basis of *NDVI* studies Gross (2005) Fig.d out the presence of two growing seasons in Egypt, one in the summer and the other in the winter months. Gross (2005) used low resolution sensor data from NOAA's AVHRR and Spot's Vegetation instruments that are provided on a decadal basis. In general Egypt's agriculture supports 2.5 harvests per year. Results of the field rotation analysis also give high-resolution information on the number of harvests in the area under study which were calculated separately. The number of harvests are compared to results of Gross (2005) to roughly estimate the quality of the crop rotation algorithm.

Except for outliers harvest stay between 7 and 10 harvest within the analyzed period of 4 years. This means that in average fields are harvested slightly above 2 times a year (see Fig. 3.13) as it has also been measured by Gross (2005). Additionally, measuring the number of field rotations or harvests is very useful for evaluating the size and development of the agricultural space within the Nile delta. Roads, cities and the area of fish farms in the north can be easily differentiated as these surfaces lack substantial *NDVI* changes.

#### 3.6.5 Influence of palaeorivers on the vegetation performance

Prior to the modern hydraulic regulation, the Nile river arms constantly changed their course, vanished or fanned out into smaller channels. As a result the modern channels

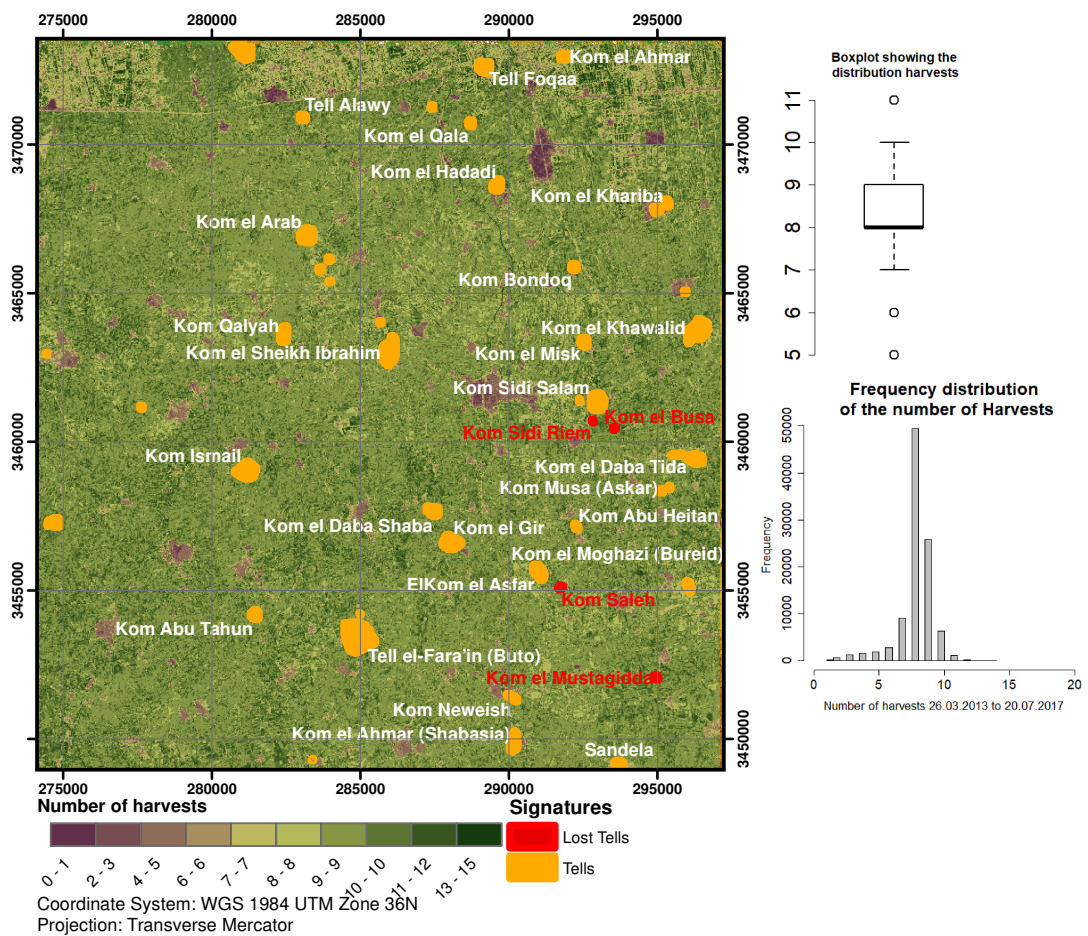


**Fig. 3.13: Estimation of the number of harvests** - The number of harvests are illustrated for the area under study together with a boxplot diagram and histogram showing the distribution of data of the harvests.

### 3. ARTICLE 1, REMOTE SENSING ANALYSIS

---

do not reflect the courses of past river arms. In general the channels are responsible for transport and deposition of the nutritious alluvial Nile muds in their closer surroundings. The relevant processes for the formation of floodplain deposits are best described by Aslan & Autin (1999), who showed that overbank flooding or crevassing and avulsion are the dominant processes in floodplain formation and leave behind a complex architecture with high variation in texture. Sediment accumulation occurs primarily in the river beds and on the associated levees which are natural dams that slightly incline towards the river. Ginau *et al.* (2019) mapped several of these elevated palaeorivers on the basis of a TanDEM-X elevation model from the German Aerospace Center and sedimentological investigations in the area. These are compared with the results on the Vegetation performance in Fig. 3.14. Especially the elevated lobe that stretches out between Kom el'Gir and Tell el-Fara'in shows higher values. It lies between the forking branches of the palaeorivers and very likely overbank flood deposits of both branches mixed and formed this slightly elevated plateau. Similar processes can be attributed to the area around Kom el Arab. In essence, past Nile flood deposits formed these nutritious elevated areas which are less susceptible to salinization due to greater groundwater depths and the presence of coarser material reducing the adsorption capacity of the soil. Such influences of the texture and depths of the groundwater table on salinization and groundwater ascension were researched by the author in Ginau *et al.* (2013). It is worth mentioning that the former settlement sites lie almost entirely along the palaeorivers (Ginau *et al.*, 2019). The vegetation performance seems to be higher on the elevated areas along the palaeorivers. And often it seems as if the settlement sites lie not only along the palaeorivers but also in direct vicinity of the areas with best vegetation performances. Agricultural practices of the settlements comprised tapping of the Nile channels for irrigation of fields and concentrated floodings and accumulation of nutritious Nile material in the irrigated areas next to the settlements and could explain such patterns. These could be important plateaus or areas where larger amounts of flood deposits accreted along the rivers and therefore offered best agricultural conditions.

#### 3.6.6 Soil salinization and other applications

In general the area under study is at the margin between the ocean and the inner delta. In this region agriculture deals with severe problems and is at its limit. Here the agricultural landscape faces a low lying delta body with a shallow water table, the intrusion of marine sea waters and low quality of irrigation water at the end of the supply chain (Beltrán, 1999; Kashef, 1983; Sefelnasr & Sherif, 2014). Therefore, such factors affect the vegetation performance and emasculate the relationship between fertile archaeological soils and the vegetation performance.

Systematic studies have introduced the soil's salinity as an important factor affecting plant growth (Munns, 1993; Shrivastava & Kumar, 2015). Soil salinization possibly explains the lower vegetation performance in the areas surrounding lake Burullus in the northern half of the study region. Kotb *et al.* (2000) point out that croplands in

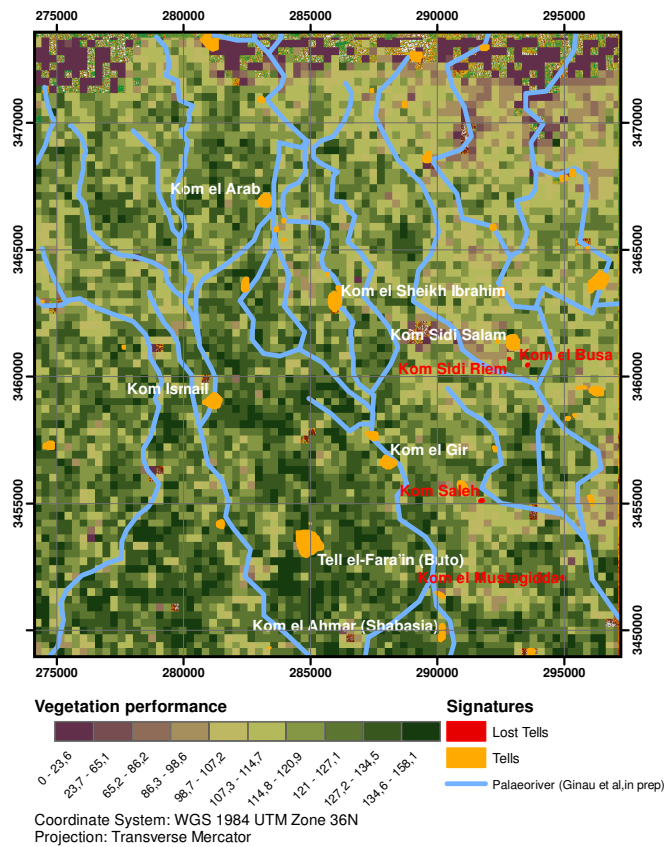


**Fig. 3.14: Vegetation performance in contrast to former palaeorivers** - The palaeorivers represent our recent state of research on our sedimentological analyzes in the area around Buto and detailed analyzes of a TanDEM-X elevation model supported by the German Aerospace Center (DLR)

### 3. ARTICLE 1, REMOTE SENSING ANALYSIS

---

Egypt are 100% irrigated and evaporation is very high. Thus, the intense irrigation of cropland under an arid climate is the main reason for secondary soil salinization. Previous work by the author in the Taklamakan desert (Ginau *et al.*, 2013) indicated that floods are important to desalinate and renew the soils. A cessation of floods in this area led to increasing soil salinization. The study region in the Nile delta may suffer the same fate as due to the termination of the nutritious Nile floods the washing of soils came to a halt. Such influence was demonstrated by Abd-El Monsef *et al.* (2015) in a study dealing exclusively with the environmental effects of the construction of the high damn of Aswan. El-Guindy (1989) indicates that the study area lies in the transition zone of moderately saline soils in the south and highly saline soils in the north. To balance the soils' salinity the following practices were introduced by the government and farmers: a better water management and land improvement programs, the use of sub-soiling or chiselling, leveling by laser beam (observed in the field), the cleaning of water courses (see Kotb *et al.*, 2000) and the cultivation of rice. Rice cultivation leads to the same effects as floodings as the fields are constantly provided with fresh water to keep a permanent water body over the field. For this reason soils regenerate and desalinate in the course of rice cultivation.

Field use classification results reveal that rice cultivation takes place throughout the area. In accordance with these findings El-Quosy (1994) states that rice cultivation occurs at an average of 50% in this area. Soils in the north are however still more affected by salinization as water quality decreases northwards. Results of the land-use classification in this study find a total area of rice fields of 1 %. However, this is partly because the date of classification lies after the rice harvest.

Most of the barren fields showed indications of rice cultivation. Counting barren fields as rice areas, the share of rice fields of the total area amounts to 15 %, which is still comparably lower than the results of El-Quosy (1994). But algorithms and methods of this study can also be adopted in other fields of remote sensing. Many studies focusing on remote sensing data covering the Nile delta deal with detection of land-use changes, surface characteristics and the phenomenon of urban sprawl (Belal & Moghanm, 2011; El-Asmar *et al.*, 2013; Elhag *et al.*, 2013; Shalaby, 2012). Methods presented in this study, however, allow the identification of unused agricultural areas and separation of urban areas on the basis of *NDVI* change detection that very likely enhances the quality of existing approaches. In general, knowledge about unused areas and the vegetation performance can be very important for planning and the designation of settlement areas to control the phenomenon of urban sprawl and protect agriculturally productive areas.

### 3.7 Conclusion

This study assessed methods for the identification and mapping of different classes of tells. The identification is based on the supervised classification of a set of images to monitor existing high tells. In a second approach, vegetation performances are calculated on the basis of *NDVI* time series derived from Landsat 8 and RapidEye imagery. The vegetation performance is indirectly related to the presence of nutritious ancient



settlement material in the subsoil and allows non-invasive discovery of lost tells. Especially the latter part that deals with the identification of lost tells via analyzing plant growth in *NDVI* time series is of high interest. Describing plant growth in the delta is difficult, as fields are very small, constantly change and show different plant covers. Only statistical measures and the analysis of *NDVI* time series helped to describe this plant growth for the Nile delta in a reliable way that allows the uncovering of lost tells or former river channels. The overall performance of results show that there exists a relationship between vegetation performance and the appearance of archaeological material in the topsoil and such information can be useful for planning of archaeological surveys. For example, our study showed that Kom esh-Scheikh Ibrahim had once been bigger and had extended further to the northwest. Interesting is the juxtaposition of vegetation performance with the location of the former palaeorivers. Remarkably areas of higher vegetation performances follow the course of these former palaeorivers researched by Ginou *et al.* (2019) because the levees of these former rivers were areas of deposition and aggradation of the nutritious Nile floods.

Nevertheless, several factors such as water availability or salinity largely affect plant growth and mask this relationship. These phenomena especially occur in the area situated in the transitional zone between sea and delta where agriculture is at the maximum tolerable limit. Additionally, this weak tangibility of the category of lost tells is not only related to the disturbed symbiosis between soil and vegetation but also a problem of recognition. The category of lost tells shows only small sizes and is hard to recognize in the image products.

Additionally, modern agricultural techniques comprising chemical fertilization and intensive irrigation contributed to a decoupling of the link between edaphic properties and the vegetation performance that was assessed in this study. Therefore, ascertained geochemical results proving the higher amounts of nutritious elements within the tell material only slightly exert influence on the growth of plants.

Nevertheless, the variation of the vegetation performance can be evidence of other environmental factors such as the soil's salinity. Similar to results on soil salinity, the vegetation performance reflects a north-south gradient. Low salinities correspond with high vegetation performances in the south while high soil salinities might negatively affect vegetation in the north.

Additionally, the analysis of the number of crop rotations and *NDVI* time series is a useful tool to differentiate and analyze agricultural space in the Nile delta. Analysis helps to separate settlements and enables identification of unused agricultural areas. Therefore, the methods used in this study may be of limited use in the identification of lost tells, but offer important insights on aspects of urban sprawl and agricultural space in the Nile delta and beyond.

The method design of this study is based on freely available Landsat data products as well as commercial RapidEye products. The RapidEye products were obtained for free in the course of a scientific application directed at BlackBridge Ltd.. Nowadays RapidEye is owned by Planet Labs. Classification of high tells can be easily extended to wider regions with the Landsat data, but precise contours of high tells can only be

### 3. ARTICLE 1, REMOTE SENSING ANALYSIS

---

achieved with costly higher resolution data. Identification of lost tells and analysis of *NDVI* time series could also be extended to a wider region or different regions but involves a lot more processing, automation and programming.

#### 3.8 Acknowledgments

We thank the Cairo Department of the German Archaeological Institute (DAI) for funding and support in the field. BlackBridge AG for delivering high resolution multispectral RapidEye images for RESA Projekt ID 1002. Landsat Data available from the U.S. Geological Survey.

4

# **Integrative geoarchaeological research on settlement patterns in the dynamic landscape of the northwestern Nile delta**

The identical content of this chapter was published in different formatting in:

Ginau, A., Schiestl, R., Wunderlich, J., 2019. Integrative geoarchaeological research on settlement patterns in the dynamic landscape of the northwestern Nile delta. *Quaternary International* 511, 51-67.

## 4. ARTICLE 2, INTEGRATIVE GEOARCHAEOLOGICAL RESEARCH

---

### 4.1 Abstract

Settlement activity in the Nile delta is characterized by its profound connection to the branches of the river Nile. Major ancient settlements were founded next to waterways. The constant shifting of these Nile branches – coming either too close or moving too far away – was a fundamental challenge for settlements. This research focuses on the region around Buto (Tell el-Fara'in) in the northwestern Nile delta. The massive increase in settlements in the Ptolemaic, Roman and in particular late Roman periods (4<sup>th</sup> c BC – 7<sup>th</sup> c AD) needs to be connected with a fundamental change in the landscape and the way people interacted with the landscape. A particular challenge to reconstructing the ancient land and waterscape was posed by the regional lack of an indicative modern surface relief. A linear settlement pattern of ancient sites was interpreted as showing the distribution along a defunct river branch. A combination of remote sensing data, in particular a new high resolution DEM based on TanDEM-X data, and a program of over thirty cores on the ground, have clarified the landscape, especially its fluvial pattern, and the placements of associated settlements. In the north of the study region, the DEM shows elevated levees of former palaeorivers belonging to a finely ramified subdelta, with all settlements placed on alluvial levees. The corings uncovered different artificial channels and identified ancient natural riverbeds at a deep level but similar depth, suggesting that the streams were active during the occupation of these sites and the ancient settlements were either in direct vicinity of the natural rivers or connected via artificial channels. These artificial channels found in corings next to the settlements show characteristics of slack water regimes.

In essence, the massive increase of settlements spread over the northwestern delta in Classical Antiquity was spurred by multiple branches that provided routes of transportation, fresh water for irrigation and good conditions for agriculture on their elevated and fertile levees

### 4.2 Introduction

Archaeological research suggests that large parts of the northwestern Nile delta had been widely settled since the Ptolemaic period (4<sup>th</sup> c BC – 1<sup>st</sup> c BC) with the settlement activity reaching its peak in the Roman and late Roman periods (1<sup>st</sup> c BC – 7<sup>th</sup> AD) (Schiestl, 2012a; Wilson, 2015). Previous archaeological and geoarchaeological research hypothesized that ancient settlements within the delta were closely related to branches of the Nile (Bietak, 1975). Up to seven major water courses flowing through the delta were described by classical authors from the 5<sup>th</sup> c BC to 4<sup>th</sup> c AD. It was suggested that settlements of this time period mainly flanked these branches as higher elevated levees along the channels served as appropriate places for settlement. Moreover, the delta branches of the Nile were important transport routes. However, a closer view to the pattern of ancient settlements indicates that they are not only confined to the few major natural water courses but are more widely spread over the whole delta plain. This might be due to the high variability and shifting of the water courses that caused

## 4.3 Historical and Geological setting of the Nile delta

---

the abandonment and new foundation of settlements. Furthermore, it has to be taken into account that a number of smaller channels and artificial canals must have existed within the delta giving rise to a dispersed settlement pattern.

In order to uncover the relationship between the highly variable waterscape and the settlement distribution in the northwestern Nile delta from the Ptolemaic to the late Roman period an integrated approach has been applied. It combines archaeological research, modern methods of remote sensing, and sedimentological studies on different spatial scales (see Fig. 4.2). The concept of this research is summarized in Fig. 4.1. On a large scale we juxtapose the location and distribution of archaeologically verified ancient settlements with the fluvial network which could be detected by means of a TanDEM-X DEM. The fluvial network manifests itself primarily via positive elevation anomalies in the form of former river levees, which later on were heavily transformed by agricultural usage as this could be verified with GPS measurements on the ground. On the smaller scale, individual core sites are studied in detail. The results serve as a ground truthing for larger-scale findings. Furthermore, results on the finer scale elucidate how settlements lying apart from major channels were possibly connected to these watercourses. Based on the analysis of sediments a differentiation between high energy (natural rivers) and low energy watercourses (man-made canals, oxbows) is suggested on the finer scale. Dating of former channels at different localities and analyzing their depth profiles can clarify whether we are dealing with a network of channels that existed in a certain period of time.

The following sections will give an overview of the research history on the fluvial landscape of the Nile delta based on various archaeological sources as well as on the results of landscape archaeological projects focusing on the reconstruction of watercourses and settlements in the Nile delta. Subsequently the settlement history and the physical setting of the study area in the northwestern Nile delta and relevant environmental changes and processes will be summarized. An integrative approach will be presented that combines archaeological findings, remote sensing data and sedimentological results from corings and we shed new light on the relationship between the Ptolemaic to late Roman settlement pattern, the waterscape and the environmental conditions to get a better understanding how a changing waterscape affected the occupation of the study area at distinct time periods.

## 4.3 Historical and Geological setting of the Nile delta

### 4.3.1 Research history on the fluvial landscape of the Nile delta

The investigations into the ancient landscape of the Nile delta have mostly focused on the reconstruction of the courses of defunct Nile branches. Other features of the ancient landscapes of the delta, such as lagoons, marshy regions, flood plains and the vegetation of the Nile delta, remain much less studied (for an up to date overview see Pennington *et al.* (2017)). This prioritization is due to the archaeological background of most research and the linking of watercourses and settlements, the latter mostly

## 4. ARTICLE 2, INTEGRATIVE GEOARCHAEOLOGICAL RESEARCH

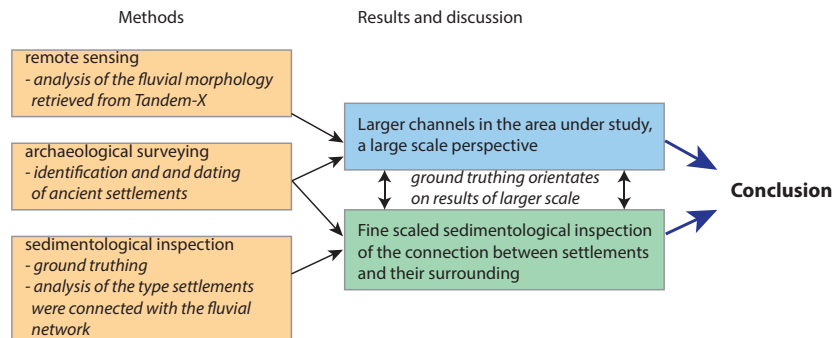


**Fig. 4.1: Research design** - The design gives an overview of this research. The different entities relate to the sections within this article.

representing the primary research interest. The first suggestions for reconstructions of river branches were based on textual sources from classical antiquity. Classical authors from the 5<sup>th</sup> c BC to 4<sup>th</sup> c AD have named and described, in varying detail, the branches and mouths of the Nile. Most authors (Diodorus, 1<sup>st</sup> c BC; Strabo, 1<sup>st</sup> c AD; Pomponius Mela, 1<sup>st</sup> c AD; Ammianus Marcellinus, 4<sup>th</sup> c AD) list seven mouths of the Nile, with different names and courses (Ball, 1942; Toussoun, 1922). The existence of further smaller mouths, connected to minor branches, is occasionally mentioned, for example, by Diodorus (Oldfather, 1933) and Strabo (Radt, 2005), but these smaller features remain mostly nameless. Human intervention into the waterscape is already mentioned in the earliest source, Herodotus (5<sup>th</sup> c BC), who notes two man-made mouths, the Bolbitine and the Bucolic (Feix, 2006). By the 1<sup>st</sup> c BC the Bolbitine was, however, considered natural and no longer is listed among the man-made mouths (Diodorus). Ptolemy (2<sup>nd</sup> c AD) lists nine mouths and six branches of the Nile (Stückelberger *et al.*, 2006) and gives the greatest amount of detail on the location of the water courses, providing coordinates and the relationship to important cities. However even this data, lacking details, allows only very rough placements of branches. Modern maps of the ancient delta (Kessler *et al.*, 1980; Talbert, 2000; Wittke *et al.*, 2012) have two fundamental shortcomings: firstly, they depict branches whose courses are unknown. The courses shown are essentially rough approximations. Secondly, maps tend to present an ahistorical static image, failing to convey the dynamic changes of the fluvial system over time. The maps of the *Tübinger Atlas des Vorderen Orients* and *Historischer Atlas der Antiken Welt* show the same fluvial system with nine mouths of Nile branches from the Old Kingdom (Kessler *et al.*, 1980; Wittke *et al.*, 2012) to the Third Intermediate Period 1st millennium BC, (Gomaà *et al.*, 1977; Wittke *et al.*, 2012), whereas the system is based on the description of Ptolemy of the mid 2<sup>nd</sup> c AD.

To date only the courses of two historic Nile branches have been reconstructed in their entirety and in detailed resolution, namely the Tanitic and the Pelusiac branches in the eastern delta (Bietak, 1975). Sections of the course of the Canopic branch in the western delta have been traced (Cooper, 2014; El-Qady *et al.*, 2011; Pennington & Thomas, 2016; Stanley & Jorstad, 2006; Wilson & Grigoropoulos, 2009). The fol-

### 4.3 Historical and Geological setting of the Nile delta

---

lowing provides a brief overview over the methods employed (for a recent summary see also Zakrzewski *et al.* (2016)). The Pelusiac and Tanitic branches of the Nile were reconstructed based on the tracing of raised linear features by means of contour lines on maps (Bietak, 1975; Shafei, 1946). These elevated features represent alluvial levees created by the sedimentation of active river branches. The data of the surface relief was combined with textual sources, both from the Pharaonic period and classical antiquity, to provide the first full length Nile branch reconstructions.

Egypt has a rich tradition of historic maps, which show both topographic features and numerous ancient settlements which have disappeared since the publication of the maps. Of central importance for the delta are the maps of the Napoleonic expedition (1:100.000 Jacotin & Jomard, 1828), the El-Falaki map of 1871 (1:100.000), and the series of Survey of Egypt maps, from the late 19<sup>th</sup> c to the 1930s (scales 1:25.000, 1:50.000, 1:100.000). The distribution of sites in certain significant linear patterns can be indicative of ancient watercourses which connected these sites. This has been used as a guideline for the courses of the Tanitic and Pelusiac branches (Bietak, 1975), discussed above, the lower reaches of the Pelusiac branch (Sneh & Weissbrod, 1973) or at the western edge of the delta (Bunbury *et al.*, 2014; Trampier *et al.*, 2013; Trampier, 2014). Reconstructing Nile branches by tracing levees can only be applied to levees visible on the surface. Areas with barely formed levees, such as some lower reaches of rivers, levees submerged by alluvial layers and levees levelled by natural or man-made activities, prevent the use of this method. Field walking was applied to the clarification of the lower reaches of the Pelusiac branch. A slight physical depression, changes in color and properties of the surface were detected, permitting the reconstruction of the lower reaches flowing through the plain of the northeastern delta (Sneh & Weissbrod, 1973). Remote sensing methods have been introduced only relatively recently: aerial photographs were evaluated for the north eastern delta in the early 1970s (Sneh & Weissbrod, 1973). Landsat satellite imagery had been used for geologic purposes in the delta since the 1970s (El Shazly *et al.*, 1975) and was applied for the detection of ancient water courses in the northwestern delta (Wunderlich, 1989). SPOT and SOYUZ satellite images were used to study the lower reaches of the Pelusiac branch and the changes in the coastline of the northeastern delta (Marcolongo, 1992) and satellite imagery also was the basis for a suggested course of the Canopic branch of the Nile (Wilson & Grigoropoulos, 2009). Corona satellite images from the late 1960s and 1970s are the earliest regional satellite images which, however, only became generally available recently. They served as basis for studies of the Pelusiac branch of the Nile (Moshier & El-Kalani, 2008) and the ancient waterscape of the western edge of the delta (Trampier *et al.*, 2013; Trampier, 2014). Shuttle Radar Topography Mission (SRTM) data was used to clarify the lower reaches of the Canopic branch of the Nile (Stanley & Jorstad, 2006).

Submerged levees were first traced by means of a substantial coring program by the Amsterdam University Survey in the eastern delta (Sewuster & van Wesemael, 1987; van Wesemael, 1988), in the course of which both major and minor branches were detected. Core transects were placed perpendicular to assumed river courses, connecting

#### 4. ARTICLE 2, INTEGRATIVE GEOARCHAEOLOGICAL RESEARCH

---

elevated sand mounds, so called *geziras* (Arab. islands) and turtle backs (Butzer, 1976; Pennington *et al.*, 2017; Wunderlich, 1989), where settlements were located. Large scale corings were undertaken in the northwestern delta (Wunderlich, 1989, 1993; Wunderlich & Andres, 1991) and the northeastern delta (Andres & Wunderlich, 1991). In the latter region, the area of Tell el-Dab'a/Avaris (Dorner, 1993/1994, 1999), 850 cores served as the basis for the reconstruction of the course of the Pelusiac branch at the ancient cities of Avaris and Piramesse. Coring was also conducted around Sais (Wilson *et al.*, 2006) and at Naukratis, where the relationship of that town to the Canopic branch has been established with certainty (Pennington & Thomas, 2016). Electrical resistivity tomography served as the basis for delineating buried channels in the central delta (El-Gamili, 1988; El-Gamili *et al.*, 2001) and sections of the Canopic branch (El-Gamili *et al.*, 1994; Pennington & Thomas, 2016). Magnetic investigations have also been added to the study of water courses (Fattah & Frihy, 1988; Pennington & Thomas, 2016). In general, most projects currently combine above mentioned methods, depending on the specific questions addressed. To summarize, research has focused on the western and eastern parts of the delta. The central delta remains understudied – in archaeological terms, as well as concerning the ancient landscape and its water courses.

While most archaeological projects in the delta address issues of the ancient landscape, it is now generally done on a local or regional scale. New methods have led to the intensification of research, but also a reduction in spatial scope. This, on the one hand, allows for new levels of detail and constructions are investigated in connection with waterways, such as inland harbors (river ports), reinforced riverbanks, terracing and quays. Such features are evaluated, for example, at Avaris/Tell el-Dab'a (Herbich & Forstner-Müller, 2013; Tronchère *et al.*, 2008), Naukratis (Thomas, 2014; Thomas & Villing, 2013) and at Schedia (Bergmann & Heinzelmänn, 2015). Smaller waterways and canals are also being investigated, e.g. at Naukratis (Thomas, 2015), and the local connection to the larger waterscape (Bunbury *et al.*, 2014), as well as the width and depth of larger waterways, which is crucial for inferring ship capacities (Pennington & Thomas, 2016; Tronchère *et al.*, 2012). On the other hand, the reconstruction of the entire length of branches has faded to the background and is currently not being tackled.

Dating of the ancient watercourses remains a major challenge. There are two approaches, an archaeological and a natural scientific one. By means of archaeological data, watercourses are, on a general level, dated by the association with dated settlements flanking the route. On a more detailed level, archaeological artefacts, generally pottery embedded in sediment cores, serve as indicators for dating (Toonen *et al.*, 2017). The transportation and redeposition of such material in a fluvial environment, however, weakens this method as a dating tool. By scientific means, the crucial dating tool for fluvial deposits, OSL (Optically Stimulated Luminescence) dating, is not possible in Egypt. Based on sedimentation rates, the thickness of sediments has been used as a general dating tool (Sewuster & van Wesemael, 1987). Radiocarbon dates currently provide crucial chronological anchors. For example, based on a  $^{14}\text{C}$  date the end of the activity of the Pelusiac branch was dated to the first half of the 1<sup>st</sup> c AD (Sneh &



Weissbrod, 1973).

#### 4.3.2 Research history of ancient settlements in the study region

Our current level of knowledge of the settlement history of the northwestern delta remains sparse and uneven. The annual Nile flood covered most of the delta plain with water. In order for settlements to remain dry, the delta only provided two elevated areas above the flood line: Holocene (western delta) or Pleistocene (eastern delta) turtle backs or geziras and the alluvial levees of active or former Nile branches. There is, however, also evidence for ancient settlements in the alluvial plain (Sais, Wilson & Grigoropoulos (2009), and possibly Ezbet el Qerdahi, Wunderlich *et al.* (1989)). The occupation of the large important site of Buto (Tell el-Fara'in) has been intensively studied. Its settlement history is unusual in two respects: its great age and a long interruption. It was founded in the 4<sup>th</sup> millennium and the latest traces of occupation are from the Early Islamic period (7<sup>th</sup> c AD). This early occupation and very long settlement history is unique in the region. This long settlement continuity, however, is interrupted by a major gap: between the late Old Kingdom (late 3<sup>rd</sup> millennium BC) and the Third Intermediate Period (early 1<sup>st</sup> millennium BC), there is no evidence of occupation (Ballet *et al.*, 2011; Hartung *et al.*, 2009). The site seems to have been abandoned as a settlement for almost 1500 years, with possibly only the important temple of Wadjet, the main goddess of the site, persisting (Bedier, 1994; Schiestl, 2012b). The reason for this settlement gap remains unclear, but partial flooding of the late Old Kingdom site point to environmental reasons, possibly caused by a shifting Nile branch (Hartung *et al.*, 2009).

The hinterland of Buto (Tell el-Fara'in) has long been archaeologically neglected and its settlement history remains only partially understood. Following some early small scale investigations (Daressy, 1926; Edgar, 1911; Hogarth, 1904; Petrie, 1896; Petrie *et al.*, 1905) it was only in recent decades that more field surveys took this region into focus (Ballet & von der Way, 1993; Schiestl, 2012a, 2015; Schiestl & Rosenow, 2016; Spencer, 1992; Wilson, 2012a,b, 2015; Wilson & Grigoropoulos, 2009) and <https://www.ees.ac.uk/delta-survey>.

#### 4.3.3 Physical setting and environmental history

The current Nile delta is traversed by two large branches of the Nile, that of Rosette and that of Damietta, and numerous smaller watercourses. In the northwestern delta, most of the watercourses are man-made and consist of a system of drains and canals cut mostly since the late 19<sup>th</sup> c AD, when this part of the delta was being developed for modern agricultural purposes. The research area (Fig. 4.2) lies about 7 km south of the Burullus Lake and 20 km south of the Mediterranean coast. The land surface of the delta is almost flat with slight elevation differences of only several meters (Butzer, 1975; Wunderlich, 1989). The delta plain slightly dips for 15 m over a distance of 170 km from Cairo in a north-northwest direction to the coastline. The modern landscape is entirely covered by fields to grow crops, and settlements, which are rapidly expanding.

#### 4. ARTICLE 2, INTEGRATIVE GEOARCHAEOLOGICAL RESEARCH

---

No natural environment remains within this densely settled and agriculturally intensely used delta (Said, 1993).

The ancient landscape is obscured by the natural sedimentation of the yearly Nile flood, which ultimately ended in the 1970s with the construction of the Aswan High dam and the sediments being trapped in lake Nasser. Processes such as sea level changes, tectonic and isostatic movements also control the evolution of the Nile delta and are subject to many studies (Arbouille & Stanley, 1991; Butzer, 1975; Krom *et al.*, 2002; Marriner *et al.*, 2012b; Pennington *et al.*, 2017; Stanley & Warne, 1993). In summary, the modern surface relief and the current waterscape seem to offer very few traces of the ancient landscape. The investigations into the ancient landscape of this region by J. Wunderlich in the 1980s (Wunderlich, 1988, 1989, 1993) fundamentally changed our understanding of the northwestern delta. This large scale sediment core program showed that after the late Pleistocene, the flat delta body with local dunes and deeply incised main channels was affected by transgression due to rapid sea level rise. This caused a southward movement of the coastline and the deposition of peat layers on top of the former Pleistocene surface at about 5000 cal BC. Remnants of this great landscape change shaped the early period of Buto's occupation. A marshy region, a precursor of the later Burullus lake, extended much further south, rendering the region between Buto and the coast unsuitable for permanent settlements. This was followed by a phase of decreasing sea level rise and increasing clastic sedimentation which caused this movement to rebound and the marshy environment moved northwards again. Since then the floodplain deposits are constantly aggrading in the delta and nowadays cover former levees, dunes or slowly growing settlements reaching thicknesses of about 7 to 10 m (Wunderlich, 1989). What remains unclear as of yet is the date and the pace of landscape changes which permitted settling or caused abandonment in this region. The general stratigraphy of Wunderlich (1989) focused on larger scaled changes, namely the change from brackish lagoonal conditions to the development of the Nile floodplain. It does not further differentiate the Holocene floodplain deposits, which accumulated during about four millennia, and roughly amalgamates these sediments as a single homogeneous unit.

The present study focuses on the development of this sediment sequence and the information contained therein about changes of the fluvial system and the settlement history of this region. In a study on the Mississippi River, which serves as a standard for interpreting fine-grained floodplain deposits of meandering rivers, Aslan & Autin (1999) showed that floodplains develop by overbank flooding, crevassing and avulsion. Especially the latter processes leave behind a complex alluvial architecture with a high local variety in texture. Nile river arms as well constantly changed their courses, vanished, reappeared or even fanned out (see section 4.3.1) into several smaller channels. In the Mississippi delta Aslan *et al.* (2005) demonstrated that avulsions were a key process in the development of river channel belts and subdeltas.

Within the channels coarser material is deposited that differs in texture from the finer grained levees and the silty to clayey floodplain deposits. Especially the shifting meander belts cause a sediment body of remarkable thickness and horizontally and vertically

### 4.3 Historical and Geological setting of the Nile delta

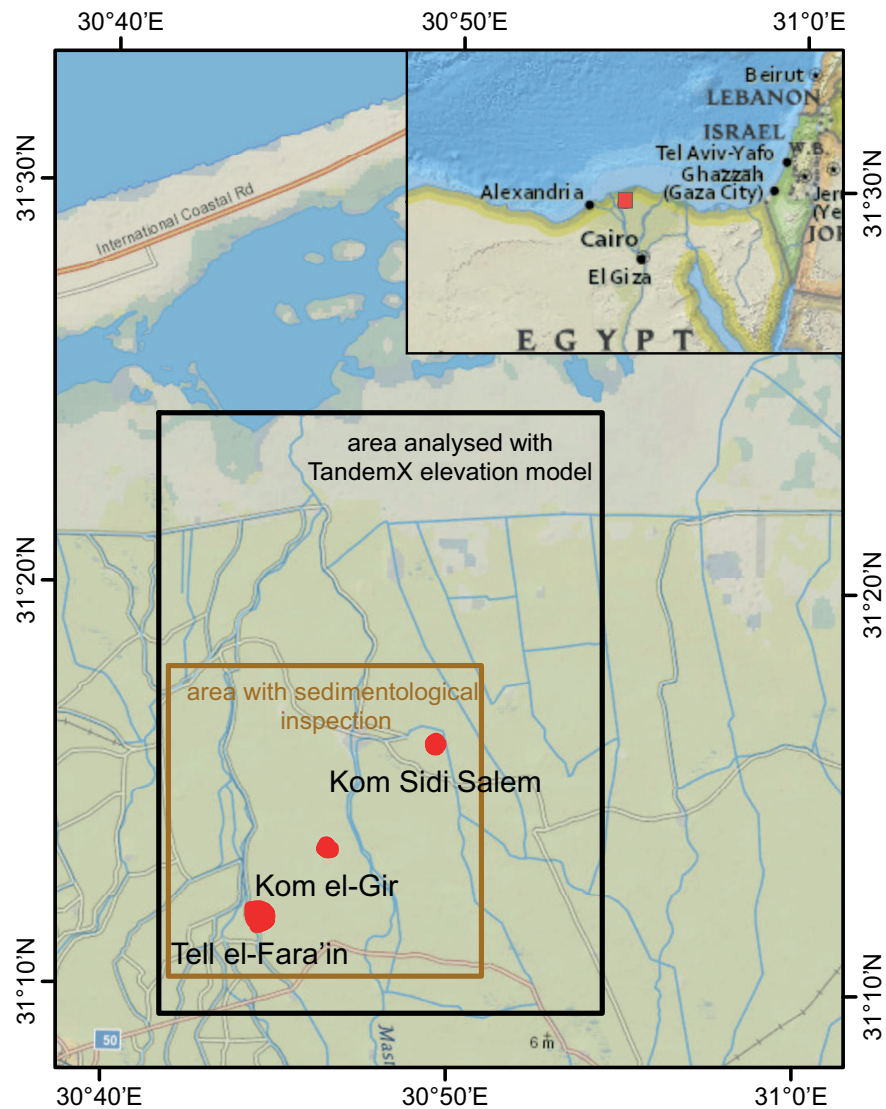


**Fig. 4.2: Location of the study area** - The study area is located in the northwestern Nile delta and comprises the area of the TanDEM-X (large scale approach) model and the area with the sedimentological inspection (small scale approach). Most important tells (red) and settlements are illustrated. Map Copyright 2014 Esri, Sources: National Geographic, Esri, DeLorme, HERE, UNEP-WCMC, USGS, NASA, ESA, METI, NRCAN, BEBCO, NOAA, increment P Corp.

## 4. ARTICLE 2, INTEGRATIVE GEOARCHAEOLOGICAL RESEARCH

---

varying texture of sediment (Aslan & Autin, 1999).

Within this context, levees are of special interest. They appear as positive height anomalies along rivers. Especially the latter qualifies levees as important witnesses for rivers in contour maps (Bietak, 1975; Shafei, 1946) or high resolution elevation models processed from Lidar and TanDEM-X elevation data (Erasmí *et al.*, 2014; Palaseanu-Lovejoy *et al.*, 2014). According to Branß *et al.* (2016), levees form directly next to the main channel. They show a steep slope directed towards the channel and fall off gradually towards the floodplain. Levees tend to be made of fine sand, but grain size decreases with transport distances, resulting in the fining-up of sediments towards the floodplain (Aslan & Autin, 1999; Cazanacli & Smith, 1998; Smith & Pérez-Arlucea, 2008). Additionally, the slope of the levees decreases with the average grain size decrease (Cazanacli & Smith, 1998). In the Nile delta floodplain levees reach some meters in height with a wide lengthwise extension and a convex body that very slightly dips towards the floodplain (Butzer, 1976). The absence of visible indications for the ancient landscape on the modern surface terrain, in particular in the southern part of the study region, led to the application of the integrative approach discussed in the following.

### 4.4 Methods

Our methods focus on two different scales. On a larger scale archaeological prospection aimed at the localization, documentation, and dating of ancient sites (section 4.4.1) This was supported by recent satellite imagery which furthermore were analyzed to trace levees of ancient watercourses (section 4.4.2).

On a smaller scale landscape units and ancient watercourses were studied via coring (section 4.4.3). The core localities were chosen based on their proximity to archaeologically relevant settlement sites. Our core transects focused on the transition between the settlements and the closer environment. Methods applied at this smaller scale concentrate on pinpointing ancient river channels and by chance we reached fluvial sediments of ancient watercourses.

#### 4.4.1 Archaeological methods

The region investigated by archaeological means (Schiestl, 2012a,b, 2015) overlaps with, but is not identical to, the study region discussed here. The survey region is bordered approximately by the area of Kom Sidi Salem in the North, the modern towns of Qellin in the South, Kafr esh-Sheikh in the East and by Buto (Tell el-Fara'in) in the West (Schiestl, 2012b, fig.1). As no prior systematic survey of the region had taken place, the aims of the archaeological investigation of the region were primarily threefold: firstly, location and identification of ancient sites, secondly, documentation and further prospection of these sites based on field walking, and thirdly, dating of the occupation of the sites based on pottery fragments from the surface and from core material. The identification of sites in agricultural lands is challenged by an Egyptian particularity: the wide spread use of ancient settlement remains (sebakh) as fertilizer on fields (Bai-

ley, 1999; Quickel & Williams, 2016). The ceramic sherds embedded in this material were thus dislocated from their original context and redistributed. Surface material alone cannot be considered an indicator for ancient activity. Positive identification of ancient sites requires further evidence. Therefore, within the survey region areas of interest were defined which were investigated more closely on the ground. The areas were chosen based on information from historical maps, editions of 1828, 1872, 1900s–1930s and 1940s, aerial photography from the 1950s, Corona satellite images from 1968 and satellite images from Google Earth from the 2000s. The areas of interest are composed of ancient settlement sites, tells, rising above the surrounding ground, partially or entirely leveled ancient sites, identified based on historic maps, and elevated areas identified on historic topographic maps, mainly the Survey of Egypt editions, 1:25.000, from the 1920s/30s. 31 sites were investigated by field walking in these designated areas and their current state was documented. Combining this information with changes traceable on satellite images, in particular the Corona images from 1968, and historic maps, in particular the Survey of Egypt series from the 1920s/30s, allows us to document the taphonomic processes affecting the site, primarily shrinkage and leveling of sites (Schiestl, 2012b). Dating of sites is primarily based on pottery sherds collected on the surface. Other artifact categories encountered are glass sherds, coins, metal objects and stone objects, but these play quantitatively a minor role. The pottery is dated typologically based on comparisons with dated examples from other sites. Additionally, 43 cores were placed at 14 sites in order to investigate the land the settlements were founded on and to retrieve pottery fragments from lower layers.

#### 4.4.2 TanDEM-X digital elevation model

Elevation data is of high importance in geoarchaeology, especially when working on a broader landscape scale in flat areas. The TanDEM-X satellite formation consists of two twin radar satellites flying in close formation to allow precise digital elevation measurements based on state-of-the-art radar technology. The TanDEM-X digital elevation model (DEM) is available globally and shows a pixel spacing of up to 12 m and with less than 10 m absolute vertical accuracy and around 2 m relative vertical accuracy in flat terrains (DLR Product Specification). Especially the new TanDEM-X data enhances the detection of fluvial structures significantly and allows a view of the Nile delta at a very detailed perspective. To give better quality information, the relative vertical accuracy was estimated via comparison with ICESAT elevation data (see Fig. 4.3, Zwally *et al.* (2011)). Several studies (Erasmi *et al.*, 2014; Huber *et al.*, 2009; Rao *et al.*, 2014) showed the potential of ICESAT data for the quality assessment of TanDEM-X elevation data. Results of this quality assessment show that height residuals between ICESAT and TanDEM-X data stay around 0.7 m (1sigma). TanDEM-X data reflects the surface and consequently settlements and other solid man-made structures appear within the TanDEM-X model.

Vegetation, especially fields with higher canopies, only slightly manifests itself within the data as the X-band waves partly penetrate vegetation. In general, Pipaud

## 4. ARTICLE 2, INTEGRATIVE GEOARCHAEOLOGICAL RESEARCH

*et al.* (2015) showed the great potential of the TanDEM-X DEM for geomorphological applications in high mountainous areas in Tibet. This potential can be expanded to flat terrains such as the Nile delta as the TanDEM-X elevation data allows for the detection of levees and other geomorphologic structures in unprecedented spatial resolution. A similar geoarchaeological approach was pursued by Erasmi *et al.* (2014) in the Cilician Plain in Turkey. Erasmi *et al.* (2014) focused on the potential of high resolution TanDEM-X data for the detection of landscape features such as ancient settlements and geomorphological elements and successfully uncovered old river patterns and levees of the river Seyhan in their region under study. Such structures are expected to occur in the Nile delta and manifest themselves with very low detail in SRTM data. But as Erasmi *et al.* (2014) state “the level of detail of the TanDEM-X DEM allows for a more detailed analysis of the shape and depth of those objects”.

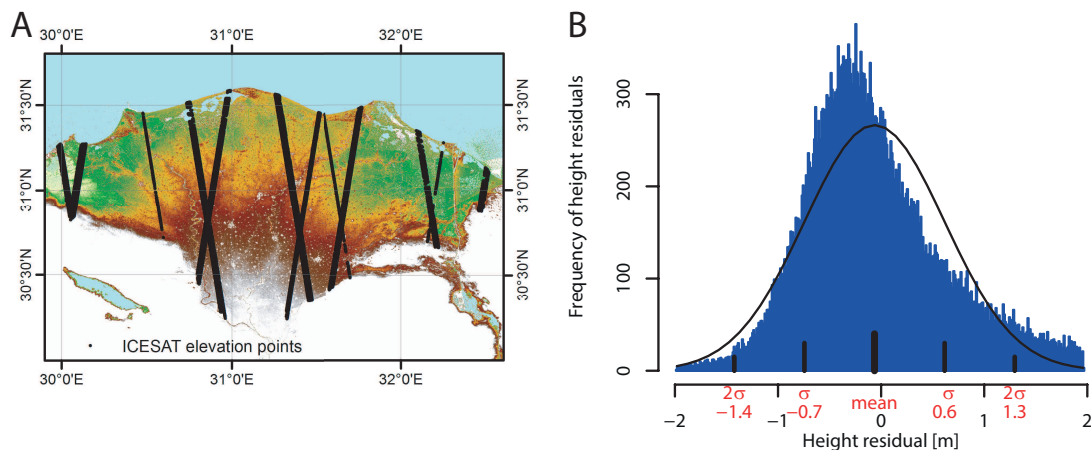


**Fig. 4.3: Quality of TanDEM-X** - Quality of the TanDEM-X is estimated for the Nile delta plain via comparison with ICESAT elevation data (Zwally *et al.*, 2011). The map (A) shows the location of the ICESAT points. The histogram (B) shows the frequency of the height residuals. TanDEM-X and ICESAT height distributions are adjusted to fit the same mean value and residuals are calculated. Additionally, outliers and ICESAT points lying on water areas are removed. The water areas are masked from Landsat 8 surface reflectance quality assessment (qa) band data of scenes acquired between April 2013 and July 2017

### 4.4.3 Corings and geochemical analyzes

The lithology of the subsurface was obtained by means of a vibracoring device (Wacker BH65) and open steel probes with varying diameters (6.0, 5.0 and 4.0 cm) and 1 m length. Especially the extraction of sediment via coring (Stein, 1986) keeps sedimentary structures and boundaries between different layers intact. The sediment cores were described in the field in terms of color (Munsell Soil Color Charts), grain size and

rounding, texture and carbonate content according to Eckelmann *et al.* (2006). Organic material was taken for radiocarbon dating and archaeological remains were used for age estimation.  $^{14}\text{C}$  dates were calibrated with Calib Rev 7.1 using IntCal13 and stated using the 2 sigma error range. For every age mentioned in the text the Radiocarbon age and the calibrated age is provided in the text. Dateable ceramic fragments were picked out by hand and analyzed by Peter French and Rita Hartmann. The sherds occurred abundantly only in very close vicinity to the settlement sites. In most cases ceramic pieces were very scarce, badly preserved and not very indicative, as they were often present within fluvial deposits, and rounded. Therefore, the dating can often be only considered a rough estimate.

The bore holes were placed along different transects with the main transects leading away from the settlement sites of Buto and Kom el'Gir and other transects focused on the levees in the north and the Bahr Nashart depression lying east of Kom el'Gir. These transects cross the delta with distances between neighboring cores of about 500 m or less. Geochemical analysis on the sample material of the corings was conducted with a Niton XL3t 980He portable XRF (pXRF) analyzer equipped with a Ag-Anode. The pXRF instrument runs at tube voltages of 9 to 50 kV and at beam currents of 0 – 40  $\mu\text{A}$ . A helium purge was used to enhance quantitative measurements of light elements, of which phosphorus is most important. The XRF spectra were quantified using a fundamental parameter algorithm "Testall geo" that combines the mining and soil mode and which is supported by the device. The measurement time was set to 180 s. To optimize the results and gather information on the accuracy of the device to detect certain elements, certified reference materials ( $\text{SiO}_2$ , NIST2780, Till4) and our own local standards, characteristic samples of our corings, were measured during each measurement series and statistical parameters such as standard deviation and mean were calculated. Precision of measurement is expressed with the coefficient of variation, which is the share of the standard deviation (2 sigma) to the mean. The element data presented within this study show the coefficients of variation given in table 4.1. Additionally, the handling of the samples was standardized in order to provide reproducible measurement conditions and to reduce influences of the sample matrix and sample surface. All samples were oven dried at 100 °C, homogenized with an achat mortar and sealed in certified XRF sample cylinders using a 4  $\mu\text{m}$  XRF foil to allow best penetration of the analyzation and fluorescence radiation.

## 4.5 Results and Discussion

Results are presented and discussed regarding the archaeological prospection and the two different spatial scales which were defined earlier. Results of the larger scale show that nearly all settlements in the Nile delta lie directly next to former rivers or in close vicinity (see Figs. 4.4 and 4.5). On a small scale we sampled several identified watercourses, landscape units and settlements and the transects cover the transition from the settlements to their wider surrounding. At this scale we could verify that the surrounding of settlements sampled via corings and sedimentological inspection reveals

## 4. ARTICLE 2, INTEGRATIVE GEOARCHAEOLOGICAL RESEARCH

---

**Table 4.1:** Coefficients of variation for elements used within this study.

<b>Al</b>	4.50%	<b>Nb</b>	16.90%	<b>Sr</b>	1.40%
<b>Ba</b>	4.40%	<b>Ni</b>	12.70%	<b>Te</b>	32.10%
<b>Ca</b>	2.15%	<b>P</b>	21.40%	<b>Ti</b>	2.20%
<b>Cr</b>	8.70%	<b>Pb</b>	3.40%	<b>U</b>	31%
<b>Cs</b>	11%	<b>Rb</b>	1.70%	<b>V</b>	9%
<b>Cu</b>	3.70%	<b>S</b>	2.50%	<b>W</b>	27.80%
<b>Fe</b>	0.10%	<b>Sb</b>	19.70%	<b>Y</b>	11.40%
<b>K</b>	1%	<b>Sc</b>	42.40%	<b>Zn</b>	5.30%
<b>Mg</b>	11.30%	<b>Si</b>	2.30%	<b>Zr</b>	2.50%
<b>Mn</b>	5.40%	<b>Sn</b>	20.70%		

associated channels. These channels are also of artificial origin and likely linked with the natural rivers present in the area. These findings are presented and discussed in detail according to the two scales adopted within this study.

### 4.5.1 Archaeological results

To summarize the results of the archaeological survey: numerous new settlements could be documented, none, however, with a settlement history as long as Buto. Identification and closer inspection of archaeological sites in the survey region was difficult as most sites are overbuilt by modern cemeteries and settlements. Many sites are partially or entirely leveled. Free standing, non-overbuilt sites, are the exception (Schiestl, 2012b). This picture changes when moving to the northern part of the study region and in particular to the region between Kom Sidi Salem and the Burullus lagoon (Figs. 4.2, 4.4). This region shows a large amount of remarkably well preserved free standing and non-overbuilt sites. As no site in this region has yet been excavated, dating of these sites relies to date on pottery from surface surveys and corings. The following picture has emerged for the settlement history of this region: In the vicinity of Buto (Tell el-Fara'in) there is evidence of traces of further early sites from the 4<sup>th</sup> millennium BC (Wunderlich, 1989). These remain, however, exceptional. What follows is a very long gap: no settlements of the 3<sup>rd</sup> or 2<sup>nd</sup> millennium BC are to date documented on a regional scale. The early 1<sup>st</sup> millennium BC provides the first evidence for new settlements, such as at Kom Asfar. This is followed by a period of growth in the Ptolemaic period, and strong growth in the Roman and late Roman periods (Schiestl, 2012b; Schiestl & Rosenow, 2016; Wilson, 2012b, 2017; Wilson & Grigoropoulos, 2009, 4<sup>th</sup> c BC – 7<sup>th</sup> c AD). Some sites show continuity into the Early Islamic period. Individual sites, such as Kom Sidi Salem, contain substantial amounts of Medieval remains. The wide spread settlement growth in the northwestern delta can only be understood in connection with a fundamental change in the ancient waterscape and landscape. The basis for the



economic development of this region must have been a network of Nile branches, in order to provide for the settlements, the irrigation of fields and the transport routes for people and goods. The modern surface offers no indication of the ancient land- and waterscape. Based on the settlement pattern, a linear distribution was interpreted as possibly flanking a central defunct Nile branch, roughly where today the Bahr Nashart and Masraf Nashart flow. The term Bahr refers to a larger irrigation watercourse and Masraf to a drain. This hypothesis was to be tested by the integrated methods of remote sensing, in particular the TanDEM-X DEM, and sedimentological ground truthing with corings.

### 4.5.2 Larger channels in the area under study, a large scale perspective

In the Nile delta, the TanDEM-X DEM allows the visualization of traces of levees which are not visible with the naked eye (Fig. 4.4). Only the largest of these levees are traceable on historic maps, even on the detailed topographic maps of Survey of Egypt (1:25.000, 1920s/30s editions). With the new data, a picture emerges of a subdelta of finely ramified larger and smaller branches between Kom el'Gir and the Burullus lagoon. The levees are isolated in Fig. 4.5 via thresholding for heights between 17.6 and 20 m and applying focal median filtering. They mostly appear as single elongated ridges which evolved when both levees flanking a channel merged together. Only in few cases are both levees still preserved with a channel depression in between. Palaeorivers are reconstructed based on the evidence of the levees and highlighted with blue lines.

It becomes evident that all settlements in this region (see Fig. 4.5) are situated on levees alongside these palaeorivers. Very likely the levees in the delta did not only attract settlements as safe and elevated places along rivers. The levees also offered best conditions for agriculture with high soil fertility and access to irrigation water. Ginau *et al.* (2017) studied vegetation performances in the Nile delta on the basis of NDVI time series. In their results, the areas along the palaeorivers, namely the elevated levees that slightly dip away from the channels, show highest vegetation performances. Several factors contribute to the high vegetation performances. Nutritious Nile flood deposits accumulate primarily on the levees and best soils formed along the rivers. Secondly, higher elevation and coarser sediments reduce ascension of groundwater and prevent soil salinization (Ginau *et al.*, 2013, 2017). Results of Ginau *et al.* (2017) also showed that large settlement mounds show larger areas of high vegetation performances in their surroundings. They state that agricultural practices comprise tapping of the Nile channels for irrigation of fields resulting in the accumulation of nutritious Nile material in the irrigated areas next to the settlements which can explain the observed patterns of vegetation performance. The eccentric position of some settlements on the elongated ridges is notable, e.g. Kom el-Arab, Kom Sheikh Ibrahim and Tell Alawi are lying on the western side, Kom el-Misk, Kom Bondoq on the eastern side. These positions place the sites on the western bank and eastern bank of the branches respectively. Kom el-Nashwia actually is a double site, as expressed by the second name, Kom el-Nashawein,

#### 4. ARTICLE 2, INTEGRATIVE GEOARCHAEOLOGICAL RESEARCH

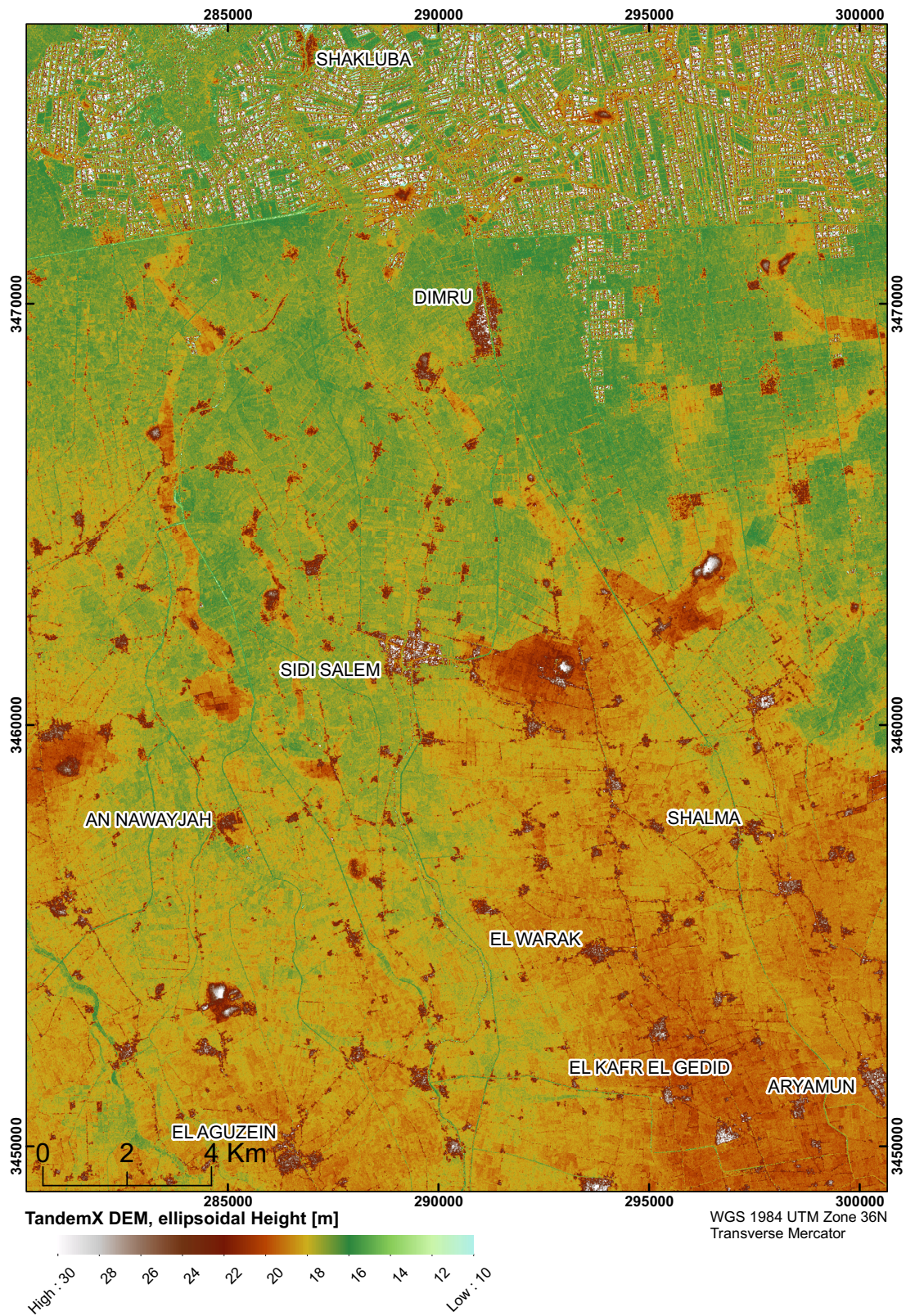


**Fig. 4.4:** TanDEM-X DEM - Undisturbed elevation models including names of prominent modern settlements. TanDEM-X elevation map (German Aerospace Center, DLR).

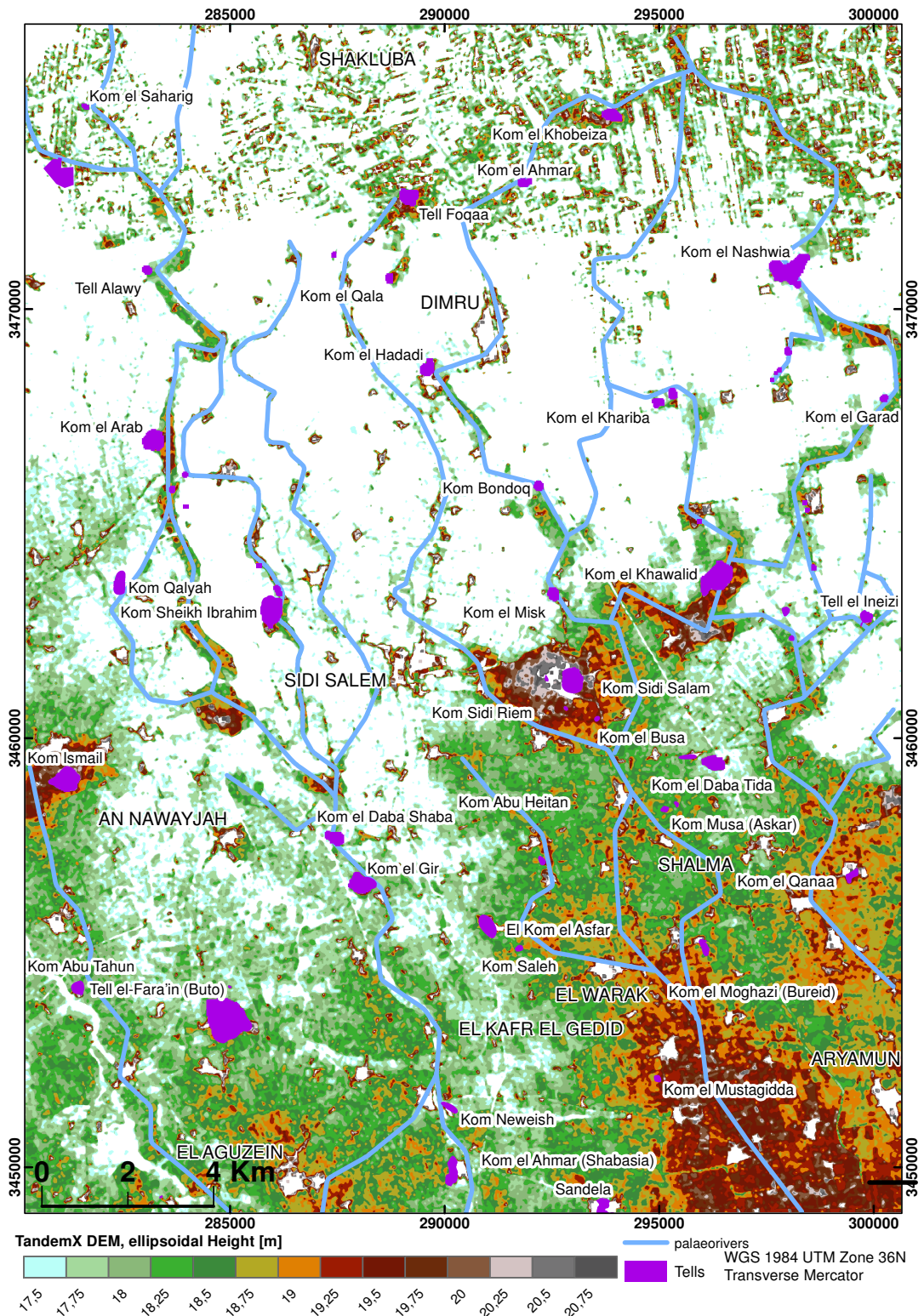


**Fig. 4.5: Thresholded TanDEM-X DEM** - Elevation values are thresholded for elevations lying between 17.6 and 20 m. Prominent palaeorivers are highlighted with lines. Additionally position and names of ancient settlements are included as well as modern settlements highlighted with capital letters. TanDEM-X elevation map (German Aerospace Center, DLR).

#### 4. ARTICLE 2, INTEGRATIVE GEOARCHAEOLOGICAL RESEARCH

---

which is a dual construction. The two sites are separated by a depression, which, as suggested by Wilson (2017) represents the ancient watercourse.

It is actually easier to identify levees and consequently the system of palaeorivers in the northern part of the study area, where these features contrast clearly with the flat surrounding flood plain. Continuing these features further south is more difficult. Kom el'Gir seems to have been erected on a levee about 2 km south of the forking off into four smaller features. The southern part of the study area (Fig. 4.4, south of Sidi Salem) is generally higher and here levees tend to be wider and often are cut by other channels. Incised structures leading away from the levees directly into the lower lying areas possibly resulted from crevassing and formation of new channels. Incised structures running along the levees may be interpreted as remnants of the former river channel situated between the levees. This higher diversity in the southern half of the study area together with profound anthropogenic influence makes it much harder to perceive the location of former watercourses whereas we can clearly outline them in the north. Additionally, Wunderlich (1989) showed that north of Buto peat layers occur within the sediments and their thickness increases northwards. In a study dealing with the effects of peat on delta evolution, van Asselen *et al.* (2009) name peat as the most compressible of all natural sediments. This may lead to substantial subsidence in the northern delta areas and explains the considerable local variability of subsidence rates observed by Marriner *et al.* (2012b) as they are influenced by variations in texture and organic content of the sediments. Along former channels and within the channel sediments no peat but fine to coarse sand deposits of remarkable thickness occur. As a result, these channel and levee deposits were not affected by compaction. The great difference in compaction rates between the sandy sediments and the surrounding peat layers very likely helped to enhance the traces of former watercourses. Taking a closer look at the area between Tell el-Fara'in and Kom el'Gir, we hardly find any of these structures in the digital elevation model and the area in general seems to be heavily disturbed and transformed due to the intensive agricultural usage. This is due to the fact that the Nile delta is one of the most intensely cultivated areas on the earth and is shaped by the interplay of urbanization and intensive agriculture. Even the well pronounced levees in the northern part of the study area were substantially modified for agricultural purposes.

A very good example is the levee running from Kom Sidi Salem northwards along Kom el Qala, exemplified in Fig. 4.6. The DGPS track reveals the levee as a flattened and leveled structure with cross profiles resembling a stepped pattern. This pattern possibly results from differences in height and size of the two levees situated at the former slip-off slope and eroding bank of the channel. The question why these levees were not completely leveled might be answered with their positive effects in preventing soil salinization. They increase the distance to the ground water table and reduce ascension and evaporation of ground water. Especially the northern delta suffers soil salinization (Kotb *et al.*, 2000). Soils in this low lying area are categorized as highly saline by El-Guindy (1989). Even with sediment compaction and subsidence of the surrounding, clearly the levees are the result of a considerable period of fluvial activity

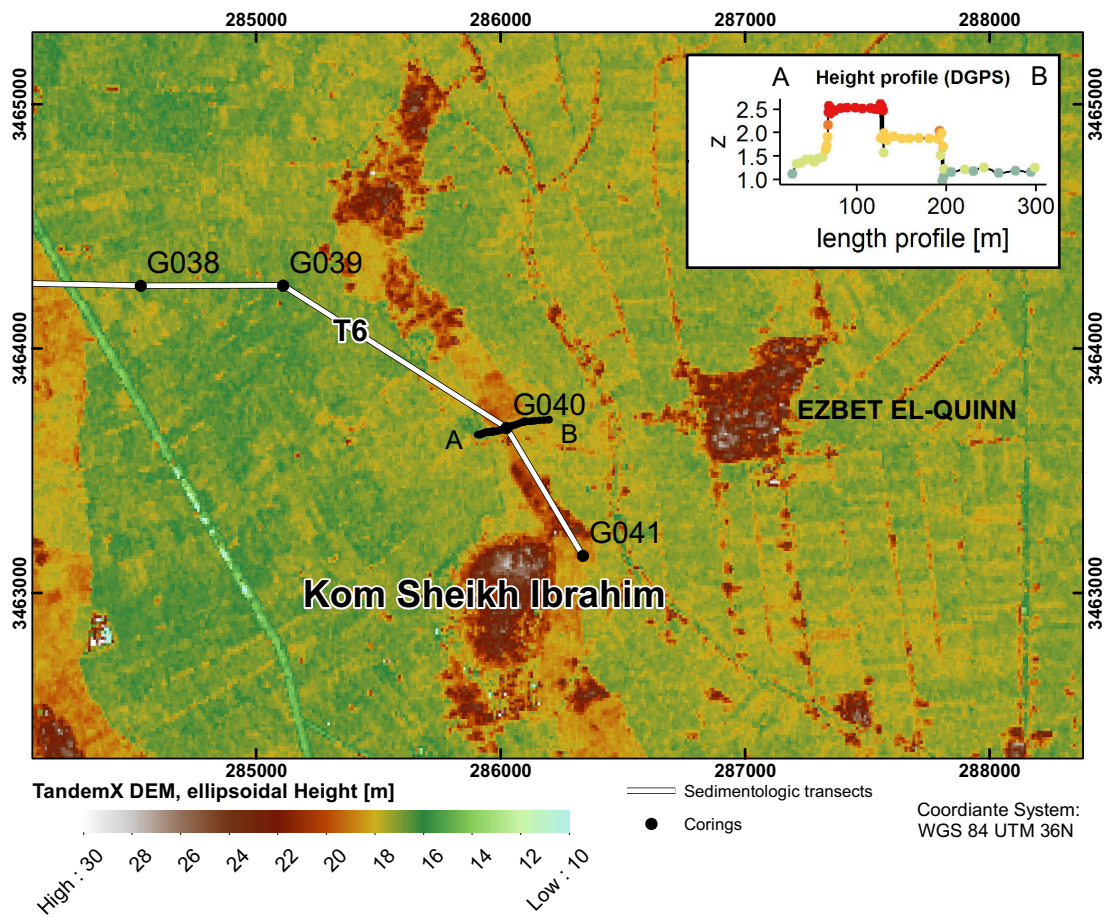


**Fig. 4.6: Transformation of levees** - Elevation profile of an elevated levee north of Buto. The cross profile through the levee was measured with a Topcon GR-5 DGPS and its location is illustrated in the TanDEM-X elevation map (German Aerospace Center, DLR) and in ESRI satellite maps.

## 4. ARTICLE 2, INTEGRATIVE GEOARCHAEOLOGICAL RESEARCH

---

and sedimentation. In a rough assessment, the levees had been forming since the 2<sup>nd</sup> millennium BC as a substantial amount of time is required to aggrade 2.5 m or more on which the settlements were founded. This raises the question why the area only seems to have been settled starting in the 1<sup>st</sup> millennium BC. Likely new methods of land-use for the areas of the low lying alluvial plains between levees played a crucial role. This expansion into the northern fringes of the delta opened huge swaths of new land (Butzer, 1976) and commercial opportunities. The challenges of agricultural activities in this marginal region are evident by papyrological sources from the region of Thmuis, in the eastern delta (Blouin, 2014).

### 4.5.3 Fine scaled sedimentological inspection of the connection between settlements and their surrounding

Our sedimentological work concentrates on the closer region around Buto (see marked area in Fig. 4.2) and Kom el'Gir. In this area hardly any recognizable fluvial structures appear in the remote sensing imagery. Finding watercourses and channels in the subsurface is challenging and time consuming as a dense net of corings is necessary to describe the courses of identified channels. Yet, it is the scope of this study to show that in this superficially disturbed region many channels and watercourses appear in the subsurface and especially alongside the settlements. In general, alluvial material of the subsurface reveals a complex lithology with inclusions of small sandy patches in the fine grained alluvial material. The coarse grained inclusions possibly originate from crevasse splays, levees or small channels. In addition, massive sequences of sand that cover widths of several hundred meters and a thickness of several meters occur and can only be explained via the action of moving meander belts.

Different core transects (see Figs. 4.7 and 4.8) are placed in this area. Fig. 4.7 gives an overview of the location of six different transects we studied in detail and Fig. 4.8 shows their lithological cross sections. In case of the transects and as a consequence of the high distances of several hundred meters between the cores it is unclear whether we touched individual watercourses at the margin or the base of the channel bed and the estimation of the channel depth is only a rough estimate. No statement can be made regarding the width of the channel. Nevertheless, our work provides important indications for further scientific studies on individual watercourses. It is planned to apply high resolution coring transects and geoelectrical measurements in future campaigns.

Transect 1 crosses Buto in W–E direction and includes results from Wunderlich (1989); Wunderlich & Ginou (2016). On both sides of the tell we find deeply incised channels that reach down to about 7 m below the sea level (bsl). The channel east of Buto dates back to Late Antiquity (4<sup>th</sup> c - 7<sup>th</sup> c AD) or earlier, as only the infill is dated, which comprises rounded Roman pottery at the channel bed at 7 m bsl and two radiocarbon dates (<sup>14</sup>C) (Wunderlich, 1989) from 1980±100 BP (HD11563-11388), or 350 cal BC – cal AD 253 (2σ) at 3.60 m bsl and 1595±115 BP (HD11563-11388), or cal AD 177 – 659 (2σ) at 5.60 m bsl. The age inversion testifies to the channel dynamics

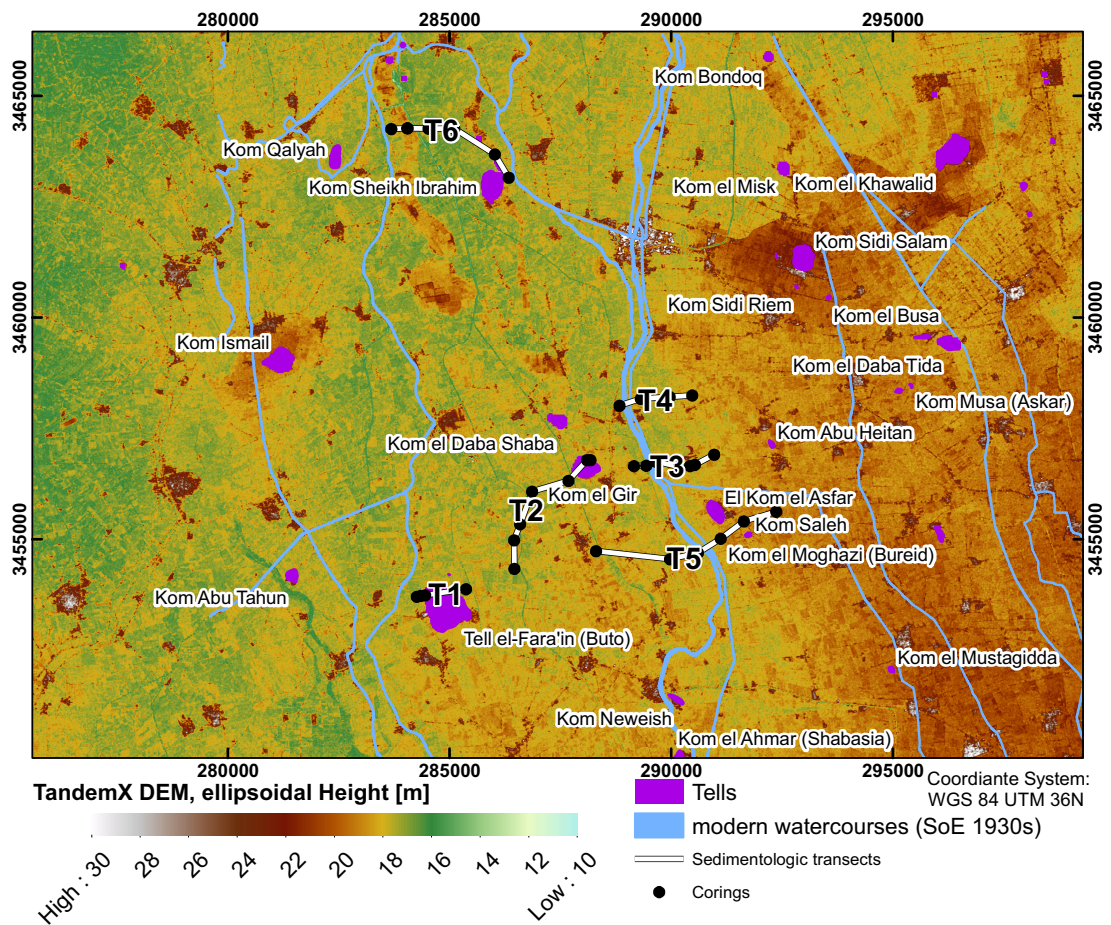


Fig. 4.7: Location of sedimentological transects - Transects are illustrated on top of the TanDEM-X elevation map (German Aerospace Center, DLR).

#### 4. ARTICLE 2, INTEGRATIVE GEOARCHAEOLOGICAL RESEARCH

---

with the reworking and redeposition of sediments. The channel infill is dominated by silty material and is rich in ceramic flitters, mollusk fragments and organic material between 3.25 and 7 m bsl. Together with the ceramic fragments, gravels occur at its bedline which is cut into underlying clayey alluvial Nile material. To the west of Buto at core site G3, predominantly loamy fine sandy material appears between 1 m and 7.5 m bsl with small gravels found at 7 m bsl (Wunderlich and Ginau, 2016). Below 1.2 m bsl the sediments are brighter with only small proportions of clay. Yet a thin darker layer containing plant remains is found at 5.2 m bsl and seeds from this layer date back to about  $2210 \pm 30$  BP (Beta-354940), or 370 – 199 cal BC( $2\sigma$ ) and corroborate the existence of younger channel infill material at such depths. Also indications for the Pleistocene surface such as the typical calcic horizon, which formed during stable conditions with soil formation (Wunderlich, 1989) are missing at this location due to incision of the channel. This calcic horizon can be found in the neighboring core G2 at 4.75 m bsl and G1 shows the presence of gezira material upon which Buto was founded (Wunderlich, 1989) at about 2 m bsl and below.

Transect 2 leads SW–NE and crosses the settlement mound Kom el’Gir, which lies 5 km northeast of Buto. It reveals the typical lithostratigraphy that Wunderlich (1989) uncovered displaying the occurrence of peat layers on top of the Pleistocene surface. Radiocarbon dates of this peat layer undertaken by Wunderlich (1989) provided a date of about  $5930 \pm 120$  BP (HD10629-10561), or 5206 – 4503 cal BC( $2\sigma$ ). In the southwestern part of this transect at coring G10 these peat layers are replaced by channel deposits consisting of fine sand and clayey silt which occur below the clayey Nile alluvium between 2.5 and 5 m bsl. At 4 to 5.2 m bsl the sandy material contains many ceramic fragments, mollusk shells and carbonate concretions that concentrate at this depth. Several of these ceramic fragments can be assigned to the Ptolemaic and Roman periods (332 BC – AD 400). The fragments measure on average 1 cm in diameter; one Ptolemaic sherd at 5.1 m bsl has a diameter of about 4 cm. The concentration of these larger fragments suggest this being the channel bed but a clear boundary to the underlying fine sandy material cannot be drawn. But in general no ceramic fragments occur within this sandy layer below. Between 7 and 8 m bsl the fine sandy material contains thin organic enriched layers. At location G13 a smaller channel reaching down to about 2 m bsl lies above the peat layers below. It is filled with non-diagnostic ceramic fragments, mollusk shells and shows organic enriched silty material at 0 m above the sea level (asl). More significant is the channel uncovered directly next to the eastern edge of Kom el’Gir (G21) that reaches down to about 6 m bsl and cuts through the older peat layers that were eroded at this location. The channel infill of loamy fine sand shows concentrations of ceramic fragments as well as mollusk shells at two different sections from 2 to 3 m bsl and from 4 and 5.5 m bsl. In this lowermost section, charcoal fragments and plant roots appear whereas the upper section shows thin organic layers. Also many ceramic fragments occur at the surface reaching down to about 2 m bsl. These were eroded at the adjacent tell and redeposited as colluvial material in the surroundings of Kom el’Gir.

Transect 3 is located east of Kom el’Gir and crosses the Bahr Nashart depression in



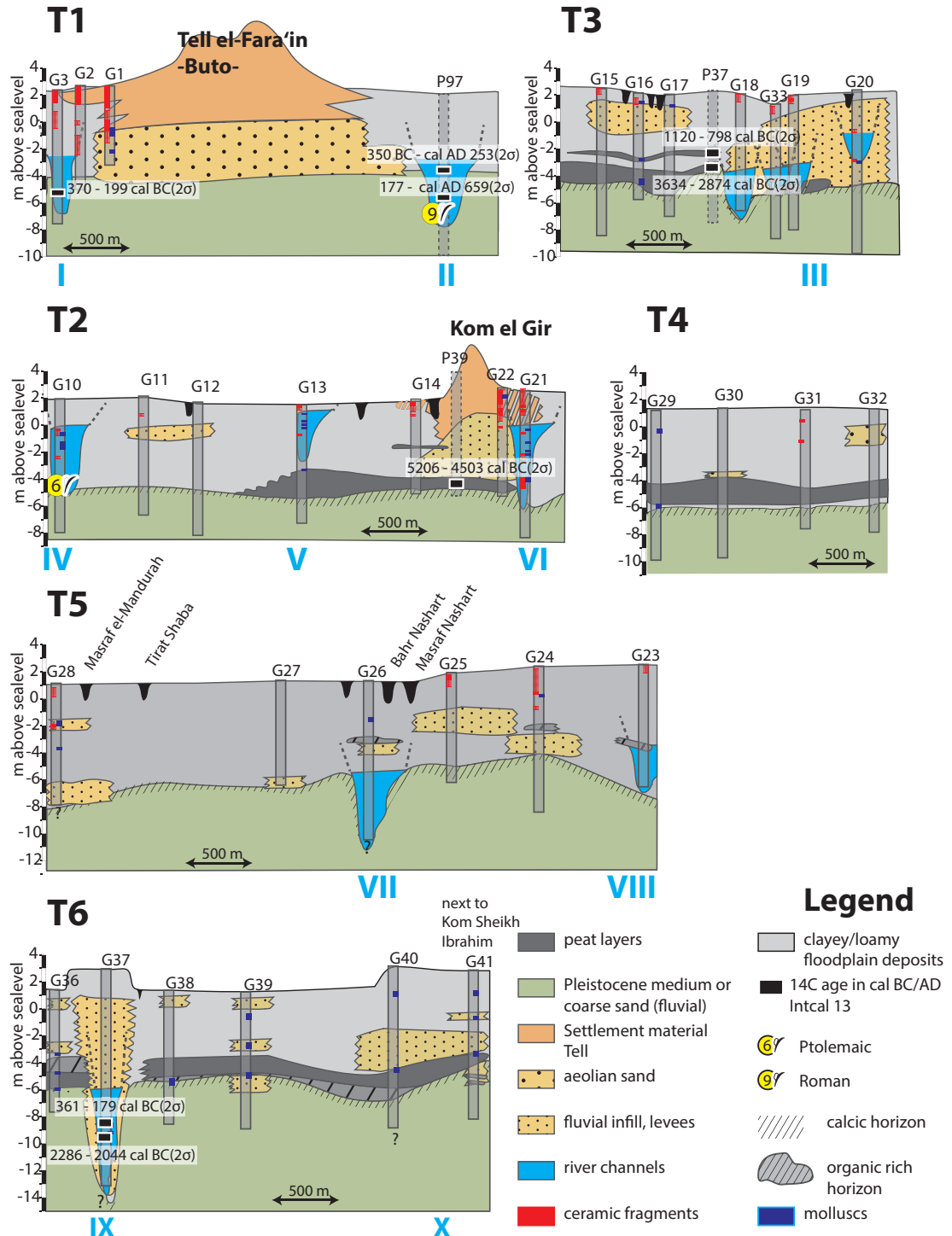


**Fig. 4.8: Cross sections of sedimentological transects** - Different cross sections of sedimentological transects were channels were found. The different channels within the cross sections are labeled with blue Roman numbers. A legend explaining the different signatures is included.

#### 4. ARTICLE 2, INTEGRATIVE GEOARCHAEOLOGICAL RESEARCH

---

a W–E direction. The western half of this transect reveals the typical lithostratigraphy of two peat layers intercalated in silty clayey Holocene Nile alluvium and overlying the Pleistocene surface (cf. Wunderlich, 1989). According to Wunderlich (1989) the lowermost peat layer at about 3 to 5 m bsl dates back to  $4490 \pm 150$  BP (HD10628-10558), or 3634 – 2874 cal BC( $2\sigma$ ) and the thinner layer above (2 m bsl) to  $2765 \pm 80$  BP (HD10627-10557), or 1120 – 798 cal BC( $2\sigma$ ) (cf. Wunderlich, 1989). These layers appear in all corings of the western half of the study area west of G18. Additionally, between 1.5 m asl and 1 m bsl of these corings show clayey material with intercalated graded fine sandy layers possibly resulting from flood events. The corings of the eastern half including G18 are almost entirely made up of coarser material alternating between fine and coarse sand partly containing gravels. Layers containing gravels occur in corings G18 at 5.8 m and 6.4 m bsl, in G19 at 3.4 m and G20 at 0.2 m bsl. The coarse material represents channel deposits of a former prominent channel. In G33 a rounded ceramic fragment occurred at 4.3 m bsl. Peat material also occurs in this eastern part, specifically in corings G19 and G33 between 4.75 and 5.25 m bsl. But here the peat appears to be reworked and mixed with sand when the channel cut into the peat layers. As a consequence, activity and incision of the river is younger than the reworked peat material included within the channel sediments. In the eastern reach of the transect, fine grained material is restricted to a layer close to the surface that increases in thickness from only 0.5 m (G20) to 3 m (G18) westwards.

Transect 4 lacks any indications for deeply incised channels and reveals an intact horizontally layered sequence with the Pleistocene surface at about 6 m bsl and a layer of peat lying above with 2 m in thickness. Northwards the brackish environment in which the peat was formed (Wunderlich, 1989; Wunderlich & Ginau, 2016) prevailed longer causing the deposition of thicker peat layers than further south. The peat is overlain by clay deposits and only at very few locations in the profile do we find sand or fine sand layers originating from overbank floodings or crevasse events.

Transect 5 lies further in the south and does not cut through the area where the peat formed in the early to mid Holocene. In this transect two channels can be verified in corings G26 and G23. The channel at coring G26 reaches down to about 10.7 m bsl or more as the base could not be found. Below 3.5 m bsl coarse sand with fine-sand layers appear and gravels occur at 6.8 and 8.1 m bsl. Additionally, the sandy layers show segments enriched with heavy minerals. Similar findings occur in coring G23 below 3.5 m bsl with gravels at 6.5 m bsl. The channel bed was not reached at this location. Both channels are topped by organically enriched alluvial clays for which datings cannot be provided. At G24 we also find organically enriched material intermixed with sand at 2 m bsl.

Transect 6 lies further away in the north west of the study area and crosses the elevated channels that are observable in the TanDEM-X elevation data. Underneath the elevated structure at coring G37 a deeply incised channel was identified. The associated levees were leveled to different heights as described in the previous section. The channel fill reaches down to about 13 m bsl or more and cuts through the peat layers, which are present in the other corings of this transect. Also here a clear channel

base could not be found. This elevated channel shows alluvial clay enriched with a downward increasing share of fine sand or intercalated sequences of differently sized sand. Gravels occur at 9.25, 11.75 and larger ones at 12.5 m bsl. Additionally, thin organic layers appear at 8.75 and between 10 and 10.75 m bsl. Mollusk shells occur between 8.5 and 9 m bsl and 9 and 9.5 m bsl. Radiocarbon ages of shells from these two layers date back to  $2190 \pm 30$  BP (Beta-450880), or 361 – 179 cal BC( $2\sigma$ ) for the upper layer and  $3760 \pm 30$  BP (Beta-450879), or 2286 – 2044 cal BC( $2\sigma$ ) for the lower layer. Very likely the younger date resembles the age of this channel and the much older shell fragment was reworked and redeposited. The other corings show the typical stratigraphy as described for transect 4. The Pleistocene surface lies at about 6 m bsl and is slightly incised to the east. Except for corings G37 and G38, mollusks occur at different depths and especially at the top or base of the peat layer which is present between 4 and 6 m bsl approximately.

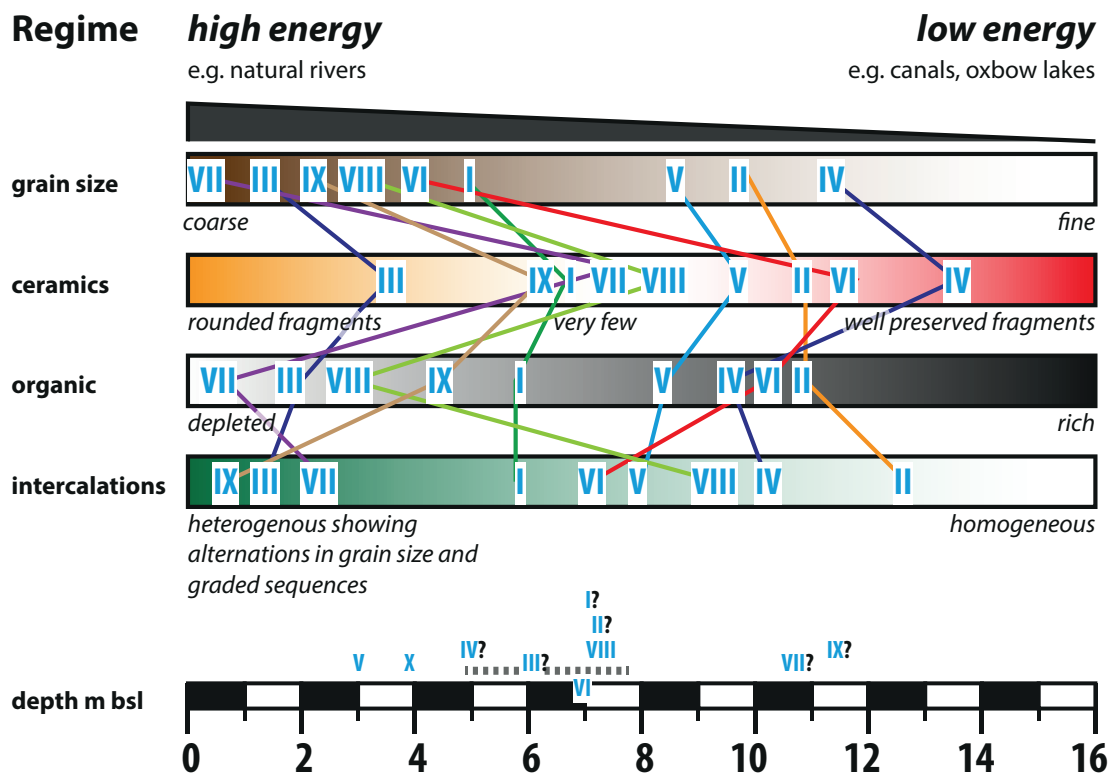


**Fig. 4.9: Categorization of channels** - Channels are compared according to the results of the field documentation. Individual parameters are only roughly differentiated and results of the channels are compared relatively to each other.

In Fig. 4.9 the channels (see Roman numerals in Fig. 4.8) are compared according to the findings of the field documentation. On the basis of the work of Tronchère *et al.* (2012) and our own observations, parameters of the field documentation are chosen that

#### 4. ARTICLE 2, INTEGRATIVE GEOARCHAEOLOGICAL RESEARCH

---

help to differentiate between high and low energy watercourses. Especially parameters such as grain size, amount of ceramic fragments, organic layers and the layering of the sediments help to answer the question whether we are dealing with slack water and low energy conditions such as in canals or oxbows or high energy regimes, such as natural rivers.

The classification presented in Fig. 4.9 shows that channels VI, II, V and IV can be more likely attributed to the low energy domain, whereas channels VII, III, IX, VIII to high energy watercourses. Channel VI also shows characteristics of a natural stream as it is filled with coarser material, but this probably originates from Kom el'Gir which is founded on coarser grained levees. A similar relation can be drawn for the channel west of Buto (I) as Buto is located on top of a sandy gezira. Generally the channel west of Buto shows characteristics of both classes of watercourses. On the one hand, it comprises a great deal of ceramic fragments, and on the other hand alternations of sandy sediment sequences are visible that show higher contents of organic matter compared to the natural rivers.

Tronchère *et al.* (2012) also made use of such parameters to discriminate between river and fluvial harbor sediments and they observed a slowing down of the water regime and anthropoization of the harbor basins resulting in the transformation of these deposits. According to Tronchère *et al.* (2012) these deposits are enriched with organic matter and show fine grainsizes due to a low energy flow regime, high magnetic susceptibilities, many mollusk fragments and are littered with potsherds. Additionally, the layering is an important discriminating factor as the fluvial regime of the Nile river constantly changes and therefore layers with different grainsizes, graded sequences and discordances alternate in natural rivers. Low energy watercourses such as man-made canals are controlled waterways and the magnitude of change of their flow regime is weaker and sediments appear more homogeneous. On the one hand, changes in grain size are harder to recognize and on the other hand, biological mixing processes can be higher in canals as mollusks and plants are more abundant in these environments.

Results of geochemical analyzes on the sample material hint at significant differences between sediments from low or high energy watercourses. PXRF results illustrated with the help of boxplot diagrams in Fig. 4.10, show significant differences between rivers with high stream velocities and the low energy watercourses. In general, the river sediments are bleached and sandy, therefore ion absorption is low and the river sediments contain only minute amounts of elements compared to the fine grained sediments of low energy regimes. In conclusion, the element contents reflect the grain size of the material. Such effects should diminish if ratios of these elements are plotted. The data distribution of the ratios shows that canals and rivers might show similar values, but the canals show very distinct ratios that do not fluctuate as much as the values of the river sediments, which cover a wide span of values. This corroborates the heterogeneous nature of the river sediments consisting of an alternation of different layers showing different compositions. Looking in detail on the ratios we see that such a discrepancy is especially high for Al/Ti and Cu/Zn ratios. Both Al and Ti are extremely resistant to weathering (Wayne Nesbitt & Markovics, 1997; Wei *et al.*, 2003) and tend to reflect

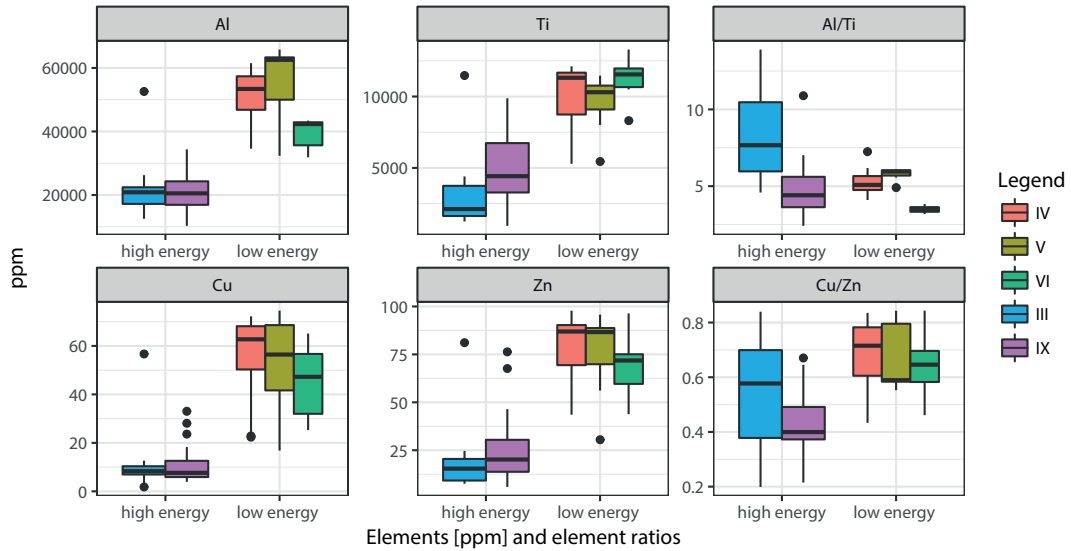


**Fig. 4.10: Data distribution between channels with different energy domains** - Boxplot diagrams showing the data distribution of pXRF results from high and low energy watercourses with the following frequencies: IV n=18, V n=7, VI n=10, III n=13, IX n=26. Results for different elements (Al, Ti, Cu, Zn) and element ratios (Al/Ti, Cu/Zn) are presented.

the supply of siliciclastic materials of fluvial or aeolian origin (Arz *et al.*, 1998; Chen *et al.*, 2011; Jansen *et al.*, 1998). Ratios of these two elements describe changes in the habitus of the transported sediments of the rivers such as density differences in siliciclastic materials derived from fluvial or Aeolian sources (Chen *et al.*, 2013). In the case of the natural watercourses, the sediments constantly varied with flooding events and changes in the Nile basin and, therefore, Ti/Al ratios show a wide span of values compared to the small data range of the canals, caused by the relatively stable sedimentary conditions. Similar findings can be shown for the Cu/Zn ratio, where we also notice this significantly higher data range for the Cu/Zn ratio in the case of the natural watercourses. But it is also interesting to notice that this difference is not so obvious in man made canals, which also show a wider range of values. This might relate to the fact that copper and zinc played an important role in Ptolemaic and Roman times (Healy, 1978) to which the man made canals can be dated. These man made canals lie close to the settlements and are connected with them. Therefore, they might be influenced by these elements, which explains the great variation, especially of copper, within the canal sediments.

Fig. 4.11 plots a selection of elements along the x-axis against the ratio of the element to the concentration of the same element in reference Nile clay material. According to Reimann (2008) this technique was developed to compare the distribution of Rare Earth Elements between different rock types. The reference Nile clay mate-

## 4. ARTICLE 2, INTEGRATIVE GEOARCHAEOLOGICAL RESEARCH

rial has been selected according to a spatial selection from the pXRF measurements. Specifically it is the clayey material outside a 600 m radius of the settlements found in depths between 3 and 10 m bsl in corings lacking any indications for channels. This subset allows us to exclude the modernly affected surface and material older than the Holocene era. In this plot, distinctive changes between low energy (curves with dots and continuous lines) and high energy watercourses (triangles with dotted lines) manifest themselves. Generally sediments in natural watercourses are depleted in many elements compared to the Nile clay material and show high changes between different elements. The sediments from low energy watercourses are slightly enriched with a wide variety of elements and of interest are higher contents of Al, Ca, Cu, Mn and Sn as they reveal information on the anthropogenic influence.

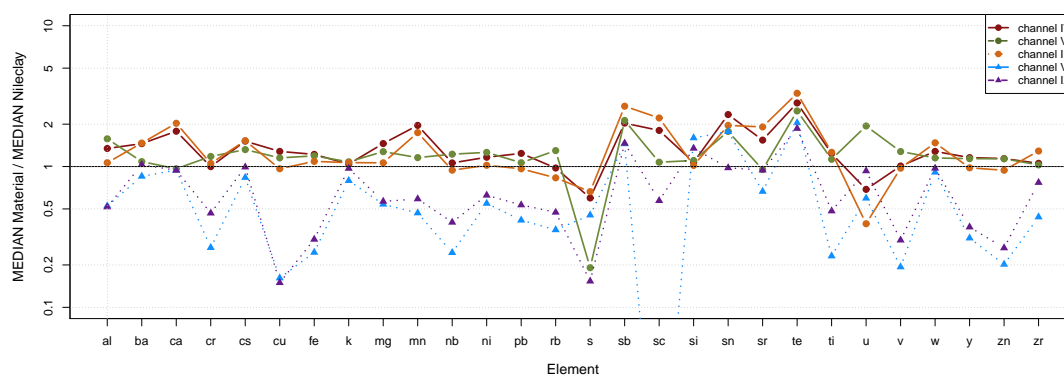


**Fig. 4.11: Spiderplot showing pXRF profiles** - A selection of elements is plotted along the x-axis against the ratio of the element to the concentration of reference Nile material. The element contents of the reference Nile material as well as the different channels are calculated as median element values. Additionally, samples representing the reference Nile material are spatially selected as fine grained material lying outside a 600 m radius of ancient settlements and within depths between 3 and 10 m bsl. The elements have been ordered alphabetically (according to chemical abbreviation from Ag to Zn).

Looking at the distribution of these low energy watercourses on the map we see that they appear east of the settlement sites Kom el’Gir and Buto and between these sites whereas natural river channels were identified in the Bahr Nashart depression and north of Buto, where the elevated channels can be traced in the elevation data. Most of the channels reach down to depths of about 6 to 8 m bsl. Deeper channels (VII, IX) show depths of about 11 m bsl and occur in transect 5 crossing the Bahr Nashart depression and further to the north below the larger elevated channel structures (IX). Channel VII is an older channel that is overlain by a thin peat layer and shows neither ceramic fragments nor thick layers of sand. Channel IX, situated within the elevated levee north west of Sidi Salem, cuts very deep into the sediments and shows thick layers of sand. It is important to emphasize that the depth of this channel is mainly shaped

by flooding events. Such rhythmic events convey the biggest part of the flood waters. During such events the river cuts through the sediments well below its erosional base, which explains the greater depth of this channel. This over-deepening of the river beds in the Nile delta is first mentioned in Butzer (1976). The fact that most channels show similar depths suggests that they belonged to the same river system and were set to the same erosional basis of the main river or were part of the finely ramified subdelta that manifests itself on the larger scale. Additionally, channel activity in channels I,II,IV,IX can be dated, based on a combination of radiocarbon dates and pottery dating, to Greek and Roman times. For the activity of channel III we can establish a terminus postquem of 832 BC or younger as the channel eroded into the peat layers of coring P37 which Wunderlich (1989) dated to  $4490 \pm 150$  BP (HD10628-10558) or 3634 – 2874 cal BC( $2\sigma$ ) for the upper peat layer and  $2765 \pm 80$  BP(HD10627-10557) or 1120 – 798 cal BC( $2\sigma$ ). In essence, the existence of these interconnected channels fall together with the strong period of settlement growth in the Ptolemaic, Roman and late Roman periods (4<sup>th</sup> c BC – 7<sup>th</sup> c AD), (Schiestl, 2012b; Schiestl & Rosenow, 2016; Wilson, 2012b, 2017; Wilson & Grigoropoulos, 2009). But as the settlements were erected on tall levees, these watercourses already existed previously and the area was later colonized.

All settlements were situated along natural rivers. To this natural fluvial network artificial canals are added or old river branches were used. They all show similar depths as the natural waterways they were connected with. These are primarily in immediate vicinity of settlements, e.g. Buto and Kom el’Gir, as well as, in one case, between those settlements. The function of these canals is not yet clear. Possibly they served as branch canals between settlements and the adjacent natural watercourses and as connections between sites. Such infrastructural measures could reflect adaptive practices in a dynamic fluvial landscape, which is characterized by meandering courses.

## 4.6 Conclusion

Archaeological investigations aiming at the localization and dating of ancient settlements in the northwestern Nile delta showed that this area was widely settled. Based on a linear distribution of mainly Roman and late Roman settlements, the existence of a single defunct Nile branch was suggested. In the present study an interdisciplinary archaeological and geoscientific approach has been applied to verify this hypothesis. The approach views landscape and ancient settlements of the delta at two different scales: a large scale that incorporates archaeological prospection as well as satellite data, maps and elevation data, and at a smaller scale we focus on different sedimentological transects crossing archaeological sites and landscape units in the study area to prove and to refine results gained on the landscape scale. Our new results show that in the study area the situation is much more complicated and diverse. Single Nile branches could be traced with great reliability but these branches together form a subdelta with ramified larger and smaller branches whose elevated levees are merged and thus allow for a more dispersed settlement pattern. This larger perspective on the northwestern delta was realised using historic maps, satellite imagery and modern satellite elevation data from

## 4. ARTICLE 2, INTEGRATIVE GEOARCHAEOLOGICAL RESEARCH

---

the TanDEM-X satellite configuration, allowing for an integrative view on the whole landscape. Especially modern satellite elevation data from the TanDEM-X satellite configuration of the German Aerospace Center reveals many incised and elevated linear structures in the flat delta and the subdelta. Detailed sedimentological research gave evidence that this subdelta formed prior to Ptolemaic and Roman times, and the levees and watercourses formed the basis for human settlements in the area studied. Remarkably, a remote sensing approach of the authors (Ginau *et al.*, 2017) dealing with NDVI time series showed the high fertility of the levee sediments and their positive influence against soil salinization compared to the former remote and low lying swampy areas. This further qualifies levees as targets for the formation of settlements as they do not only offer a safe ground but also ground for the production of food.

Furthermore, with a closer look at the different sedimentological transects in the area under study and the channels we sampled, it is possible to gain a better understanding of different landscape units. We sampled elevated levees visible in the elevation map and we identified different categories of channels within the transects. Our field results and geochemical pXRF measurements on sample material of these channels allow us to discriminate between high and low energy watercourses. In the case of the channels next to settlements, such as Buto and Kom el'Gir, it is suggested that these sites were connected via canals with the larger watercourses. Moreover, these sedimentological transects crossing the northwestern Nile delta show the complex and changing nature of the Holocene delta landscape and its floodplain deposits. As described in the introduction, it is especially a result of the changing river patterns and processes such as crevassing and overbank flooding (see Aslan & Autin, 1999; Aslan *et al.*, 2005) that lead to such complex sediment patterns and which very likely were responsible for the termination of this subdelta. An avulsion event upstream could have changed the entire network of watercourses and rendered this subdelta inactive.

The integration of both scales into this study supported new insights and made us reverse our original hypothesis of a single defunct Nile branch that could explain the linear pattern of settlement sites. The TanDEM-X DEM opens fundamentally new possibilities to investigate the ancient delta landscape and a first reconstruction of a fluvial network with associated settlements can be presented. On the larger scale artificial channels were identified and they are the result of adaptive practices of the settlements in a dynamic fluvial landscape.

### 4.7 Acknowledgments

We thank the Egyptian Ministry of State for Antiquities for their assistance and support of our work in the field. We thank the Cairo Department of the German Archaeological Institute (DAI) and especially Prof. Dr. Seidlmayer for funding and support in the field, the Eurasia Department of the German Archaeological Institut (DAI) for supporting pXRF measurements in Egypt, namely Dr. Daniel Steiniger. German Aerospace Center (DLR) for the provision of Tandem-X elevation data under science application DEM\_HYDR1426. We also thank Janice M. Schiestl for proofreading the article and



## 4.7 Acknowledgments

---

correcting our English. Finally, we thank the anonymous reviewers for their helpful comments.

#### 4. ARTICLE 2, INTEGRATIVE GEOARCHAEOLOGICAL RESEARCH

5

# **What settlements leave behind - pXRF compositional data analysis of archaeological layers from Tell el-Fara'in (Buto, Egypt) using machine learning**

The identical content of this chapter was published in different formatting in:

Ginau, A., Steiniger, D., Hartmann, R., Hartung, U., Schiestl, R., Altmeyer, M., Seeliger, M., Wunderlich, J., 2020. What settlements leave behind - pXRF compositional data analysis of archaeological layers from Tell el-Fara'in (Buto, Egypt) using machine learning. *Palaeogeography, Palaeoclimatology, Palaeoecology* 546.

### 5.1 Abstract

Modern portable and handheld XRF devices (pXRF) allow quick measurement of large geochemical datasets without the necessity for laboratory facilities. Such facilities are rare in Egypt and modern dating techniques which are indispensable in Geoarchaeology to establish a robust chronology are not available, as sample transport is restricted and Egypt does not provide OSL or AMS  $^{14}\text{C}$  laboratories. With these preconditions, we evaluate the usability of pXRF geochemical data for the dating of archaeological sediments with machine learning techniques. The sample material was collected via sampling of archaeological sections and profile walls from archaeological excavations in the northwestern Nile delta at the settlement site Buto (Tell el-Fara'in) and Kom el'Gir. Additionally, samples were taken from sediments and cultural layers uncovered from their surroundings using vibracore corings with open steel auger heads. In this methodological approach, we examine the applicability of pXRF methods and test the sample data for distinct geochemical differences between the main settlement phases with multivariate statistical methods. The dating is based on the training of artificial neural networks with pXRF data from archaeological material of well-dated context to date test data of cultural layers within the vibracores. This allows us to link fundamental changes in the landscape with the settlement history of Buto and neighboring tells.

### 5.2 Introduction

Despite all research undertaken in the last decades, no concise picture of the archaeological and palaeoecological evolution of the northwestern Nile delta can be drawn. The archaeological records show significant population dynamics and long lasting phases of abandonment of sites that still need explanation and may very likely be the result of changing environmental conditions. Consequently, the archaeological and sedimentological records are the subject of intensive studies that reach far back in the past. For more than three decades, the ancient settlement site Tell el-Fara'in (Buto) and its surroundings have been the target of archaeological excavations and prospections conducted under the auspices of the German Archaeological Institute (DAI) (Faltings *et al.*, 2000; Hartung, 2014; Hartung *et al.*, 2009; von der Way, 1997) and the Paris Nanterre University (Ballet & Marouard, 2015; Ballet *et al.*, 2011), to name but a few publications (see Fig. 5.1).

Ancient settlement sites (tells) in the surrounding area have been surveyed since 2010 (Schiestl, 2012a,b; Schiestl & Rosenow, 2016) with a strong focus on the neighboring settlement site Kom el'Gir. Additionally, sedimentological investigations by the University of Frankfurt concentrate on a larger region around Buto and Kom el'Gir and aim to reconstruct the Holocene landscape change of the area. They uncovered the lithology of the subsurface and aim to trace larger landscape changes and fluvial changes within the sediment sequences. Especially palaeogeographic investigations in the 1980s (Wunderlich, 1988, 1989, 1993) showed the change from brackish lagoonal conditions

with deposition of peat layers on top of the former Pleistocene surface at about 5000 cal BCE to the development of the modern Nile delta floodplain with constantly aggrading clastic sediments reaching a thickness of about 7 to 10 m today (Wunderlich, 1989).

Current investigations of the authors concentrate on the closer region around Buto (see marked area in Fig. 5.1) and Kom el'Gir and focus on the identification of small-scaled landscape changes such as changes in the net of watercourses and channels in the sedimentological records and the application of geochemical methods on the sample material. Ginau *et al.* (2019) showed that the massive increase of settlements in the northwestern delta from the Ptolemaic to Late Roman period (late 4th c. BCE - 7th c. CE) was spurred by a net of multiple branches that provided routes of transportation, fresh water for irrigation and probably good conditions for agriculture on the adjacent elevated and fertile levees.

Furthermore, they state that the ancient settlements either were in direct vicinity of the natural rivers or connected via artificial channels. While the net of former river branches and the location of settlement sites is well documented by Ginau *et al.* (2019) and Schiestl (2012b), their temporal relationships are poorly understood. Out of the few ceramic fragments present in the corings, only a small fraction is datable and other dating techniques such as OSL or AMS  $^{14}\text{C}$  are not available in Egypt. In this paper, we will draw temporal relationships between the well documented and dated settlement layers and the landscape units such as the watercourses.

In essence, we link the environmental history stored in the Nile alluvium with the settlement history starting in prehistoric times and ending in the early Islamic period. The innovative character of this work is the establishment of geochemical connections between sediment samples from archaeological layers and samples taken from auger corings from the surrounding landscape to date archaeological or human influenced sediment layers that are present within the corings. Often archaeological material is found especially within the corings located near the settlement mounds. As local authorities forbid sample export, our approach of sediment dating is based on the analysis of XRF data measured with a portable device (pXRF, Niton XLT3) from Nile alluvial material from sections and profiles of archaeological excavations. We test the usability of pXRF data in terms of accuracy and applicability for machine learning techniques. Despite their coarser resolution compared to elaborated lab systems (ICP-MS, AAS etc.) pXRF data show a wide range of elements and can easily be produced for a high number of samples. This allows the establishment of new methods of data analysis, visualization and machine learning techniques which we intend to apply to large pXRF datasets. Lastly, we need to find new alternatives for elaborated sediment dating and geochemical analyzes.

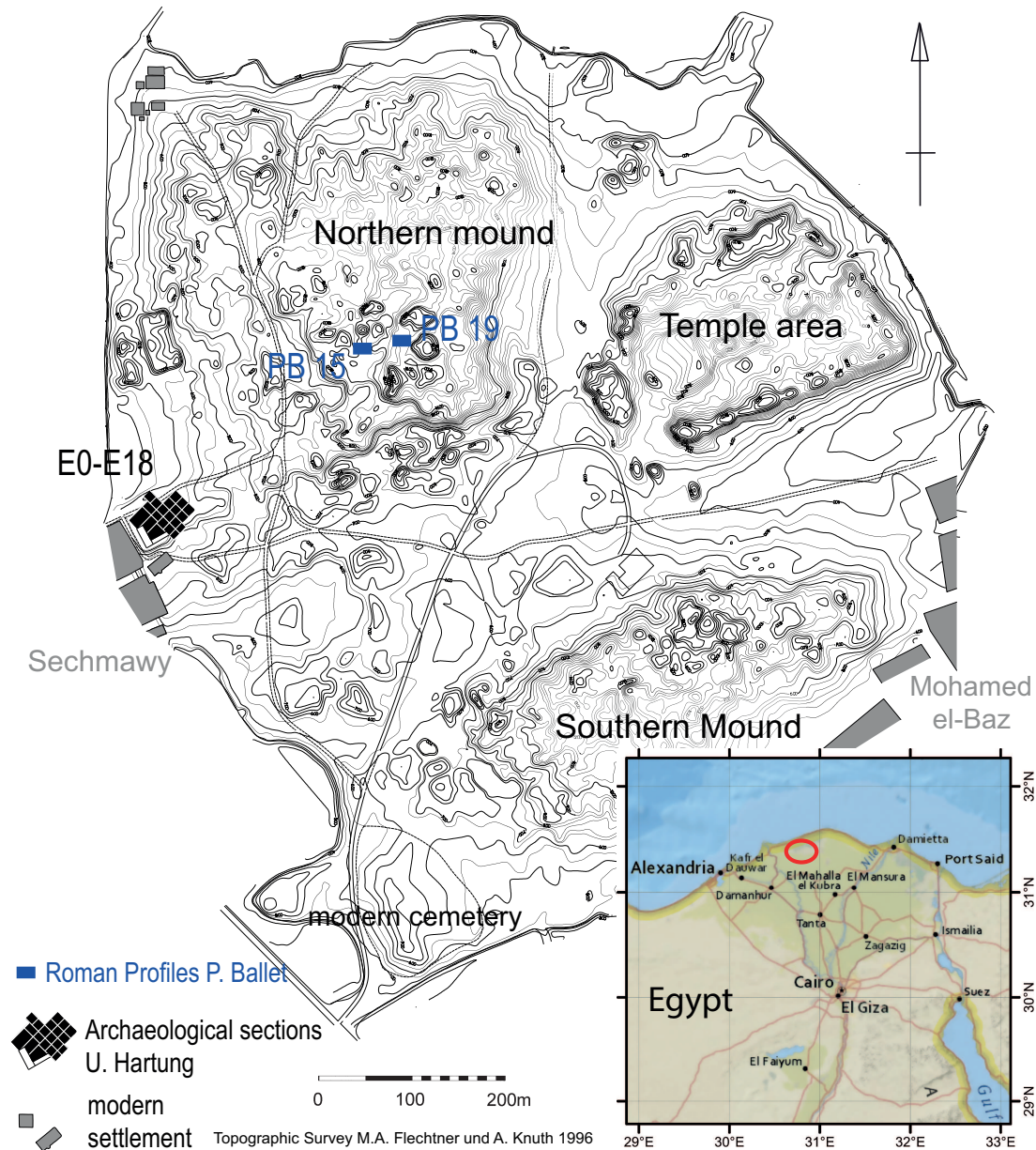


**Fig. 5.1: Location of archaeological profiles** - Tell el-Fara'in lies in the northwestern Nile delta and sampling was performed on archaeological sections and section walls E0-E18 (black) covering all cultural periods in Buto as well as the Roman-age profiles PB15/19. The sections lie at the western edge of Tell el-Fara'in close to the village of Sechmawy and cut older low lying settlement layers.

## 5.3 An overview of pXRF analyzes in geoarchaeological contexts

Earth sciences such as geology, geomorphology or soil science are experiencing a fast spread in the application of pXRF analyzes of sediment and soil samples. Exemplary are the papers of Birks & Birks (2006); Lubos *et al.* (2013); Nowacki (2016); Sritrairat (2013) that inferred palaeoclimatic or environmental conditions from pXRF results of sediments and soil samples from different geoarchives such as peat layers, soils or colluvial material. Studies in scientific literature corroborate the spread of pXRF analyzes in archaeological and earth sciences (Frahm & Doonan, 2013; Hall *et al.*, 2014), which is especially true for archeology. Frahm & Doonan (2013) and Shackley (2010) state that pXRF analyzes in archeology have the potential to produce significant changes in this discipline. Frahm & Doonan (2013) differentiate between different types of pXRF devices that range from larger “benchtop systems” to small transportable devices called handheld pXRF analyzers (HHpXRF). The latter type of device is used in this study (Niton XL3t 980He from Analyticon) and simply referred to as pXRF in the following.

As more and more studies adopted the use of pXRF methods, methodological approaches mushroomed that tried to evaluate the precision and the potential for specific geoscientific applications of pXRF analyzers. Lubos *et al.* (2016); Rocheford (2014); Schneider *et al.* (2016) compared the application of pXRF analyzes of sediment and soil samples with elaborated laboratory methods such as ICP-AES, ICP-MS, AAS, XRF and ICP-OES, and highlight pXRF results as applicable and comparable in earth sciences. Many of those studies recommend worst or best-suited elements (Hall *et al.*, 2014; Kenna *et al.*, 2011; Rocheford, 2014). In addition, effects of sample preparation are analyzed by Schneider *et al.* (2016) who recommend the application of pXRF analyzes in the field as moisture effects can be excluded by these devices.

In practice, pXRF analyzes of archaeological material focus mainly on ceramics, small fragments, metals (Forster *et al.*, 2011; Frankel & Webb, 2012; Hunt & Speakman, 2015; Shackley, 2011; Shugar & Mass, 2012) and archaeological records such as walls, ovens, floors or debris layers (Bernasconi & Stanley, 1994; Kanthilatha *et al.*, 2017; Rocheford, 2014) which are named cultural layers within this work. Major aims of these studies dealing with pXRF data are provenance analyzes and the classification of ceramics or other materials into different cultural phases based on pXRF geochemical fingerprints.

Due to the speed and accessibility of modern pXRF devices, we gathered a large set of measurement data in just a couple of field campaigns. This fuels the application of modern data analytics such as multivariate statistical methods or machine learning techniques. There are many studies that use methods such as principal component analysis, non-metric multidimensional scalation (NMDS) or factor analysis to detect clusters of parameters or visualize geochemical effects (Forster *et al.*, 2011; Frankel & Webb, 2012; Gauss *et al.*, 2013; Kanthilatha *et al.*, 2017; Speakman *et al.*, 2011).

### 5.4 Methods

The applied methods of this study encompass fieldwork, sample measurements and data handling and processing.

#### 5.4.1 Sampling of archaeological layers on-site

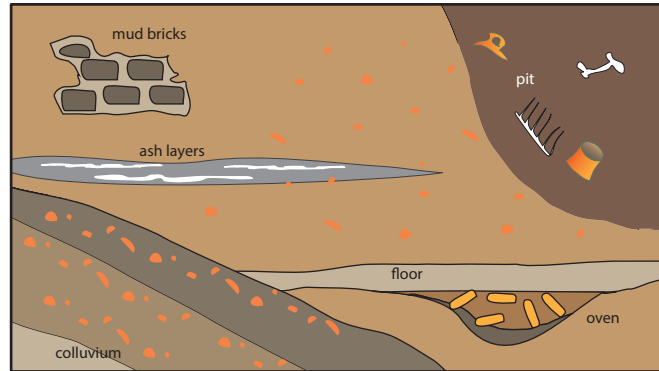
Sampling focuses on archaeological records of the different cultural layers or cultural phases (see Fig. 5.2) exposed in the excavation sections. Records targeted are bricks, floors, ovens, pits and ash layers or other forms of burned residues. Mainly samples are taken from three sections and their walls (E9, E14, E18) and two profile walls (PB15, PB19), (Fig. 5.1). Supplementary Figs. A.1 and A.2 illustrate the sampling of the main profile walls together with the ages estimation of the samples. Additionally, soil samples from squares taken during excavation works are added to the analysis. They cover different altitudes and settlement periods; E9 is more elevated and comprises layers from the 4th Dynasty (c. 2575-2465 BCE). E18 shows prehistoric to Saitic (664 - 525 BCE) material, whereas E14 covers layers of Prehistoric times. Profiles PB15 and PB19 lie in the highest areas of Buto and cover Roman settlement periods. Sample material from prehistoric times is categorized as Predynastic (>3150 BCE), material from the Early Dynastic period to the Old Kingdom as Dynastic (3150 - 2181 BCE) and material from Saitic or Roman layers (332BCE - 641 CE) as Roman.

Fig. 5.3 visualizes the sampling of the southwestern wall in profile section E18. Archaeological records are repeatedly sampled at different positions within the profile (single samples) and some samples are taken twice from neighboring positions within the same archaeological record (double sampling with upper and lower sample limits). This double sampling allows estimation of the difference between neighboring sample material that is very likely caused by post-sedimentary alterations such as leaching, precipitation of salts or due to a heterogeneous matrix of the record. These effects are additionally studied by sampling one record, namely a cultural layer, a Predynastic floor (record 928) in profile section E13 with 32 individual samples. Again, the distribution of elements within this set of samples is analyzed for the same reason as the double samples.

#### 5.4.2 Sampling of sediment corings

Auger core samples are retrieved by means of a vibracore device (Wacker BH65) and open steel auger heads with diameters of 6.0, 5.0 and 4.0 cm. The use of auger cores keeps sedimentary structures and boundaries between different layers intact. The sediment cores are described in the field in terms of color (Munsell Soil Color Charts), grain-size and rounding, texture and carbonate content according to Eckelmann *et al.* (2006). They are placed along different transects with the main transects leading away radially from the settlement sites of Buto and Kom el'Gir and other transects focusing on the levees in the north and the Bahr Nashart depression lying east of Kom el'Gir. Due to the huge extent of the study area, corings of the transects show spacings of about





**Fig. 5.2: Archaeological records targeted by pXRF measurements** - Illustrated are the different archaeological records within the profile walls that are sampled. Sampling focused on mud bricks, floors, ovens, pits, ashlayers and colluvial deposits. This Fig. acts as an illustration and is not in scale.

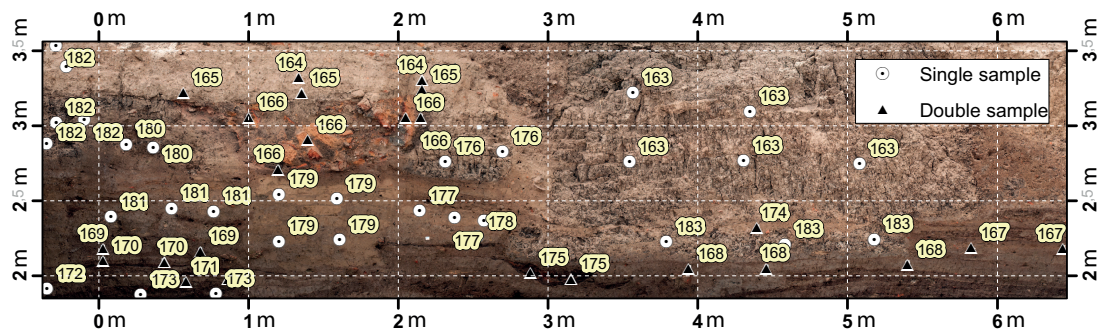


**Fig. 5.3: Sampling of the southwestern wall in profile section E18** - Exemplary sampling of the southwestern profile wall in section E18 (sections near Sechmawy, Fig. 5.1). Each archaeological record is sampled at different positions (single sampling) and some samples are taken twice from the same position (double sampling, upper and lower sample).

## 5. ARTICLE 3, DATA ANALYTICS AND MACHINE LEARNING

---

500 m. The cores are described in Ginau *et al.* (2019) focusing on the sedimentological description and interpretation of the cores placed in the northwestern Nile delta.

### 5.4.3 Sample preparation

The handling of the samples is standardized in order to provide reproducible measurement conditions and to reduce influences of the sample matrix and sample surface. All samples are oven dried at 100 C, homogenized with an achat mortar and sealed in certified XRF sample cylinders using a 4  $\mu\text{m}$  foil to allow best penetration of the analyzation and fluorescence radiation. Supplement Fig. A.3 illustrates the different steps of the on-site sample preparation performed during our fieldwork in Egypt.

### 5.4.4 pXRF measurements

pXRF measurements are performed with a Niton XL3t 980He portable XRF (pXRF) analyzer equipped with a Ag-Anode. The pXRF instrument runs at tube voltages of 9 to 50 kV and at beam currents of 0-40  $\mu\text{A}$ . A helium purge is used to enhance quantitative measurements of light elements, of which phosphorus (P) is most important. The XRF spectra are quantified using a fundamental parameter algorithm “Testall geo” that combines the mining and soil mode of the device. The measurement time is set to 180 s with the following filter settings: main 45 s, low 45 s, high 30 s and light 65 s. To optimize the results and gather information on the accuracy of the device to detect certain elements, certified reference materials ( $\text{SiO}_2$ , NIST2780, Till4) and our own standards originating from the surroundings of Buto (STRS1-5) are repeatedly measured during each measurement campaign to allow calculation of precision values and statistics. Precision of measurement is expressed as relative standard deviation (RSD). Supplement Figs. A.4 and A.5 present the relation between a sample’s element concentration and the standard deviation over repeated measurements of the different reference materials. Standard deviations increase with increasing sample concentration. This was shown for certain elements (highlighted in bold letters) in Table 5.1. Elements with high slope values (e.g. As, Cr, Ni) tend to be less precise at higher concentrations compared to elements with low slopes and, therefore, more evenly distributed measurement precisions. The intercept gives information on the detection limit or the amount of initial error.

Element concentrations where the coefficient of variation exceeds the 50 % line mark the detection limit, as the error is nearly as high as the measurement value. In short, detection limits (see results) are calculated based on the element standard deviation curves as presented in supplement Figs. A.4 and A.5. In some cases, the reference materials do not cover the transition to high coefficients of variation. Detection limits for elements marked with a star in Table 5.2 are taken from the guidebook of Thermo Scientific Niton XL3t 500/900 GOLDD Analyzers with elemental limits of detection for a  $\text{SiO}_2$  matrix in the mining mode (2009 Thermo Fisher, AN44815\_E060).

Another aspect is the normalization of the pXRF data (Helfert & Ramming, 2012; Iserlis *et al.*, 2019) that involves conversion of the main elements except sodium into

**Table 5.1:** Linear regression parameters for the relationship between x:mean and y:standard deviation

Element	Slope	Intercept	R <sup>2</sup>	Element	Slope	Intercept	R <sup>2</sup>
As	0.086	3.228	0.122	P	0.111	71.873	0.103
Al	0.045	832.139	0.231	Pb	0.011	5.352	0.455
Ba	0.011	12.668	0.213	Rb	0.028	0.064	0.110
<b>Ca</b>	0.024	150.143	<b>0.662</b>	<b>S</b>	0.021	14.523	<b>0.964</b>
Ce	-0.031	29.625	0.041	Sc	0.328	4.544	0.565
<b>Cl</b>	0.023	37.640	<b>0.646</b>	Si	0.040	128.321	0.226
Cr	0.083	1.295	0.138	Sr	-0.001	3.318	0.001
Cs	0.024	1.262	0.104	Ti	0.005	167.693	0.010
<b>Cu</b>	0.029	3.634	<b>0.613</b>	U	0.154	1.312	0.413
Fe	0.003	214.346	0.100	V	0.014	10.836	0.073
K	0.024	108.954	0.345	W	0.115	5.332	0.237
Mg	0.026	562.328	0.087	Y	0.014	0.946	0.032
<b>Mn</b>	0.016	15.940	<b>0.764</b>	<b>Zn</b>	0.072	0.341	<b>0.620</b>
Nb	0.011	1.051	0.017	Zr	0.029	2.722	0.132
<b>Ni</b>	0.092	-0.131	<b>0.828</b>				

## 5. ARTICLE 3, DATA ANALYTICS AND MACHINE LEARNING

oxides and scaling to 100 wt%. Fig. 5.4 shows the calculated normalization factors for the different grain size compositions. In our data, normalization factors remain stable between 1.3 and 1.5. All samples were dried and pestled. As a consequence matrix, moisture effects and the porosity are comparable between the samples and contribute to the stability of the normalization factor. Nevertheless, normalization factors are higher with a larger error in samples that contain organic material or mainly consist of peat. Carbon cannot be registered by pXRF but suppresses the registration of other elements. Normalization of these samples will completely ignore the organic material, but this information can be essential and is additional information the neural network can process (e.g. samples with low contents of all main elements belong to the group of Nile material from the peat layers). Additionally, samples containing higher amounts of clay also show slightly higher normalization factors with slightly higher deviations. This is related to the presence of crystal water within the clayey sample material. In essence, the stability of the normalization factor and the importance of the indirect registration of carbon via overall low contents of the main elements is essential and, therefore, normalization of the pXRF data is ignored.

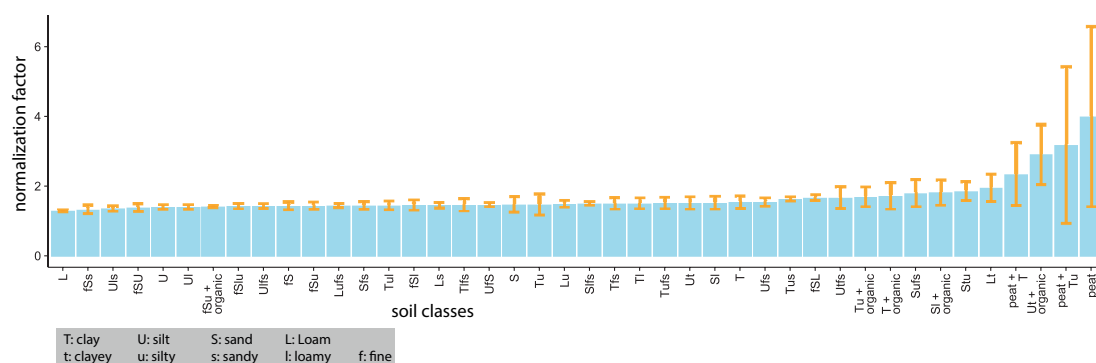


**Fig. 5.4: Normalization factor in relation to the different grain-size classes** - Normalization factor is calculated after Helfert & Ramminger (2012); Iserlis *et al.* (2019) and shown as the mean for the different grain size classes (blue bars). Error bars (yellow) indicate the standard variation of the aggregated normalization factors

### 5.4.5 Data management and analysis

For our data new methods of data storage, selection and analysis. In consequence, our data is stored in a “relational database management system”(RDBMS, PostGIS) that allows querying and selection of data based on attribute values and spatial relations. Analyzes such as robust factor analysis (PFA), clusterization, or machine learning techniques are performed using the software package R. Generally, the analysis of element compositions requires specific statistical methods and procedures (Aitchison, 2003; Filzmoser *et al.*, 2009; van den Boogaart & Tolosana-Delgado, 2013) that are supported by R-libraries Compositions and robCompositions (Reimann, 2008).

Chemical differences along the large-scale sedimentological transects are analyzed with a robust factor analysis, (chapter 5.5.2.1). Only elements are chosen that were measured in more than 50 % of the sediment or archaeological sample material (Fig. 5.6). This ensures that elements that show either an archaeological or sedimentological significance are not excluded, e.g. P which is important for tracing archaeological material. Furthermore, data preparation includes the replacement of zero values as these show negative consequences for plotting, descriptive statistics, estimation of parameters or statistical tests (van den Boogaart & Tolosana-Delgado, 2013). Zero values are considered as trace zeros meaning that values are below the detection limit (BDL). According to Hijazi (2011) and Palarea-Albaladejo & Martín-Fernández (2008) trace zeros should be replaced to allow log-ratio based factor analysis of the data set. This is achieved with EM-based replacement of zeros in compositional data (Palarea-Albaladejo *et al.* (2007), function `impRZilr` from `robCompositions`) without distorting the covariance structure of the data (Martín-Fernández, 2003). The robust factor analysis with varimax rotation (Filzmoser *et al.*, 2009; Reimann, 2008) is based on covariance estimation using the Minimum Covariance Determinant (MCD) estimator (Hubert *et al.*, 2012; Rousseeuw & Leroy, 1987) of log transformed XRF data.

Differences between the chemistry of the cultural layers and reference Nile clay material are visualized by a spiderplot in Fig. 5.9. Spiderplots are frequently used in petrology and were developed to analyze rare earth elements (REEs) between different rock types (Reimann, 2008; Rollinson, 1995). In this case, selected elements of this study (y-axis) are plotted as the ratio of that element to reference Nile material (samples outside a 600 m radius of ancient settlements and within depths between 3 and 10 m below the surface (bts). Through normalization different element curves are aligned and deviations from the reference material become immediately visible. Those geostatistical procedures are used to identify suitable elements for machine learning with neural networks. We define suitable elements as elements that are measurable in a majority of the total sample material and that tend to correlate with the different cultural phases in Buto, meaning that they bear a geochemical fingerprint, and which are less affected by post-sedimentary processes such as precipitation of salts and dissolving.

Neural networks are used to register patterns within the data that allow “indirect” dating of the sediments. Very generally and simply stated, neural networks mimic human learning. Information is processed by processing elements called neurons that act analogously to nerve cells of the human body in a way that inputs are received, weights attached and an output value is passed to connected neurons (Bell & Croson, 1998). Input values are multiplied by the weighting factor, summed and passed on by the transfer function to the next neurons.

This design allows neural networks to detect non-linear relations and to analyze a plurality of parameters. Many studies in archaeology use neural networks for shape analysis, texture analysis, rock-art studies, archeometry, burial analysis etc (Barceló, 2004, 2009; Bell & Croson, 1998). Supervised machine learning relies on prior knowledge. We use neural networks to classify the geochemistry of sediment samples to corresponding ages of the anthropogenic material or classify it as alluvial Nile material.

## 5. ARTICLE 3, DATA ANALYTICS AND MACHINE LEARNING

---

A training set is used to construct models that allow classification of the test data, namely, the geochemical data of the samples belonging to the different corings.

A similar approach that also used pXRF data in a supervised approach to train neural networks and classify archaeological soils was applied by Oonk & Spijker (2015). Learning of the network is achieved with the resilient backpropagation algorithm with weight backtracking (Riedmiller, 1994). In this iterative process, training data is presented to the network and the results are compared to the desired output. The weights of the network are adjusted using back propagation of the error until results are equal to the desired output. In essence, the network learns by examples and self-correction (Bell & Croson, 1998). The network converges when a local minimum in the error function is found (Guenther & Fritsch, 2010). In order to perform the neural network analysis with the R-package neuralnet (Guenther & Fritsch, 2010) a training and test data set is to be defined. Our training set comprises in total 539 samples, 95 dated sediment samples from the corings, 141 dated archaeological samples taken from walls and floors of the archaeological profiles, and 303 samples from alluvial Nile material. The latter are the sediment samples surrounding dated pottery in the corings. To ensure that cultural sediments are not included, training data for the alluvial Nile material is selected as samples lying outside a 600 m radius of settlements and in depths below 6 m. Considering the quantities for the different cultural phases, the training data consist of 74 Roman, 109 Dynastic, 47 Predynastic, and 303 alluvial Nile samples.

The test data comprises 1747 sediment samples from the different auger cores shown in Fig. 5.5. Zeros in training and test data are treated as trace zeros (see 5.4.5) and replaced. The categorical dating of each sample is marked in a one-hot encoding. Therefore, a new binary variable is added for each unique date and “1” is placed for the binary variable with the date and “0” for the other dates or the alluvial Nile material.

The structure of the neural network is presented in supplement Fig. A.6 and consists of two hidden layers with 16 and 5 neurons. Input are the elements presented in Table 5.1 and output are the three cultural phases or the alluvial Nile material to which the pXRF data are assigned. Neural network analysis has been performed two times. In a first run (colored crosses in Fig. 5.11, 5.12, 5.13 and 5.14, training data consisted of the 539 samples as described earlier. In a second run (colored dots), the training data is artificially simulated. This is done by imputing values within the  $\pm 1\sigma$  ranges for the different elements. As a result, the training set of the second run consists of 5390 artificial samples.

### 5.5 Results and discussion

Results are divided into two sections. The first section presents results regarding measurement precision and the general quality of the sample data. This also involves the quantification of post-sedimentary effects that alter element concentrations. Secondly, statistical methods such as multivariate factor analysis shed more light on the geochemical differences between different cultural phases in Buto.

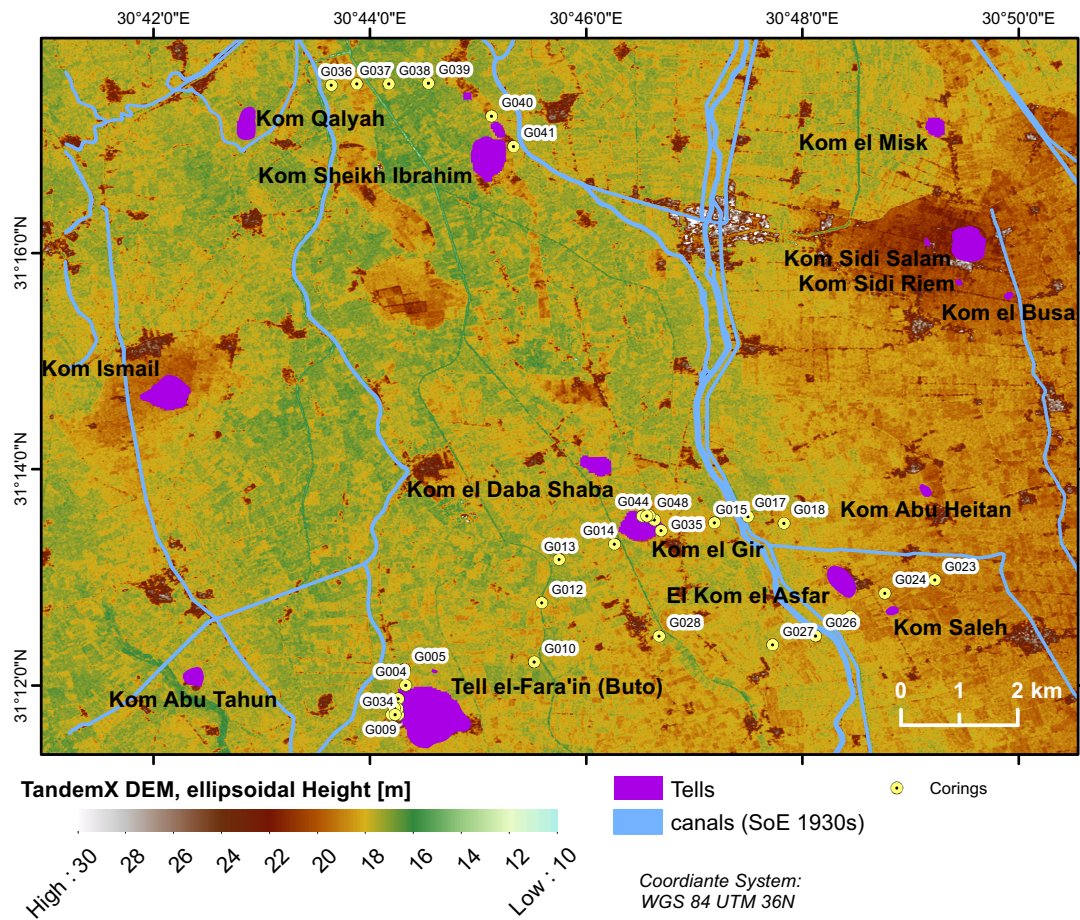


Fig. 5.5: Location of sedimentological corings analyzed with pXRF - Corings are illustrated on top of the TanDEM-X elevation map (German Aerospace Center, DLR).

## 5.5.1 XRF methodology

Detection limits (see table 5.2) are calculated based on repeated measurements of reference materials showing different element concentrations. Table 5.3 expresses the measurement precision as the average coefficient of variation of repeated measurements of standards. Coefficients of variation for elements such as Au,Bi,Co,Cd,Pd are rather high as they seldom reach concentrations that can be registered by the xrf device.

Table 5.2: Limits of detection (LOD) for selected elements

Element	LOD [ppm]	Element	LOD [ppm]	Element	LOD [ppm]
<b>Ag</b>	3	<b>Fe*</b>	25	<b>Se*</b>	4
<b>As</b>	3	<b>K</b>	25	<b>Si</b>	1
<b>Al*</b>	750	<b>Mg</b>	1000	<b>Sn</b>	4.5
<b>Au</b>	4	<b>Mn*</b>	30	<b>Sr*</b>	8
<b>Ba*</b>	50	<b>Mo</b>	1.6	<b>Te</b>	15
<b>Bi</b>	4	<b>Nb*</b>	3	<b>Th</b>	1.2
<b>Ca*</b>	65	<b>Ni</b>	10	<b>Ti</b>	13.6
<b>Cd</b>	4	<b>P</b>	40	<b>U</b>	2.3
<b>Ce</b>	60	<b>Pb*</b>	4	<b>V*</b>	12
<b>Cl</b>	40	<b>Pd</b>	5.5	<b>W</b>	15
<b>Co</b>	30	<b>Rb*</b>	6	<b>Y*</b>	1.5
<b>Cr</b>	30	<b>S</b>	50	<b>Zn*</b>	6
<b>Cs</b>	3	<b>Sb</b>	6.5	<b>Zr*</b>	3
<b>Cu</b>	6	<b>Sc</b>	3.5		

These first analyzes identified reliable elements for the classification of settlement layers via pXRF signals on the basis of precision values. Secondly, it is necessary to compare these results with the high amount of sediment samples that were measured. Fig. 5.6 gives an overview of the percentage of samples that lie over the detection limit for each element. In total 1611 samples were analyzed. Fig. 5.6 points out that the elements Ag, Au, Bi, Cd, Co, Mo, Pd, Se, Te, Th only showed concentrations above the detection limits in 20% or less of all analyzed samples and are excluded from the analyzes. Additionally, coefficients of variations are rather low for these elements. Cl, P and Te show high differences between archaeological and sedimentological samples. In contrast to their concentrations in the sedimentological samples, Cl and P are generally higher in archaeological material and exceed detection limits. Te shows a similar less pronounced and opposite effect, with Te concentrations being higher in the sedimentological samples. By definition elements with element concentrations exceeding detection limits in more than 50 % of the alluvial Nile material and archaeological sample material are taken into consideration. These are As, Al, Ba, Ca, Ce, Cl, Cr,



**Table 5.3:** Coefficient of variation (CV) for selected elements

Element	CV [ppm]	Element	CV [ppm]	Element	CV [ppm]
<b>Ag</b>	18.3	<b>Fe</b>	1.0	<b>Se</b>	0.9
<b>As</b>	27.4	<b>K</b>	4.1	<b>Si</b>	4.0
<b>Al</b>	6.7	<b>Mg</b>	13.3	<b>Sn</b>	38.8
<b>Au</b>	46.6	<b>Mn</b>	5.1	<b>Sr</b>	1.8
<b>Ba</b>	3.8	<b>Mo</b>	26.1	<b>Te</b>	47.8
<b>Bi</b>	42.0	<b>Nb</b>	9.2	<b>Th</b>	14.9
<b>Ca</b>	3.8	<b>Ni</b>	8.9	<b>Ti</b>	4.5
<b>Cd</b>	27.1	<b>P</b>	65.0	<b>U</b>	35.5
<b>Ce</b>	16.9	<b>Pb</b>	10.7	<b>V</b>	9.8
<b>Cl</b>	27.7	<b>Pd</b>	49.0	<b>W</b>	35.4
<b>Co</b>	66.1	<b>Rb</b>	2.8	<b>Y</b>	5.7
<b>Cr</b>	8.9	<b>S</b>	9.3	<b>Zn</b>	6.6
<b>Cs</b>	16.2	<b>Sb</b>	20.5	<b>Zr</b>	4.2
<b>Cu</b>	11.9	<b>Sc</b>	48.0		

Cs, Cu, Fe, K, Mg, Mn, Nb, Ni, P, Pb, Rb, S, Sc, Si, Sr, Ti, U, V, W, Y, Zn and Zr. Results on the effects of post-sedimentary alteration or heterogeneity of element concentrations are presented in Fig. 5.7 (a). These differences most likely result from the precipitation of salts, leaching of elements or the presence of inhomogeneities caused by microlayers, crustations or concretions. They are analyzed by describing the differences between element concentrations of directly neighboring samples from the same records. Results are expressed as the share of the difference between the two samples to the standard deviation for each particular element. The standard deviation is calculated as the mean standard deviation of the repeated reference sample measurements. However, standard deviations for elements showing  $R^2$  values  $>0.6$  in Table 5.1 are calculated from the regression equation by inserting the average of both samples. Elements Ca, Cl, Fe, Mn, P, S and Sr show differences that exceed 3 times the standard deviation for that particular element. Therefore, these element concentration changes are considered significant.

Similar to this approach, element concentrations within one archaeological record, namely, a Predynastic floor (E13/928) are analyzed. Overall 32 samples of this floor are measured, see supplement Fig. A.7 (b). The standard deviations of the different samples within the floor is divided by the standard deviation of the measurement precision for each element. Likewise to the prior approach with the double sampling, the variation can in this way be expressed as a factor of measurement precision. Again, elements Cl, Fe, Mn, P, S and Sr show differences that exceed 3 times the standard deviation of measurement precision for that particular element. Compared to the prior

## 5. ARTICLE 3, DATA ANALYTICS AND MACHINE LEARNING

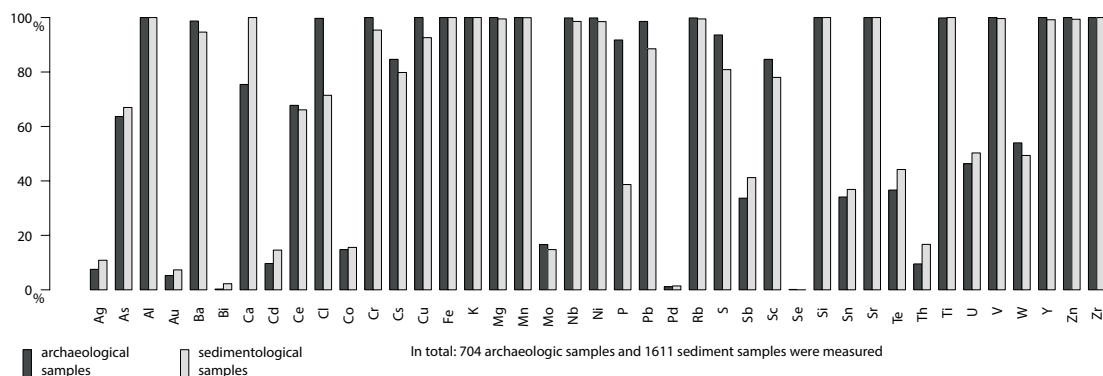


**Fig. 5.6: Selection of elements** - Percentage of the number of archaeological and sedimentological samples lying over the detection limits of the different pXRF elements.

approach, Cs shows significantly lower resolutions.

### 5.5.2 Geostatistical analysis

In a first attempt, sample material of the large-scale coring transects tending rectangular to the settlements (Ginau *et al.*, 2019) are analyzed. This material not only exposes differences between the different sediment layers, especially the Holocene alluvial material and the Pleistocene layers, but also differences relating to the influence of former settlements on element concentrations. Secondly, the element concentrations of the different archaeological layers from the excavations (E, PB Profiles) are further researched to shed more light on the internal element characteristics of the archaeological sample material. These analyzes should not only verify that there exist different elemental characteristics or fingerprints between the archaeological layers of the different phases but also characterize these differences. Results of both steps are used to refine and choose the right set of training data for the application of machine learning techniques that are used to link settlement layers of unknown origin with a specific cultural phase.

#### 5.5.2.1 Chemical differentiation along large-scale sedimentological transects

Sample material of the large-scale coring transects (Ginau *et al.*, 2019) are analyzed via multivariate statistics described in the previous chapter. These are 1611 samples from 32 different corings (see Fig. 5.5). Moreover, Fig. 5.8 displays the results of this spatiostatistical analysis that tends to identify representative element concentrations for different sediment units or environments. The position of each coring is plotted according to the distance to the next neighboring settlement mound. Therefore, all corings next to Tell el-Fara'in or Kom el'Gir show low distances and are located in the western area of Fig. 5.5.

The five factors explain 63 % of the data variability. Each factor is shaped by

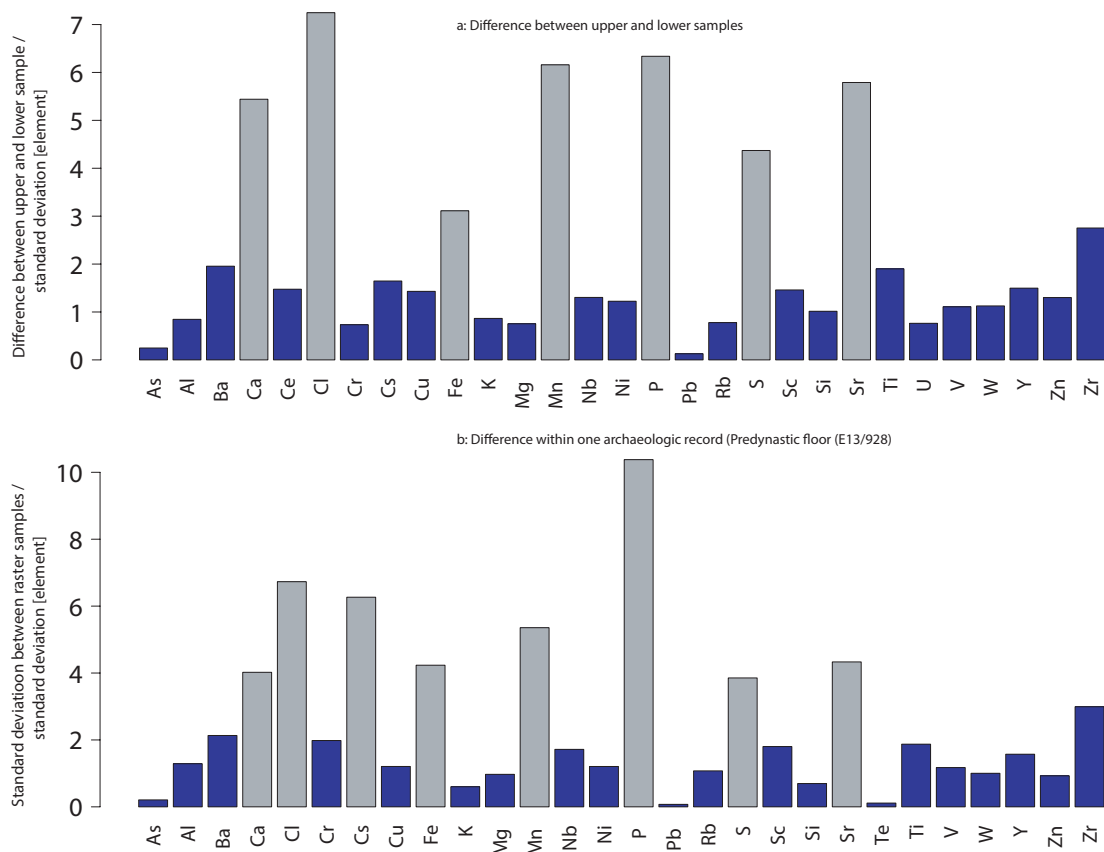


**Fig. 5.7: Post-sedimentary affected elements** - Deviation between the element contents of a: upper and lower samples, b: directly neighboring samples within the same record, as a factor of the standard deviation describing the measurement precision for each particular element. Elements with differences greater  $3\sigma$  are highlighted in gray.

## 5. ARTICLE 3, DATA ANALYTICS AND MACHINE LEARNING

---

a specific set of elements that tends to correlate with the sedimentary layers or the distance to the next settlement sites. Factor 1 seems to react to individual cores showing fine-grained channel deposits which are located along the Bahr Nashart and in the surroundings of Buto. Especially elements Cr, Ni, P, Mg, Cu, and Si show higher loadings to factor 1. Overall, factors 2 and 3 show higher loadings in the upper 4 to 8 m and reflect the strong chemical differences in the alluvial Nile mud lying on top of Pleistocene sands. In the case of factor 2, elements with positive loadings representing the Nile alluvial material are e.g. Fe, Al, Cu, Mg, Cr, V, Y, Ti and Rb. Especially elements typical for clay minerals or rare elements enclosed by higher adhesion forces occur within the upper clayey meters. Below lying Pleistocene sands often show a high concentration of salts, especially in the form of carbonate concretions. This is reflected by high negative loadings at the boundary resulting from higher contents of P, K, Sr and Ca (factor 2) and Si (factor 3). Nevertheless, factor 3 also bears a strong anthropogenic component, as loadings tend to be higher in corings close to the settlements. Also higher loadings in the corings do not reach as deep as in factor 2. So higher loadings in the upper meters tend to reflect the anthropogenic signal stored within the Holocene surface. Consequently, loadings for elements such as P, Pb, Ca, K, Sr are higher for factor 3. Factor 4 seems to be a combination of factors 1 to 3. It shows higher values for surface samples of specific cores with a general tendency towards higher loadings for corings close to the settlements. Factor 5 shows the highest loadings in corings located near the settlements and comparably higher loadings in the upper meters for the other corings. This factor reflects only 3 % of the variability in the data but seems to describe the anthropogenic impact best and elements such as Cu, Pb, P, Zn, Ca, K, Rb show higher loadings.

### 5.5.2.2 Chemical differences within archaeologic samples

In this section, pXRF results of the archaeologic sample material are presented. Analyzes are chosen to evaluate the different elements for their quality to distinguish between different cultural phases or settlement periods. Generally, element concentrations are thought to vary depending on the cultural phase in which they were deposited. This can be due to the variation of element fluxes in the course of technological revolutions, changes of the population in composition and density and abandonment or colonization of new sites. This work tries to differentiate between the main settlement periods occurring in Buto, which are the Predynastic, Dynastic and Roman period. The spiderplot of Fig. 5.9 with element curves of the three different settlement periods shows that compared to the Nile reference the settlement material is generally enriched in Zn, W, Sr, Sc, P, Mn, K, Cl, Ca and Ba. It is also noticeable that the curve for the Roman period shows concentrations of W, Sr, Sc, Pb, P, K, Cu, Cl and Ca. Of high interest are the higher S, Pb, Cu, Cl and Ca concentrations compared to the other two periods. Predynastic and Dynastic sample material show similar trends with greater differences for elements U, Sc, P, Cl and Ca.

The strong differences in the element concentrations of U, Ca and Cl might be related to post-sedimentary alterations. Highest Ca and Cl contents in the uppermost

## 5.5 Results and discussion

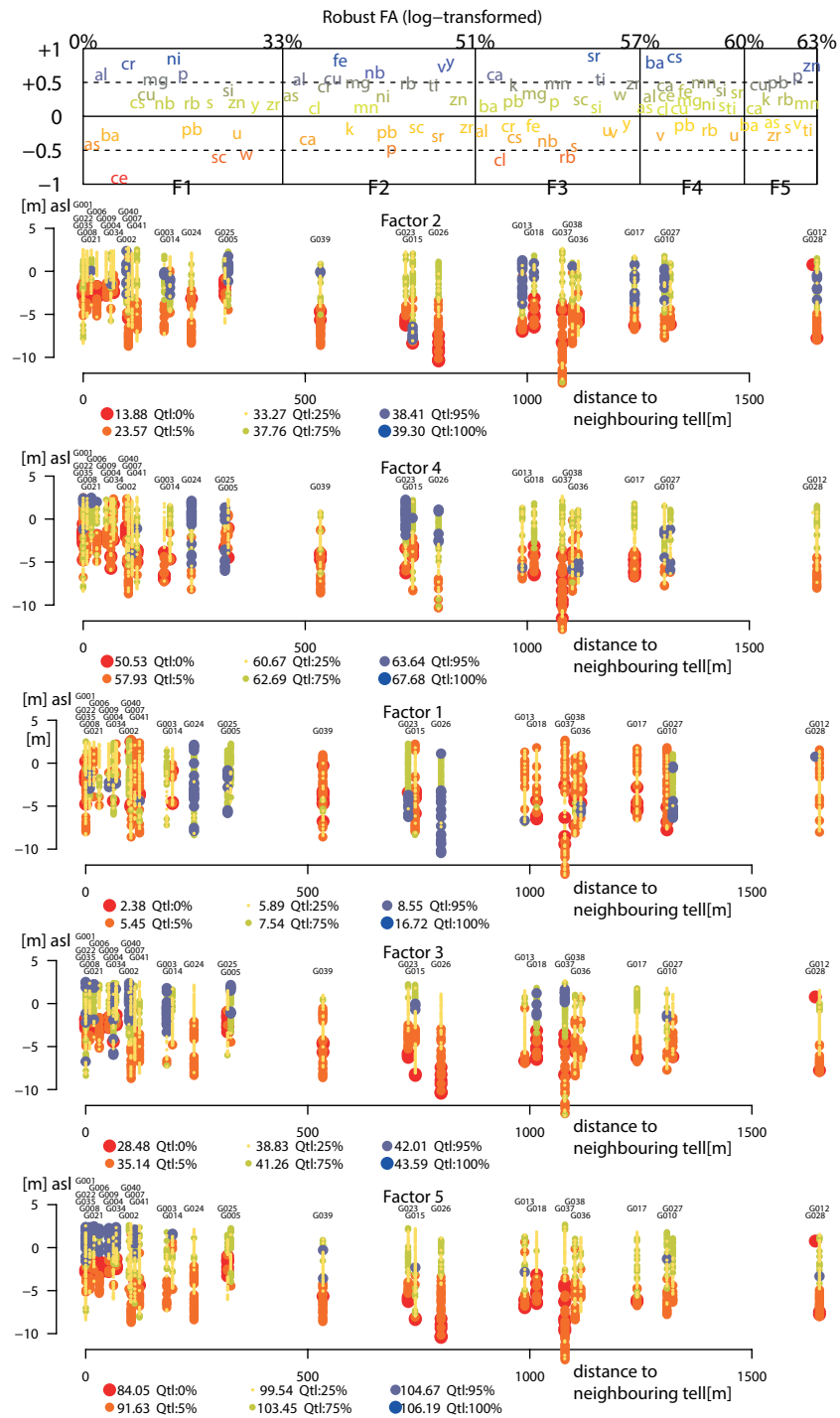


**Fig. 5.8: Chemical differences along large-scale transects** - Results of a robust factor analysis with varimax rotation and log-transformed data. The factor map shows the assemblage of elements belonging to the different factors. Sample points are plotted against sample distance to next neighboring settlement mounds and depth of the sample in m above sea level (asl). The color of the sample points represents the factor scores. For each factor the colors represent different quantiles and a legend is included for each factor.

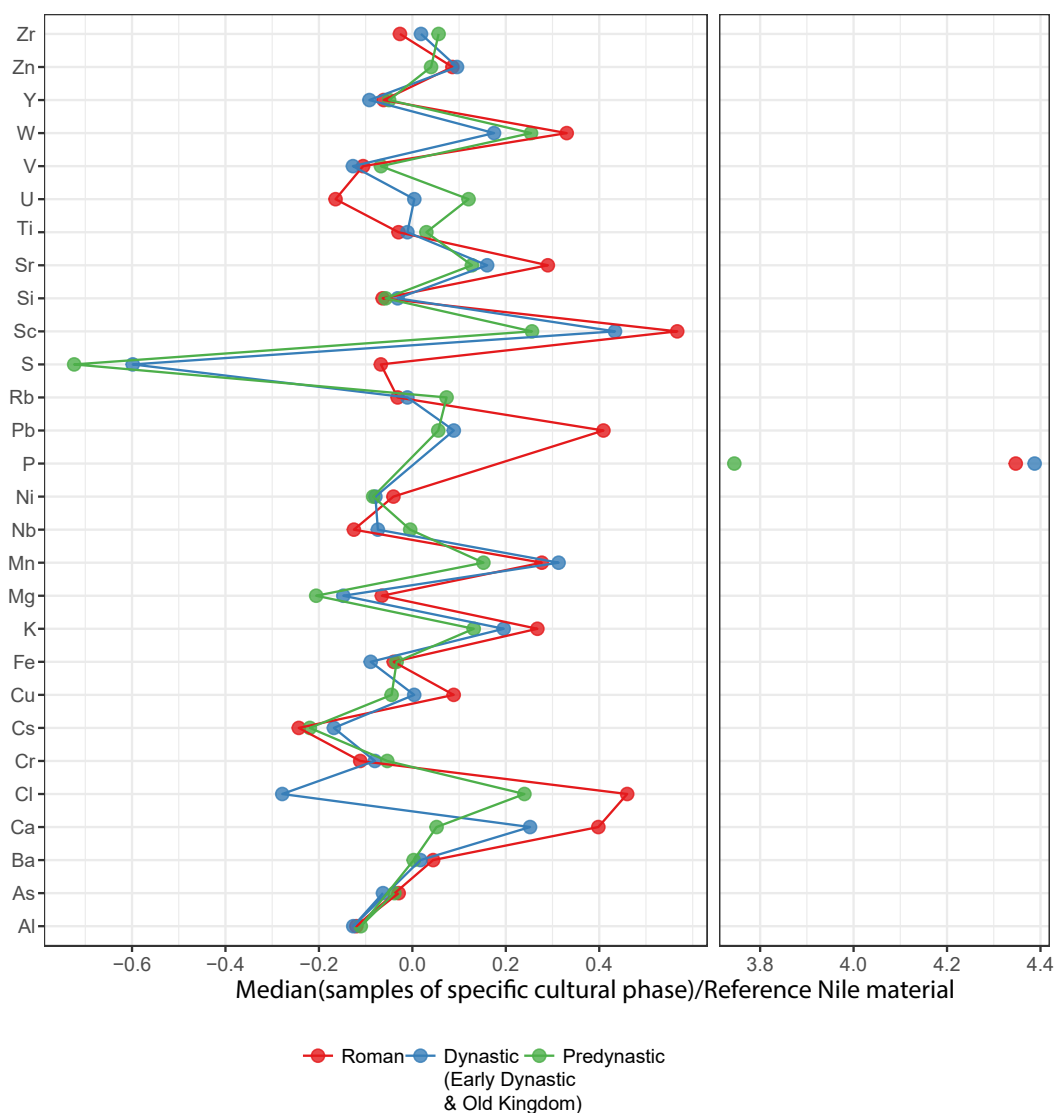


**Fig. 5.9: Spiderplot showing pXRF profiles** - A selection of elements is plotted along the x-axis against the ratio of the element concentration to the concentration of reference Nile material. The element contents of the reference Nile material as well as samples belonging to the three major archaeological periods are calculated as median element values of the complete pXRF dataset. Additionally, samples representing the reference Nile material are spatially selected as fine-grained material lying outside 600 m radius of ancient settlements and within depths between 3 and 10 m bts

Roman material can be explained by precipitation of salts and ascension of soil moisture. And the fact that the lower lying Predynastic samples show higher Ca contents than the Dynastic samples might relate to the foundation of the settlement on top of the Ca enriched Pleistocene surface or the different dynamics between sea-level rise, accretion of tell material and ground water changes. Also descendent mobilization of precipitation water may have contributed to this stratification of elements. In contrast to this, U shows lowest concentrations in the surface material, which might be related to the solvation and enrichment of U in the ground water. Therefore, lowest samples show highest U concentrations.

Fig. 5.10 shows the chemical differentiation between the different archaeological records for selected elements, for an overview of all measured elements, see supplement Figs. A.8 and A.9. Elements with at least one highly distinctive or more than two slightly distinctive records are Ca, Cl, Cu, Fe, K, Mg, Mn, P, Pb, Rb, S, Sc, Si, Sr, Ti, Zn and Zr. The element distributions highlight that many metals (Cu, K, Mg, Pb, Sr, K) show higher contents in Roman sample material. This is especially true for samples belonging to floors or cultural layers but not for debris. Predynastic material shows low Al, Cl and Fe contents in wall samples and is generally enriched in Sr, K, and depleted in Rb. Dynastic cultural layers and floors are enriched in Pb. In many cases, floors tend to show distributions with specific and condensed violins that do not spread over broad value ranges (eg. Ca, K, Fe, Nb, Rb, Sr, Y, Zr) and are regarded as records storing the cultural fingerprint best.

This analysis shows that there exist not only differences between tell material and the alluvial Nile sediments but between the different cultural layers. Especially floors show strongest chemical differences between the cultural phases. Secondly, Predynastic walls seem to be distinguishable as they are depleted in many elements. Cultural layers such as house fillings or erosional debris are left out as they tend to be intermixed with material of different cultural phases. In addition, our methodological approaches showed that the measurement precision varies significantly for the different elements and the sediment and archaeological layers experienced mobilization and leaching of elements.

### 5.5.2.3 First application of neural networks

In this section, we confront the artificial neural network described in 5.4.5 in a supervised machine learning approach with these preconditions and verify if they are suitable to date the sediments of the different corings placed in the surrounding of the settlement sites Buto, Kom el'Gir and Kom Sheikh Ibrahim.

For each of the four classes the network outputs values that should range between 0 and 1 and the sample is assigned to the class with the maximum value. Comparing the two runs, it is obvious that the second run, where the network is trained with a much greater set of simulated sample data, shows less scattering in the output data. Classified outputs stay more or less exactly around 1.

Both approaches produce classification errors especially for Predynastic sample material. Predynastic material is hard to differentiate, as it bears only slight geochemical

## 5. ARTICLE 3, DATA ANALYTICS AND MACHINE LEARNING

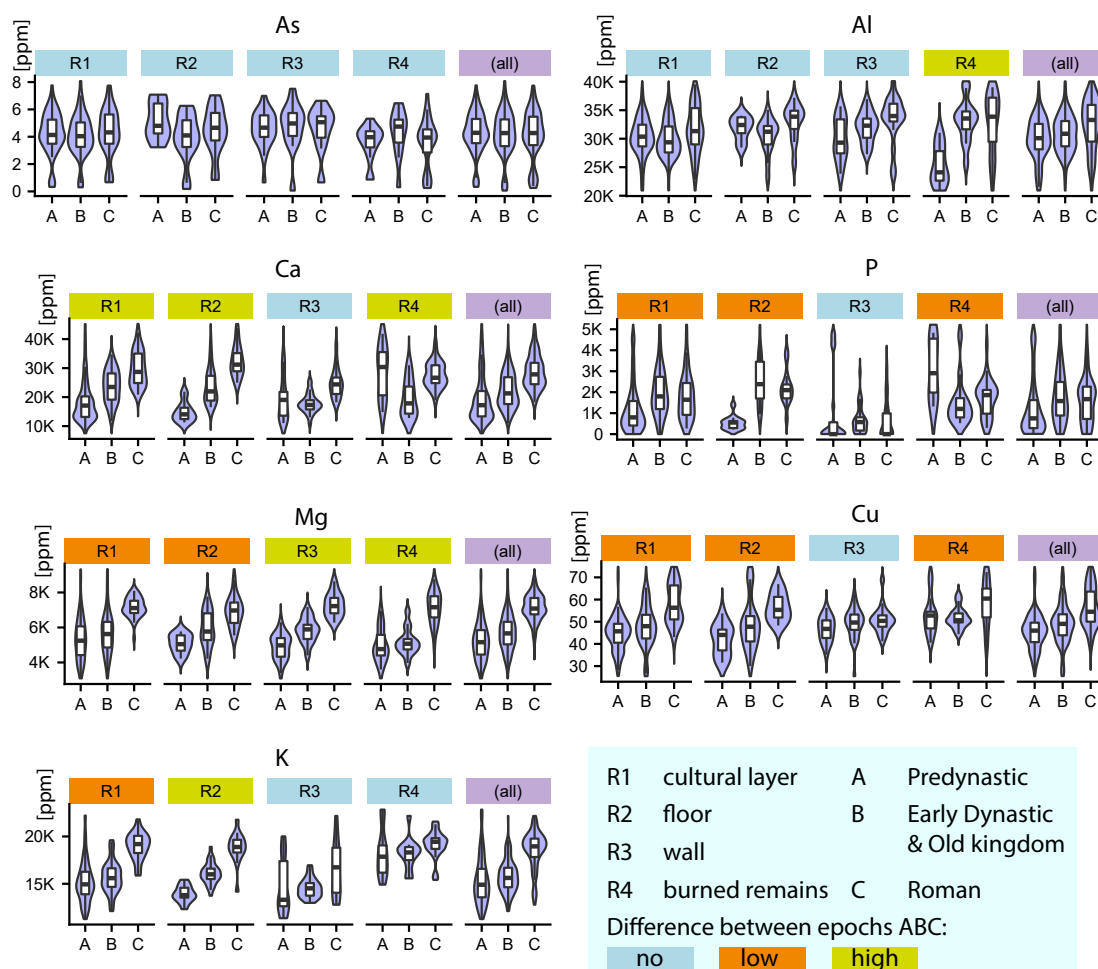


**Fig. 5.10: Chemical differentiation between archaeological records and main epochs for selected elements** - Illustrated are the pXRF data distribution of elements selected in chapter 5.5.1. The results are presented in form of violin plots. In addition to normal box plots, they show the smoothed probability density of the data on each side. Results are presented separately for the different archaeological records and epochs. The last violin plot on the right for each element shows the distribution of all records for the three different epochs. Records of elements with a distinctive pattern for only one or all three epochs are marked in orange if they show slight differences in their distributions and in green if the differences tend to be high and significant. This differentiation is applied qualitatively based on violin plots. An overview of all elements is given in the supplement



differences to the Dynastic material and furthermore, Predynastic material shows the lowest share within the training set. Simulation of data allows the network to compensate misinterpretations based on elements that are hard to measure. On the other hand, the network can misinterpret simulated data. Another aspect is that the surface is mostly interpreted as Roman material. Training data with Roman material was taken from near surface layers in Buto and Roman material generally occurs mostly near the surface. Processes such as precipitation of salts or leaching create specific element compositions that superimpose the geochemical fingerprint of the cultural layers. And it was a common practice in the past to use tell material as fertilizers and spread it on fields (Ginau *et al.*, 2019; Schiestl, 2012a,b). Generally, it is very hard to validate the results of the neural network. Nevertheless, results will be compared to sedimentological results of the corings, especially the ceramic findings.

In the following, results of the neural network analysis are presented and discussed for the settlement mounds Buto, Kom el'Gir and Kom Sheikh Ibrahim and the larger area around Buto and Kom el'Gir where corings show greater distances to the previous mentioned settlement sites.

Results of both networks suggest for most corings close to Buto (see Fig. 5.11) the typical sequence with Roman layers at the top, followed by Dynastic material below. As stated above, both neural networks mostly classify surface layers as Roman material. Thin layers of Predynastic material on top of the alluvial Nile sediments occur in corings G8, G9 and G34. The second network identifies Predynastic material in corings G1, G2, G4, G6 and G5. Only in case of G6, the first network identified Predynastic material. In most cases, cultural layers reach down to about -2.5 m asl. Both networks suggest the presence of Dynastic material on top of Roman material in coring G1. Pottery datings correspond with the results of the neural network, but often the dated cultural layers of both neural networks reach deeper than ceramic findings in the corings suggest. This might be related to the vertical dislocation of elements within the sediment columns. Cultural layers of Roman or Dynastic origin reach down very deep in corings G2 (-4 m asl), G4 (-3.5 m asl) and G1 (-3 m asl), whereas, cultural material at the base of corings G6 and G7 are suggested as misinterpretations by the neural network.

At core site G3, loamy fine sandy material appears between -0.5 m and -7.5 m asl with small gravel found at -7 m asl (Ginau *et al.*, 2019; Wunderlich & Ginau, 2016). At -5.3 m asl a thin, darker layer containing plant remains is found and seeds from this layer date back by  $^{14}\text{C}$  dating to about  $2210 \pm 30$  BP (Beta-354940), or 358 - 207 cal BCE( $1\sigma$ ) which is interpreted by Ginau *et al.* (2019) as channel infill. Both networks suggest at singular points the presence of Roman cultural material. Very likely because the channel infill is mostly composed of sand intermixed with other material; the chemical fingerprint is completely altered and cannot resemble the silty and clayey material of the cultural layers.

Four corings in the direct vicinity of Kom el'Gir are analyzed with the pXRF device. Both networks suggest the presence of Roman material on top of Nile clay material.

## 5. ARTICLE 3, DATA ANALYTICS AND MACHINE LEARNING

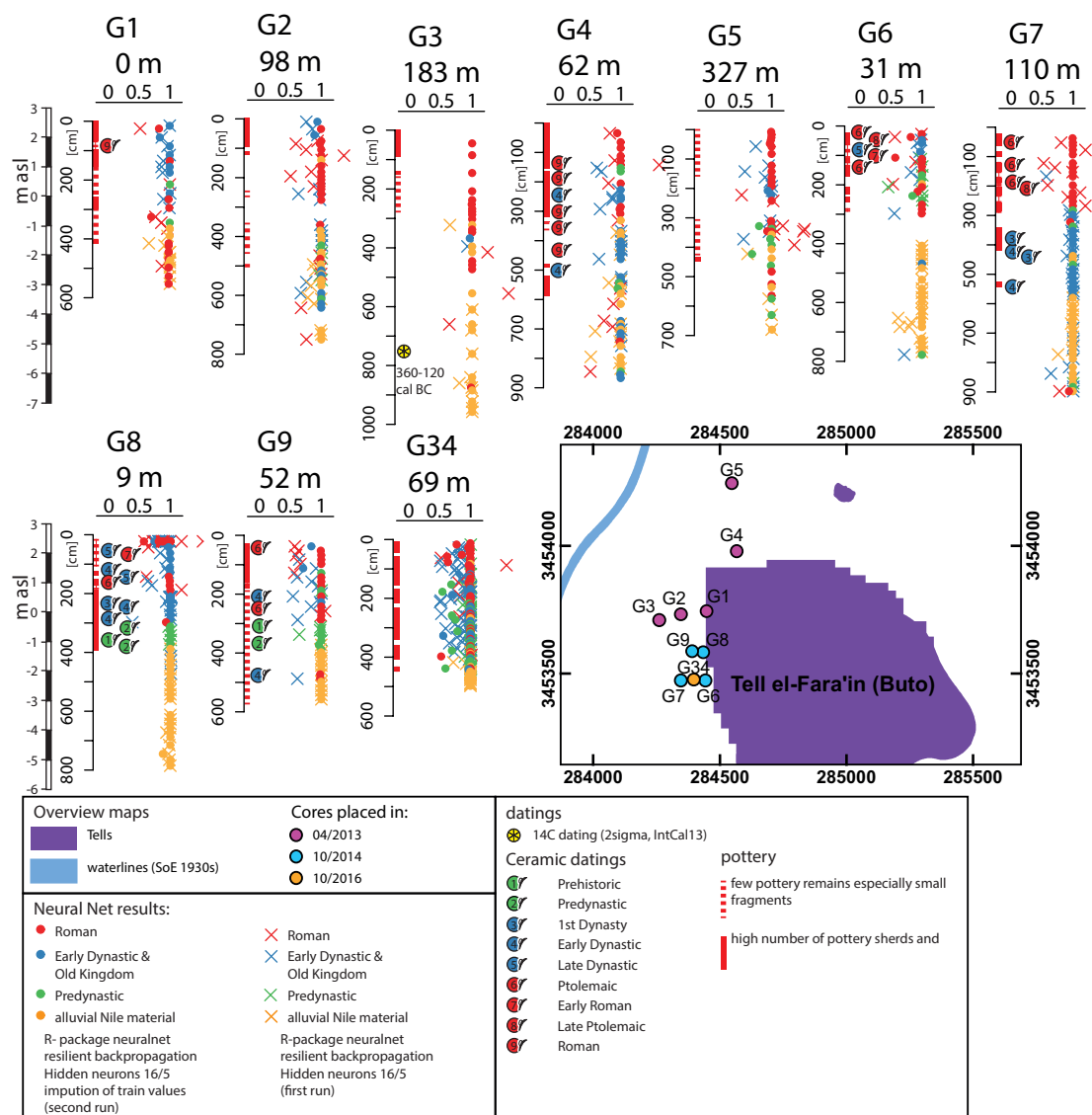


**Fig. 5.11: Neural network results - Dating of core sediments in the area around Buto.** The enclosed map shows the location of the corings. Below the coring number the distance to the next neighboring tell is given. The unit of the x-Axis shows the probability of the neural net.

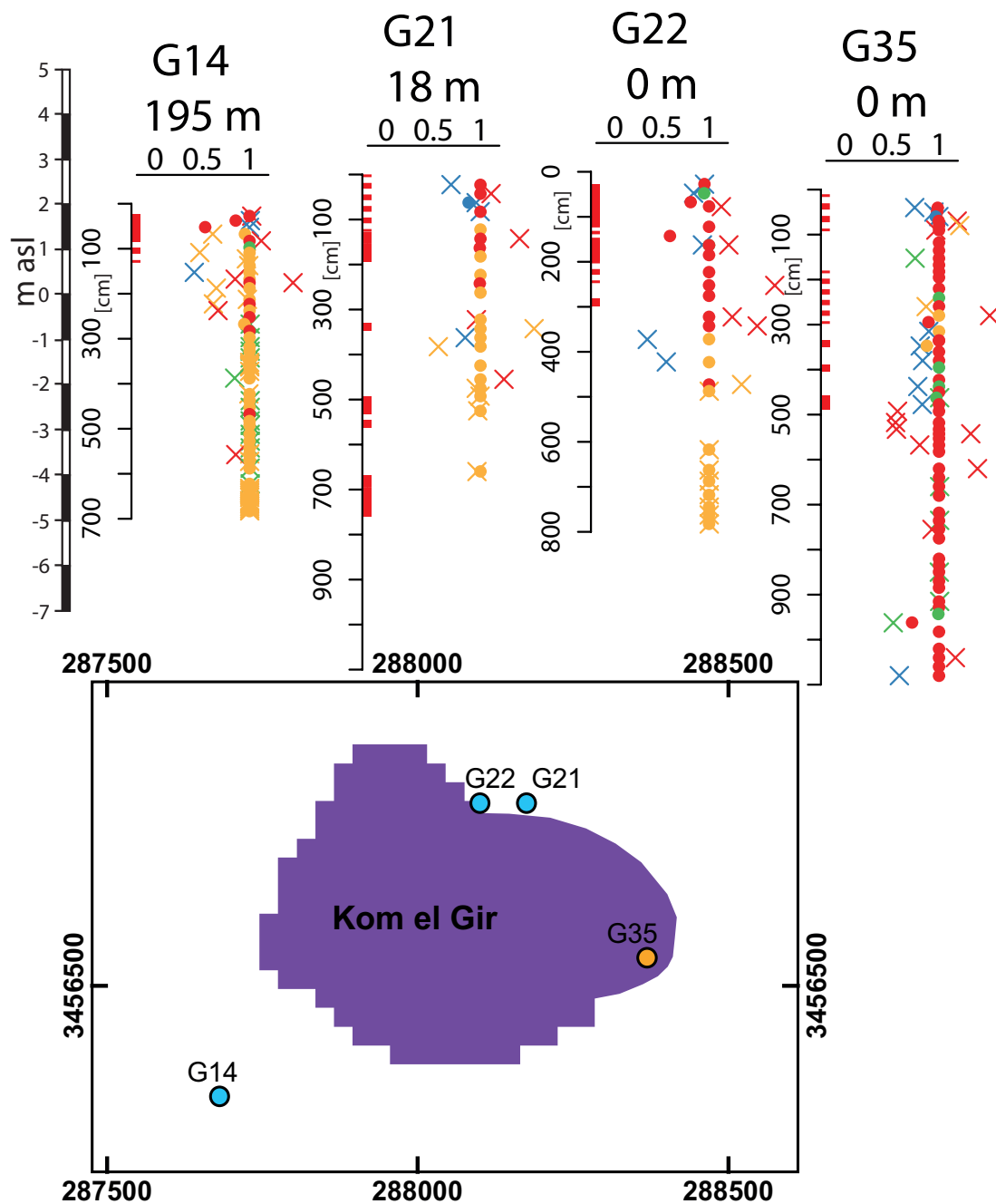


**Fig. 5.12:** Neural network results - Dating of core sediments in the area around Kom el'Gir. The enclosed minimap shows the location of the corings. Below the coring number the distance to the next neighboring tell is given. The unit of the x-Axis shows the probability of the neural net. The legend is presented in Fig. 5.11.

## 5. ARTICLE 3, DATA ANALYTICS AND MACHINE LEARNING

---

Identified Roman layers reach a bit deeper than ceramic findings suggest in coring G14, G21 and G22. The first network identifies Predynastic material in coring G14 in depths between -0.5 and -4 m asl, which is interpreted as Nile material by the second network. The depths of the identified Roman material correspond with the depths of ceramic fragments present in the corings. Corings G21 and G22 show in-situ tell material lying on top of silty or fine sandy alluvial Nile material. Nevertheless, both networks do not recognize layers with ceramic fragments in G21 that occur at -2.5 and -4.5 m asl. Coring G35 is actually located very close to the tell and is fully interpreted by both networks as cultural material of Roman origin reaching to about -9 m asl. Additionally, the first network suggests the presence of Dynastic material at insular locations in the upper 5 m of the core. Recent geophysical results by Robert Schiestl suggest the presence of a channel flowing along the eastern side of Kom el'Gir. Coring G35 might be located in this channel, which was filled by tell sediments of its direct surrounding.

The first meter of the more distant corings of Kom Sheikh Ibrahim (G36, G37, G38 and G39) is interpreted as Roman material, probably to surface related effects or spreading of seabkh. Only corings G40 and G41 show thicker cultural layers of up to 5 m bts. The first network trained with the original data signals the presence of Dynastic material at various locations within these layers and both networks show a small layer of Predynastic material in Coring G40. Coring G37 is located on a former large alluvial branch of the Nile (Ginau *et al.*, 2019) and almost completely interpreted as Nile material. It can be hypothesized that the channel at G37 is filled with cultural material. But even if there is cultural material at depths around 12 m bts as  $^{14}\text{C}$  datings of Ginau *et al.* (2019) might suggest, it is diluted by sandy material in a way that it cannot be detected by the neural network. Corings G37, G40 and G41 rest near elevated levees that aggregated along the former Nile branches or represent filled channels between the elevated levees.

Corings of the larger area around Buto and Kom el'Gir show cultural layers in the upper meters, ranging between 0.5 and 2 m bts, which corresponds well with sedimentation rates of about 1 m in 1000 years (Butzer, 1976; Wunderlich, 1989). Coring G10 also shows smaller Roman layers at -2 and -4 to -5 m asl. This low lying layer corresponds well with pottery findings and is interpreted as channel infill material.

### 5.6 Conclusions

Interpreting geochemical pXRF data of sedimentological samples proves to be a hard task for supervised machine learning. We simplified this task so that the neural networks used within this study were trained to differentiate between cultural material of the three phases, namely Roman, Dynastic and Predynastic or alluvial Nile material. This approach faces several difficulties that are reviewed in the following.

Our methodological approach showed that pXRF results vary in resolution and stability for the different elements. One measure describing the precision of measurements is the coefficient of variation with a high variance between the different elements. For example, metals such as Fe, Cu, or Cr show low coefficients of variation, whereas,

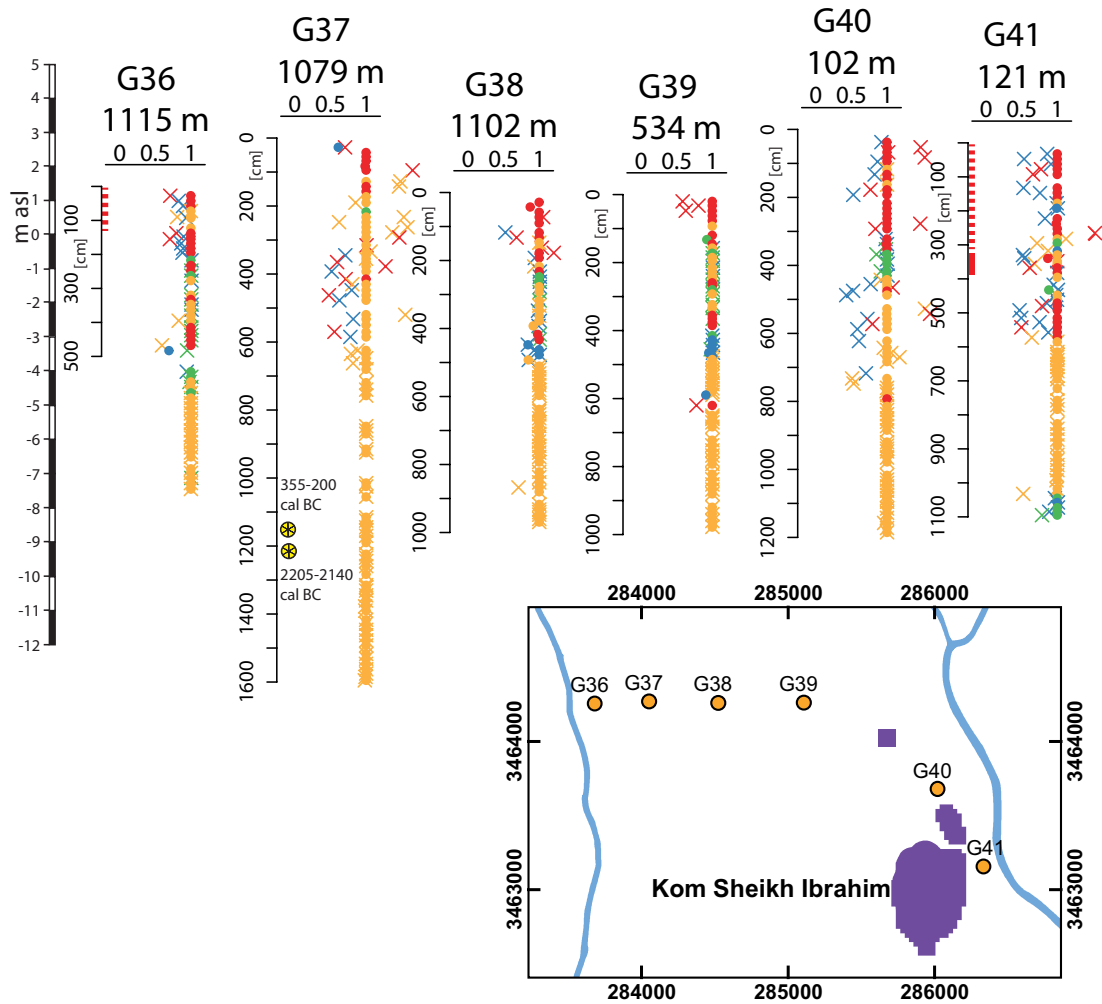


**Fig. 5.13: Neural network results** - Dating of core sediments in the area around Kom Sheikh Ibrahim. The enclosed minimap shows the location of the corings. Below the coring number the distance to the next neighboring tell is given. The unit of the x-Axis shows the probability of the neural net. The legend is presented in Fig. 5.11.

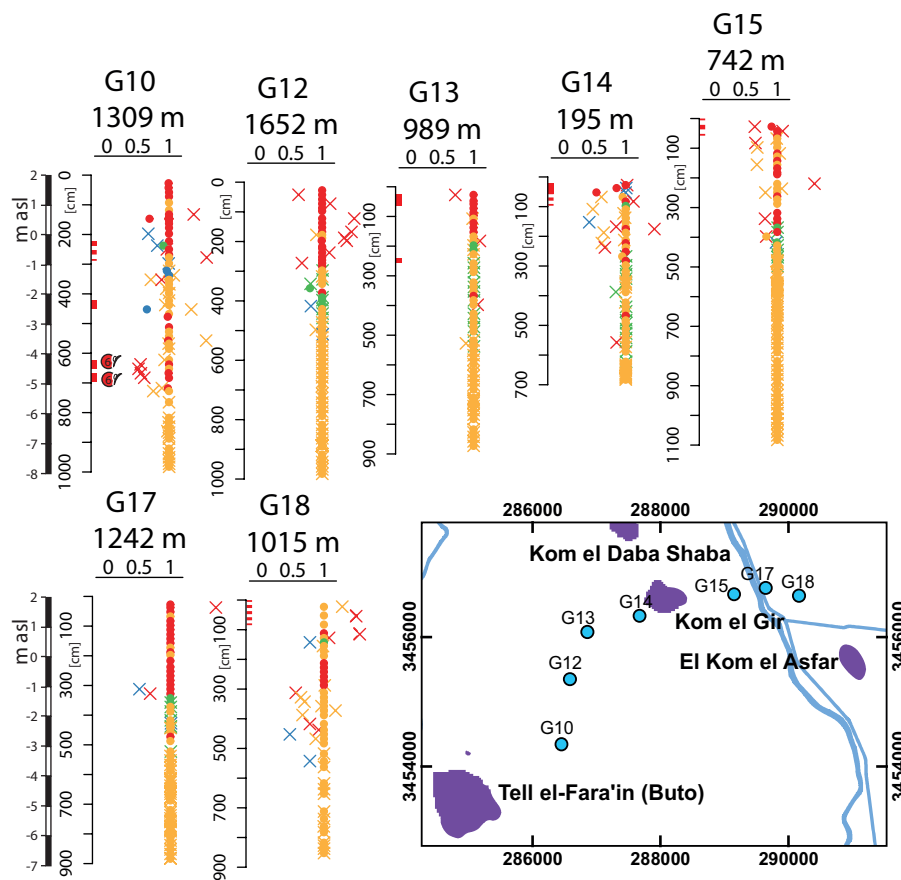


**Fig. 5.14: Neural network results** - Dating of core sediments in the larger area around Buto and Kom el'Gir. The enclosed minimap shows the location of the corings. Below the coring number the distance to the next neighboring tell is given. The unit of the x-Axis shows the probability of the neural net. The legend is presented in Fig. 5.11.

elements such as P, Co or Au show high coefficients of variation. Additionally, measurement stability varies with element concentration. Repeated measurements of pXRF standards with different element compositions show a decreasing measurement precision with an increase in element concentration. There are also many elements especially of the first and second period that the pXRF device does not register but which influence the registration of the other measurable elements. This is especially true for samples containing high amounts of organic material. Other influences such as porosity and humidity were minimized by pestling and drying the sample material. As a result, low element concentrations for the main elements suggest presence of higher amounts of non-detectable elements and to keep this information, normalization of the pXRF data was intentionally left out. Lastly, concentrations of many elements lie below the detection limit and could not be used within this study (e.g. Ag, Au, Bi, Co, Mo, Pd...). Additionally, chemical properties of sediments are altered over time by leaching of minerals or precipitation of salts as we showed by sampling individual archaeological records at several locations. Nevertheless, our statistical approaches show that there exist profound differences within the set of measurable elements that we analyzed in the archaeological material gathered from the settlements and sedimentological samples retrieved from the sediment cores. Results of a robust factor analysis revealed that along the large-scale sedimentological transects we find sets of elements that are especially enriched within the cultural material (Cu, Pb, P, Zn, Ca, K, Rb). With the help of spider and boxplots we showed that there also exist profound differences within the archaeological material that are referred to the different cultural phase the sediments were deposited. Compared to the Nile reference, the settlement material is generally enriched in Zn, W, Sr, Sc, P, Mn, K, Cl, Ca and Ba and it is noticeable that for the Roman period the curve shows higher element concentrations of W, Sr, Sc, Pb, P, K, Cu, Cl and Ca. Overall, elements showing distinctive differences between the cultural phases in at least one of the analyzed records are Ca, Cl, Cu, Fe, K, Mg, P, Pb, Rb, S, Sc, Sr, Ti and Zr.

Lastly, we used a neural network with resilient backpropagation algorithm and weight backtracking to register and learn from such differences and allow dating of sediment cores in the surroundings of Buto and Kom el'Gir. Our results correspond with dated ceramic pieces from the corings and allow a rough estimation of the cultural origin of the different core segments. Nevertheless, geochemical processes that postsedimentarily altered the sediments manifest within this interpretation, e.g. surface material with the enrichment of salts such as carbonates are always interpreted as Roman material. With this approach we could show that in some corings west of Buto we find cultural sediments reaching down to -4 m asl (G2,G9) which are possibly filled channels. Additionally, core G35 near Kom el'Gir shows cultural sediments till about -9 m asl and can be further proof of the channel that has only recently been uncovered by geoelectrical measurements east of Kom el'Gir.

The pretrained nets can be easily applied to new sample data, and results of the neural network should be further validated by testing additional material of the excavations with known context. Additionally, with larger amounts of dated material we

## 5. ARTICLE 3, DATA ANALYTICS AND MACHINE LEARNING

---

will try to make the network more sensitive and fine tune the dating. In the future we also expect to add more material from excavation works in Kom el'Gir, where from the start it is planned to systematically sample important records.

### 5.7 Acknowledgments

We thank the Egyptian Ministry of State for Antiquities for their assistance and support of our work in the field. We thank the Cairo Department of the German Archaeological Institute (DAI) and especially Prof. Dr. Seidlmayer for funding and support in the field, the Eurasia Department of the German Archaeological Institute (DAI) for supporting pXRF measurements in Egypt. German Aerospace Center (DLR) for the provision of TanDEM-X elevation data under science application DEM\_HYDR1426. We also thank Janice M. Schiestl for proofreading the article and correcting our English.



## 6

# Synthesis and conclusions

This chapter provides a synthesis of the results from chapters 3, 4 and 5. Fig. 6.1 references the three research papers that are the essential part of this thesis to the research aims presented in Fig. 1.1 and the previous sections. Additionally, it gives a concise description of the key aspects of the research and differentiates whether the chapter or paper deals with a methodological approach or whether it focuses on geoarchaeological results that contribute to the intended diachronical, geoarchaeological research. In the following the chapter comments on the research aims formulated in chapter 1.

### **6.0.1 Ad aim 1: Reconstruction of the large scale water net with location of settlement sites**

The remote sensing classification techniques performed in chapter 3 helped to complete the network of tells in the Nile delta. A method was developed that reliably differentiates existing high tells from other land use classes or surfaces like barren fields that showed similar characteristics. In a second approach, vegetation performances were calculated on the basis of *NDVI* time series derived from 66 Landsat 8 and two RapidEye scenes. Via spatial analysis, it could be proven that settlement material is enriched with plant nutritious elements and induces higher vegetation performances. In a next step the vegetation performance was related to the presence of lost tells. The results corroborated a relationship between vegetation performance and the appearance of archaeological material in the topsoil. Kom esh-Scheikh Ibrahim, for example, had once been bigger and had extended further northwest. Of far more interest is the correspondence of the vegetation performance to the routing of the former river branches researched in chapter 4. The levees of these former rivers were areas of deposition and aggradation of the nutritious Nile floods which still manifest in the results of the time series analysis.

Very important are the results of the TanDEM-X elevation model. In the elevation model levees are visible of which only the largest are traceable on historic maps or detailed topographic maps of Survey of Egypt (1:25.000, 1920s/30s editions). Comparison

## 6. SYNTHESIS AND CONCLUSIONS

---

### Development of an integrative, diachronical geoarchaeological reconstruction of the settlement and landscape history in the northwestern Nile delta



#### Aim 1

##### **Identification of historic landscape features and settlement mounds in the Western Nile Delta by means of remote sensing time series analysis and the evaluation of vegetation characteristics**

*Methodological remote sensing approach to identify ancient settlements and waterways in the northwestern Nile Delta*

- Multitemporal classification of different tell classes that are visible from the surface
- Identification of Lost tells beneath the surface via indirect analysis of the vegetation performance from an NDVI time series
- Identification of areas with high vegetation performance that follow former palaeorivers



#### Aim 1, 2, (4)

##### **Integrative geoarchaeological research on settlement patterns in the dynamic landscape of the northwestern Nile delta**

*Geoarchaeological research combining results of field work, geochemical and remote sensing analyses in order to better understand the Late Dynastic and Roman time slice*

- Analysis of remote sensing material on location of settlements and palaeorivers
- Precision estimation of TandemX material and verification of palaeorivers
- Identification channels within the geological core profiles
- Characterisation and dating of channels within the core profiles



#### Aim 2, 3

##### **What settlements leave behind: pXRF compositional data analysis of archaeological layers from Tell el-Fara'in (Buto, Egypt)**

*Methodological statistical data approach to verify the suitability and expressiveness of pXRF geochemical data for sediment dating of cultural material*

- Precision estimation of pXRF analyses in terms of resolution and application
- Statistical verification of the presence of distinctive element properties of cultural sediments
- Identification of appropriate archaeological records for the training of a neural network that can be used for age estimation of cultural layers
- development and testing of a dating method based on geochemical data and neural networks

**Fig. 6.1: Research papers** - Short overview of the research highlights and aims of the research papers included in this thesis.

---

with ICESAT laser data shows that many incised and elevated linear structures showing vertical height differences of at least 0.5 m are now visible on a high resolution scale. This renders the TanDEM-X data as a very important source for detecting ancient river channels and artificial canals in the delta. This new data allows for the identification of a finely ramified subdelta with larger and smaller branches between Kom el’Gir and the Burullus lagoon. To better identify the levees in the data they were thresholded for heights between 17.6 and 20 m together with focal median filtering. Together with the results for the settlements, it became evident that these settlements are almost exclusively situated along these palaeoriver branches. In addition to what was said before, levees did not only attract settlements as safe and elevated places along rivers with good transport conditions, but they also offered best conditions for agriculture with high soil fertility and access to irrigation water. For the time slice encompassing the Late Period up to the Roman period, a detailed picture of the northwestern Nile delta as it is described here can be drawn.

### **6.0.2 Ad aim 2: Inspection of the fine-scaled sedimentological underground**

The detailed sedimentological inspection integrated results from fieldwork remote sensing and geochemistry and gave evidence that in the northwestern Nile delta a subdelta formed prior to Ptolemaic and Roman times, and the levees and watercourses formed the basis for human settlements in the area studied. At the large scale it was verified that all settlements that were identified in the survey and via the remote sensing approach are located along the river branches. Integrated with results of the finder scale, it is possible to gain a better understanding of different landscape units especially the different sedimentological transects in the area under study and the channels we sampled. The fieldwork verified that in this intensively used and agriculturally transformed region many channels and watercourses appear in the subsurface and especially alongside the settlements that refer to the subdelta. In many cases the subsurface reveals a complex lithology with inclusions of small sandy patches in the fine grained alluvial delta material. Crevasse splays, levees or small channels lead to the deposition of coarse grained inclusions. We also found massive sequences of sand, covering widths of several hundred meters and being several meters deep that can only be the result of moving meander belts. A detailed description of the fine scaled sedimentological inspection for the different core transects is given in chapter 4.5.3. In combination with results and datings from Wunderlich (1989) it could be verified that this subdelta formed prior to Ptolemaic and Roman times, and the levees and watercourses formed the basis for human settlements in the area studied. Additionally, artificial channels and ancient natural riverbed often occur at a deep but similar depth of about 7 meters below sea level, suggesting that the streams were active during the occupation of these sites and belonged to the same system. Furthermore, a differentiation on the basis of pXRF and field data was developed that allows to distinguish between high or low energy watercourses.

## 6. SYNTHESIS AND CONCLUSIONS

---

The field results and geochemical pXRF measurements on sample material of these channels allows to discriminate between high and low energy watercourses (see Fig. 4.9). On the basis of Al/Ti and Cu/Zn ratios it was shown that natural rivers and canals show differences in their value ranges. Deposits of both water regimes significantly vary in their chemical composition or chemical stability. Natural watercourses are constantly in throughflow and sediment supply, therefore, Ti/Al ratios show a wide span of values compared to the small data range of the canals with their relatively stable sedimentary conditions. Lastly, these results are corroborated with a spiderplot showing the element distributions for different channels that were measured with the pXRF device, see Fig. 4.11. Buto and Kom el'Gir were directly connected via canals with the larger watercourses nearby. Current work in Kom el'Gir verified these results also in geoelectric measurements (Schiestl *et al.*, 2020). Yet, the function of these canals is not clear. Very likely, they were constructed to keep the connection between the sites and the moving rivers intact and reflect adaptive practices in a dynamic fluvial landscape.

### 6.0.3 Ad aim 3: Characterization and dating of settlement layers within coring transects

The methodological approach in chapter 5 did not only aim to develop a new dating method on the basis of machine learning techniques. A large number of preceding analyzes was performed that examine the applicability of pXRF methods and identify distinct geochemical differences in the archaeological sample material. The methodological approach aimed to gather important information on resolution and reproducibility for different elements. The coefficient of variation which was calculated for the different elements and different element concentrations to estimate precision of the results. We verified a decreasing precision with increasing element concentration. Secondly, it was shown that drying and pestling effectively minimizes negative influence on the measurement precision due to influences on the fluorescence radiation by porosity or water. Therefore, normalization of the pXRF data as handled by Helfert & Ramminger (2012); Iserlis *et al.* (2019) was intentionally left out and the low element concentrations of the main elements can be referred to the presence of higher amounts of non-detectable material. This is information which is important for the further processing of the data and which was verified by comparison with the results of the field description on the different soil texture classes. Many elements for both the sedimentologic and archaeological sample material lie below the detection limit and were not used in this study. Additionally, multiple samples from the same archaeological records were taken to uncover effects of leaching or precipitation of salts, which is essential information on the validity of different elements to derive past information.

This being the preconditions, different statistical approaches were applied to show that there do not only exist profound differences between archaeological material; It is rather that distinctive geochemical patterns can be registered for different archaeological records and between records of the different cultural periods. First of all, principal

---

geochemical patterns in the large-scale sedimentological transects were analyzed. Each factor of the analysis is influenced by specific elements that tend to correlate with the sedimentary layers or the distance to the next settlement sites. For example, factors 2 and 3 show high loadings in the upper meters and reflect the strong chemical differences between the alluvial Nile mud lying on top and the Pleistocene sands below. An anthropogenic component was revealed for factor 3 showing high loadings close to the settlements for elements such as P, Pb, Ca, K, Sr. Differences within the archaeological material were analyzed using spider and boxplots. Compared to the Nile reference, the settlement material is generally enriched in Zn, W, Sr, Sc, P, Mn, K, Cl, Ca and Ba, and it is noticeable that for the Roman period the curve shows higher element concentrations of W, Sr, Sc, Pb, P, K, Cu, Cl and Ca. Overall, elements showing distinctive differences between the cultural phases in at least one of the analyzed records are Ca, Cl, Cu, Fe, K, Mg, P, Pb, Rb, S, Sc, Sr, Ti and Zr.

A neural network with resilient backpropagation algorithm and weight backtracking was used to register and learn from such differences and allow dating of sediment cores in the surroundings of Buto and Kom el'Gir. The results correspond with dated ceramic pieces from the corings and allow a rough estimation of the cultural origin of the different core segments. Lastly, the robustness of the neural network was increased by enlarging the amount of data. This is done by artificial simulation of training data within the  $\pm 1$   $\sigma$  ranges for the different elements.

Nevertheless, the methodological approach also showed that geochemical processes postsedimentarily alter the sediments and manifest within this interpretation, e.g. surface material with the enrichment of salts such as carbonates are always interpreted as Roman material.

It was shown that in some corings west of Buto cultural sediments appear reaching down to -3 m asl (G2, G9) and which are possibly filled channels. Additionally, core G35 near Kom el'Gir shows cultural sediments till about -9 m asl and can be further proof of the channel that has only recently been uncovered by geoelectrical measurements east of Kom el'Gir.

#### 6.0.4 Summary and outlook

This study developed a toolbox of new creative methods in the fields of remote sensing and data analytics for geoarchaeological research. Highlight is the new dating method based on machine learning techniques that can be applied on pXRF sample data.

In the fields of remote sensing new methods are applied in the Nile delta. The analysis of time series data describes plant growth in a reliable way and allows the identification of lost tells or former river channels. Results show that there exists a weak relationship between vegetation performance and the appearance of archaeological material in the topsoil. Nevertheless, recognition of lost tells is still very difficult as they show only small sizes. The analysis of time series data is a promising tool and increasing in application. Especially platforms such as the Google Earth Engine help to apply such methods on a far larger amount of data in only a fraction of time. Today's

## 6. SYNTHESIS AND CONCLUSIONS

---

work of Ullmann *et al.* (2019) aims to use these platforms and apply such methods on data picturing the Nile delta. Future approaches should do likewise, because increasing the statistical data and large scale processing can be easily achieved with such platforms and compensates for many problems such as processing time, weak relationship between plant growth and subsoil conditions and low recognition due to small field sizes.

New astonishing insights of the Greco-Roman landscape in the Nile delta were made that let us reverse our original hypothesis of a single defunct Nile branch. Now the linear pattern of settlement sites can be explained with the location of palaeorivers nearby. Especially, the TanDEM-X DEM opens fundamentally new possibilities to investigate the ancient delta landscape and a first reconstruction of a fluvial network with associated settlements is presented. On finer scale the channels were in detail and adaptive practices of the settlements in a dynamic fluvial landscape were revealed.

This is one of the first studies that uses machine learning techniques to date archaeological sediments on the basis of pXRF data. Data that is increasingly gathered during geoscientific field campaigns. This first approach should be further developed and validated by testing additional material of the excavations with known context. As it was shown, larger amounts of dated material make the network more sensitive and allow to further refine the dating method. In the future, a similar revolution as it occurred in remote sensing with the opening of the Google Earth Platform, can be expected in data analytics for the processing of data with machine learning techniques. This will open up new possibilities to analyze geoscientific datasets.

# References

- ABD-EL MONSEF, H., SMITH, S.E. & DARWISH, K. (2015). Impacts of the Aswan High Dam After 50 Years. *Water Resources Management*, **29**, 1873–1885. 40
- ABDEL KAWY, W. & ALI, R. (2012). Assessment of soil degradation and resilience at northeast Nile Delta, Egypt: The impact on soil productivity. *The Egyptian Journal of Remote Sensing and Space Science*, **15**, 19–30. 15
- AITCHISON, J. (2003). *The Statistical Analysis of Compositional Data*. Blackburn Press, Caldwell, N.J. 84
- ANDRES, W. & WUNDERLICH, J. (1991). Late Pleistocene and Holocene evolution of the eastern Nile Delta and comparisons with the western delta. In H. Brückner & U. Radtke, eds., *Von der Nordsee bis zum Indischen Ozean*, Erdkundliches Wissen, 121–130, Franz Steiner Verlag, Stuttgart. 48
- ANTHONY, E.J., MARRINER, N. & MORHANGE, C. (2014). Human influence and the changing geomorphology of Mediterranean deltas and coasts over the last 6000 years: From progradation to destruction phase? *Earth-Science Reviews*, **139**, 336–361. 1
- ARBOUILLE, D. & STANLEY, D.J. (1991). Late Quaternary evolution of the Burullus lagoon region, north-central Nile delta, Egypt. *Marine Geology*, **99**, 45–66. 1, 50
- ARZ, H.W., PÄTZOLD, J. & WEFER, G. (1998). Correlated Millennial-Scale Changes in Surface Hydrography and Terrigenous Sediment Yield Inferred from Last-Glacial Marine Deposits off Northeastern Brazil. *Quaternary Research*, **50**, 157–166. 69
- ASLAN, A. & AUTIN, W.J. (1999). Evolution of the Holocene Mississippi River floodplain, Ferriday, Louisiana; insights on the origin of fine-grained floodplains. *Journal of Sedimentary Research*, **69**, 800–815. 3, 38, 50, 52, 72
- ASLAN, A., AUTIN, W.J. & BLUM, M.D. (2005). Causes of River Avulsion: Insights from the Late Holocene Avulsion History of the Mississippi River, U.S.A. *Journal of Sedimentary Research*, **75**, 650–664. 50, 72
- BAILEY, D.M. (1999). Sebakh, Sherds and Survey. *The Journal of Egyptian Archaeology*, **85**, 211–218. 52
- BALL, J. (1942). *Survey of Egypt: Egypt in the classical geographers*. Government Pr, Cairo. 46
- BALLET, P. & MAROUARD, G. (2015). Mutations d'une ville du nord de l'Égypte de la Basse Époque À la période byzantino-islamique. *Supplément au Bulletin de l'Institut français d'archéologie orientale*, 149–162. 2, 76
- BALLET, P. & VON DER WAY, T. (1993). Exploration archéologique de Bouto et de sa région (époques romaine et byzantine). *Mitteilungen des Deutschen Archäologischen Instituts, Abteilung Kairo*, **49**, 1–22. 2, 49
- BALLET, P., LECUYOT, G., MAROUARD, G., PITHON, M. & REDON, B. (2011). Et la Bouto tardive ? *Bulletin de l'Institut français d'archéologie orientale*, **111**, 75–111. 2, 49, 76
- BARCELÓ, J.A. (2004). Beyond Classification: Automatic Learning in Archaeology and Cultural Studies. *Intelligenza Artificiale*, **1**, 29–33. 85
- BARCELÓ, J.A. (2009). *Computational Intelligence in Archaeology*. Information Science Reference, Hershey, PA. 85
- BEDIER, S. (1994). Ein Stiftungsdekret Thutmosis' III. aus Buto. In M. Minas-Nerpel, S. Schips & E. Winter, eds., *Aspekte spätägyptischer Kultur*, Aegyptiaca Treverensia, 35–50, von Zabern, Mainz am Rhein. 49
- BELAL, A.A. & MOGHANM, F.S. (2011). Detecting urban growth using remote sensing and GIS techniques in Al Gharbiya governorate, Egypt. *The Egyptian Journal of Remote Sensing and Space Science*, **14**, 73–79. 40

## REFERENCES

---

- BELL, S. & CROSON, C. (1998). Artificial neural networks as a tool for archaeological data analysis. *Archaeometry*, **40**, 139–151. 85, 86
- BELTRÁN, J.M. (1999). Irrigation with saline water: Benefits and environmental impact. *Agricultural Water Management*, **40**, 183–194. 38
- BERGMANN, M. & HEINZELMANN, M. (2015). Schedia. Alexandria's customs station and river port on the Canopic Nile. In P. Pomey, ed., *La batellerie égyptienne*, Etudes Alexandrines, Centre d'Etudes Alexandrines, Alexandrie. 48
- BERNASCONI, M.P. & STANLEY, D.J. (1994). Molluscan biofacies and their environmental implications, Nile Delta lagoons, Egypt. *Journal of Coastal Research*, **10**, 440–465. 79
- BIETAK, M. (1975). *Tell el Dab'a. II: Der Fundort im Rahmen einer archäologisch-geographischen Untersuchung über das ägyptische Ostdelta*. Untersuchungen der Zweigstelle Kairo des Österreichischen Archäologischen Instituts 1, Denkschriften der Gesamtakademie 4, Verlag der Österreichischen Akademie der Wissenschaften, Wien. 1, 44, 46, 47, 52
- BIRKS, H.H. & BIRKS, H.J.B. (2006). Multi-proxy studies in palaeolimnology. *Vegetation History and Archaeobotany*, **15**, 235–251. 79
- BLOUIN, K. (2014). *Triangular landscapes: Environment, society, and the state in the Nile Delta under the Roman rule*. Oxford Univ. Press, Oxford. 62
- BRANSS, T., DITTRICH, F. & NÚÑEZ-GONZÁLEZ, F. (2016). Reproducing natural levee formation in an experimental flume. In G. Constantinescu, ed., *River Flow 2016*, CRC Press, Boca Raton. 52
- BUNBURY, J., HUGHES, E. & SPENCER, N. (2014). Ancient Landscape reconstruction at Kom Firin. In N. Spencer & J. Bunbury, eds., *Kom Firin*, Research publication / British Museum, Trustees of the British Museum, London. 47, 48
- BUTZER, K.W. (1975). Delta. In W. Helck & E. Otto, eds., *Lexikon der Ägyptologie*, 1043–1052, Harrassowitz, Wiesbaden. 1, 18, 49, 50
- BUTZER, K.W. (1976). *Early hydraulic civilization in Egypt: A study in cultural ecology*. Univ. of Chicago Press, Chicago u.a. 48, 52, 62, 71, 100
- BUTZER, K.W. (1998). Late Quaternary problems of the Egyptian Nile : stratigraphy, environments, prehistory. *Paléorient*, **23**, 151–173. 3
- BUTZER, K.W. (2002). Geoarchaeological Implications of Recent Research in the Nile Delta. In E.C.M. van den Brink & T.E. Levy, eds., *Egypt and the Levant*, 83–97, Leicester University Press, London, New York. 3
- CAZANAÇLI, D. & SMITH, N.D. (1998). A study of morphology and texture of natural levees—Cumberland Marshes, Saskatchewan, Canada. *Geomorphology*, **25**, 43–55. 52
- CHAVEZ, P.S. (1996). Image-Based Atmospheric Corrections - Revisited and Improved. *Photogrammetric engineering and remote sensing*, **62**, 1025–1035. 21
- CHEN, H.F., CHANG, Y.P., KAO, S.J., CHEN, M.T., SONG, S.R., KUO, L.W., WEN, S.Y., YANG, T.N. & LEE, T.Q. (2011). Mineralogical and geochemical investigations of sediment-source region changes in the Okinawa Trough during the past 100ka (IMAGES core MD012404). *Journal of Asian Earth Sciences*, **40**, 1238–1249. 69
- CHEN, H.F., YEH, P.Y., SONG, S.R., HSU, S.C., YANG, T.N., WANG, Y., CHI, Z., LEE, T.Q., CHEN, M.T., CHENG, C.L., ZOU, J. & CHANG, Y.P. (2013). The Ti/Al molar ratio as a new proxy for tracing sediment transportation processes and its application in aeolian events and sea level change in East Asia. *Journal of Asian Earth Sciences*, **73**, 31–38. 69
- COOPER, J.P. (2014). *The medieval Nile: Route, navigation, and landscape in Islamic Egypt*. The American University in Cairo Press, Cairo. 46
- DARESSY, G. (1926). Recherches géographiques. *Annales du Service des antiquités de l'Égypte*, **26**, 246–272. 49
- DORNER, J. (1993/1994). Die Rekonstruktion einer pharaonischen Flusslandschaft. *Mitteilungen der Anthropologischen Gesellschaft in Wien*, **123/124**, 401–406. 48
- DORNER, J. (1999). Die Topographie von Piramess - Vorbericht. *Ägypten und Levante / Egypt and the Levant*, **9**, 77–83. 48



## REFERENCES

- ECKELMANN, H.W., SPONAGEL, R.H., GROTTENTHALER, W., HARTMANN, K.J., HARTWICH, R., JANETZKO, P., JOISTEN, H., KÜHN, D., SABEL, K.J., TRAILD, R. & BODEN, H.A.H.A., eds. (2006). *Bodenkundliche Kartieranleitung. KA5*. Schweizerbart Science Publishers, Stuttgart, Germany. 9, 55, 80
- EDGAR, C.C. (1911). Notes from the Delta. *Annales du Service des antiquités de l'Égypte*, **11**, 87–96. 49
- EL-ASMAR, H.M., HEREHER, M.E. & EL KAFRAWY, SAMEH B. (2013). Surface area change detection of the Burullus Lagoon, North of the Nile Delta, Egypt, using water indices: A remote sensing approach. *The Egyptian Journal of Remote Sensing and Space Science*, **16**, 119–123. 40
- EL-GAMILI, M.M. (1988). Geophysical investigations for holocene palaeohydrography in the north-western Nile Delta. *The Archaeology, Geography and History of the Egyptian Delta in Pharaonic Times, Wadham College 29-31 August 1988, Oxford, Discussions in Egyptology Special Number 1*, 125–154. 48
- EL-GAMILI, M.M., SHAABAN, F. & EL-MORSI, O. (1994). Electrical resistivity mapping of the buried stream channel of the Canopic branch in the western Nile Delta, Egypt. *Journal of African Earth Sciences*, **19**, 135–148. 48
- EL-GAMILI, M.M., IBRAHIM, E.H., HASSANEEN, A.R.G., ABDALLA, M.A. & ISMAEL, A.M. (2001). Defunct Nile Branches Inferred from a Geoelectric Resistivity Survey on Samannud area, Nile Delta, Egypt. *Journal of Archaeological Science*, **28**, 1339–1348. 48
- EL-GUINDY, S. (1989). Quality of drainage water in the Nile Delta. In M.H. Amer & Ridder, N. A. De, eds., *Land drainage in Egypt*, Ministry of Public Works and Water Resources, Water Research Center, Drainage Research Institute and International Institute for Land Reclamation and Improvement, Cairo, Egypt and Wageningen, The Netherlands. 40, 60
- EL-QADY, G., SHAABAN, H., EL-SAID, A., GHAZALA, H. & EL-SHAHAT, A. (2011). Tracing of the defunct Canopic Nile branch using geoelectrical resistivity data around Itay El-Baroud area, Nile Delta, Egypt. *Journal of Geophysics and Engineering*, **8**, 83–91. 46
- EL-QUOSY (1994). Control of water consumption of rice. In *VIIIth IWRA World Congress on Water Resources*. 40
- EL SHAZLY, E.M., ABDEL-HADY, M.A., EL GHAWABY, M.A., EL KASSAS, I.A., KHAWASIK, S.M., EL SHAZLY, M.M. & SANAD, S. (1975). Geologic interpretation of Landsat satellite images for West Nile Delta area, Egypt. *Cairo, Egypt: The Remote Sensing Research Project, Academy of Scientific Research & Technology*. 47
- ELHAG, M., PSILOVIKOS, A. & SAKELLARIOU-MAKRANTONAKI, M. (2013). Land use changes and its impacts on water resources in Nile Delta region using remote sensing techniques. *Environment, Development and Sustainability*, **15**, 1189–1204. 40
- ERASMI, S., ROSENBAUER, R., BUCHBACH, R., BUSCHE, T. & RUTISHAUSER, S. (2014). Evaluating the Quality and Accuracy of TanDEM-X Digital Elevation Models at Archaeological Sites in the Cilician Plain, Turkey. *Remote Sensing*, **6**, 9475–9493. 52, 53, 54
- FALTINGS, D., BALLEET, P., FÖRSTER, F., FRENCH, P., IHDE, C., SAHLMANN, H., THOMALSKY, J., THUMSHIRN, C. & WODZINSKA, A. (2000). Zweiter Vorbericht über die neuen Ausgrabungen des DAI in Tell el-Fara'in/Buto. *Mitteilungen des Deutschen Archäologischen Instituts, Abteilung Kairo*, **56**, 131–179. 2, 76
- FATTAH, T.A.E. & FRIHY, O.E. (1988). Magnetic Indications of the Position of the Mouth of the Old Canopic Branch on the Northwestern Nile Delta of Egypt. *Journal of Coastal Research*, **4**, 483–488. 48
- FEIX, J. (2006). *Herodot Historien, Erster Band, Bücher I-V: Griechisch-deutsch*. Sammlung Tusculum, De Gruyter, Berlin, 7th edn. 46
- FILZMOSER, P., HRON, K. & REIMANN, C. (2009). Principal component analysis for compositional data with outliers. *Environmetrics*, **20**, 621–632. 84, 85
- FLAUX, C., EL-ASSAL, M., MARRINER, N., MORHANGE, C., ROUCHY, J.M., SOULIÉ-MÄRSCHKE, I. & TORAB, M. (2012). Environmental

## REFERENCES

---

- changes in the Maryut lagoon (northwestern Nile delta) during the last ~2000 years. *Journal of Archaeological Science*, **39**, 3493–3504. 1
- FLAUX, C., CLAUDE, C., MARRINER, N. & MORHANGE, C. (2013). A 7500-year strontium isotope record from the northwestern Nile delta (Maryut lagoon, Egypt). *Quaternary Science Reviews*, **78**, 22–33. 1
- FORSTER, N., GRAVE, P., VICKERY, N. & KEALHOFER, L. (2011). Non-destructive analysis using PXRF: Methodology and application to archaeological ceramics. *X-Ray Spectrometry*, **40**, 389–398. 79
- FRAHM, E. & DOONAN, R.C. (2013). The technological versus methodological revolution of portable XRF in archaeology. *Journal of Archaeological Science*, **40**, 1425–1434. 79
- FRANKEL, D. & WEBB, J.M. (2012). Pottery production and distribution in prehistoric Bronze Age Cyprus. An application of pXRF analysis. *Journal of Archaeological Science*, **39**, 1380–1387. 79
- GAUSS, R.K., BÁTORA, J., NOWACZINSKI, E., RASSMANN, K. & SCHUKRAFT, G. (2013). The Early Bronze Age settlement of Fidvár, Vráble (Slovakia): Reconstructing prehistoric settlement patterns using portable XRF. *Journal of Archaeological Science*, **40**, 2942–2960. 79
- GINAU, A., OPP, C., SUN, Z. & HALIK, Ü. (2013). Influence of sediment, soil, and micro-relief conditions on vitality of *Populus euphratica* stands in the lower Tarim Riparian Ecosystem. *Quaternary International*, **311**, 146–154. 38, 40, 57
- GINAU, A., SCHIESTL, R., KERN, F. & WUNDERLICH, J. (2017). Identification of historic landscape features and settlement mounds in the Western Nile Delta by means of remote sensing time series analysis and the evaluation of vegetation characteristics. *Journal of Archaeological Science: Reports*, **16**, 170–184. 57, 72
- GINAU, A., SCHIESTL, R. & WUNDERLICH, J. (2019). Integrative geoarchaeological research on settlement patterns in the dynamic landscape of the northwestern Nile delta. *Quaternary International*, **511**, 51–67. 38, 41, 77, 82, 90, 97, 100
- GOMAÀ, F., JÄGERLIN, K. & STAHL, W. (1977). *Tübinger Atlas des Vorderen Orients. B IV 2. Nildelta zur Zeit der lybischen Fürstentümer*. Reichert, Wiesbaden. 46
- GOVAERTS, B. & VERHULST, N. (2010). *The normalized difference vegetation index (NDVI) Greenseeker (TM) handheld sensor: toward the integrated evaluation of crop management. Part A-Concepts and case studies*. CIMMYT - International Maize and Wheat Improvement Center, Mexico. 23
- GROSS, D. (2005). Monitoring agricultural biomass using NDVI time series. *Food and Agriculture Organization of the United Nations (FAO), Rome*. 36
- GUENTHER, F. & FRITSCH, S. (2010). neuralnet: Training of neural networks. *The R Journal*, **2**, 5–15. ISSN 2073-4859.. 12, 86
- HALL, G.E.M., BONHAM-CARTER, G.F. & BUCAR, A. (2014). Evaluation of portable X-ray fluorescence (pXRF) in exploration and mining: Phase 1, control reference materials. *Geochemistry: Exploration, Environment, Analysis*, **14**, 99–123. 79
- HAMROUSH, H.A. (1987). *Geoarchaeology of the Kom el Hisn Area; Tracing Ancient Sites in the Western Nile Delta*. Cairo. 1
- HAMZA, W. (2010). The Nile Delta. In H.J. Dumont, ed., *The Nile*, vol. 89 of *Monographiae Biologicae*, 75–94, Springer, Berlin. 14
- HARTUNG, U. (2014). Buto, Ägypten. Die Siedlungsgeschichte des Fundplatzes Buto (Tell el Fara'in). *Die Arbeiten der Jahre 2012 und 2013. e-Forschungsberichte*, **2014**, 9–13. 2, 76
- HARTUNG, U., BALLETT, P., EFFLAND, A., FRENCH, P., HARTMANN, R., HERBICH, T., HOFFMANN, H., HOWER-TILMANN, E., KITAGAWA, C., KOPP, P., KREIBIG, W., LECUYOT, G., LÖSCH, S., MAROUARD, G., NERLICH, A., PITHON, M. & ZINK, A. (2009). Tell el-Fara'in - Buto. 10. Vorbericht. *Mitteilungen des Deutschen Archäologischen Instituts, Abteilung Kairo*, **65**, 83–190. 2, 49, 76
- HEALY, J.F. (1978). *Mining and metallurgy in the Greek and Roman world*. Thames and Hudson, London. 69

- HELFFERT, M. & RAMMINGER, B. (2012). *Neue Perspektiven für geochemische Untersuchungen von neolithischen Steingeräten: Ein Methodenvergleich zwischen portabler energiedispersiver Röntgenfluoreszenzanalyse (P-ED-RFA) und wellenlängendispersiver Röntgenfluoreszenzanalyse (WD-RFA) am Beispiel von bandkeramischen Dechselklingen aus Diemarden (Südniedersachsen)*. Hamburg University Press Programm. 82, 84, 108
- HERBICH, T. & FORSTNER-MÜLLER, I. (2013). Small Harbours in the Nile Delta. The Case of Tell el-Dab'a. In *Festschrift Karol Mysliwiec, Études et Travaux*, 258–272, Instytut Kultur Śródziemnomorskich i Orientalnych Polskiej Akademii Nauk, Warszawa. 48
- HIJAZI, R. (2011). An EM-Algorithm Based Method to Deal with Rounded Zeros in Compositional Data under Dirichlet Models. *Universitat de Girona. Departament d'Informàtica i Matemàtica Aplicada*. 85
- HOGARTH, D.G. (1904). Three North Delta Nomes. *The Journal of Hellenic Studies*, **24**, 1–19. 49
- HOPE, A.S., BOYNTON, W.L., STOW, D.A. & DOUGLAS, D.C. (2003). Interannual growth dynamics of vegetation in the Kuparuk River watershed, Alaska based on the Normalized Difference Vegetation Index. *International Journal of Remote Sensing*, **24**, 3413–3425. 27
- HUBER, M., WESSEL, B., KOSMANN, D., FELBIER, A., SCHWIEGER, V., HABERMEYER, M., WENDLEDER, A. & ROTH, A. (2009). Ensuring globally the TanDEM-X height accuracy: Analysis of the reference data sets ICESat, SRTM and KGPS-tracks. In *2009 IEEE International Geoscience and Remote Sensing Symposium*, 769–772. 53
- HUBERT, M., ROUSSEEUW, P.J. & VERDONCK, T. (2012). A Deterministic Algorithm for Robust Location and Scatter. *Journal of Computational and Graphical Statistics*, **21**, 618–637. 85
- HUNT, A.M. & SPEAKMAN, R.J. (2015). Portable XRF analysis of archaeological sediments and ceramics. *Journal of Archaeological Science*, **53**, 626–638. 79
- ISERLIS, M., STEINIGER, D. & GREENBERG, R. (2019). Contact between first dynasty Egypt and specific sites in the Levant: New evidence from ceramic analysis. *Journal of Archaeological Science: Reports*, **24**, 1023–1040. 82, 84, 108
- JACOTIN, A. & JOMARD, E.F. (1828). *Carte topographique de L'Égypte et de plusieurs parties des pays limitrophes: Levée pendant l'expédition de l'armée française par les ingénieurs-géographes*. L'Imprimerie Impériale, Paris. 47
- JANSEN, J., VAN DER GAAST, S., KOSTER, B. & VAARS, A. (1998). CORTEX, a shipboard XRF-scanner for element analyses in split sediment cores. *Marine Geology*, **151**, 143–153. 69
- KANTHILATHA, N., BOYD, W. & CHANG, N. (2017). Multi-element characterization of archaeological floors at the prehistoric archaeological sites at Ban Non Wat and Nong Hua Raet in Northeast Thailand. *Quaternary International*, **432**, 66–78. 79
- KASHEF, A.A.I. (1983). Salt-Water Intrusion in the Nile Delta. *Ground Water*, **21**, 160–167. 38
- KENNA, T.C., NITSCHKE, F.O., HERRON, M.M., MAILLOUX, B.J., PETEET, D., SRITRAIRAT, S., SANDS, E. & BAUMGARTEN, J. (2011). Evaluation and calibration of a Field Portable X-Ray Fluorescence spectrometer for quantitative analysis of siliciclastic soils and sediments. *J. Anal. At. Spectrom.*, **26**, 395–405. 79
- KESSLER, D., ZIBELIUS, K., POHLMANN, H. & DENK, W. (1980). *Tübinger Atlas des Vorderen Orients. B II 1. Ägypten zur Zeit des Alten Reiches*. Reichert, Wiesbaden. 46
- KOTB, T.H., WATANABE, T., OGINO, Y. & TANJI, K.K. (2000). Soil salinization in the Nile Delta and related policy issues in Egypt. *Agricultural Water Management*, **43**, 239–261. 38, 40, 60
- KROM, M.D., STANLEY, D.J., CLIFF, R.A. & WOODWARD, J.C. (2002). Nile River sediment fluctuations over the past 7000 yr and their key role in sapropel development. *Geology*, **30**, 71. 50
- KUMAR, R. & SILVA, L. (1973). Light ray tracing through a leaf cross section. *Applied Optics*, **12**, 2950–2954. 23
- LUBOS, C., DREIBRODT, S., ROBIN, V., NELLE, O., KHAMNUEVA, S., RICHLING, I., BULTMANN, U. & BORK, H.R. (2013). Settlement and environmental history of a multilayered settlement mound

## REFERENCES

---

- in Niederröblingen (central Germany) – a multi-proxy approach. *Journal of Archaeological Science*, **40**, 79–98. 79
- LUBOS, C., DREIBRODT, S. & BAHR, A. (2016). Analysing spatio-temporal patterns of archaeological soils and sediments by comparing pXRF and different ICP-OES extraction methods. *Journal of Archaeological Science: Reports*, **9**, 44–53. 79
- MA, B.L., DWYER, L.M., COSTA, C., COBER, E.R. & MORRISON, M.J. (2001). Early prediction of soybean yield from canopy reflectance measurements. *Agronomy Journal*, **93**, 1227–1234. 18, 23
- MARCOLONGO, B. (1992). Evolution du paléo-environnement dans la partie orientale du delta du Nil depuis la transgression flandrienne (8000 BP). *Cahiers de Recherches de l'Institut de Papyrologie et d'Égyptologie de Lille*, **14**, 23–31. 47
- MARRINER, N., FLAUX, C., KANIEWSKI, D., MORHANGE, C., LEDUC, G., MORON, V., CHEN, Z., GASSE, F., EMPEREUR, J.Y. & STANLEY, D.J. (2012a). ITCZ and ENSO-like pacing of Nile delta hydro-geomorphology during the Holocene. *Quaternary Science Reviews*, **45**, 73–84. 1
- MARRINER, N., FLAUX, C., MORHANGE, C. & KANIEWSKI, D. (2012b). Nile Delta's sinking past: Quantifiable links with Holocene compaction and climate-driven changes in sediment supply? *Geology*, **40**, 1083–1086. 50, 60
- MARTÍN-FERNÁNDEZ, J.A. (2003). Dealing with zeros and missing values in compositional data sets using nonparametric imputation. *Mathematical Geology*, **35**, 253–278. 85
- MENZE, B.H. & UR, J.A. (2012). Mapping patterns of long-term settlement in Northern Mesopotamia at a large scale. *Proceedings of the National Academy of Sciences of the United States of America*, **109**, E778–E787. 16, 17
- MORAN, M., JACKSON, R.D., SLATER, P.N. & TEILLET, P.M. (1992). Evaluation of simplified procedures for retrieval of land surface reflectance factors from satellite sensor output. *Remote Sensing of Environment*, **41**, 169–184. 21
- MOSHIER, S.O. & EL-KALANI, A. (2008). Late Bronze Age paleogeography along the ancient Ways of Horus in Northwest Sinai, Egypt. *Geoarchaeology*, **23**, 450–473. 47
- MUNNS, R. (1993). Physiological processes limiting plant growth in saline soils: Some dogmas and hypotheses. *Plant, Cell and Environment*, **16**, 15–24. 38
- NOWACKI, D. (2016). *Rekonstruktion der Landschaftsgenese eines Flussabschnittes der Unteren Donau anhand eines Multi-Proxy-Ansatzes an Seesedimenten im Kontext der neolithischen und kupferzeitlichen Siedlung "Mägura Gorgana", Südrumänien: Frankfurt am Main, Johann Wolfgang Goethe-Universität, Diss., 2015*. Universitätsbibliothek Johann Christian Senckenberg, Frankfurt am Main. 79
- OLDFATHER, C.H. (1933). *Diodorus Siculus: The Library of History*, vol. 279 of *Loeb Classical Library*. Harvard Univ. Press, Cambridge, Mass., 1st edn. 46
- OONK, S. & SPIJKER, J. (2015). A supervised machine-learning approach towards geochemical predictive modelling in archaeology. *Journal of Archaeological Science*, **59**, 80–88. 86
- PALAREA-ALBALADEJO, J. & MARTÍN-FERNÁNDEZ, J.A. (2008). A modified EM algorithm for replacing rounded zeros in compositional data sets. *Computers & Geosciences*, **34**, 902–917. 85
- PALAREA-ALBALADEJO, J., MARTÍN-FERNÁNDEZ, J.A. & GÓMEZ-GARCÍA, J. (2007). A Parametric Approach for dealing with compositional rounded zeros. *Mathematical Geology*, **39**, 625–645. 11, 85
- PALASEANU-LOVEJOY, M., THATCHER, C.A. & BARAS, J.A. (2014). Levee crest elevation profiles derived from airborne lidar-based high resolution digital elevation models in south Louisiana. *ISPRS Journal of Photogrammetry and Remote Sensing*, **91**, 114–126. 52
- PENNINGTON, B.T. & THOMAS, R.I. (2016). Paleoenvironmental surveys at Naukratis and the Canopic branch of the Nile. *Journal of Archaeological Science: Reports*, **7**, 180–188. 46, 48
- PENNINGTON, B.T., STURT, F., WILSON, P., ROWLAND, J. & BROWN, A.G. (2017). The fluvial evolution of the Holocene Nile Delta. *Quaternary Science Reviews*, **170**, 212–231. 45, 48, 50

## REFERENCES

- PERKO, R., RAGGAM, H., GUTJAHR, K. & SCHARDT, M. (2010). The capabilities of TerraSAR-X imagery for retrieval of forest parameters. *International Archives of the Photogrammetry, Remote Sensing and Spatial Information Sciences*, **38**, 452–456. 35
- PETRIE, W.M.F. (1896). *Naukratis I, 1884-5*. Third Memoir of the Egypt Exploration Fund, London. 49
- PETRIE, W.M.F., CURRELLE, C.T. & GRIFFITH, F.L. (1905). *Ehnasya 1904*, vol. 26 of *Memoir of the Egypt Exploration Fund*. Egypt Exploration Fund [usw.], London. 49
- PIPAUD, I., LOIBL, D. & LEHMKUHL, F. (2015). Evaluation of TanDEM-X elevation data for geomorphological mapping and interpretation in high mountain environments ? A case study from SE Tibet, China. *Geomorphology*, **246**, 232–254. 53
- QUICKEL, A.T. & WILLIAMS, G. (2016). In Search of Sibākh: Digging Up Egypt from Antiquity to the Present Day. *Journal of Islamic Archaeology*, **3**, 89–108. 53
- RADT, S., ed. (2005). *Strabons Geographika: Mit Übersetzung und Kommentar*. Vandenhoeck & Ruprecht, Göttingen. 46
- RAO, Y.S., DEO, R., NALINI, J., PILLAI, A.M., MURALIKRISHNAN, S. & DADHWAL, V.K. (2014). Quality assessment of TanDEM-X DEMs using airborne LiDAR, photogrammetry and ICESat elevation data. *ISPRS Annals of Photogrammetry, Remote Sensing and Spatial Information Sciences*, **II-8**, 187–192. 53
- REIMANN, C. (2008). *Statistical Data Analysis Explained: Applied Environmental Statistics with R*. John Wiley & Sons, Chichester, England and Hoboken, NJ. 69, 84, 85
- RIEDMILLER, M. (1994). Advanced supervised learning in multi-layer perceptrons — from backpropagation to adaptive learning algorithms. *Computer Standards & Interfaces*, **16**, 265–278. 86
- ROCHFORD, M.K. (2014). *Determining Geomorphological and Land Use Effects through Physico-Chemical Fingerprinting of Soils*. University of Iowa. 79
- ROLLINSON, H. (1995). Using Geochemical Data: Evolution, Presentation, Interpretation. *Longman Scientific and Technical Press*, **26**. 85
- ROSEN, A.M. (1986). *Cities of clay: The geoarcheology of tells*. Prehistoric archeology and ecology, University of Chicago Press, Chicago. 16
- ROUSSEEUW, P.J. & LEROY, A.M. (1987). *Robust Regression and Outlier Detection*. John Wiley & Sons, Inc, Hoboken, NJ, USA. 85
- SAID, R. (1981). *The geological evolution of the river Nile*. Springer, New York, NY. 18
- SAID, R. (1993). *The river Nile: Geology, hydrology and utilization*. Pergamon Press, Oxford u.a., 1st edn. 50
- SCHIESTL, R. (2012a). Field Boundaries and Ancient Settlement Sites: Observations from the Regional Survey around Buto, Western Delta. *Mitteilungen des Deutschen Archäologischen Instituts, Abteilung Kairo*, **68**, 175–190. 2, 5, 15, 16, 17, 35, 44, 49, 52, 76, 97
- SCHIESTL, R. (2012b). Investigating ancient settlements around Buto. *Egyptian Archaeology*, **40**, 18–20. 2, 5, 49, 52, 53, 56, 71, 76, 77, 97
- SCHIESTL, R. (2015). Landschaftsarchäologie und regionale Siedlungsnetzwerke um den Fundplatz Tell el-Fara'in, Gouvernorat Kafr esch-Scheich. Die Arbeiten des Jahres 2012: e-FORSCHUNGSBERICHTE DES DAI. 2, 3, 5, 49, 52
- SCHIESTL, R. & ROSENOW, D. (2016). Prospektion am Kom el-Gir. Einführung in eine neue Siedlung des Deltas. *Mitteilungen des Deutschen Archäologischen Instituts, Abteilung Kairo*, **72**, 169–196. 2, 3, 49, 56, 71, 76
- SCHIESTL, R., WUNDERLICH, J., ALTMAYER, M. & MÖLLER, H. (2020). Report on the Season in Autumn 2018 and Spring 2019 of the Survey around Kom el-Gir and the Test Excavation at Kom el-Gir (Governorate Kafr esh-Shaikh). *ASAE (Annales du Service des Antiquités de l'Égypte)*. 108
- SCHNEIDER, A.R., CANCÈS, B., BRETON, C., PONTHEIU, M., MORVAN, X., CONREUX, A. & MARIN, B. (2016). Comparison of field portable XRF and aqua regia/ICPAES soil analysis and evaluation of

## REFERENCES

---

- soil moisture influence on FPXRF results. *Journal of Soils and Sediments*, **16**, 438–448. 79
- SEFELNASR, A. & SHERIF, M. (2014). Impacts of seawater rise on seawater intrusion in the Nile Delta Aquifer, Egypt. *Ground Water*, **52**, 264–276. 38
- SEWUSTER, R.J. & VAN WESEMAEL, B. (1987). *Tracing Ancient River Courses in the Eastern Nile Delta: A Geo-archaeological Survey in the Sarqiya Province, Egypt*. University of Amsterdam. 47, 48
- SHACKLEY, M. (2010). Is there reliability and validity in portable X-ray fluorescence spectrometry (PXRF)? *The SAA Archaeological Record*, **10**, 17–20. 79
- SHACKLEY, M.S., ed. (2011). *X-Ray Fluorescence Spectrometry (XRF) in Geoarchaeology*. Springer, New York, NY. 79
- SHAFEI, A.B. (1946). Historical Notes on the Pelusiac Branch, the Red Sea Canal, and the Route of the Exodus. *Bulletin de la Société de Géographie d'Égypte*, **21**, 231–287. 47, 52
- SHALABY, A. (2012). Assessment of Urban Sprawl Impact on the Agricultural Land in the Nile Delta of Egypt Using Remote Sensing and Digital Soil Map. *International Journal of Environment and Sciences*, **1**, 253–262. 40
- SHERRATT, A. (2004). Spotting tells from space. *Antiquity*, **78**. 16
- SHRIVASTAVA, P. & KUMAR, R. (2015). Soil salinity: A serious environmental issue and plant growth promoting bacteria as one of the tools for its alleviation. *Saudi journal of biological sciences*, **22**, 123–131. 38
- SHUGAR, A.N. & MASS, J.L. (2012). *Handheld XRF for art and archaeology*, vol. 3 of *Studies in archaeological sciences*. Leuven University Press, Leuven, Belgium. 79
- SMITH, N.D. & PÉREZ-ARLUCEA, M. (2008). Natural levee deposition during the 2005 flood of the Saskatchewan River. *Geomorphology*, **101**, 583–594. 52
- SNEH, A. & WEISSBROD, T. (1973). Nile delta: The Defunct Pelusiac Branch Identified. *Science*, **180**, 59–61. 47, 48
- SPEAKMAN, R.J., LITTLE, N.C., CREEL, D., MILLER, M.R. & IÑÁÑEZ, J.G. (2011). Sourcing ceramics with portable XRF spectrometers? A comparison with INAA using Mimbres pottery from the American Southwest. *Journal of Archaeological Science*, **38**, 3483–3496. 79
- SPENCER, A.J. (1992). Roman sites in the north-west Delta. In U. Luft, ed., *The intellectual heritage of Egypt. Studies presented to László Kákósy by friends and colleagues on the occasion of his 60th birthday*, *Studia Aegyptiaca*, 535–539, Eötvös Loránd University, Budapest, Budapest. 2, 49
- SRITRAIRAT, S. (2013). *Multiproxy Analyses of Past Vegetation, Climate, and Sediment Dynamics in Hudson River Wetlands*. [publisher not identified], [New York, N.Y.?]. 79
- STANLEY, D.J. & WARNE, A.G. (1993). Nile Delta: Recent Geological Evolution and Human Impact. *Science*, **260**, 628–634. 18, 50
- STANLEY, D.J., ARNOLD, D. & WARNE, A.G. (1992). Oldest Pharaonic Site Yet Discovered in the North-central Nile Delta, Egypt. *National Geographic Research & Exploration*, **8**, 264–275. 1
- STANLEY, J.D. & JORSTAD, T.F. (2006). Short contribution: Buried Canopic channel identified near Egypt's Nile delta coast with radar (SRTM) imagery. *Geoarchaeology*, **21**, 503–514. 46, 47
- STEIN, J.K. (1986). Coring Archaeological Sites. *American Antiquity*, **51**, 505–527. 54
- STOW, D., DAESCHNER, S., HOPE, A., DOUGLAS, D.C., PETERSEN, A., MYNENI, R., ZHOU, L. & OECHEL, W. (2003). Variability of the Seasonally Integrated Normalized Difference Vegetation Index Across the North Slope of Alaska in the 1990s. *International Journal of Remote Sensing*, **24**, 1111–1117. 27
- STÜCKELBERGER, A., GRASSHOFF, G. & MITTENHUBER, F. (2006). *Klaudios Ptolemaios Handbuch der Geographie: Griechisch-deutsch*. Schwabe Verlag, Basel. 46
- TALBERT, R.J.A., ed. (2000). *Barrington Atlas of the Greek and Roman World*. Princeton Univ. Press, Princeton, NJ. 46

## REFERENCES

- THOMAS, R.I. (2014). Roman Naukratis and its Alexandrian context. *The British Museum Studies in Ancient Egypt and Sudan*, **21**, 193–218. 48
- THOMAS, R.I. (2015). Naukratis, ‘Mistress of ships’, in context. In D. Robinson & F. Goddio, eds., *Thonis-Heracleion in context*, Monograph / Oxford Centre for Maritime Archaeology, 239–257, Oxford Centre for Maritime Archaeology, Oxford. 48
- THOMAS, R.I. & VILLING, A. (2013). Naukratis revisited 2012: Integrating new fieldwork and old research. *British Museum Studies in Ancient Egypt and the Sudan*, **20**, 81–125. 48
- TOONEN, W.H.J., GRAHAM, A., PENNINGTON, B.T., HUNTER, M.A., STRUTT, K.D., BARKER, D.S., MASSON-BERGHOF, A. & EMERY, V.L. (2017). Holocene fluvial history of the Nile’s west bank at ancient Thebes, Luxor, Egypt, and its relation with cultural dynamics and basin-wide hydroclimatic variability. *Geoarchaeology*, **85**, 211. 48
- TOUSSOUN, O. (1922). Mémoires sur les anciennes branches du Nil. *Epoque Ancienne. Mémoire de l’Institut d’Égypte*, **4**. 46
- TRAMPIER, J. (2009). *Ancient Towns and New Methods: A GIS and Remote Sensing-Guided Archaeological Survey in the Western Nile Delta*. The University of Chicago. 16
- TRAMPIER, J., TOONEN, W., SIMONY, A. & STARBIRD, J. (2013). Missing Koms and Abandoned Channels: The Potential of Regional Survey in the Western Nile Delta Landscape. *The Journal of Egyptian Archaeology*, **99**, 217–240. 1, 47
- TRAMPIER, J.R. (2014). *Landscape Archaeology of the Western Nile Delta*, vol. 2 of *Wilbour Studies in Egypt and Ancient Western Asia*. Lockwood Press, Atlanta. 47
- TRONCHÈRE, H., SALOMON, F., CALLOT, Y., GOIRAN, J.P., SCHMITT, L., FORSTNER-MÜLLER, I. & BIETAK, M. (2008). Geoarchaeology of Avaris: first results. *Ägypten und Levante/Egypt and the Levant*, **18**, 327–339. 48
- TRONCHÈRE, H., GOIRAN, J.P., SCHMITT, L., PREUSSER, F., BIETAK, M., FORSTNER-MÜLLER, I. & CALLOT, Y. (2012). Geoarchaeology of an ancient fluvial harbour: Avaris and the Pelusiac branch (Nile River, Egypt). *Geomorphologie (Géomorphologie: relief, processus, environnement)*, **18**, 23–36. 48, 67, 68
- ULLMANN, T., SERFAS, K., BÜDEL, C., PADASHI, M. & BAUMHAUER, R. (2019). Data Processing, Feature Extraction, and Time-Series Analysis of Sentinel-1 Synthetic Aperture Radar (SAR) Imagery: Examples from Damghan and Bajestan Playa (Iran). *Zeitschrift für Geomorphologie, Supplementary Issues*, **62**, 9–39. 110
- VAN ASSELEN, S., STOUTHAMER, E. & VAN ASCH, T. (2009). Effects of peat compaction on delta evolution: A review on processes, responses, measuring and modeling. *Earth-Science Reviews*, **92**, 35–51. 60
- VAN DEN BOOGAART, G.K. & TOLOSANA-DELGADO, R. (2013). *Analyzing compositional data with R. Use R!*, Springer, Berlin and New York. 11, 84, 85
- VAN WESEMAEL, B. (1988). The relation between natural landscape and distribution of archaeological remains in northeastern Nile delta. In E.C.M. van den Brink, ed., *The Archaeology of the Nile Delta, Egypt: Problems and Priorities*, 125–134, Netherlands Foundation for Archaeological Research in Egypt, Amsterdam. 47
- VON DER WAY, T., ed. (1997). *Ergebnisse zum frühen Kontext: Kampagnen der Jahre 1983 - 1989*, vol. 83 of *Archäologische Veröffentlichungen*. von Zabern, Mainz am Rhein. 2, 76
- WAYNE NESBITT, H. & MARKOVICS, G. (1997). Weathering of granodioritic crust, long-term storage of elements in weathering profiles, and petrogenesis of siliciclastic sediments. *Geochimica et Cosmochimica Acta*, **61**, 1653–1670. 68
- WEI, G., LIU, Y., LI, X., SHAO, L. & LIANG, X. (2003). Climatic impact on Al, K, Sc and Ti in marine sediments: Evidence from ODP Site 1144, South China Sea. *Geochemical Journal*, **37**, 593–602. 68
- WILSON, C.A., CRESSER, M.S. & DAVIDSON, D.A. (2006). Sequential element extraction of soils from abandoned farms: an investigation of the partitioning of anthropogenic element inputs from historic land use. *Journal of Environmental Monitoring*, **8**, 439–444. 48

## REFERENCES

---

- WILSON, P. (2012a). The ancient landscape around Lake Burullus. *Egyptian Archaeology*, **41**, 18–20. 2, 49
- WILSON, P. (2012b). Waterways, settlements and shifting power in the north-western Nile Delta. *Water History*, **4**, 95–117. 2, 49, 56, 71
- WILSON, P. (2015). Baltim, Parallos, and Mutubis: Late Period and Ptolemaic antecedents for Late Antique ports and settlements in northern Egypt. In D. Robinson & F. Goddio, eds., *Thonis-Heracleion in context*, Monograph / Oxford Centre for Maritime Archaeology, 297–315, Oxford Centre for Maritime Archaeology, Oxford. 2, 44, 49
- WILSON, P. (2017). Landscapes of the Bashmur. Settlements and Monasteries in the Northern Egyptian Delta from the Seventh to the Ninth Century. In H. Willems & J.M. Dahms, eds., *The Nile: natural and cultural landscape in Egypt*, Mainz Historical Cultural Sciences, 345–368, transcript, Bielefeld. 56, 60, 71
- WILSON, P. & GRIGOROPOULOS, D. (2009). *The West Nile delta regional survey, Beheira and Kafr el-Sheikh provinces*, vol. 86 of *Excavation Memoir*. Egypt Exploration Society, London. 2, 46, 47, 49, 56, 71
- WITTKÉ, A.M., OLSHAUSEN, E. & SZYDLAK, R. (2012). *Historischer Atlas der antiken Welt*. Der neue Pauly. Supplemente, ungekürzte Sonderausgabe des 2007 als Bd. 3 der Reihe 'Der Neue Pauly. Supplemente' erschienen Werks, Metzler, Stuttgart. 46
- WUNDERLICH, J. (1988). Investigations on the development of the western Nile Delta in Holocene times. In E.C.M. van den Brink, ed., *The Archaeology of the Nile Delta, Egypt: Problems and Priorities*, 251–257, Netherlands Foundation for Archaeological Research in Egypt, Amsterdam. 2, 50, 76
- WUNDERLICH, J. (1989). *Untersuchungen zur Entwicklung des westlichen Nildeltas im Holozän: Zugl.: Marburg, Univ., Diss., 1989*, vol. 114 of *Marburger Geographische Schriften*. Marburger Geograph. Gesellschaft, Marburg/Lahn. iii, iv, v, vii, 1, 2, 6, 9, 47, 48, 49, 50, 56, 60, 62, 64, 66, 71, 76, 77, 100, 107
- WUNDERLICH, J. (1993). The natural conditions for pre- and early dynastic settlement in the western Nile Delta around Tell el-Fara'in-Buto. In L. Krzyzaniak, M. Kobusiewicz & J. Alexander, eds., *Environmental change and human culture in the Nile Basin and northern Africa until the second millennium B.C.*, Studies in African Archaeology, 259–266, Poznan Archaeological Museum, Poznan. 1, 2, 48, 50, 76
- WUNDERLICH, J. & ANDRES, W. (1991). Late Pleistocene and Holocene evolution of the western Nile delta and implications for its future development. In H. Brückner & U. Radtke, eds., *Von der Nordsee bis zum Indischen Ozean*, Erdkundliches Wissen, 105–120, Franz Steiner Verlag, Stuttgart. 18, 48
- WUNDERLICH, J. & GINAU, A. (2016). Paläoumweltwandel im Raum Tell el Fara'in/Buto. Ergebnisse und Perspektiven geoarchäologischer Forschung. In D. Polz & S.J. Seidlmayer, eds., *Gedenkschrift für Werner Kaiser*, vol. 70/71 of *Mitteilungen des Deutschen Archäologischen Instituts, Abteilung Kairo*, 485–498, De Gruyter, Berlin, Boston. 1, 62, 66, 97
- WUNDERLICH, J., VON DER WAY, T. & SCHMIDT, K. (1989). Neue Fundstellen der Buto-Maadi-Kultur bei Ezbet el-Qerdahi. *Mitteilungen des Deutschen Archäologischen Instituts, Abteilung Kairo*, **45**, 309–318. 49
- ZAKRZEWSKI, S., SHORTLAND, A. & ROWLAND, J. (2016). *Science in the Study of Ancient Egypt*, vol. 3 of *Routledge Studies in Egyptology*. Routledge, New York. 47
- ZEYDAN, B.A. (2005). The Nile Delta in a global vision. In *Ninth International Water Technology Conference, IWTC9*, 31–40. 18
- ZWALLY, H.J., SCHUTZ, B.E., BENTLEY, C.R., BUFTON, J.L., HERRING, T.R., MINSTER, J.B., SPINHIRNE, J.D. & THOMAS, R.H. (2011). *GLAS/ICESat L1B Global Elevation Data, Version 33*. NASA National Snow and Ice Data Center Distributed Active Archive Center, Boulder, Colorado USA. 53, 54



# Appendices



## Appendix A

### additional figures

## A. ADDITIONAL FIGURES

---

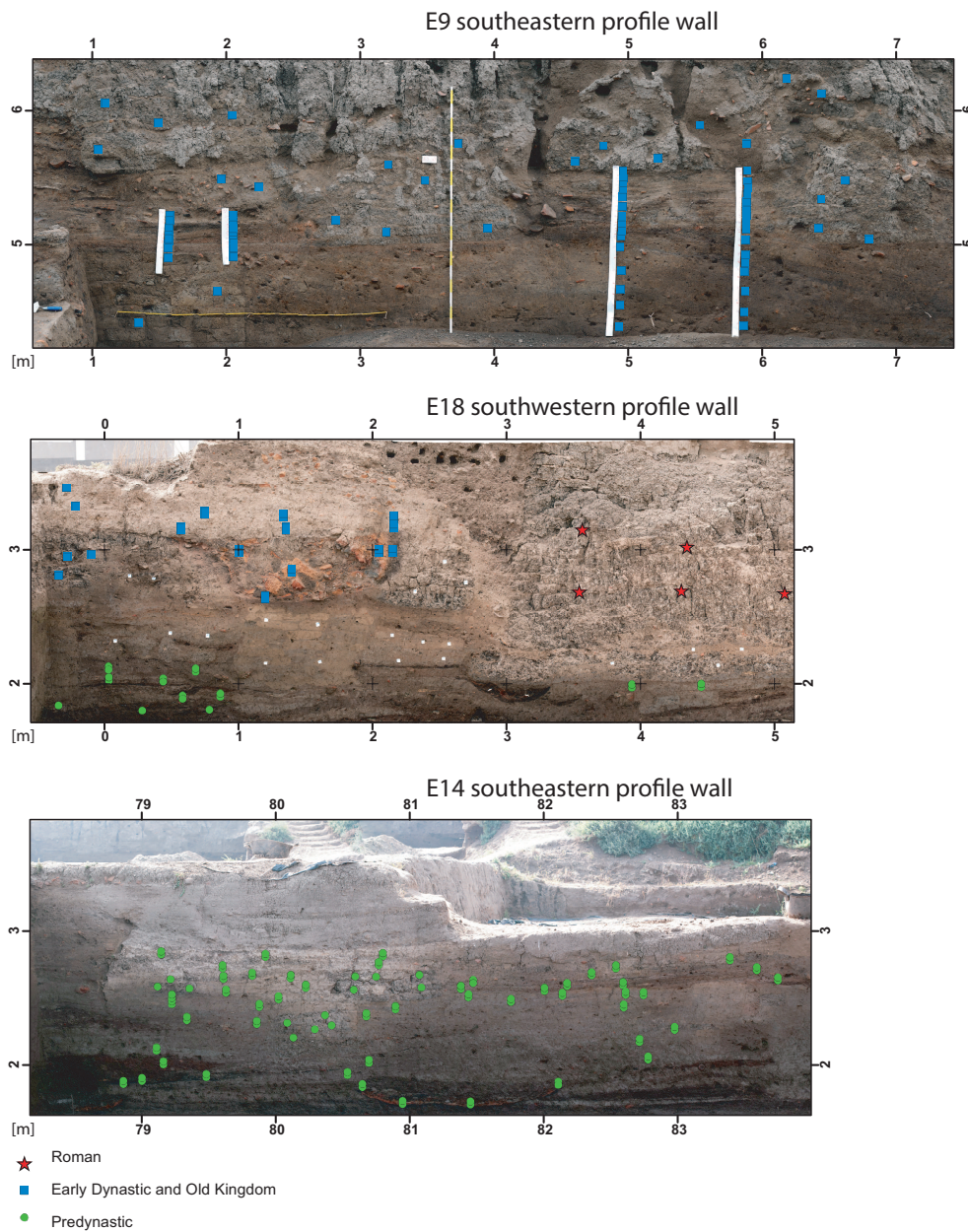


**Fig. A.1: Profile walls PB15 and PB19** - The figure shows the sampling and age composition of the profile walls from the excavation of Dr. Pascale Ballet.

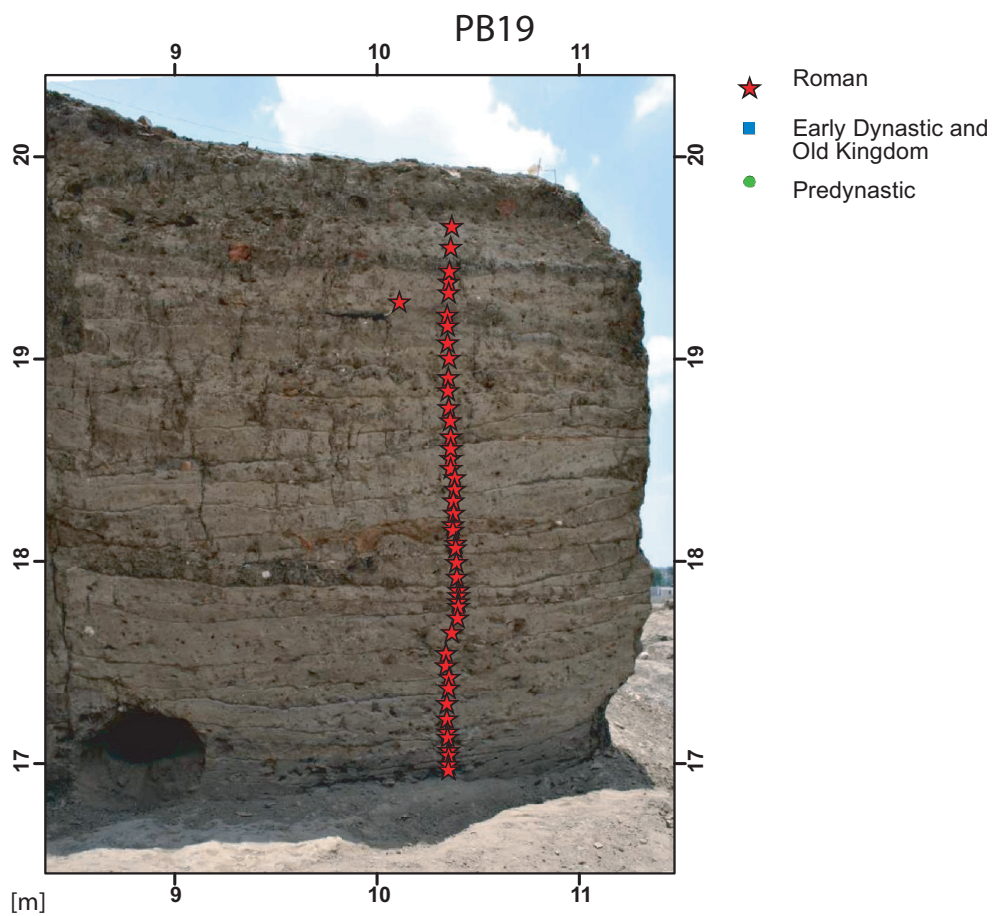
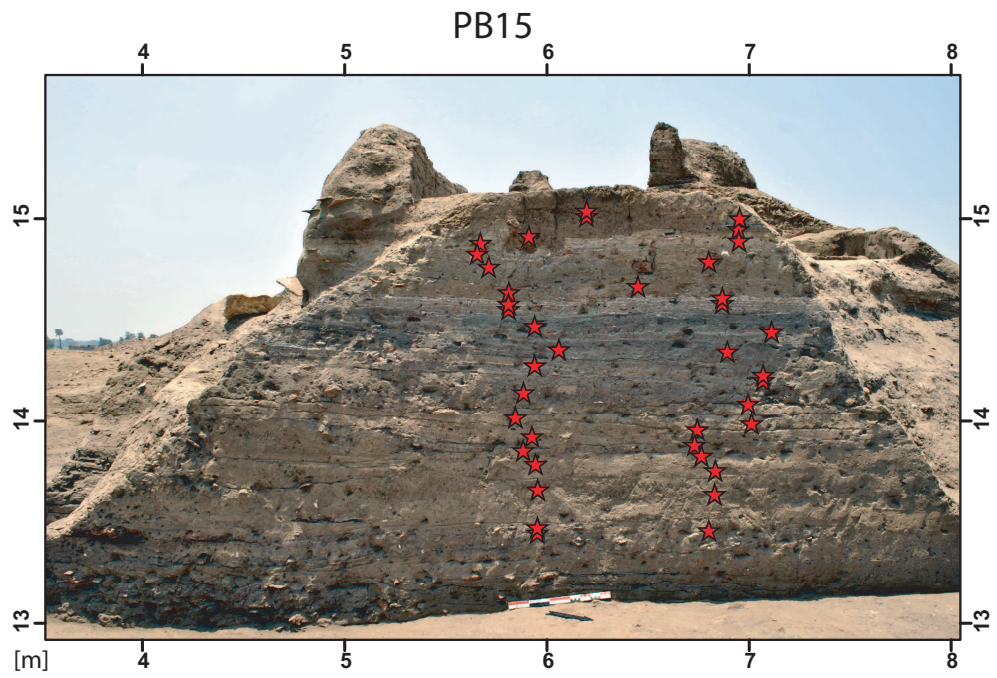


**Fig. A.2: Profile walls E9, E14 and E18** - The figure shows the sampling and age composition of the profile walls from the excavation of Dr. Ulrich Hartung.

## A. ADDITIONAL FIGURES

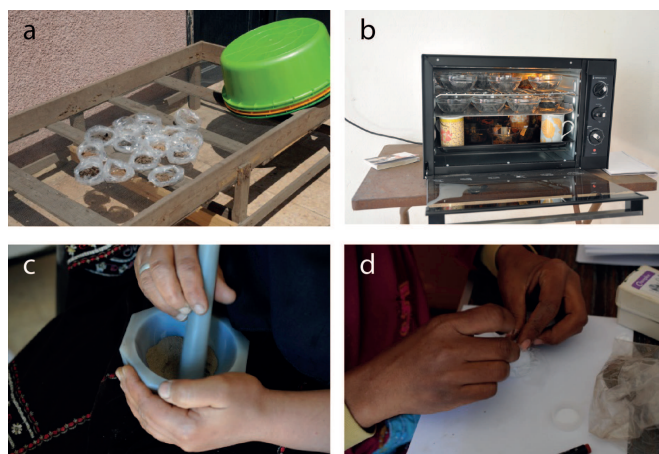


**Fig. A.3: On site sample preparation** - a/b drying of sediment samples, c fine grinding with an achat pestle, d preparation of xrf cylinders with 4 µm foil

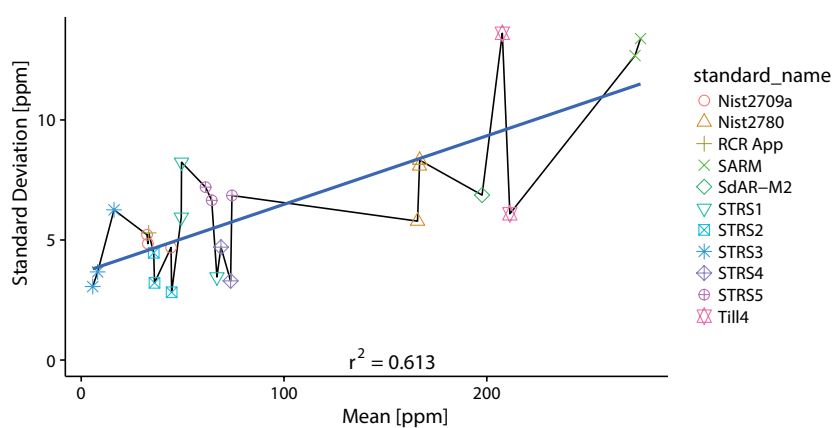


**Fig. A.4:** - Relation between standard deviation and mean sample concentrations for Copper (Cu). Each point represents repeated measurements of a standard reference sample from one measurement campaign.

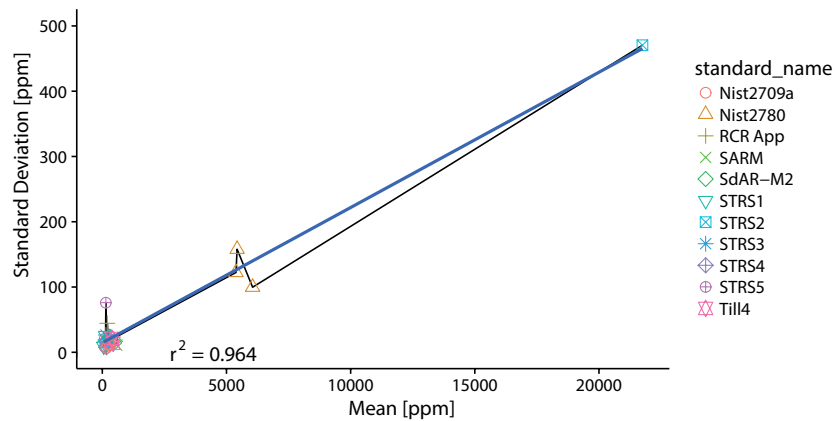


**Fig. A.5:** - Relation between standard deviation and mean sample concentrations for Sulphur (S). Each point represents repeated measurements of a standard reference sample from one measurement campaign.

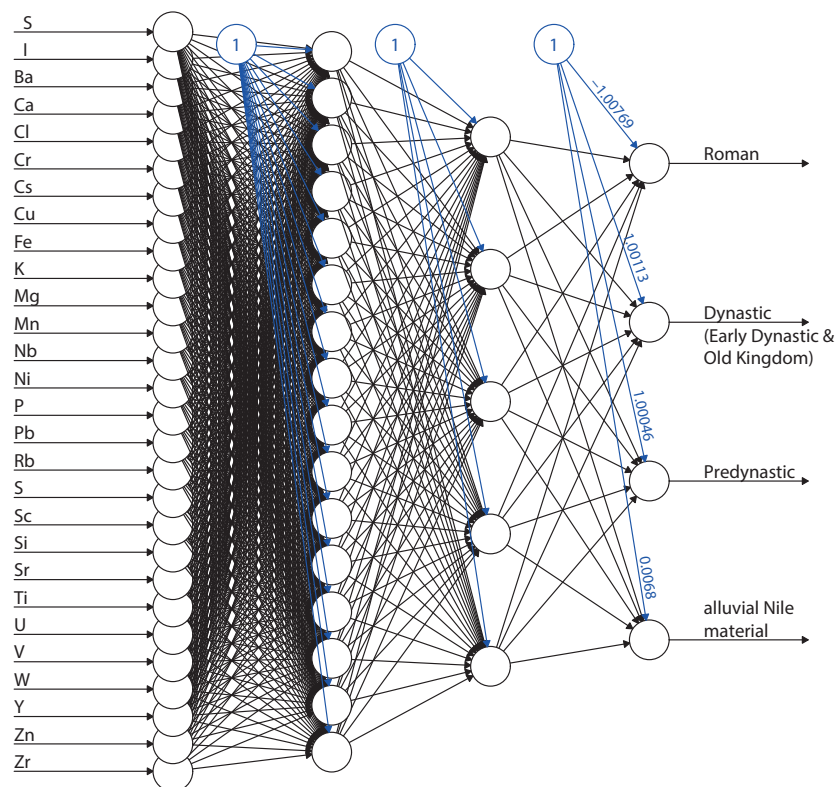


**Fig. A.6: Structural design of the neural network** - The structure shows the input variables, the two hidden layers with 16 and 5 neurons and as output variables the three cultural phases as well as the alluvial Nile material.

## A. ADDITIONAL FIGURES

---

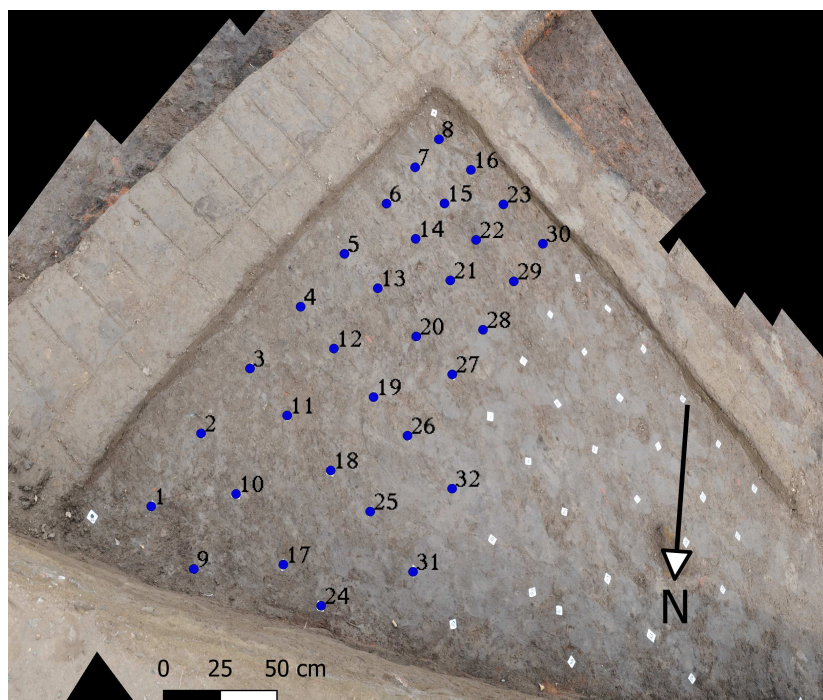


**Fig. A.7: Post-sedimentary affected elements** - Location of measured samples within the Predynastic floor (record 928) in section E13.



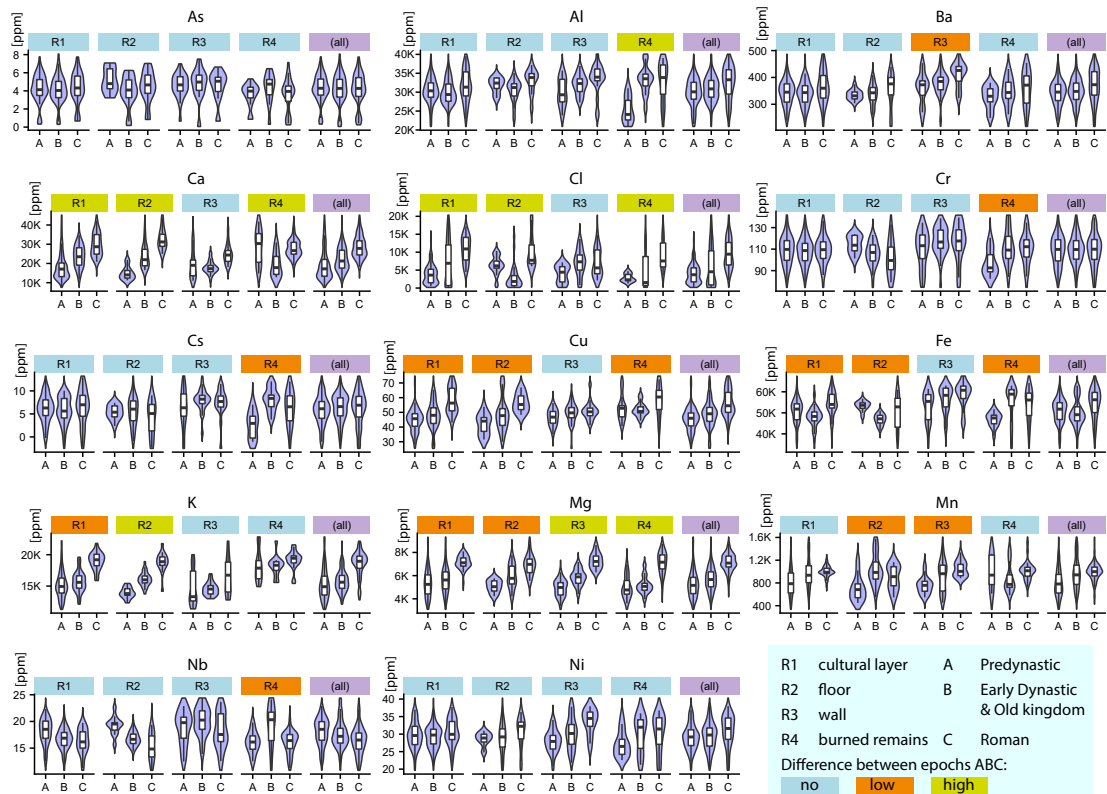


**Fig. A.8: Chemical differentiation between archaeological records and main epochs for selected elements.** - Illustrated are the pXRF data distribution of elements selected in chapter 5.5.1. The results are presented in form of violin plots. In addition to normal box plots, they show the smoothed probability density of the data on each side. Results are presented separately for the different archaeological records and epochs. The last violin plot on the right for each element shows the distribution of all records for the three different epochs. Records of elements with a distinctive pattern for only one or all three epochs are marked in orange if they show slight differences in their distributions and in green if the differences tend to be high and significant. This differentiation is applied qualitatively based on violin plots.

## A. ADDITIONAL FIGURES

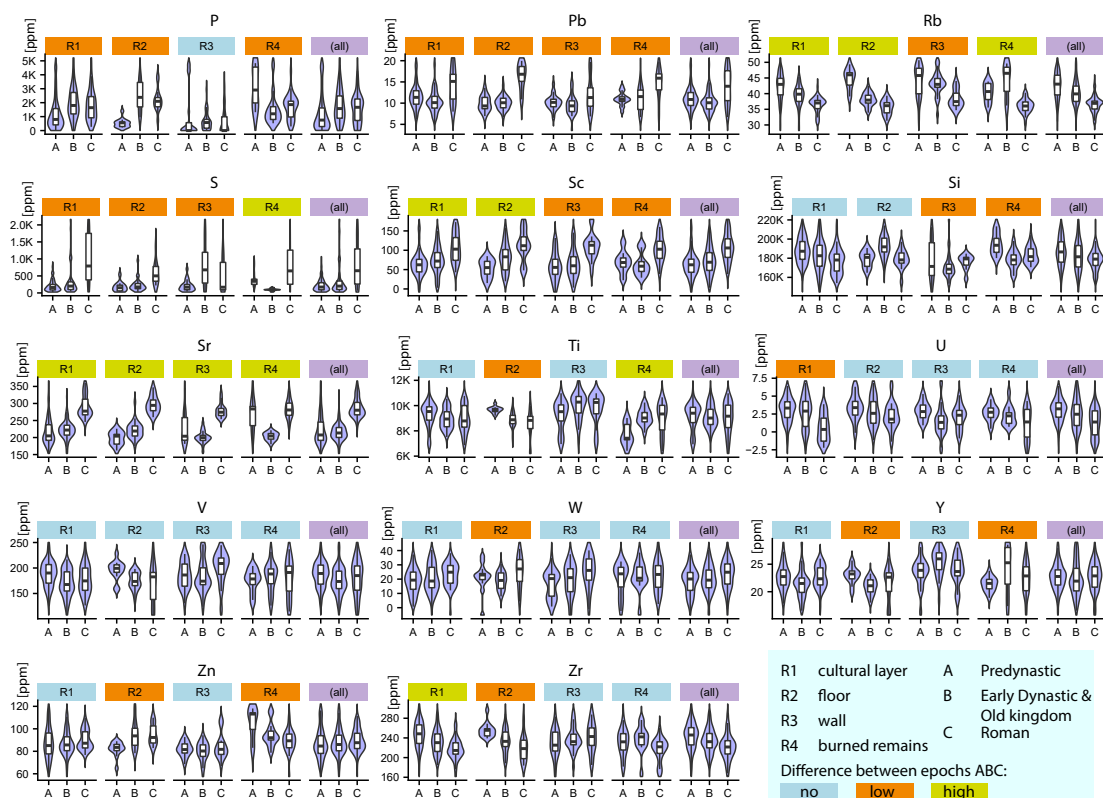


**Fig. A.9: Chemical differentiation between archaeological records and main epochs for selected elements** - Illustrated are the pXRF data distribution of elements selected in chapter 5.5.1. The results are presented in form of violin plots. In addition to normal box plots, they show the smoothed probability density of the data on each side. Results are presented separately for the different archaeological records and epochs. The last violin plot on the right for each element shows the distribution of all records for the three different epochs. Records of elements with a distinctive pattern for only one or all three epochs are marked in orange if they show slight differences in their distributions and in green if the differences tend to be high and significant. This differentiation is applied qualitatively based on violin plots.

## Appendix B

### corings

## B. CORINGS

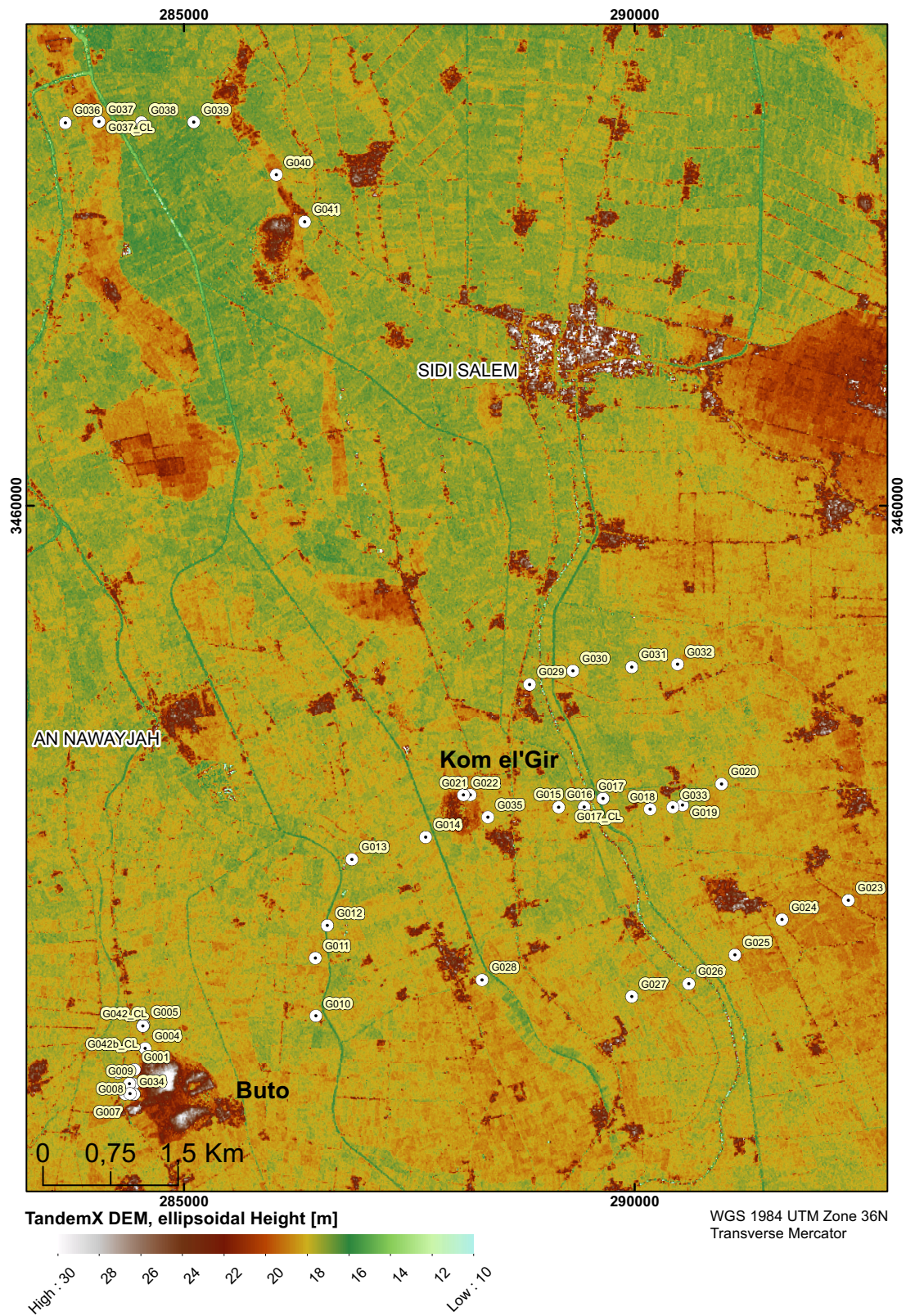


**Fig. B.1: Location of sediment corings** - Overview map showing the location of all sediment corings that are important for this study.



## B. CORINGS

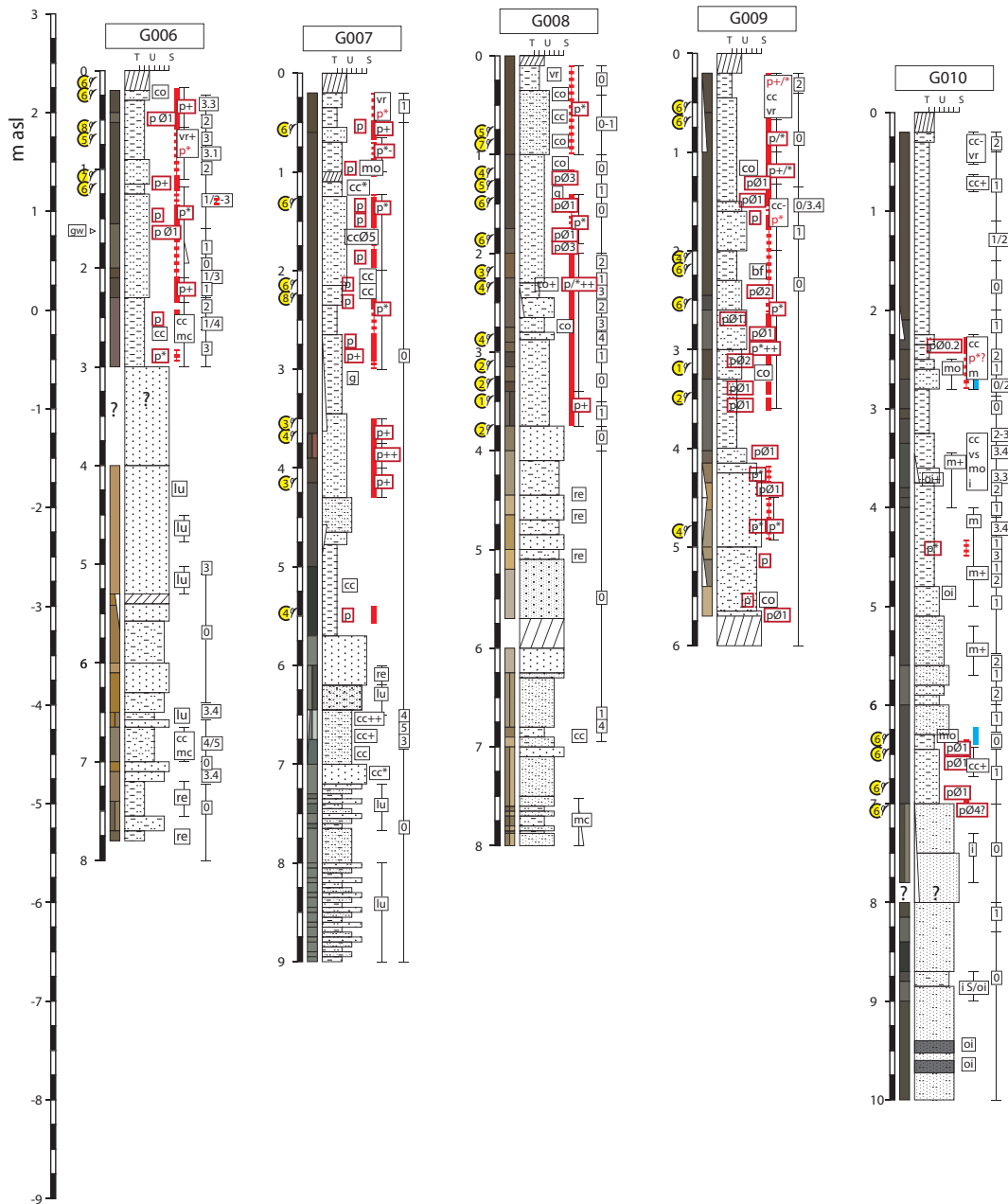
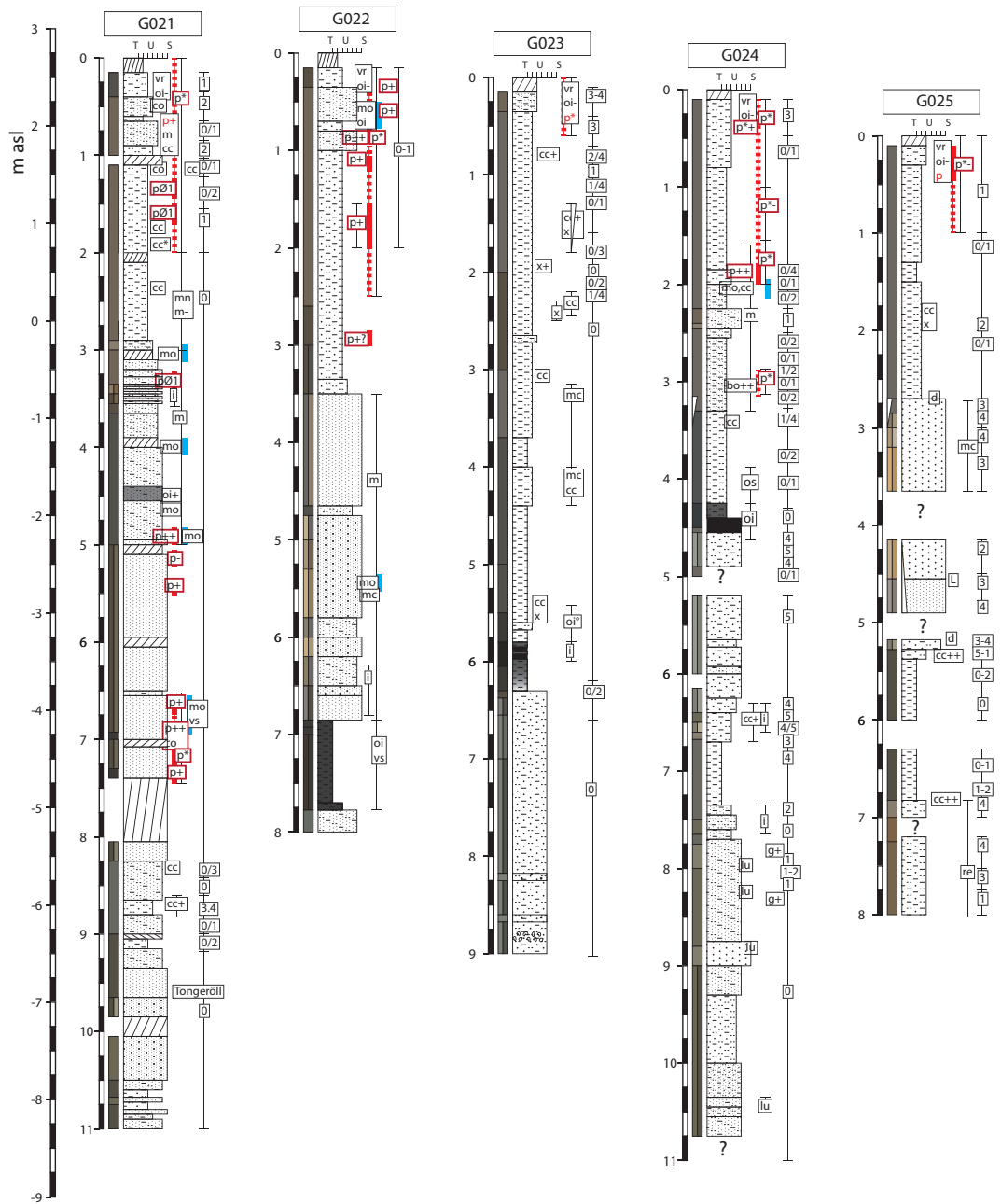


Fig. B.3: Coring descriptions G6-G10 - Graphical illustration of the field description. The legend is included in figure B.10









**Fig. B.6: Coring descriptions G21-G25** - Graphical illustration of the field description. The legend is included in figure B.10

## B. CORINGS

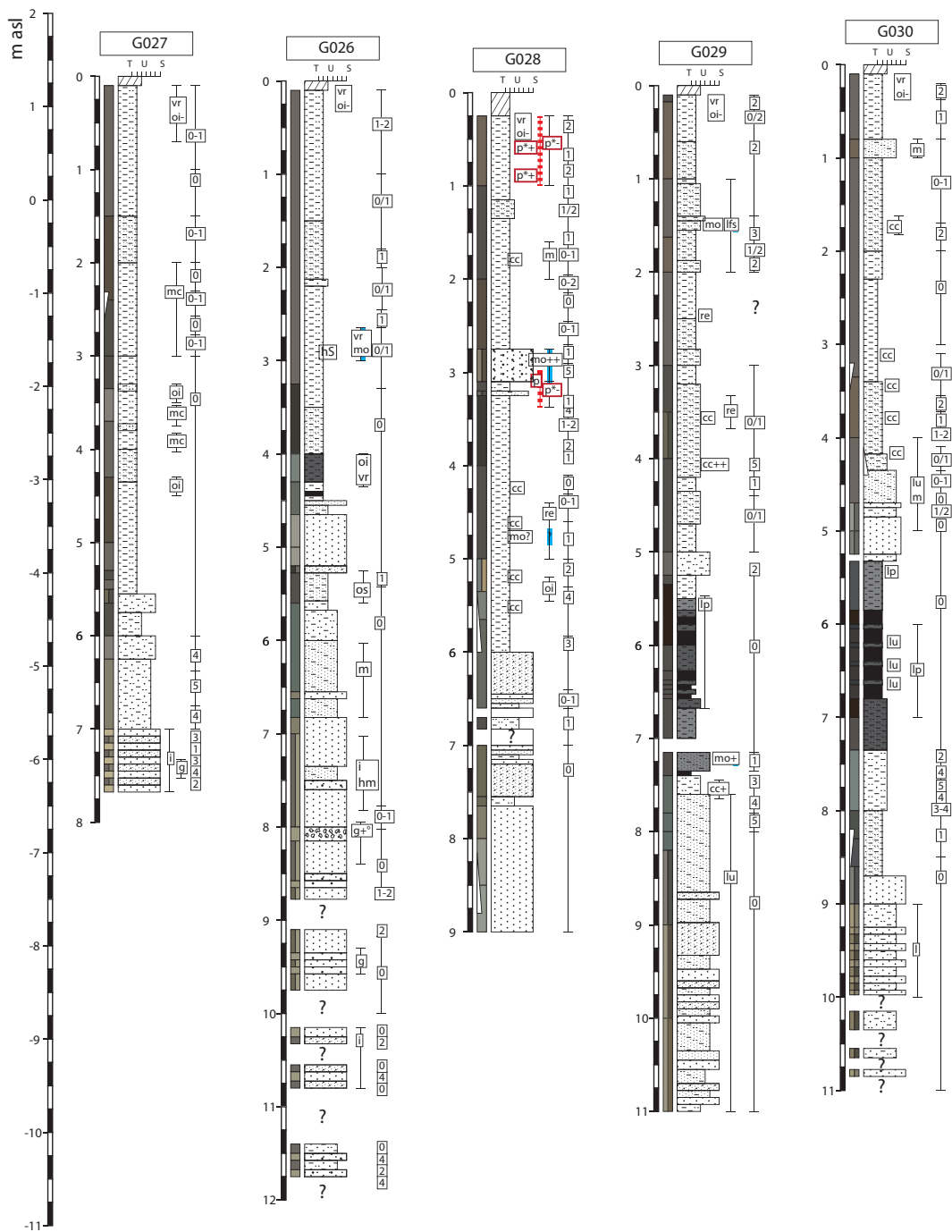


**Fig. B.7: Coring descriptions G26-G30** - Graphical illustration of the field description. The legend is included in figure B.10

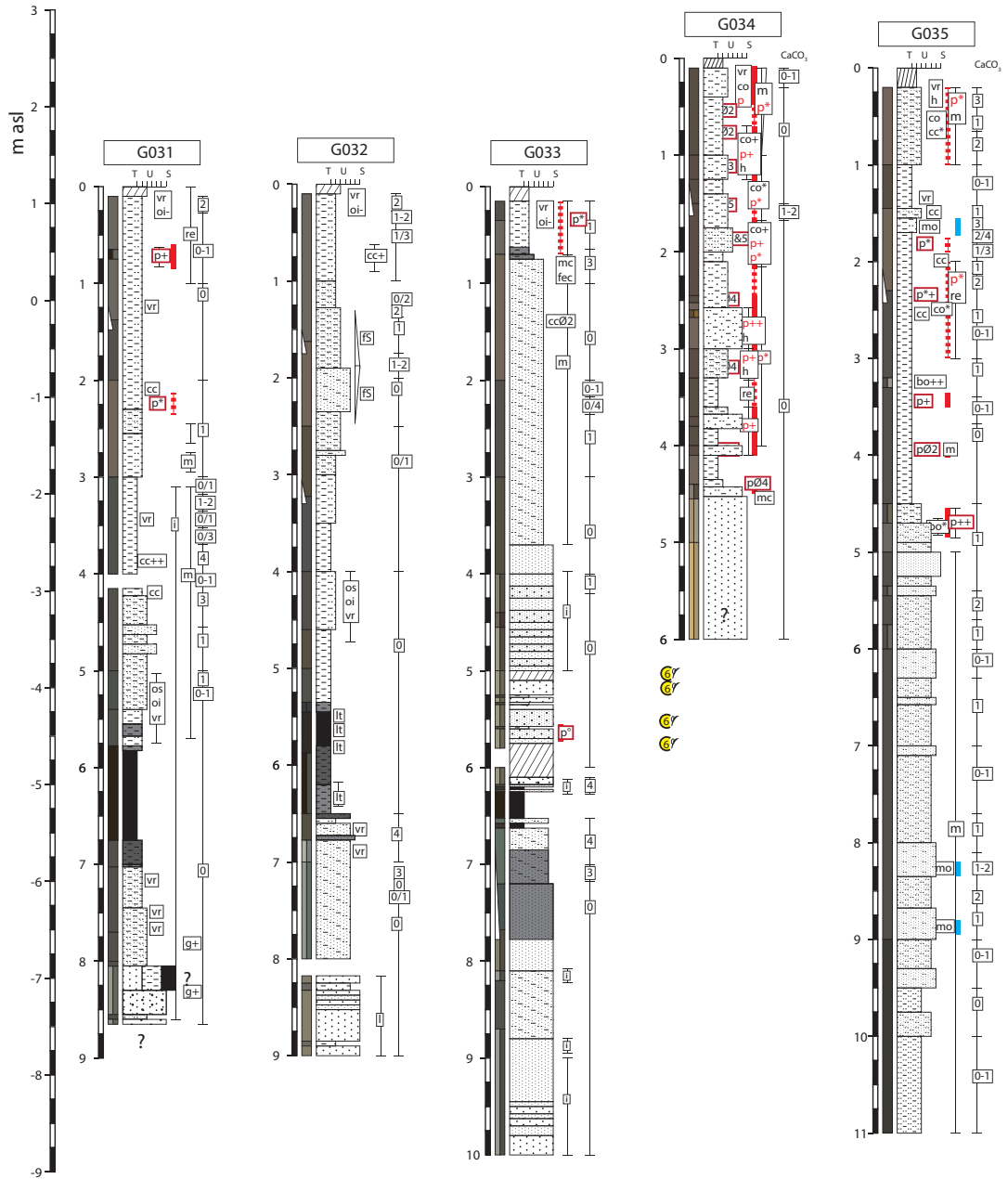


Fig. B.8: Coring descriptions G31-G35 - Graphical illustration of the field description. The legend is included in figure B.10



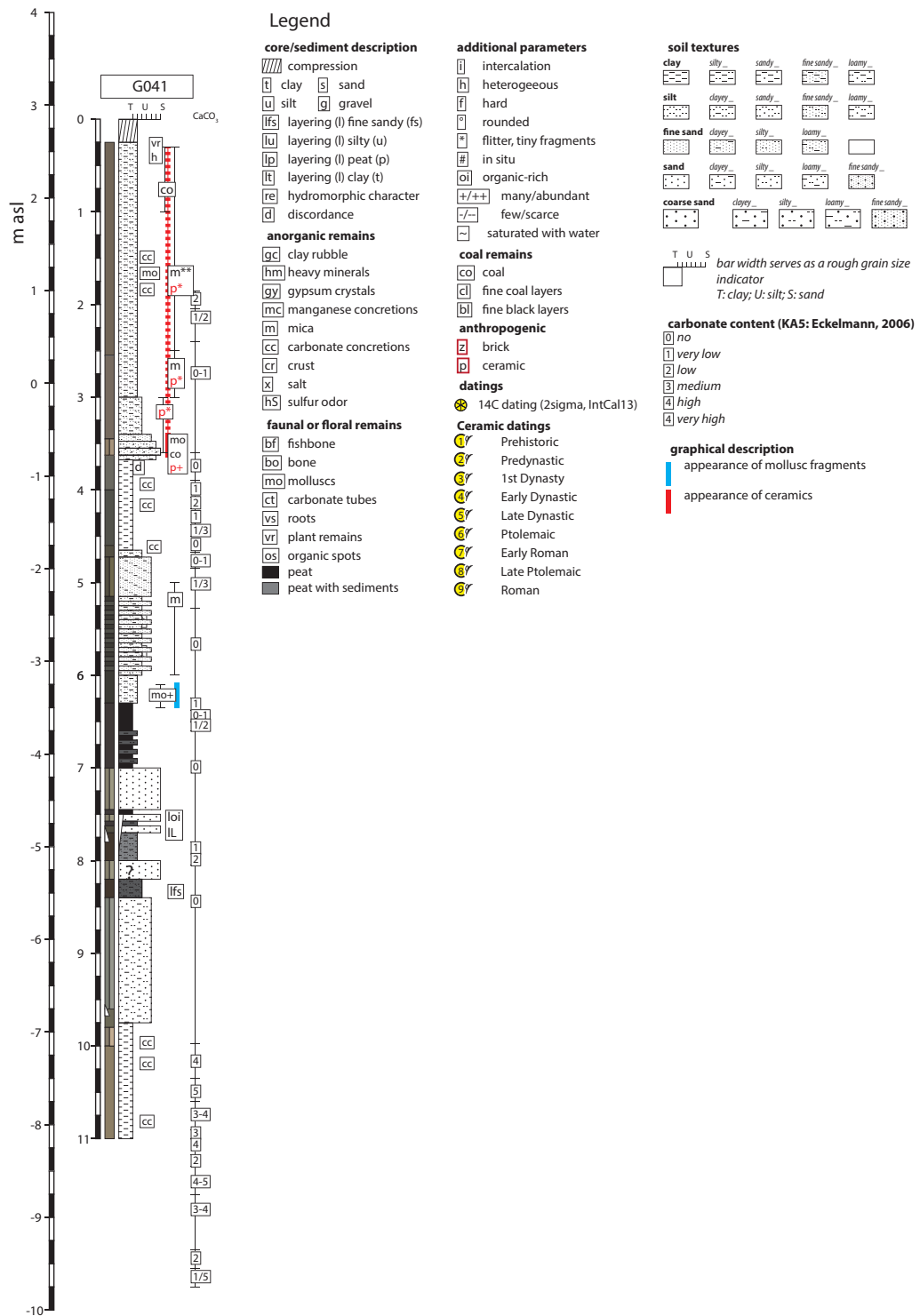


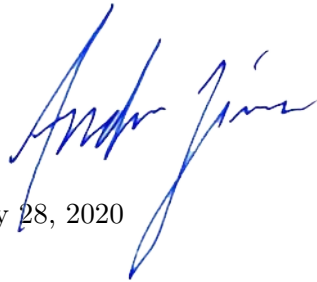
Fig. B.10: Coring descriptions G041 - Graphical illustration of the field description with legend.

## Declaration

Ich versichere an Eides statt durch meine eigene Unterschrift, dass ich die vorstehende Arbeit selbständig und ohne fremde Hilfe angefertigt und alle Stellen, die wörtlich oder annähernd wörtlich aus Veröffentlichungen genommen sind, als solche kenntlich gemacht habe. Die Versicherung bezieht sich auch auf in der Arbeit gelieferte Zeichnungen, Skizzen, bildliche Darstellungen und dergleichen.

Datum:

Unterschrift:

A handwritten signature in blue ink, appearing to read 'Andreas Jünke', written over the date line.

Assenheim, July 28, 2020